UNIVERSITY OF ALBERTA

The *Saccharomyces cerevisiae* Succinate Dehydrogenase: Studies on the Structure and Function of the Anchor Polypeptides

by

Kayode Stephen Oyedotun ©

A thesis submitted to the Faculty of Graduate Studies and Research in partial
fulfillment of the requirements for the degree of Doctor of Philosophy.

Department of Biochemistry

Edmonton, Alberta

Fall, 1999

National Library
of Canada

Acquisitions and
Bibliographic Services

395 Wellington Street
Ottawa ON K1A 0N4
Canada

Bibliothèque nationale
du Canada

Acquisitions et
services bibliographiques

395, rue Wellington
Ottawa ON K1A 0N4
Canada

Your file Votre référence

Our file Notre référence

The author has granted a non-exclusive licence allowing the National Library of Canada to reproduce, loan, distribute or sell copies of this thesis in microform, paper or electronic formats.

The author retains ownership of the copyright in this thesis. Neither the thesis nor substantial extracts from it may be printed or otherwise reproduced without the author's permission.

L'auteur a accordé une licence non exclusive permettant à la Bibliothèque nationale du Canada de reproduire, prêter, distribuer ou vendre des copies de cette thèse sous la forme de microfiche/film, de reproduction sur papier ou sur format électronique.

L'auteur conserve la propriété du droit d'auteur qui protège cette thèse. Ni la thèse ni des extraits substantiels de celle-ci ne doivent être imprimés ou autrement reproduits sans son autorisation.

0-612-46900-X

Canada

University of Alberta

Library Release Form

Name of Author: Kayode Stephen Oyedotun

Title of Thesis: The *Saccharomyces cerevisiae* Succinate Dehydrogenase: Studies on the Structure and Function of the Anchor Polypeptides

Degree: Doctor of Philosophy

Year this Degree Granted: 1999

Permission is hereby granted to the University of Alberta Library to reproduce single copies of this thesis and to lend or sell copies for private, scholarly, or scientific purposes only.

The author reserves all other publication and other rights in association with the copyright in the thesis, and except as hereinbefore provided, neither the thesis nor any substantial portion thereof may be printed or otherwise reproduced in any form whatever without the author's prior written permission.

Kayode Stephen Oyedotun
114 RH Michener Park
Edmonton, Alberta, Canada

Dated August 23/99

University of Alberta

Faculty of Graduate Studies and Research

The undersigned certify that they have read, and recommend to the Faculty of Graduate Studies and Research for acceptance, a thesis entitled "The *Saccharomyces cerevisiae* Succinate Dehydrogenase: Studies on the Structure and Function of the Anchor Polypeptides" submitted by Kayode Stephen Oyedotun in partial fulfillment of the requirements for the degree of Doctor of Philosophy.

Bernard Lemire
Dr. B. D. Lemire (supervisor)

Dr. M. Michalak

Dr. M. Glerum

Dr. M. Schultz

Gary Cecchini
Dr. G. Cecchini (external examiner)

Dated June 22/99

To the memory of my mother, Ruth Ayoka Oyedotun

ABSTRACT

Succinate dehydrogenase (SDH) is an enzyme that participates in both the Krebs cycle and the aerobic respiratory chain by coupling the oxidation of succinate to the transfer of electrons to ubiquinone. The enzyme is composed of two domains: a catalytic domain, comprised of a flavoprotein and an iron-sulfur protein subunit (designated Sdh1p and Sdh2p, respectively); and a membrane-anchoring domain, typically comprised of two smaller hydrophobic polypeptides (designated Sdh3p and Sdh4p). The membrane-anchoring domain interacts with ubiquinone and in some cases, one or two *b*-type cytochromes. Using the *Saccharomyces cerevisiae* SDH as a model, the structure and function of the anchor polypeptides were investigated.

The loss of either of the anchor polypeptides results in the absence of membrane-associated SDH, suggesting the essential role of these polypeptides in the docking of the catalytic domain and in electron transfer. Moreover, analysis of the difference absorption spectra of mitochondria showed that the *S. cerevisiae* SDH contains a fumarate-oxidizable cytochrome b_{562} in stoichiometric amounts. Based on the covalent FAD content, there is one heme per SDH holoenzyme. The spectrum is absent in the *SDH3* or the *SDH4* gene disruption mutants, suggesting that axial ligands for the heme are contributed by both subunits.

The function of the unusual carboxyl-terminal extension of the yeast Sdh4p subunit was investigated by sequential truncations. The Sdh4p residues 128-135

were found to be critical for the formation of a conformation that is compatible with high affinity quinone binding. Residues 136-140 were found to be necessary for optimal quinone reduction. Site-directed mutagenesis at Lys-132 suggests that the Sdh4p C-terminus is involved in protein-protein interactions, possibly via the formation of salt-bridges.

We explored protein-quinone interactions by performing random mutagenesis on the *SDH3* gene. Our studies determined that three amino acid residues, Phe-103, His-113, and Trp-116 in the Sdh3p subunit are important for the formation of a quinone-binding site. On the basis of kinetic analysis of inhibition by the quinone analog, 2-*sec*-butyl-4,6-dinitrophenol and the asymmetric locations of mutations that affect quinone reduction, a dual quinone-binding site model is proposed for the *S. cerevisiae* SDH.

Acknowledgments

I would like to acknowledge my indebtedness to the many people who contributed to the success of this thesis.

Words can not adequately express my profound gratitude to my supervisor, Dr. Bernard Lemire, for his limitless patient, his humane disposition, and his guidance. I have benefited immensely from his scientific approach to issues, his ingenuity, and enthusiasm.

I am thankful to my supervisory committee members, Drs. Merek Michalak, Colin Rasmussen, and Moira Glerum, for their invaluable suggestions, constructive criticisms and directions.

I thank the entire members of Dr. Lemire Laboratory–Bonnie Bullis, Karen Robinson, Elena Dibrov, Jennifer Douglas, and William Tsang. Their openness and friendly dispositions have contributed in no small way to making the Laboratory a conducive atmosphere for learning and research.

I am immensely grateful to my family–my dad, Nathaniel Olaoye, my mom, Ruth Olaoye (of blessed memory), my sister and brother, Williams and Cecilia, my wife, Arinade, and my sons, Kayode Jr. and Ifeloluwa for their unalloyed support, encouragement and prayers.

Finally, I thank the Almighty God for sparing my life and for illuminating my paths in the tortuous terrain of life.

Financial supports from the Department of Biochemistry and the Medical Research Council of Canada are gratefully acknowledged.

TABLE OF CONTENTS

Chapter 1 General Introduction 1

1.1. Introduction 2

1.2. Energy Transduction in Mitochondrion 3

1.2.1. Mechanism of Energy Transduction: The Chemiosmotic Theory 6

1.3. The Mitochondrial Respiratory Chain 7

1.3.1. The Respiratory Chain of *S. cerevisiae* 10

1.3.2. Structure and Function of the Energy Transducing Units 12

1.3.2.1. Complex I 13

1.3.2.2. Complex IV 15

1.3.3. Complex III 16

1.3.3.1. Structure 17

1.3.3.2. Intramolecular Electron Transfer and Energy Conservation 18

1.3.3.3. Electron Transfer at the Q_o Site 21

1.4. The SDH and FRD Complexes 23

1.4.1. Structural and Functional Properties of SDH and FRD 24

1.4.2. Molecular Biology of SDH and FRD 30

1.4.3. The Flavoprotein Subunit 31

1.4.4. The Iron-sulfur Protein Subunit 36

1.4.5. The Anchor Polypeptides 38

1.4.6. Interaction with Heme 38

1.4.7. Interaction with Quinones 43

1.4.8. Intramolecular Electron Transfer 44

1.4.9. Topological Organization of SDH and FRD 47

1.5. Assembly of Succinate-quinone Oxidoreductases 50

1.5.1. The Temporal Order of Assembly 51

1.5.2. Incorporation of the Prosthetic Groups 52

1.5.3. Assembly of Eukaryotic SDHs 54

1.6. The Mechanism of Q-mediated Electron Transfer: The Two Quinone-binding Site Hypothesis 55

1.6.1. Structure and Properties of Quinones 56

1.6.2. Quinone-binding Sites in SDHs and FRDs 59

1.6.3 The Q_A and Q_B Sites of Bacterial Photosystems 62

1.7. Thesis Problem 66

1.8. Bibliography 68

Chapter 2 The *S. cerevisiae* SDH Contains Stoichiometric Amounts of Heme *b*.................... 92

2.1. Introduction 93

2.2. Materials and Methods 95

2.3. Results 101

2.4. Discussion 109

2.5. Bibliography 116

Chapter 3 Function of the Sdh4p Carboxyl-terminal Extension....... 121

3.1. Introduction 122

3.2. Materials and Methods 123

3.3. Results 128

3.4. Discussion 142

3.5. Bibliography 148

Chapter 4 Mutagenesis of the *S. cerevisiae* Sdh4p Lys-132............. 152

4.1. Introduction 153

4.2. Materials and Methods 154

4.3. Results 158

4.4. Discussion 168

4.5. Bibliography 173

Chapter 5 Identification and Characterization of *S. cerevisiae SDH3* Mutants Involved in Quinone Interaction 176

5.1. Introduction 177
5.2. Materials and Methods...180
5.3. Results 181
5.4. Discussion 197
5.5. Bibliography 204

Chapter 6 General Discussion and Conclusions 211

6.1. Bibliography 223

List of Tables

Table 1.1 Properties of Quinones and Hemes in Selected SDHs and FRDs.......... 41

Table 2.1 Enzymatic Activities of Submitochondrial Particles.......... 104

Table 2.2 Concentrations of Cytochromes in Yeast Mitochondrial Membranes.......... 107

Table 3.1 Respiratory Chain Activities of Mitochondrial Membranes..... 132

Table 3.2 Apparent Michaelis Constants for Quinone Reduction.......... 136

Table 3.3 Apparent Inhibition Constants for Quinone Reduction.......... 141

Table 4.1 Succinate Dehydrogenase Activities of Mitochondrial Membranes.......... 161

Table 4.2 Enzymatic Activities of Mitochondrial Particles.......... 163

Table 4.3 The Apparent Michaelis Constants for the Reduction of Exogenous Quinone Analog.......... 165

Table 5.1 Summary of UV- and EMS-induced Mutations in the *SDH3* Gene.......... 183

Table 5.2 Covalent Flavin Levels and Succinate-PMS/DCPIP Reductase Activities in Mitochondrial Membranes of *S. cerevisiae* Strains.......... 186

Table 5.3 Quinone-mediated Enzymatic Activities of *SDH3* Mutants and Wild Type Mitochondrial Membranes.......... 189

Table 5.4 The Apparent Michaelis Constants for DB Reduction.......... 191

Table 5.5 The Apparent Inhibition Constants for Quinone Reduction..... 196

List of Figures

Figure 1.1 Schematic Diagram of the Mitochondrion........................ 4

Figure 1.2 Schematic Diagram of the Chemiosmotic Coupling............. 8

Figure 1.3 Schematic Diagram of the Mitochondrial Respiratory Chain... 9

Figure 1.4 The Sequence of Electron transfer in the Mitochondrial Respiratory Chain... 11

Figure 1.5 The Protonmotive Q-cycle Mechanism of Electron Transfer Through the Cytochrome bc_1 Complex.......................... 19

Figure 1.6 Schematic Diagram of the Electron Transfer Events at the Q_o Site.. 22

Figure 1.7 The Krebs Cycle.. 26

Figure 1.8 Schematic Representation of the Electron Transport Chain in Facultative Anaerobic Eukaryotes................................ 27

Figure 1.9 The Structure of the 8α-[*N*3]-Histidyl Flavin Adenine Dinucleotide.. 32

Figure 1.10 The Structure of Heme *b*.. 39

Figure 1.11 Topological Model of Succinate Dehydrogenase and Fumarate Reductase.. 48

Figure 1.12 Structures of Quinones, Quinone Analogs, and Inhibitors....... 57

Figure 1.13 The Oxidation States of Ubiquinone.............................. 58

Figure 1.14 Quinone-Mediated Electron Transport in the Bacterial Reaction Center.. 64

Figure 2.1 Agarose Gel Analysis of PCR Products........................... 102

Figure 2.2 Western Blot Analysis of Mutants and Wild Type Mitochondrial.. 103

Figure 2.3 Fumarate-Oxidizable Absorption Spectrum of Mitochondria Isolated from Lactate-grown MH125 Cells....................... 106

Figure 2.4 Difference Absorption Spectrum of Mitochondria Isolated from Lactate-Grown MH125 Cells.................................. 108

Figure 2.5 Difference Absorption Spectrum of Mutants and Wild Type *S. cerevisiae* Strains.. 110

Figure 2.6 Fumarate-Oxidizable Spectra of Mutants and Wild Type *S. cerevisiae* Strains.. 111

Figure 2.7 Alignment of the *S. cerevisiae* Sdh3p Subunit and its Homologue, YMR118Cp... 113

Figure 2.8 Alignment of the *S. cerevisiae* Sdh4p Subunit and its Homologues.. 114

Figure 3.1 Multiple Sequence Alignment of the Sdh4*p Subun*its............ 125

Figure 3.2 Topological Model of the S. cerevisiae Sdh4p Subunit.......... 129

Figure 3.3 Growth of Yeast Strains on Galactose Media.................... 131

Figure 3.4 Stimulation of the SDH4ΔC23 Succinate-DB Reductase Activity.. 135

Figure 3.5 Stabilities of Mutants and Wild Type Enzymes.................. 137

Figure 3.6 Double-Reciprocal Plots for the Inhibition of the Wild Type Enzyme by *s*-BDNP.. 139

Figure 3.7 Nonlinear Kinetics of Inhibition of Quinone Reduction by *s*-BDNP.. 140

Figure 3.8 Secondary Plot Showing Linear Inhibition Kinetics for the Reduction of Exogenous Quinone................................... 143

Figure 3.9 Plot of maximal Velocities versus Substrate Concentrations at Fixed Inhibitor Concentration for the SDH4ΔC23 Mutant Enzyme... 144

Figure 4.1 Schematic Diagram of the *in vitro* Mutagenesis Procedure Using the pALTER-1 Vector.. 157

Figure 4.2 Growth of Yeast Strains on galactose Media.................... 160

Figure 4.3 Thermal Stability Profiles of Succinate-DB Reductase Activities of Mutant and Wild type Enzymes.................... 166

Figure 4.4 Thermal Stability Profiles of Succinate-PMS Reductase Activities of Mutant and Wild type Enzymes.................... 167

Figure 4.5 Spectra of SDH-associated Heme in Mitochondria from Wild Type and Mutant Yeast Strains.................................. 169

Figure 5.1 Growth of Yeast Strains on galactose Media...................... 184

Figure 5.2 Western Blot Analysis of Mutant and Wild Type Mitochondria... 188

Figure 5.3 Thermal Stability Profiles of Succinate-DB Reductase Activities of Mutant and Wild type Enzymes.................... 193

Figure 5.4 Inhibition of Quinone Reduction by 2-*sec*-butyl-4,6-dinitrophenol... 195

Figure 5.5 Spectra of SDH-associated Heme in Mitochondria from Wild Type and Mutant Yeast Strains.................................. 198

Figure 5.6 Topological Model of the Yeast Sdh3p Showing the Mutations Identified in this Study.................................. 200

Figure 6.1 A Model of Quinone Interactions for the *S. cerevisiae* SDH.... 222

List of Abbreviations

ADP	adenosine diphosphate
ATP	adenosine triphosphate
b_L	low potential cytochrome *b*
b_H	high potential cytochrome *b*
Co A	coenzyme A
Coenzyme Q	ubiquinone
cyt.	cytochrome
Cu_A/Cu_B	primary and secondary copper-binding sites of cytochrome *c* oxidase
D	bacteriochlorophyll dimer
DABS	diazobenzene sulfonate
DB	2,3-dimethoxy-5-methyl-6-decyl-1,4-benzoquinone or decylubiquinone
DCPIP	2,6-dchlorophenol indophenol
DTT	dithiothreitol
$E^{0\prime}$	standard redox potential
$E_{m,7}$	midpoint redox potential at pH 7
EDTA	ethylenediaminetetraacetic acid
EMS	ethyl methanesulfonate
EPR	electron paramagnetic resonance
ETC	electron transport chain
FAD/ $FADH_2$	oxidized and reduced flavin adenosine dinucleotide
Fe-S	iron-sulfur cluster
FMN	flavin adenosine mononucleotide
FRD	fumarate reductase
H	heavy polypeptide subunit of photosynthetic reaction center
HEPES	4-(2-hydroxyethyl)-1-piperazineethanesulfonic acid

HQNO	2-*n*-heptyl-4-hydroxyquinoline-*N*-oxide
ISP	iron-sulfur protein subunit
K_m	apparent Michaelis constant
K_{i1}/K_{i2}	apparent high affinity and low affinity inhibition constants
L	light polypeptide subunit of photosynthetic reaction center
M	medium polypeptide subunit of photosynthetic reaction center
MCD	magnetic circular dichroism
MMQ	methylated menaquinone or thermoplasmaquinone
MQ	menaquinone
NAD^+/ NADH	oxidized and reduced nicotinamide adenine dinucleotide
OD	optical density
PAGE	polyacrylamide gel electrophoresis
PCR	polymerase chain reaction
PMS	phenazine methosulfate
$Q^{\cdot}$	semiquinone radical
Q_A/Q_B	primary and secondary quinone-binding sites of photosynthetic reaction center
Q/QH_2	oxidized and reduced quinone
Q_o	ubiquinone oxidation site of complex III
Q_i	ubiquinone reduction site of complex III
RC	photosynthetic reaction center
RQ	rhodoquinone
S-1/S-2/S-3	Iron-sulfur cluster 1, 2 and 3
s-BDNP	2-*sec*-butyl-4,6-dinitrophenol
SDH	succinate dehydrogenase
S.E.M.	standard error of the mean
SQO	succinate:quinone oxidoreductase
SSE	sum of squares error

TTFA	2-thenoyltrifluoroacetone
UQ/UQH_2	oxidized and reduced ubiquinone
UV	ultraviolet radiation
V_{max}	apparent maximal velocity
Δp	protonmotive force
ΔpH	proton concentration gradient
$\Delta\psi$	membrane potential
$\Delta\mu_{H+}$	proton electrochemical potential

Chapter 1

General Introduction

1.1. Introduction

Electron transfer reactions are essential for life. In photosynthesis, they provide the means for harnessing solar energy, while in respiration, they orchestrate the transformation of the chemical energy of foodstuffs into a readily utilizable form. Energy-transductions in respiration and photosynthesis are fundamentally similar. They are composed of a series of membrane-intrinsic multiprotein complexes that catalyze vectorial electrogenic reactions (Bixon *et al.*, 1991; Parson, 1996; Rich, 1996; Skulachev, 1992; Trumpower and Gennis, 1994). The redox energy is conserved via the formation of transmembrane electrochemical potential gradients that can be used to synthesize ATP, the energy currency of life. Electrochemical potentials also participate in secondary active transport (Rich, 1996; Skulachev, 1992). However, the molecular mechanisms underlying biological electron transfer processes are only partially understood (Gray and Winkler, 1996; Larsson, 1998; Moser and Dutton, 1996; Trumpower and Gennis, 1994). To date, the molecular structures of only a few energy-transducing complexes have been described (Crofts and Berry, 1998; Deisenhofer and Michel, 1992; Michel *et al.*, 1998; Parson, 1996; Yoshikawa *et al.*, 1998; Yu *et al.*, 1998).

Although it is not an energy-transducing unit, succinate dehydrogenase is a unique member of the respiratory chain. It directly links the Krebs cycle, the confluence point for the oxidation of intermediary metabolites, with the respiratory chain. Amongst the respiratory chain complexes, SDH is the simplest in terms of subunit composition (Ackrell *et al.*, 1992; Hägerhäll, 1997; Hatefi, 1985; Hederstedt and Ohnishi, 1992). Nevertheless, it possesses some of the redox carriers that are found in many energy-transducing complexes and, as such, it is a good model system for studying the molecular mechanism of electron transfer. This thesis addresses structural aspects of the *Saccharomyces cerevisiae* SDH anchor polypeptides that are germane to understanding the mechanism of intramolecular electron transport.

The aim of this chapter is to introduce the major enzymes involved in energy transduction in the mitochondrion, review our current understanding of succinate dehydrogenases and related enzymes, and discuss a model for electron transfer within this enzyme.

1.2. Energy Transduction in Mitochondria

The mitochondrion is the typical energy transducing organelle in eukaryotic cells. By energy transduction is meant any process whereby the energy leaving a system (e.g. chemical energy) differs in form from the energy entering the system (e.g. radiant energy). The apparatus for energy transduction in mitochondria is the respiratory chain, which is located in the inner membrane of the organelle (Hatefi, 1985; Nicholls and Ferguson, 1992; Trumpower and Gennis, 1994). Mitochondria are delimited by a double membrane system as depicted in Fig. 1.1 (Addink *et al.*, 1972; Korman *et al.*, 1970; Packer, 1974; Palmer and Hall, 1972). The outer membrane contains large pores constructed of three mitochondrial porin molecules. Mitochondrial porin is structurally and functionally analogous to the porin molecules of gram-negative bacteria (Jap and Walian, 1990; Shulz, 1995). These pores allow molecules of less than 10 kDa to enter the intermembrane space, making the outer membrane freely permeable to ions and most metabolites. The outer membrane also contains proteins involved in post-translational protein import into mitochondria (Attardi and Schatz, 1988; Neupert, 1997; Schatz, 1996).

The inner membrane encloses the matrix space. This compartment is the domain of enzymes of the Krebs cycle, with the exception of succinate dehydrogenase, which is bound to the inner face of the inner membrane. Unlike the outer membrane, the inner membrane is impermeable to most small molecules and ions, allowing only uncharged molecules of 100–150 Da to pass. This feature

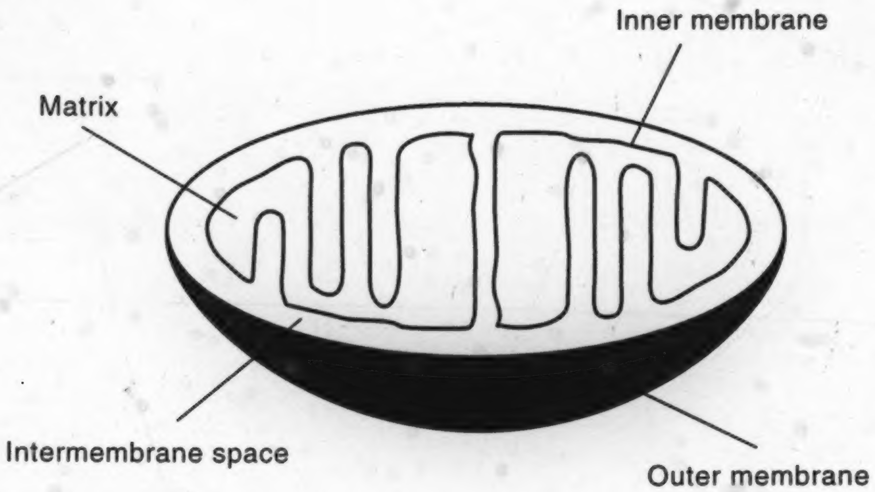
Inner membrane
Matrix
Intermembrane space
Outer membrane

Figure 1.1 Schematic Diagram of the Structure of the Mitochondrion.

is necessary for energy transduction and is a universal characteristic of energy-transducing membranes, including the bacterial plasma membranes and the thylakoid membrane of the chloroplast (Packer, 1974). The majority of charged molecules of physiological importance pass through the inner membrane by means of specific translocators associated with this membrane (Aquila *et al.*, 1987; Krämer and Palmieri, 1992). The inner mitochondrial membrane's most abundant proteins are those participating in oxidative phosphorylation. In bovine heart mitochondria, they constitute more than 50 % of inner membrane proteins. The inner mitochondrial membrane can be treated with detergents to release five discrete protein complexes (complexes I–V), which together make up the oxidative phosphorylation system (Hatefi, 1985). These are:

Complex I : NADH-ubiquinone oxidoreductase;

Complex II: Succinate-ubiquinone oxidoreductase;

Complex III :ubiquinol-cytochrome *c* oxidoreductase (also known as cytochrome bc_1 complex);

Complex IV: cytochrome *c* oxidase; and

Complex V: ATP synthase (also known as F_0F_1-ATPase).

Complexes I, III, and IV are energy-transducing units that can function with the ATP synthase system to produce ATP. In addition, these complexes or the ATP synthase can generate the driving force for various ion translocators present in the mitochondrial inner membrane (Skulachev, 1992). The molecular mechanisms of biological electron transfer and energy transduction are subjects of extensive research and intense speculation (Chance, 1977; Gray and Winkler, 1996; Larsson, 1998; Mitchell, 1977; Moser and Dutton, 1996; Papa *et al.*, 1995).

The mitochondrion, like the chloroplast, is notable among eukaryotic organelles in possessing its own genome. Some of the polypeptides that make up the respiratory complexes are encoded by the mitochondrial genome (Bonen, 1991; Gray, 1993; Poyton and McEwen, 1996; Taanman, 1999). SDH is not usually encoded by this genome (Ackrell *et al.*, 1992; Hägerhäll, 1997; Hederstedt and Ohnishi, 1992; Scheffler, 1998).

1.2.1. Mechanism of Energy Transduction: The Chemiosmotic Theory

It is now well established that the electron-transport systems associated with the inner mitochondrial membrane, the thylakoid membrane of chloroplasts, and the plasma membrane of respiring and photosynthetic prokaryotes are functionally linked to an ATP-synthesizing system by a common mechanism, called chemiosmotic coupling. The chemiosmotic theory provides a conceptual framework for understanding the mechanism by which energy-generating electron transfer processes can be coupled to those which require energy (Mitchell, 1961; Mitchell, 1969; Mitchell, 1977). It has four basic postulates:

(i) the electron transfer chain is vectorially arranged across a membrane in such a manner that electron transfer is linked to proton translocation across the membrane;

(ii) the ATP synthase is arranged asymmetrically across the same membrane such that the proton gradient can drive ATP synthesis;

(iii) the membrane is impermeable to protons and is osmotically sealed;

(iv) there are proton-linked transporter systems for osmotic stabilization and metabolite transport.

The four fundamental postulates of the chemiosmotic theory have survived years of rigorous experimental scrutiny. The theory describes the central feature of biological energy transduction as the creation of a transmembrane proton electrochemical gradient ($\Delta\mu_{H+}$), also called the protonmotive force (Δp), from redox energies of photosynthesis and respiration. There are two components to $\Delta\mu_{H+}$: one is due to concentration difference of protons across the membrane, ΔpH, and the other, to the difference in electrical potential between the two aqueous phases separated by the membrane, the membrane potential, $\Delta\psi$. In the mitochondrion, redox energy liberated at three sites (complexes I, III, and IV) is coupled to the generation of an electrochemical proton gradient across the inner mitochondrial membrane (Fig. 1.2). This gradient is harnessed by the ATP synthase to drive ATP synthesis and also provides energy for the translocation of ions and other metabolites across the inner mitochondrial membrane (Hatefi, 1985; Rich, 1996; Skulachev, 1992; Trumpower and Gennis, 1994).

While it is generally accepted that redox energy is conserved as a transmembrane electrochemical potential, the molecular mechanism by which redox proteins generate this energized stated is still not fully understood (Papa *et al.*, 1995; Rich, 1996; Wikström *et al.*, 1998). It is only in the case of complex III that the mechanism is reasonably well established (Brandt, 1996; Brandt, 1998; Mitchell, 1976; Trumpower, 1990a; Trumpower, 1990b; Trumpower and Gennis, 1994). This will be discussed in section 1.3.3.

1.3. The Mitochondrial Respiratory Chain

The mitochondrial respiratory chain is a structured array of multisubunit complexes that mediate the vectorial transport of electrons from respiratory substrates in the form of reduced pyridine and flavin nucleotides to molecular oxygen (Fig. 1.3). Typically, the respiratory chain is composed of four discrete multisubunit protein complexes, complexes I–IV, and the ATP synthase, complex V (Hatefi, 1985; Mitchell, 1987; Trumpower and Gennis, 1994; Wikström and Saraste, 1984). Reducing equivalents generated from the oxidation of pyruvate or fatty acids by the Krebs cycle are transferred to the respiratory chain via NADH and $FADH_2$, and finally to molecular oxygen. Ubiquinone (also known as coenzyme Q) is thought to shuttle electrons and/or protons between the primary dehydrogenases, complexes I and II, and complex III (Chazotte and Hackenbrock,

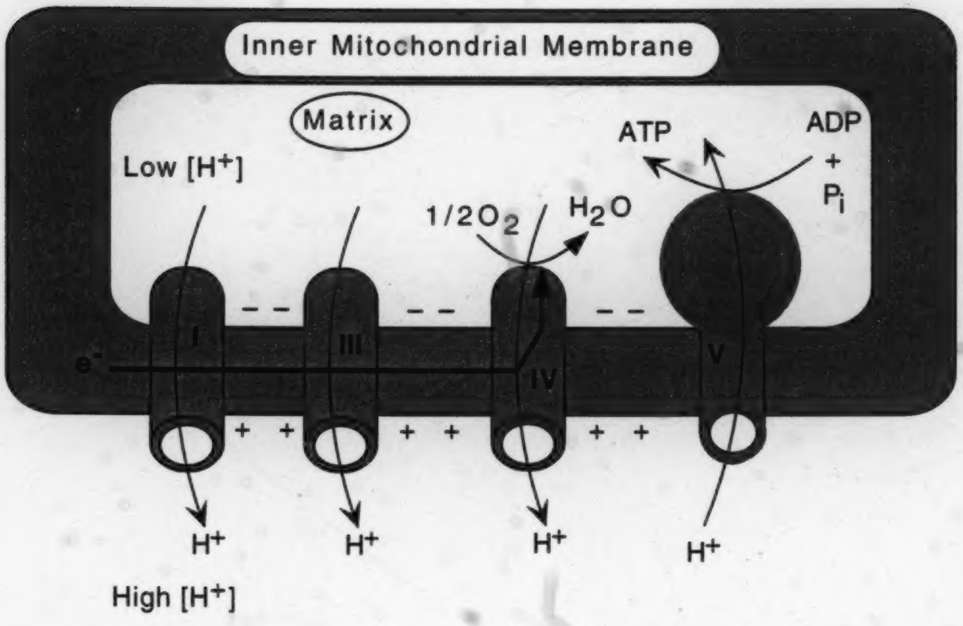
Inner Mitochondrial Membrane
Matrix
Low [H+]
ATP
ADP
+
Pi
1/2O2
H2O
I
III
IV
V
e-
− −
− −
− −
+ +
+ +
+ +
H+
H+
H+
H+
High [H+]

Figure 1.2 Schematic Diagram of the Chemiosmotic Coupling.

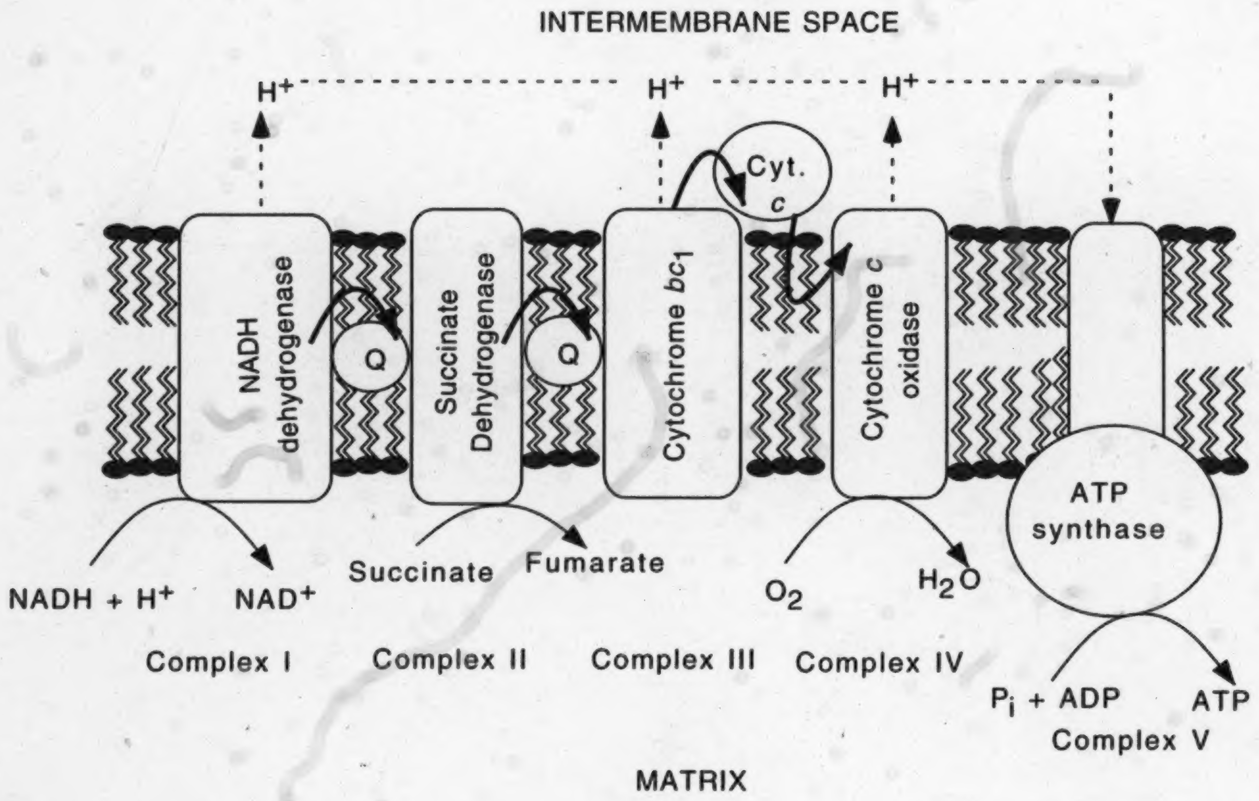

INTERMEMBRANE SPACE
H+
H+
H+
NADH dehydrogenase
Q
Succinate Dehydrogenase
Q
Cytochrome bc_1
Cyt. c
Cytochrome c oxidase
ATP synthase
NADH + H+
NAD+
Succinate
Fumarate
O_2
H_2O
P_i + ADP
ATP
Complex I
Complex II
Complex III
Complex IV
Complex V
MATRIX

Figure 1.3 Schematic Diagram of the Mitochondrial Respiratory Chain

1989; Mitchell, 1987; Trumpower, 1980; Zhu *et al.*, 1982). A similar role is played by cytochrome *c* between complexes III and IV (Gupte and Hackenbrock, 1988a; Gupte and Hackenbrock, 1988b). Fig. 1.4 depicts the linear sequence of electron carriers in the respiratory chain. However, in practice, the electron carriers may not operate in a simple linear sequence. For example, in complex III, electrons may divide between parallel carriers (Brandt, 1996; Brandt, 1998; Trumpower, 1990b). Moreover, electrons may be temporarily stored on components to enable multi-electron reduction to occur, as is the case in the $4e^-$ reduction of molecular oxygen to water in cytochrome *c* oxidase (Karpefors *et al.*, 1998; Rottenberg, 1998; Trumpower and Gennis, 1994).

1.3.1. The Respiratory Chain of S. cerevisiae

The baker's yeast, *S. cerevisiae*, an ascomycete fungus, is a metabolically versatile unicellular eukaryote. It can grow on a wide variety of carbon and nitrogen sources. The carbon sources can be classified into two main categories: fermentable substrates (the saccharides) and nonfermentable substrates (mainly glycerol, ethanol, pyruvate, or acetate). Different metabolic pathways are operative depending on the growth conditions (de Vries and Marres, 1987). Fermentable substrates may be metabolized anaerobically in which case chemical energy is transduced into ATP solely by glycolytic substrate level phosphorylation. However, growth on nonfermentable carbon sources requires the respiratory chain and oxidative phosphorylation for energy transduction. Hence, the organism is facultatively anaerobic; a feature that is exploited in the mutational study of respiratory chain proteins (Brown *et al.*, 1993; Colson, 1993; Tzagoloff and Dieckmann, 1990).

S. cerevisiae has a well-developed respiratory chain, which is very similar to those of mammals (de Vries and Marres, 1987; Trumpower and Gennis, 1994). However, perhaps due to its metabolic versatility, the respiratory chain of *S.*

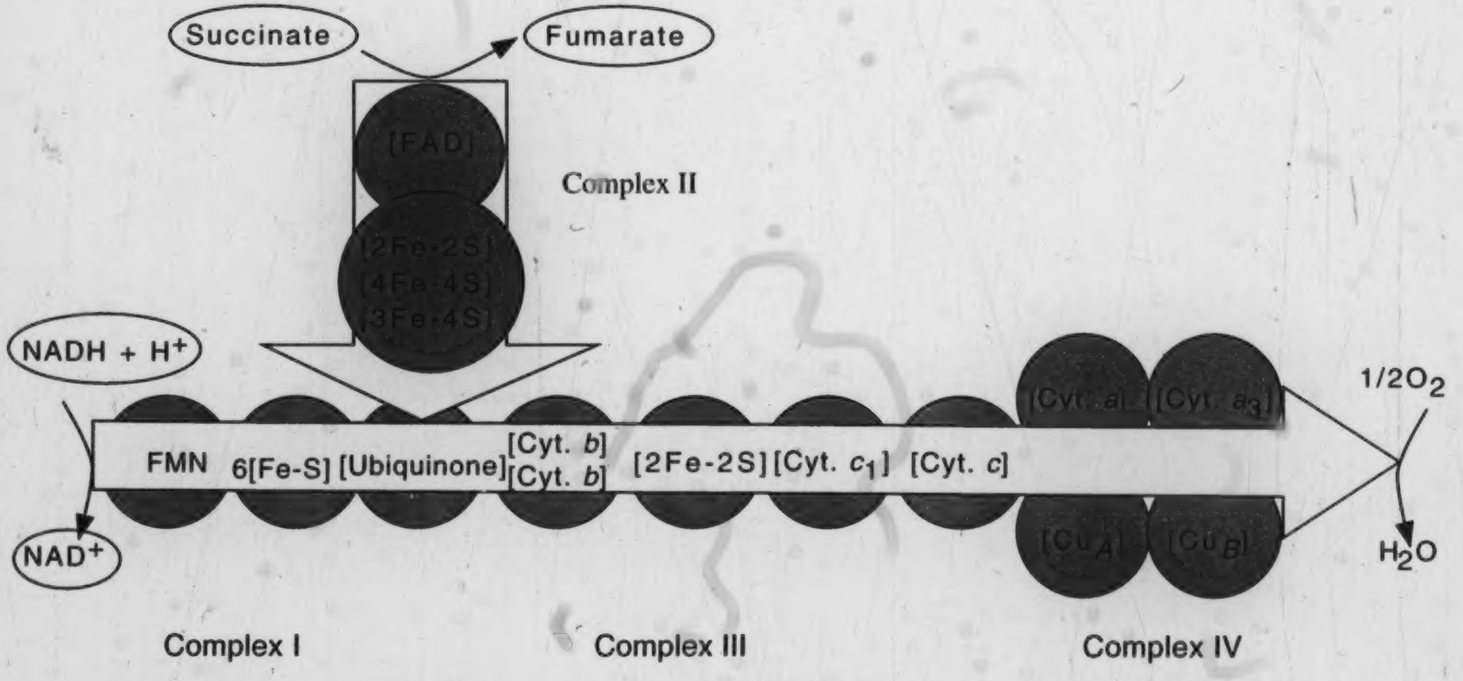

Succinate
Fumarate
[FAD]
Complex II
[2Fe-2S]
[4Fe-4S]
[3Fe-4S]
NADH + H+
NAD+
FMN
6[Fe-S]
[Ubiquinone]
[Cyt. b]
[Cyt. b]
[2Fe-2S]
[Cyt. c1]
[Cyt. c]
[Cyt. a]
[Cyt. a3]
[CuA]
[CuB]
1/2O2
H2O
Complex I
Complex III
Complex IV

Figure 1.4 The Sequence of Electron Transfer in the Mitochondrial Respiratory Chain.

cerevisiae possesses some unique features. Unlike the mammalian respiratory chain, that of *S. cerevisiae* is devoid of complex I. *S. cerevisiae* possesses internal and external NADH dehydrogenases that are distinct from complex I (de Vries *et al.*, 1992; Møller *et al.*, 1993; Moore *et al.*, 1978). They are insensitive to the classical inhibitors of complex I (e.g. rotenone or piericidin) and they are not coupling sites. The external NADH dehydrogenase is associated with the inner mitochondrial membrane and has an externally facing NADH binding site that can serve to oxidize cytosolic NADH. On the other hand, the internal NADH dehydrogenase faces the mitochondrial matrix. It oxidizes internally generated NADH produced mainly by the operation of the matrix-localized Krebs cycle. *S. cerevisiae* is also unique in that it can bypass complex III and transfer electrons directly from L-lactate to cytochrome *c*. This reaction is catalyzed by an L-lactate:cytochrome *c* oxidoreductase, a flavohemoprotein containing cytochrome b_2 and FMN, which is located in the intermembrane space (Lederer, 1991). Electrons from L-lactate are transferred via cytochrome b_2 to cytochrome *c* of the respiratory chain, which in turn donates the electrons to cytochrome oxidase.

1.3.2. Structure and Function of the Energy Transducing Units

Due to their importance in energy transduction, the structural and mechanistic properties of complexes I, III, and IV have been intensively investigated. The proteins comprise multiple subunits and redox-active prosthetic groups. High-resolution crystal structures of complexes III and IV are now available, significantly enhancing our ability to define the mechanistic properties of these proteins at the molecular level. Nevertheless, significant gaps still exist in our understanding of many mechanistic aspects of electron transfer and proton translocation. In this section, only a cursory survey of the structure and mechanism of complexes I and IV will be presented. Complex III, which interacts with quinone substrates at two distinct binding sites, may share some mechanistic properties with SDH. The pathway of intramolecular electron transfer and the mechanism of proton pumping is well established in this complex (Mitchell, 1976; Trumpower, 1990a; Trumpower, 1990b; Trumpower and Gennis, 1994). As such, its structural and mechanistic properties will be discussed in some detail in section 1.3.4.

1.3.2.1. Complex I

The NADH-ubiquinone oxidoreductase segment is the most structurally complicated and the least understood energy-coupling device in the electron-transport chain of most organisms. This enzyme is absent in *S. cerevisiae* (see section 1.3.1). Many fundamental aspects such as the number of subunits, the quaternary structure, and the number of iron-sulfur clusters remain controversial (Fearnley and Walker, 1993; Finel, 1993; Finel, 1998; Friedrich *et al.*, 1995; Friedrich *et al.*, 1997; Vinogradov, 1993; Weiss *et al.*, 1991). To date, only low-resolution structures are available for the enzymes isolated from *Neurospora crassa* (Hofhaus *et al.*, 1991) and from *E. coli* (Guénebaut *et al.*, 1998). The smallest form of the enzyme has so far been found in *E. coli* and comprises 14 subunits, one non-covalent FMN, and up to nine iron-sulfur clusters. The eukaryotic enzyme contains up to 29 additional polypeptides whose functions remain unclear (Fearnley and Walker, 1993). Some of the eukaryotic complex I subunits are mitochondrially encoded (Friedrich *et al.*, 1995; Walker, 1992; Weiss *et al.*, 1991). The gross three-dimensional structures of the bacterial (Guénebaut *et al.*, 1998) and the mitochondrial (Hofhaus *et al.*, 1991) complexes show that the subunits are arranged into the same L-shaped structure. This structure consists of two elongated protein domains: a peripheral arm, which protrudes into the matrix or the cytoplasm, and an integral arm, which is buried in the inner mitochondrial membrane or the bacterial plasma membrane. The peripheral arm contains FMN and iron-sulfur clusters, and it functions as an NADH dehydrogenase. On the other hand, the integral arm, which comprises the hydrophobic subunits, is thought to be involved in ubiquinone reduction and proton translocation (Friedrich *et al.*, 1998; Friedrich *et al.*, 1993).

Complex I catalyzes electron transfer from NADH to ubiquinone coupled to vectorial proton translocation. The classical inhibitor of this reaction is rotenone (Singer and Ramsay, 1992). However, a plethora of structurally different natural and synthetic compounds are now known to inhibit this reaction (Degli Esposti, 1998; Friedrich *et al.*, 1993; Miyoshi, 1998; Singer and Ramsay, 1992). These inhibitors act at or close to a ubiquinone reduction site, and have been instrumental in delineating the quinone-binding sites (Lenaz, 1998). Consequently, it is generally accepted that complex I has multiple quinone-binding sites (Degli Esposti, 1998). Most models of proton translocation require a minimum of two quinone-binding sites (Degli Esposti and Ghelli, 1994; Ragan, 1990; Vinogradov, 1993; Weiss and Friedrich, 1991).

Despite the substantial progress made in defining the overall structural organization, in determining the subunit structure and composition, and in characterizing the iron-sulfur clusters of complex I, little is known about the mechanism of proton translocation. Models for coupled proton translocation are at best speculative (Krishnamoorthy and Hinkle, 1988; Ragan, 1987; Vinogradov, 1993). This is due to the complex structure of the enzyme, the complexity of its redox components, and the uncertainty in numbers and positions of redox centers. The available observations seem to favor a simple mechanistic variation of the Q-cycle (Brandt, 1997; Dutton *et al.*, 1998), which is well established for complex III (see section 1.3.3.2). Nevertheless, the available structural and functional information is insufficient to evaluate the models.

1.3.2.2. Complex IV

The cytochrome *c* oxidase segment catalyses the terminal act of respiration by reducing molecular oxygen to H_2O. This electrogenic reaction is coupled to proton translocation, generating a Δp. Cytochrome *c* oxidases are members of the superfamily of heme/copper-containing terminal oxidases, which include the bacterial cytochrome *bo* complex (Calhoun *et al.*, 1994; Capaldi, 1990; Saraste, 1990; Trumpower and Gennis, 1994). The structure of the mitochondrial enzyme is very complicated, comprising 7–13 non-equivalent subunits, the largest three (subunits I–III) of which are encoded by the mitochondrial genome. These three subunits constitute the minimal catalytic core of the enzyme. In contrast, the bacterial enzymes are simpler in composition, and yet can carry out all known functions of the enzyme. For example, the *Paracoccus denitrificans* enzyme comprises three core polypeptides, subunits I—III, and a small non-conserved polypeptide, subunit IV (Michel *et al.*, 1998). Generally, subunits I and II contain the redox-active centers, consisting of two copper centers, designated Cu_A and Cu_B, and two spectrally distinct, though chemically identical, heme *a* species, *a* and a_3. One copper ion at the Cu_B-center, together with heme a_3, forms a copper-heme binuclear center, which is the catalytic site for O_2 reduction. Similarly, two copper ions at the Cu_A-center form a copper-copper binuclear complex, the entry port of electrons arriving from cytochrome *c*. Heme *a* forms electron conduit between the two binuclear centers.

As a consequence of their central position in energy transduction, the cytochrome *c* oxidases have been intensively studied using biochemical, genetic, spectroscopic, and crystallographic tools. The structures of cytochrome *c* oxidases from mammalian (Tsukihara *et al.*, 1995; Tsukihara *et al.*, 1996) and bacterial (Iwata *et al.*, 1995; Ostermeier *et al.*, 1997) sources have been resolved at atomic levels by x-ray crystallography. The core subunits (subunits I—III) of the two crystal structures have nearly identical structures. Subunit I, which contains 12 transmembrane helices, harbors the two heme groups, heme *a* (a low-spin heme) and heme a_3 (a high-spin heme). On the other hand, subunit II consists of 2 transmembrane helices interacting with subunit I and a large C-terminal membrane-extrinsic domain containing the Cu_A-center. The crystal structures provide details of the redox groups, including their relative distances, orientations, ligands, and the intervening amino acid residues. This makes it possible to gain a deeper insight into the intramolecular electron transfer pathway. The Cu_A-center functions as a one-electron donor/acceptor and is the entry port of electrons arriving from cytochrome *c*. Heme *a* accepts electrons from Cu_A and delivers them to the second binuclear center, heme a_3-Cu_B, which reduces molecular oxygen to H_2O.

Despite the progress made in understanding the structural and functional aspects of cytochrome *c* oxidase, the mechanism by which electron transfer is coupled to proton translocation is poorly understood (Karpefors *et al.*, 1998; Michel *et al.*, 1998; Rottenberg, 1998; Wikström *et al.*, 1998).

1.3.3. Complex III

Complex III is the best understood among the proton translocating respiratory chain complexes of mitochondria. It is a member of the superfamily of *bc*-type complexes that includes the cytochrome *bf* complexes found in chloroplasts, algae, and some gram-positive bacteria (Bechmann *et al.*, 1992; Knaff, 1993; Trumpower, 1990a; Trumpower and Gennis, 1994). The general function of the complex is electron transfer between two mobile redox carriers, for example ubiquinol (QH_2) and cytochrome *c* in mitochondria. This reaction is coupled to transmembrane proton translocation, thus generating a protonmotive force. Electron transfer in complex III is carried out by 5 redox-active components: two *b*-type cytochromes, cytochrome c_1, a high potential binuclear iron-sulfur cluster, and ubiquinone. The protonmotive Q-cycle has been well established as the mechanism of intramolecular electron transport and proton translocation in this enzyme (Mitchell, 1976; Trumpower, 1990a; Trumpower, 1990b; Trumpower and Gennis, 1994).

1.3.3.1. Structure

The minimal catalytic core of complex III comprises 3 redox proteins: cytochrome *b*, cytochrome c_1, and a Rieske-type iron-sulfur protein (ISP). This core structure exhibits a high degree of evolutionary conservation across species. Some bacterial bc_1 complexes consist of only the core structure (Trumpower, 1990a; Trumpower and Gennis, 1994). Variable numbers of additional non-redox subunits (termed supernumerary subunits) are present, especially in the mitochondrial enzymes. For example, 8 additional polypeptides are found in the bovine complex (Schägger *et al.*, 1986) and six in the complex from *S. cerevisiae* (Trumpower, 1990a). These supernumerary subunits are not essential for catalysis, as evidenced by the fact that no significant functional differences have been found in the more complex enzymes as compared to the bacterial enzyme in which only the three redox polypeptides are present (Robertson *et al.*, 1993).

Recently, the molecular structures of complex III from avian (Zhang *et al.*, 1998) and mammalian (Iwata *et al.*, 1998; Kim *et al.*, 1998; Xia *et al.*, 1997; Yu *et al.*, 1998; Zhang *et al.*, 1998) sources have been solved at high resolution. The structures confirm many known structural and functional properties of the enzyme (Degli Esposti *et al.*, 1993; Link *et al.*, 1993; Trumpower, 1990b; Trumpower and Gennis, 1994). Complex III exists in the crystal as a closely interacting pear-shaped dimer, suggesting that the dimer is a functional unit. Each monomer has 13 membrane-spanning helices, spanning a membrane which is ~42 Å thick. More than half of the molecular mass of the complex extends 75 Å from the membrane-spanning region into the mitochondrial matrix. Similarly, the major parts of cytochrome c_1 and the ISP extend 38 Å into the intermembrane space. Each of these subunits contains a single terminal transmembrane helix, which anchors them to the membrane.

The cytochrome *b* subunit, which is the only subunit encoded by the mitochondrial genome, consists of 8 transmembrane helices and 4 horizontal helices on the intermembrane space side. There are two *b*-type hemes that are ligated by two pairs of histidine residues on opposite sides of the second and third membrane-spanning helices. The low potential heme, b_L (b_{566}, $E_{m,7}$ = -40 mV) is located near the positive outer surface while the high potential heme, b_H (b_{562}, $E_{m,7}$ = +40 mV) is located near the negative inner surface. In addition to hemes, the subunit also interacts with quinols via at least 2 quinone-binding sites, the Q_o and Q_i sites (quinone oxidation and reduction sites, respectively). The most powerful evidence for the existence of 2 quinone-binding sites comes from inhibitor studies showing that: (i) the electron-transfer reactions occurring at either of the two sites can be independently inhibited; and (ii) mutations leading to inhibitor resistance map to opposite sides of the membrane (Colson, 1993; Link *et al.*, 1993). Crystallographic analysis of the bc_1-inhibitor complexes has revealed two separate inhibitor binding pockets, thought to be equivalent to the Q_o and Q_i sites (Iwata *et al.*, 1998; Yu *et al.*, 1998; Zhang *et al.*, 1998).

1.3.3.2. Intramolecular Electron Transfer and Energy Conservation

On the basis of functional data, the proton-motive Q-cycle is well favored as the mechanism of intramolecular electron transfer and proton translocation (Mitchell, 1976; Trumpower, 1990a; Trumpower, 1990b; Trumpower and Gennis, 1994). According to this model (Fig. 1.5), two quinone sites are asymmetrically arranged on opposite sides of the membrane, with the di-heme forming an electron conduit between them. The protonmotive Q-cycle is initiated by the oxidation of ubiquinol at Q_o leading to the release of two protons into the intermembrane space and the release of two electrons, which bifurcate in different directions. One

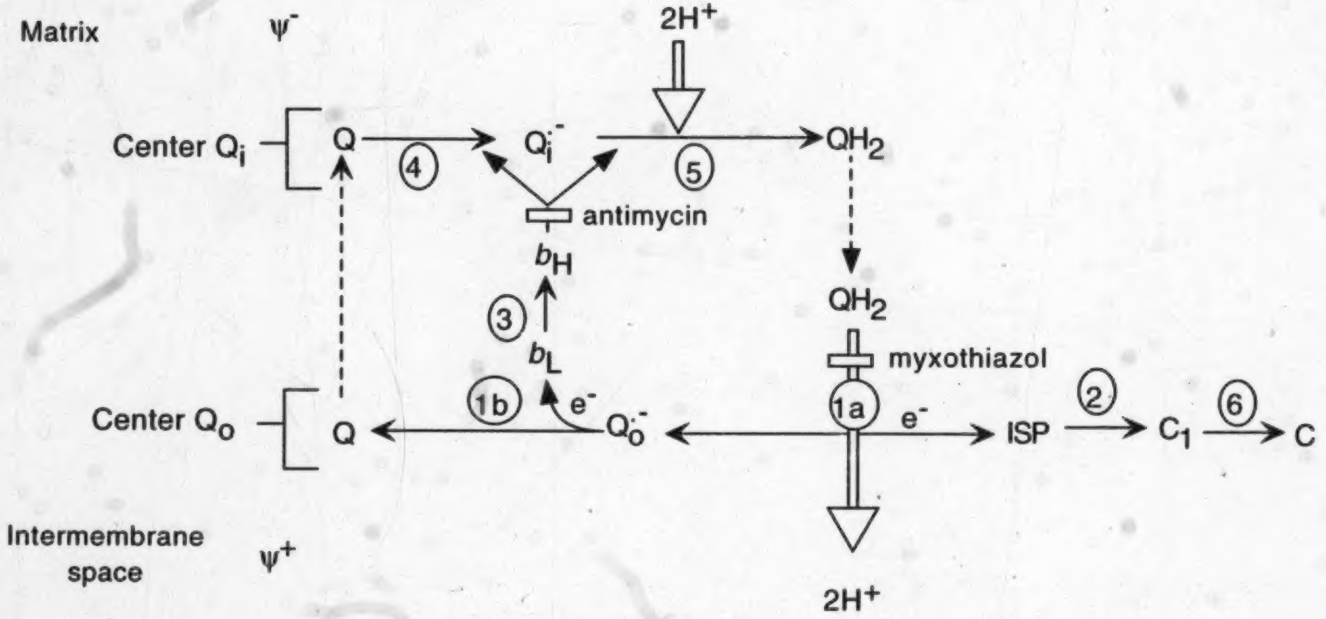
Matrix
ψ⁻
2H⁺
Center Qi
Q
4
Qi˙⁻
5
QH2
antimycin
bH
3
bL
QH2
myxothiazol
Center Qo
Q
1b
e⁻
Qo˙⁻
1a
e⁻
ISP
2
C1
6
C
Intermembrane space
ψ⁺
2H⁺

Figure 1.5 The Protonmotive Q Cycle Mechanism of Electron Transfer Through the Cytochrome *bc*$_1$ Complex.

The scheme shows the bifurcated, cyclic pathway of electron transfer from ubiquinol (QH_2) to cytochrome *c* (C) through the four redox centers of the cytochrome *bc*$_1$ complex. The circled numbers designate the sequence of electron transfer reactions. Dashed arrows represent movement of ubiquinol and ubiquinone (Q) between the site where ubiquinol is oxidized at the positive side of the membrane ("Center Q_o") and the site where ubiquinone and ubisemiquinone are reduced at the negative side of the membrane ("Center Q_i"). Open bars indicate sites of action of Q_i and Q_o inhibitors. ISP, iron-sulfur protein; b_L and b_H, low and high potential heme, respectively.

electron is transferred to cytochrome *c* via the Rieske iron-sulfur protein and cytochrome c_1. The other electron is transferred across the membrane via cytochromes b_L and b_H to ubiquinone bound at Q_i. The ubisemiquinone thus formed at Q_i remains protein-bound until a second ubiquinol is oxidized at Q_o and a second electron is transferred to Q_i to complete the reduction of ubiquinol. The two protons required for the formation of ubiquinol are taken up from the matrix space. One complete Q-cycle requires two redox turns at Q_o and two successive electron transfers to Q_i. The Q_o and Q_i sites are not equivalent. EPR studies have shown that only the Q_i site binds a semiquinone tightly, while a semiquinone has only a transient existence at Q_o (de Vries *et al.*, 1981; de Vries *et al.*, 1980; Meinhardt *et al.*, 1987; Ohnishi and Trumpower, 1980). The 2-step reduction of quinone to ubisemiquinone and ubiquinol at Q_i is reminiscent of the gated reduction of ubiquinone by the photosynthetic reaction center (see section 1.6.3). A similar mechanism has also been proposed for Q-mediated electron transport in SDH (section 1.6.2).

The Q-cycle is strongly supported by many lines of experimentation. These include: evidence for the oxidant-induced reduction of cytochrome *b* (Erecinska *et al.*, 1972; Wikström and Berden, 1972); the existence of antimycin-sensitive and -insensitive transient ubisemiquinone radicals (Ohnishi and Trumpower, 1980; Yu *et al.*, 1978); the ejection of 2 protons per electron transferred in the bc_1 complexes from many sources (Brand *et al.*, 1976; Mitchell *et al.*, 1986; West, 1986); and the binding of specific inhibitors at the Q_i and Q_o sites (Link *et al.*, 1993). Finally, the emerging x-ray crystal structures support the protonmotive Q-cycle as the overall electron- and proton-pathway within the bc_1 complex (Brandt, 1998; Crofts and Berry, 1998).

1.3.3.3. Electron Transfer at the Q_o Site

The bifurcation of electron flow into high and low potential pathways at the Q_o site is critical for the energy conservation scheme described by the Q-cycle. This step is obligatory for the cyclical electron transfer to the Q_i site, which results in vectorial proton translocation. How this electron bifurcation is achieved is poorly understood (Brandt, 1998; Crofts and Berry, 1998; Yu *et al.*, 1998). Information accruing from the crystal structures suggests the existence of two transient quinone-binding subsites within the Q_o pocket (Iwata *et al.*, 1998; Xia *et al.*, 1997; Zhang *et al.*, 1998). In addition, binding of two quinone molecules per Q_o site in the bacterial bc_1 complex has been indicated by EPR characteristics of the iron-sulfur cluster (Ding *et al.*, 1995; Ding *et al.*, 1992). Similarly, studies of the mammalian bc_1 complex with the noncompetitive Q_o site inhibitors, E-β-methoxyacrylates and stigmatellin, show the existence of two distinct inhibitor binding sites within the Q_o pocket (Brandt *et al.*, 1991; Brandt *et al.*, 1988). Quite recently, it has been demonstrated that the fully reduced bc_1 complex has two binding sites for E-β-methoxyacrylate inhibitors at Q_o (Brandt and Djafarzadeh-Andabili, 1997). These data have led to the speculation that there may be two quinone-binding sites within the Q_o pocket (Brandt, 1996; Ding *et al.*, 1995; Ding *et al.*, 1992). One of these putative sites, denoted P1, is proximal to ISP subunit while the other site, denoted P2, is proximal to the low potential heme, b_L. The P1 site has higher affinity for QH_2 while the P2 site has higher affinity for ubisemiquinone. A model for an electron transfer event consistent with the available data is schematized in Fig. 1.6. One implication of the model is the movement of the ISP subunit, which facilitates electron movement between P1 and cytochrome c_1. This has been confirmed by the molecular structure of the bc_1 complex. The extramembrane domain of the iron-sulfur protein can take up different positions in different crystals, suggesting a novel mechanism for electron transfer through domain movement (Crofts and Berry, 1998; Iwata *et al.*, 1998;

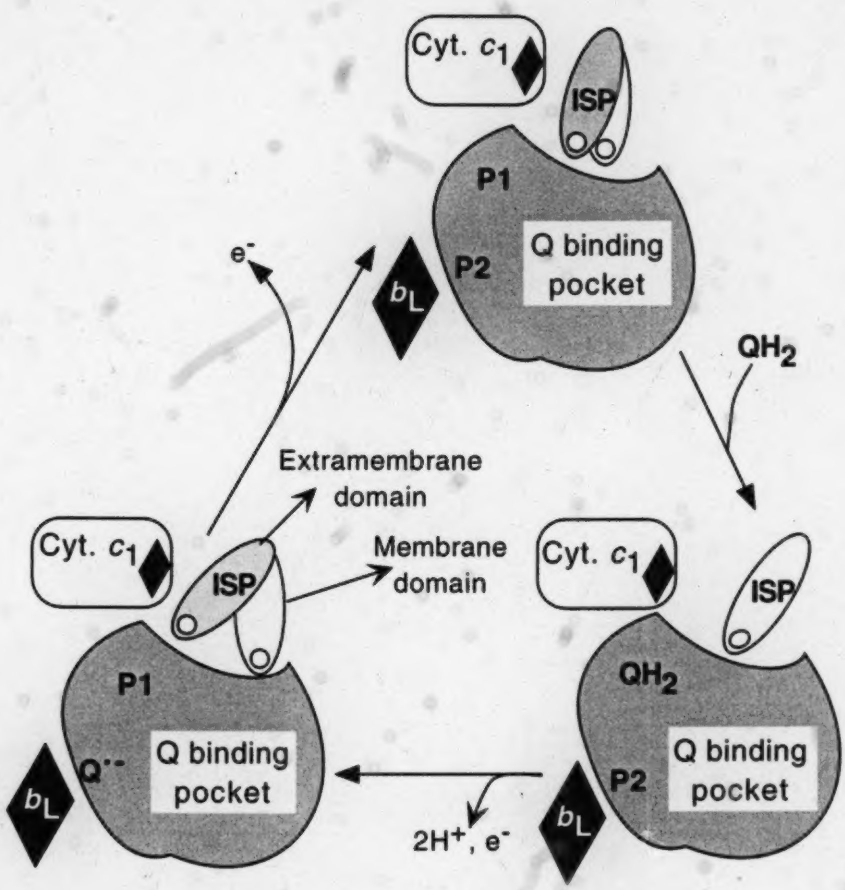
Cyt. c_1
ISP
P1
Q binding pocket
P2
b_L
e^-
QH_2
Extramembrane domain
Membrane domain
Cyt. c_1
ISP
P1
$Q^{\cdot -}$
Q binding pocket
b_L
Cyt. c_1
ISP
QH_2
Q binding pocket
P2
b_L
$2H^+$, e^-

Figure 1.6 **Schematic Diagram of the Electron Transfer Events at the Qo Site.**

When a ubiquinonol molecule (QH_2) binds to the Qo pocket, it first occupies the P1 site, stabilizing ISP presumably by a conformational change in cytochrome *b*. The stabilization of the ISP facilitates the transfer of the first electron from ubiquinol to ISP and releases two protons. The resulting ubisemiquinone ($Q^{\cdot -}$) is then switched to the second binding site, P2. This switch in position and the subsequent electron transfer from b_L to b_H may cause a conformational change in cytochrome *b* and thus, result in the release of the reduced ISP to a second position near cytochrome c_1 (cyt. c1) to deliver its electron. The abbreviations used are: ISP, iron-sulfur protein; P1 and P2, quinone-binding sites proximal to ISP and heme b_L, respectively.

Zhang *et al.*, 1998). The model also predicts the existence of a ubisemiquinone radical at P2. However, this prediction has yet to be experimentally verified.

1.4. The SDH and FRD Complexes

Succinate dehydrogenase and fumarate reductase (FRD) are fundamentally similar in structure and function (Ackrell *et al.*, 1992; Cole *et al.*, 1985; Hägerhäll, 1997; Hederstedt and Ohnishi, 1992; Ohnishi, 1987; Van Hellemond and Tielens, 1994). They belong to a superfamily of succinate:quinone oxidoreductases, SQO (E.C.1.3.5.1). The hallmark of this superfamily is the possession of a heterodimeric catalytic domain containing covalent FAD and 3 iron-sulfur clusters, which can catalyze the reversible oxidoreduction of succinate and fumarate. This catalytic domain is anchored to the membrane by a heterodimeric or in some cases, a monomeric hydrophobic domain that interacts with quinone and/or heme. SDH and FRD will be used to denote the respective intact enzymes comprising both the catalytic and membrane domains, while succinate:quinone oxidoreductase will be used when referring to both enzymes.

Despite the fact that SDH was discovered about 10 decades ago (Hatefi, 1985), our understanding of this enzyme is incomplete. Some of the aspects of this enzyme that are not fully understood are its biogenesis, its structure and its mechanism of intramolecular electron transfer. Bovine heart complex II has been the most extensively studied, but this system is not easily amenable to genetic manipulation. As such, attention is now turning to microbial systems that can be genetically modified to answer questions of structure and function that are not possible with the mammalian system (Ackrell *et al.*, 1992; Hägerhäll, 1997; Hederstedt, 1998; Hederstedt and Ohnishi, 1992; Van Hellemond and Tielens, 1994).

1.4.1. Structural and Functional Properties of SDH and FRD

SDH is an enzyme of the Krebs cycle (Fig. 1.7), a central metabolic pathway that is found in all aerobic organisms. The Krebs cycle has a dual role in aerobically respiring cells. It has an oxidative function in energy metabolism and it also provides intermediates for anabolic pathways. SDH catalyzes the oxidation of succinate to fumarate. Electrons released in the process are transferred to the respiratory chain via quinone (Hatefi, 1985; Mitchell, 1987; Trumpower and Gennis, 1994; Wikström and Saraste, 1984). Thus, SDH is unique in linking the Krebs cycle with the respiratory chain, suggesting that it may play a key regulatory role in energy metabolism (Escobar Galvis *et al.*, 1998).

On the other hand, FRD catalyzes the reduction of fumarate to succinate coupled to the oxidation of quinol, the reverse of the reaction catalyzed by SDH. It is a key enzyme for anaerobic respiration with fumarate as the terminal electron acceptor. In *E. coli*, where the enzyme has been intensively studied, fumarate by virtue of its relatively high redox potential ($E^{\circ\prime}$ +30 mV), can serve as terminal electron acceptor in the oxidation of glycerol-3-phosphate, lactate, formate, hydrogen, or dihydroorotate (Cole *et al.*, 1985; Van Hellemond and Tielens, 1994). This occurs via a membrane-associated electron transport chain composed of a primary dehydrogenase, a *b*-type cytochrome, lipid soluble quinone, and fumarate reductase (Cole *et al.*, 1985). FRD has also been found in many facultative anaerobic eukaryotes such as protozoa, parasitic helminths, green algae, and some marine organisms where fumarate reduction may be necessary for maintaining a redox balance during anoxia (Tielens and Van Hellemond, 1998). The reduction of fumarate is linked to a shortened electron-transport chain (Fig. 1.8). Soluble FRDs, which differ structurally from membrane-attached FRD and SDH enzymes, have been found in many organisms including *S. cerevisiae* (Arikawa *et al.*, 1998; Enomoto *et al.*, 1996; Muratsubaki and Enomoto, 1998).

Figure 1.7 The Krebs Cycle

The enzymes are: 1, Succinate dehydrogenase; 2, Fumarase; 3, Malate dehydrogenase; 4, Citrate synthase; 5, Aconitase; 6, Isocitrate dehydrogenase; 7, α-ketoglutarate dehydrogenase; 8, Succinyl-CoA synthetase.

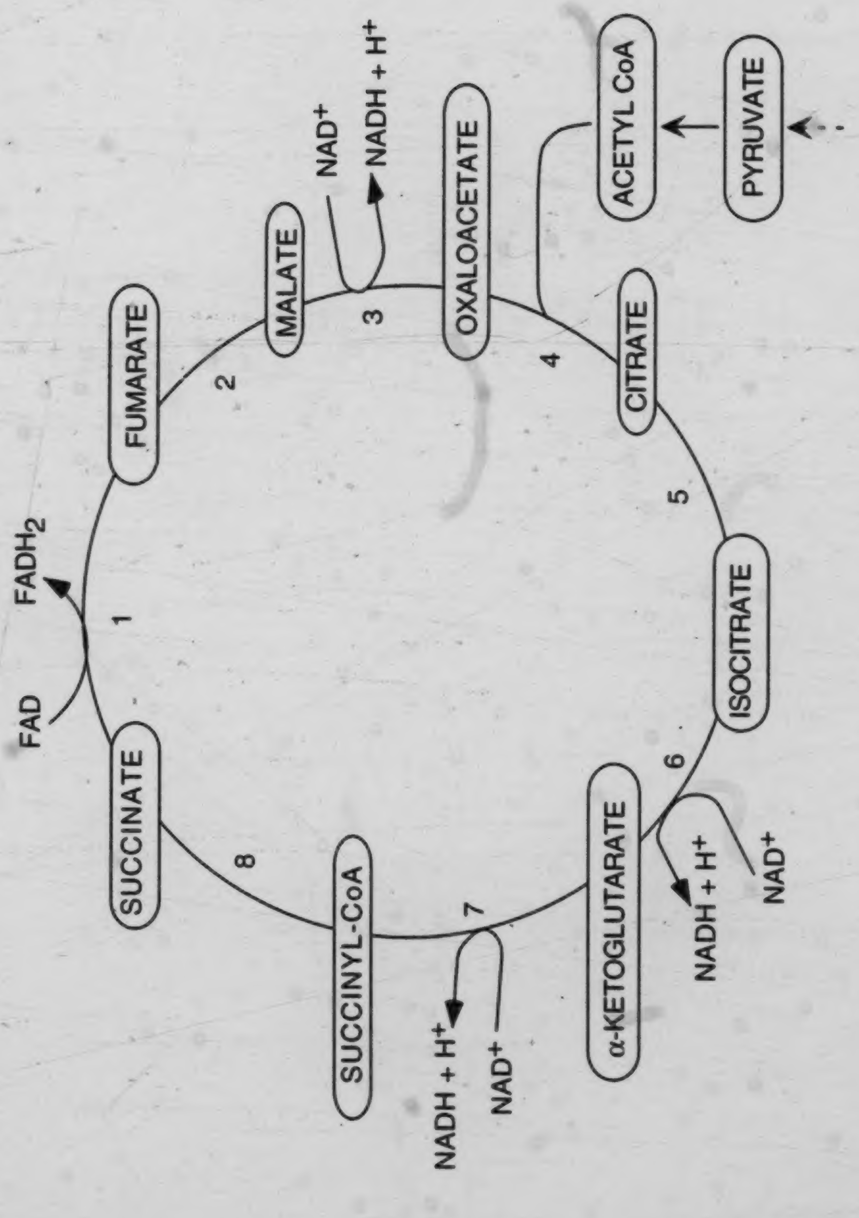
PYRUVATE
ACETYL CoA
OXALOACETATE
CITRATE
ISOCITRATE
α-KETOGLUTARATE
SUCCINYL-CoA
SUCCINATE
FUMARATE
MALATE
1
2
3
4
5
6
7
8
FAD
$FADH_2$
NAD^+
$NADH + H^+$
NAD^+
$NADH + H^+$
NAD^+
$NADH + H^+$

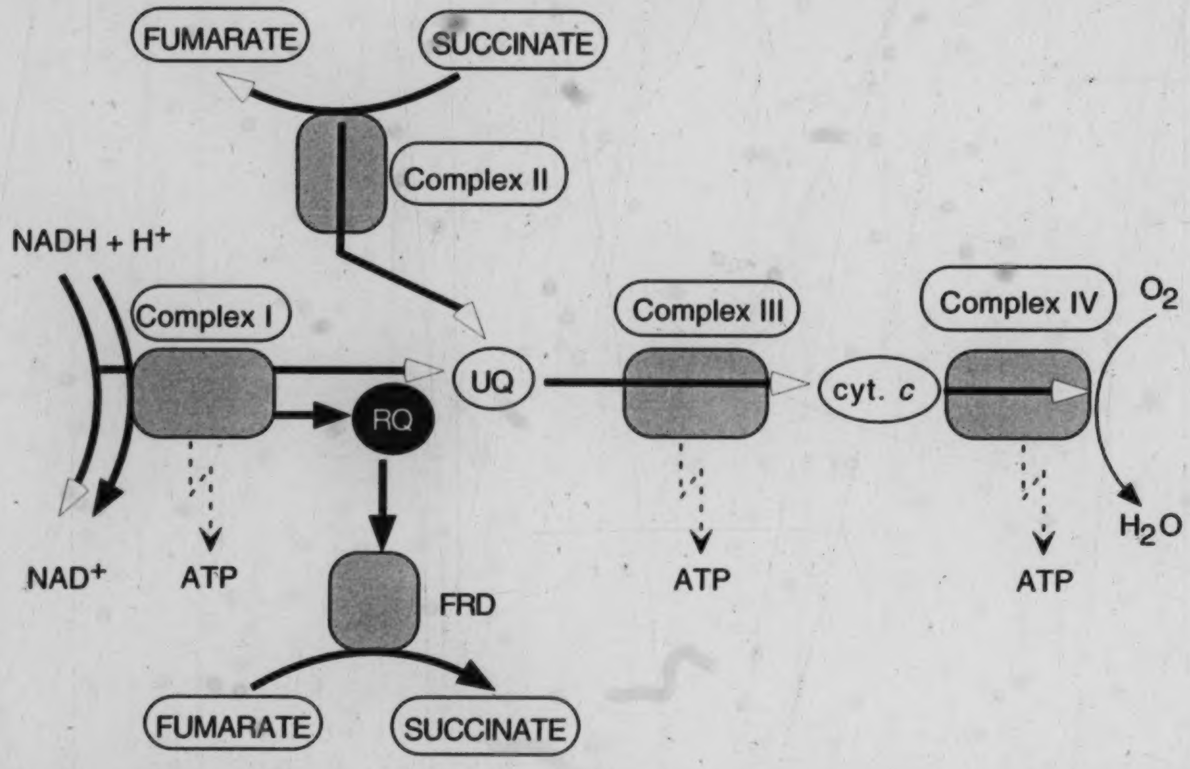
FUMARATE
SUCCINATE
Complex II
NADH + H+
Complex I
UQ
RQ
Complex III
cyt. c
Complex IV
O2
H2O
NAD+
ATP
ATP
ATP
FRD
FUMARATE
SUCCINATE

Figure 1.8 Schematic Representation of the Electron Transport Chain in Facultative Anaerobic Eukaryotes.

Open arrows indicate electron flow to oxygen during aerobic respiration, while solid arrows indicate electron flow during fumarate reduction. Sites of ATP synthesis are indicated by arrows with broken lines. The abbreviations used are: cyt. c, cytochrome *c*; FRD, fumarate reductase; RQ, rhodoquinone; UQ, ubiquinone.

The functional similarity of these enzymes is illustrated by the fact that SDH and FRD can catalyze their respective reverse reactions *in vitro*. This similarity has been further demonstrated in the *E. coli* enzymes *in vivo*. The *E. coli* FRD, when overexpressed aerobically, can function as an SDH *in vivo* (Cecchini *et al.*, 1986a; Guest, 1981; Sucheta *et al.*, 1993), although the SDH activity of the FRD complex is drastically reduced compared to its FRD activity. Recently, anaerobically overexpressed SDH has been shown to function as a FRD in *E. coli* (Maklashina *et al.*, 1998). Furthermore, SDHs from *Desulfobulbus elongatus* (Samain *et al.*, 1987), *A. suum* (Kita *et al.*, 1988; Saruta *et al.*, 1995), and *Haemonchus contortus* (Roos and Tielens, 1994) have been shown to function as both SDH and FRD *in vivo*. The *A. suum* and the *H. contortus* SDHs have the remarkable ability to switch between SDH and FRD at different developmental stages.

Apart from their functional similarity, SDH and FRD are also remarkably similar in structure. SDH is typically composed of 3–4 nonequivalent subunits. These subunits are designated Sdh1p, Sdh2p, Sdh3p, and Sdh4p, in order of decreasing molecular weights in eukaryotes. Analogous subunits from prokaryotes are designated SdhA–SdhD. In the facultative anaerobe *Bacillus subtilis* and the strict aerobe, *Neurospora crassa*, SDH is composed of 3 subunits (Hägerhäll, 1997). Purified SDHs have been shown to consist of 2 reconstitutively active domains, the catalytic and the membrane anchoring domains (Cecchini *et al.*, 1986a; Hatefi and Galante, 1980; Yang *et al.*, 1997). Sdh1p (also referred to as the flavoprotein subunit or Fp; 64–79 kDa) and Sdh2p (also referred to as the iron-sulfur protein subunit or Ip; 27–31 kDa) constitute the catalytic domain exposed to the mitochondrial matrix or to the prokaryotic cytoplasm. The catalytic domain is anchored to the inner mitochondrial membrane or the prokaryotic plasma membrane by a hydrophobic domain comprising the Sdh3p/SdhC and the Sdh4p/SdhD subunits (13–16 kDa and 11–16 kDa respectively). In addition, the hydrophobic domain interacts with quinone and, in some cases, with *b*-type heme (Hägerhäll, 1997; Hederstedt, 1998). The catalytic domain is capable of catalyzing the oxidation of succinate in the presence of artificial electron acceptors such as ferricyanide and PMS. However, the reduction of quinone and quinone analogs requires the presence of a functional hydrophobic domain (Trumpower and Katki, 1979).

This basic structure of SDH (subunit organization, redox cofactors structural organization, and localization) is also found in membrane-bound FRDs (Ackrell *et al.*, 1992; Cole *et al.*, 1985; Hederstedt and Ohnishi, 1992; Van Hellemond and Tielens, 1994). Like SDH, tetrameric FRD is composed of two distinct domains. Analogous FRD subunits are designated FrdA–FrdD, with FrdA and FrdB comprising the catalytic domain and FrdC and FrdD, the hydrophobic domain. *Wolinella succinogenes* and *B. macerans* FRD are each composed of three subunits. The hydrophobic domain contains a single protein of approximately twice the size of the individual subunits in dimeric hydrophobic domains. The catalytic domain is exposed to the cytoplasm, which is topologically analogous to the mitochondrial matrix.

Despite their structural and functional similarities, SDH and FRD are distinct enzymes with distinct physiological roles. SDH is especially adapted for aerobic respiration while FRD is adapted for anaerobic respiration. In *E. coli*, for instance, FRD and SDH are differentially expressed depending on environmental conditions, mainly the availability of O_2 and fumarate (Cole *et al.*, 1985; Van Hellemond and Tielens, 1994). Similarly, during anaerobic growth of parasitic helminths, the synthesis of SDH is repressed and fumarate reductase is induced in the presence of fumarate (Tielens and Van Hellemond, 1998). Another difference is indicated by the thermodynamic properties of the quinone substrates with which the enzymes interact. Generally, FRD interacts with quinone having a lower standard redox potential like menaquinone ($E^{\circ\prime} = -70$ mV), whereas SDH complexes interact with quinones having higher standard redox potentials like ubiquinone ($E^{o\prime}$ = +100). Eukaryotic fumarate reductases are known to interact with rhodoquinone (a benzoquinone), whereas most prokaryotic fumarate reductases interact with the napthtoquinones, menaquinone or demethylmenaquinone (Hägerhäll, 1997; Tielens and Van Hellemond, 1998; Van Hellemond and Tielens, 1994). Hence, *in vivo*, the forward reactions are thermodynamically favored, despite the fact that SDH and FRD can catalyze the reverse reactions *in vitro*. In addition, the mechanism of the reverse reaction catalyzed by each enzyme is kinetically different as determined in cyclic voltammetry experiments (Heering *et al.*, 1997; Sucheta *et al.*, 1992; Sucheta *et al.*, 1993). Catalysis in the direction of fumarate reduction by SDH is controlled by a potential gating effect, with activity decreasing as the electrochemical driving force increases. The phenomenon has been called a 'diode-like' behavior and is not observed in FRD.

1.4.2. Molecular Biology of SDH and FRD

The structural genes encoding SDH and FRD, designated *sdh* and *frd* respectively, from many prokaryotic and eukaryotic sources have been isolated and sequenced (Ackrell *et al.*, 1992; Cole *et al.*, 1985; Hägerhäll, 1997; Hederstedt and Ohnishi, 1992; Scheffler, 1998; Van Hellemond and Tielens, 1994). In most prokaryotes, the genes encoding the SDH and FRD subunits are organized as operons. In all cases, they are clustered on the chromosome and are co-transcribed into polycistronic mRNAs. The genes for the *E. coli* FRD are encoded by the *frd* operon, which contains 4 cistrons, *frdA–frdD*, arranged in tandem (Cole *et al.*, 1985; Cole and Guest, 1980; Lohmeier *et al.*, 1981; Van Hellemond and Tielens, 1994). A remarkable feature of the *frd* operon is the extreme sequence economy. *frdA* and *B* cistrons overlap by 5-bp, and the intercistronic regions are atypically short with the translational stop codons being incorporated into the ribosome binding site of the following gene. This sequence economy and cistronic organization may account for the unusually high level of overexpression that has been reported for the *frd* operon (Cole *et al.*, 1985; Lohmeier *et al.*, 1981). Similarly, the genes encoding the *E. coli* SDH subunits are polycistronic, but the gene order is *sdhCDAB* (Darlison and Guest, 1980; Wood *et al.*, 1984). A similar gene order is found in the *sdh* operons of many gram-negative bacteria, including *P. denitrificans* and *Coxiella burnettii*. In prokaryotes with a trimeric SDH (e. g. *B. subtilis*) or FRD (e. g. *W. succinogenes* and *B. macerans*), the gene order is *sdhCAB* and *frdCAB*, respectively (Hägerhäll, 1997).

In eukaryotes, SDH subunits are generally encoded by nonclustered nuclear genes (Ackrell *et al.*, 1992; Hägerhäll, 1997; Hederstedt and Ohnishi, 1992; Scheffler, 1998). The subunits are post-translationally imported into the mitochondrion by an elaborate import machinery (Neupert, 1997; Pfanner and Meijer, 1997; Schatz, 1996). However, there are exceptions to this generalization. The Sdh3p and the Sdh4p of the liverwort, *Marchantia polymorpha*, the zooflagellate, *Reclinomonas americana*, and the photosynthetic red algae, *Porphyra purpurea*, *Chondrus crispus*, and *Cyanidium caldarium* are encoded by the mitochondrial genomes (Burger *et al.*, 1996; Viehmann *et al.*, 1996). In some cases (e. g. *C. crispus, P. purpurea,* and *R. americana*), the *SDH2* genes are also mitochondrially encoded. The *SDH3* and *SDH4* genes of *P. purpurea* and *R. americana*, and the *SDH2* and *SDH3* genes of *C. crispus* are clustered as in bacteria.

1.4.3. The Flavoprotein Subunit

The dicarboxylate-binding site is harbored by Sdh1/FrdA, which also contains a covalently bound FAD prosthetic group, attached via an 8(α)-N(3)-histidyl linkage (Fig. 1.9). This basic structure of the flavoprotein subunit has been found in all the prokaryotic and eukaryotic SDH preparations that have been

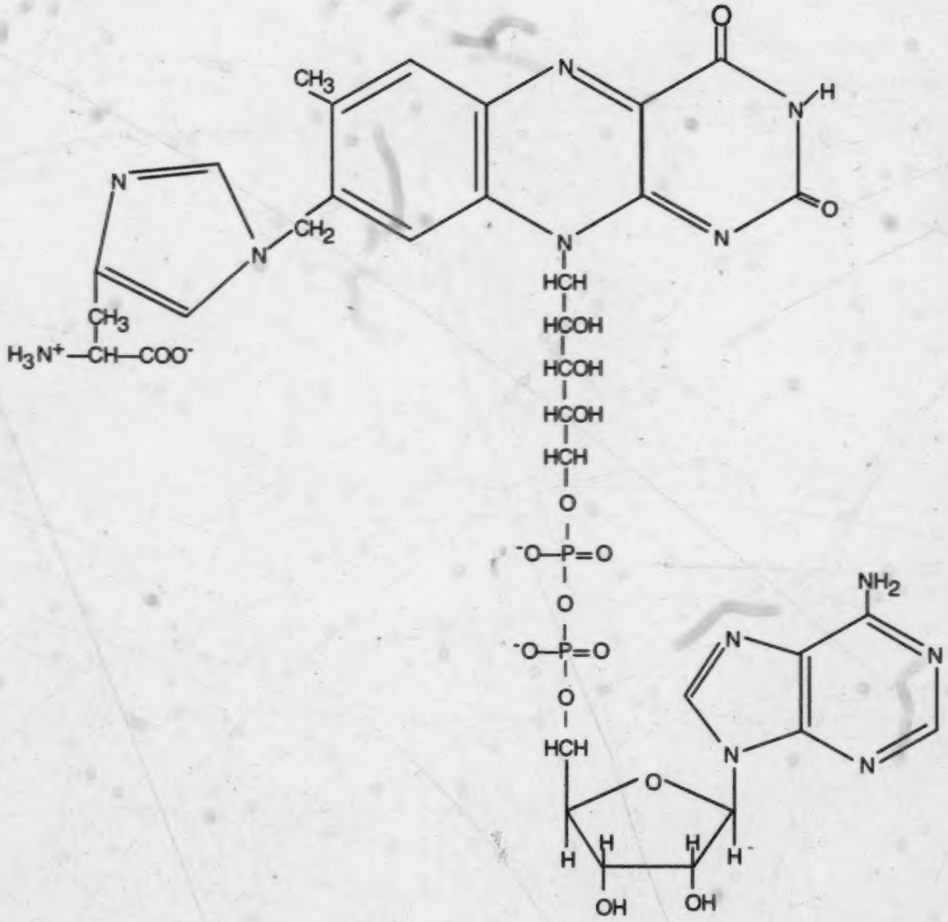
CH3
N
O
N-H
O
N
N
N
CH2
N
CH3
H3N+—CH—COO-
N
HCH
HCOH
HCOH
HCOH
HCH
O
-O—P=O
O
-O—P=O
O
HCH
NH2
N
N
N
N
O
H
H
H
H
OH
OH

Figure 1.9 The Structure of 8a-[*N*3]-Histidyl Flavin Adenine Dinucleotide.

examined to date (Ackrell *et al.*, 1992; Cole *et al.*, 1985; Hägerhäll, 1997; Hederstedt and Ohnishi, 1992; Mewies *et al.*, 1998; Scheffler, 1998; Van Hellemond and Tielens, 1994). Sdh1 or FrdA is a hydrophilic 79–65 kDa polypeptide exposed to the matrix side of mitochondrial inner membrane or to the prokaryotic cytoplasmic membrane. The flavoprotein subunit exhibits a high degree of primary sequence conservation across species.

The active site is known to bind a variety of dicarboxylate substrates. These include succinate, fumarate, L-chlorosuccinate, and malate, all of which are substrates for the enzyme (Ackrell *et al.*, 1992; Hägerhäll, 1997; Hederstedt and Ohnishi, 1992; Singer *et al.*, 1973). The affinity of the active site for dicarboxylates depends on the redox state of the enzyme. In their oxidized forms, both SDH and FRD have higher affinities for dicarboxylates than in their reduced forms (Ackrell *et al.*, 1989; Kotlyar and Vinogradov, 1984b). These observations suggest that the conformation of the active site is controlled by its redox state. Malonate and oxaloacetate are potent competitive inhibitors of succinate:quinone oxidoreductases. The affinity of malonate binding to the active site does not change significantly with the oxidation state of the enzyme. Hence, it is conceivable that bound malonate mimics a transition state between succinate and fumarate. D- and natural L-stereoisomers of malate are poor substrates for succinate:quinone oxidoreductases since they are oxidized to enol-oxaloacetate, which inhibits the enzyme. However, the oxidation of malate, a metabolite of the Krebs cycle, is of practical importance since it may account for oxaloacetate-induced inactivation of succinate:quinone oxidoreductases observed in cell-free extracts. This often precludes the meaningful measurement of succinate oxidation rates or studies with other inhibitors unless the oxaloacetate is removed by reduction (Ackrell *et al.*, 1975; Ackrell *et al.*, 1992). In their oxidized forms, both SDHs and FRDs bind oxaloacetate very tightly at the active site in a 1:1 stoichiometric ratio and with a loss of activity (Ackrell *et al.*, 1989; Kotlyar and

Vinogradov, 1984b). The possibility that this inhibitor may bind at a regulatory site has been ruled out (Ackrell *et al.*, 1992).

Many approaches, including chemical modifications, primary sequence comparisons, and mutagenesis, have been used to map the dicarboxylate-binding site (Ackrell *et al.*, 1992; Hägerhäll, 1997; Hederstedt and Ohnishi, 1992). Although this has led to the identification of amino acid residues in the flavoprotein subunit that are located in or close to the active site , the mechanisms of substrate binding and oxidation are still poorly understood. The available data indicate that residues likely to participate in catalysis are the essential arginine and histidine residues at the active site (Kotlyar and Vinogradov, 1984a; Schröder *et al.*, 1991; Vik and Hatefi, 1981). Two conserved arginine residues have been suggested to each form a bidentate ionic pair with one of the carboxylate groups of succinate and other dicarboxylate substrates, thereby orienting the substrate at the active site (Schröder *et al.*, 1991). The histidine residue at the active site has been suggested to function as the general acid-base catalyst (Vik and Hatefi, 1981), thereby aiding in protonation or deprotonation of the dicarboxylate substrate.

FAD is the redox-active center of the flavoprotein subunit and is essential for succinate oxidation and fumarate reduction (Ackrell *et al.*, 1992; Cole *et al.*, 1985; Hägerhäll, 1997; Hederstedt and Ohnishi, 1992; Singer and Johnson, 1985). It is probably located close to the substrate binding site and is most likely the first electron acceptor during succinate oxidation. The flavoprotein subunit binds FAD via both covalent and non-covalent interactions (Hägerhäll, 1997; Mewies *et al.*, 1998), raising the question of the necessity of the covalent attachment. Possible roles for covalent flavin attachment may include the alteration of the midpoint redox potential, the prevention of cofactor loss in low flavin environments, the creation of an improved reaction pathway, or the prevention of competing side reactions (Decker, 1993; Mewies *et al.*, 1998). Covalent FAD can be isolated from the holoenzyme by acid precipitation followed by proteolytic digestion to generate flavinylated peptides. This forms the basis for the determination of covalent flavin contents of SDH/FRD. Flavinylated peptides can be estimated fluorometrically at acid pH (Singer and McIntire, 1984).

The mechanism of covalent flavin attachment is unknown. Many studies have examined the role of covalent flavinylation in catalysis and whether the mechanism of covalent flavin attachment is protein-mediated or autocatalytic (Ackrell *et al.*, 1992; Decker, 1993; Hägerhäll, 1997; Hederstedt and Ohnishi, 1992; Mewies *et al.*, 1998). In the *S. cerevisiae* SDH, the flavin moiety is attached to His-90 of Sdh1p via an 8(α)-N(3) linkage (Robinson and Lemire, 1995; Robinson *et al.*, 1994). It has been shown that covalent flavin attachment is necessary for succinate oxidation in this species (Robinson *et al.*, 1994). However, the reverse reaction, fumarate reduction, is not affected. Similar experiments in *E. coli* show that mutant FRD containing non-covalent FAD can still catalyze fumarate reduction, but is defective in succinate oxidation (Blaut *et al.*, 1989). These observations have been rationalized in terms of thermodynamic considerations (Ackrell *et al.*, 1992; Mewies *et al.*, 1998). The inability of mutant complexes to oxidize succinate might reflect an altered flavin redox potential, as a consequence of the lack of covalent linkage and/or changes in the active site microenvironment. Bound FAD has been shown to have a more positive redox potential than the free FAD (Edmondson and Singer, 1973; Singer and Edmondson, 1974). Hence, a role for covalent flavinylation may be to adapt the enzyme for succinate oxidation.

Immunological and molecular genetic approaches have been used to study the mechanism of covalent flavin attachment in *S. cerevisiae* SDH (Robinson and Lemire, 1995; Robinson and Lemire, 1996a; Robinson and Lemire, 1996b; Robinson *et al.*, 1994). Several observations are consistent with the hypothesis that the folded conformation is the substrate for covalent flavinylation and that the reaction is autocatalytic. The Sdh2p subunit, tricarboxylate substrates, and the mitochondrial chaperone, hsp60, enhance the flavinylation reaction (Robinson and Lemire, 1996a; Robinson and Lemire, 1996b). In addition, C-terminal truncations of Sdh1p, at sites that are far removed from the putative FAD binding site, prevent covalent FAD attachment (Robinson and Lemire, 1996a). These results suggest that a folding of the polypeptide must precede covalent modification. This requirement for folding indirectly obviates the need for protein-mediation, suggesting that the specificity for autocatalysis is acquired after folding. However, when the *B. subtilis* SDH is heterologously expressed in *E. coli*, the enzyme is not flavinylated (Hederstedt *et al.*, 1987). This has been argued to rule out an autocatalytic mechanism of flavinylation in this organism.

1.4.4. The Iron-sulfur Protein Subunit

The iron-sulfur protein subunit, Sdh2/SdhB/FrdB, readily interacts with the flavoprotein subunit to constitute the catalytic dimer. Like the flavoprotein subunit, the basic structure of the iron-sulfur protein subunit is well conserved across species. A variety of biophysical techniques, notably electron paramagnetic resonance (EPR) and magnetic circular dichroism (MCD) spectroscopies, have been used to unravel the natures of the iron-sulfur clusters (Ackrell *et al.*, 1992; Cole *et al.*, 1985; Hägerhäll, 1997; Hederstedt and Ohnishi, 1992; Singer and Johnson, 1985). Three different iron-sulfur clusters have been identified in this subunit. These are: center 1, a $[2Fe\text{-}2S]^{2+,1+}$ cluster, center 2, a $[4Fe\text{-}4S]^{2+,1+}$ cluster, and center 3, a $[3Fe\text{-}4S]^{1+,0}$ cluster. The 3 clusters are found in most succinate:quinone oxidoreductases (Ackrell *et al.*, 1992), though with different thermodynamic parameters, which often reflect the physiological functions of the enzyme. In most SDHs, centers 1 and 3 have apparent E_m's that are high enough to be reducible by the substrate, succinate ($E_{m,7}$ = +30 mV). In FRD, both centers 1 and 3 have much lower E_m values compared to those of SDH. The midpoint potentials are almost equipotential to that of menaquinone/menaquinol couple

($E_{m,7} = -74$mV). Center 1 is most likely the immediate electron acceptor from FAD in SDHs and the immediate electron donor to FAD in FRDs. On the other hand, the thermodynamic properties of center 3 suggest that it is the immediate electron donor to/acceptor from quinones. In general, the E_m for center 3 in different succinate:quinone oxidoreductases seems to be influenced by the nature of the quinone substrate, with higher E_m values in SDH that interact with ubiquinone (E_m = +112 mV) rather than menaquinone as electron acceptor. This observation is consistent with the direction of electron flow in the two systems. Thus, center 3 exhibits a redox potential commensurate with a role as a ubiquinone/menaquinone oxidoreductant. In addition, there are indications that center 3 may perform a structural role in the membrane docking of both subunits of the catalytic domain (Manodori *et al.*, 1992). In contrast to centers 1 and 3, the iron-sulfur center 2 generally has apparent E_m's that are much lower than the succinate/fumarate couple. This has prompted speculation that it may not participate in electron transfer (Hägerhäll, 1997; Hederstedt, 1998). However, this cluster may play an important structural role as demonstrated by mutagenesis studies of the *E. coli* FRD (Kowal *et al.*, 1995).

Analysis of the intercluster magnetic interactions of the iron-sulfur clusters has provided information on their spatial proximity. The available data show that each redox-active center in succinate:quinone oxidoreductase (FAD, iron-sulfur clusters, quinone and possibly cytochrome *b*) interacts with at least one neighboring redox component. The distance between the FAD and center 1 is 12–18 Å (Ohnishi *et al.*, 1981). Centers 1 and 2 are 9–12 Å apart (Salerno *et al.*, 1979) while clusters 1 and 3 are estimated to be 10–20 Å apart (Crowe *et al.*, 1983; Maguire *et al.*, 1986). Strong spin-coupling between centers 2 and 3 has also been observed, indicating a much closer proximity of these centers (Ackrell *et al.*, 1992; Hederstedt and Ohnishi, 1992). Recent EPR data from the *P. denitrificans* SDH have shown that the three iron-sulfur clusters are arranged in the Ip subunit within 2 nm of each other (Waldeck *et al.*, 1997). Evidence for the proximity of center 3 to ubiquinone and to heme *b*, which will be discussed in the following section, has also been obtained.

1.4.5. The Anchor Polypeptides

The SDH/FRD membrane domain comprises two smaller hydrophobic polypeptides, Sdh3/SdhC/FrdC (13–18 kDa) and Sdh4/SdhD/FrdD (11–16 kDa) or one larger hydrophobic polypeptide, SdhC/FrdC (23–30 kDa). Anchor domains with a single hydrophobic polypeptide are found in trimeric succinate:quinone oxidoreductases. Apart from this variability in subunit composition, the anchor polypeptides generally show little conservation of amino acid sequence. However, the patterns of hydrophobic segments are conserved across species (Hägerhäll, 1997; Hägerhäll and Hederstedt, 1996; Hederstedt, 1998). They are predicted to each contain three transmembrane helices or in the case of one polypeptide, five. The hydrophobic domain is essential for electron transfer through the complex. It interacts with one or two redox cofactors, quinone and/or *b*-type heme.

1.4.6. Interaction with Heme

SDHs and FRDs from most organisms contain a *b*-type heme (protoheme IX; Fig. 1.10a) that is associated with one or two anchor subunits (Ackrell *et al.*, 1992; Hägerhäll, 1997; Hägerhäll and Hederstedt, 1996; Hederstedt, 1998). The protoheme IX is usually coordinated by histidine residues (Fig. 1.10b) in the anchor subunits (Crouse *et al.*, 1995; Hägerhäll *et al.*, 1995; Lee *et al.*, 1998; Nakamura *et al.*, 1996; Peterson *et al.*, 1994; Shenoy *et al.*, 1999; Simon *et al.*, 1998; Vibat *et al.*, 1998). However, the functional role of heme in these enzymes is not known. Preparations of bovine heart complex II or its hydrophobic polypeptides contain heme in substoichiometric amounts (Ackrell *et al.*, 1980; Hatefi and Galante, 1980; Tushurashvili *et al.*, 1985; Yu *et al.*, 1987; Yu and Yu,

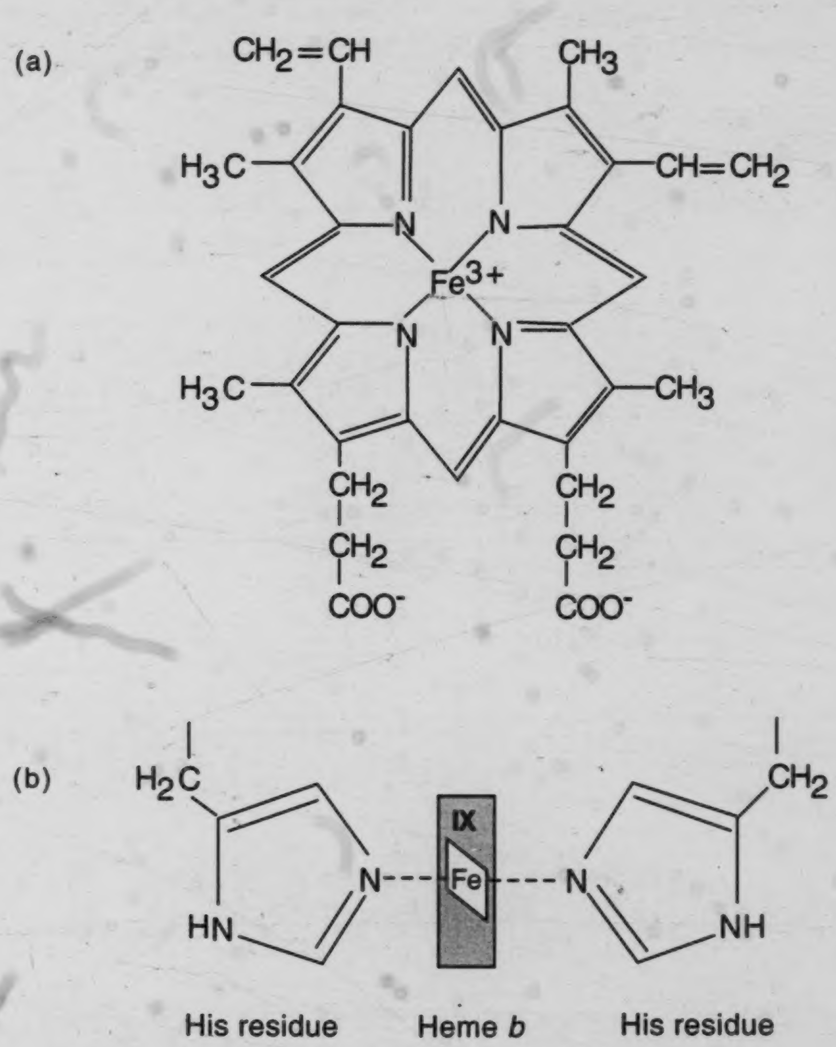
(a)
CH2=CH
CH3
H3C
CH=CH2
N
N
Fe3+
N
N
H3C
CH3
CH2
CH2
COO-
CH2
CH2
COO-
(b)
H2C
CH2
IX
N
Fe
N
HN
NH
His residue
Heme b
His residue

Figure 1.10 The Structure of Heme *b*.

(a) Iron-protoporphyrin IX (heme *b*) (b) Axial liganding of the heme iron by histidine residues.

1982). This has led to an initial skepticism on the presence and role of heme in this class of oxidoreductases. The controversy was put to rest by spectroscopic studies that indicated that this cytochrome is distinct from the *b* cytochromes of complex III (Davis *et al.*, 1973; Yu *et al.*, 1987). It was subsequently shown in *N. crassa* that the *b* cytochrome of SDH is nuclear-encoded as opposed to the *b* cytochrome of complex III, which is encoded by the mitochondrial genome (Weiss and Kolb, 1979). When *N. crassa* cells are grown in the presence of chloramphenicol to inhibit mitochondrial protein synthesis, cytochrome *b* can still be detected in this organism. It is now well established that many SDHs/FRDs contain endogenous heme (Hägerhäll, 1997; Hederstedt, 1998). The number of protoheme IX groups per enzyme complex, and the thermodynamic and the redox properties of heme *b* within the proteins vary among species (Table 1.1).

The *B. subtilis* and *Thermoplasma acidophilum* SDHs, and the *W. succinogenes* FRD each contain two hemes, while the *A. suum*, *E. coli*, *P. denitrificans*, and bovine SDHs contain one heme per enzyme molecule (Hägerhäll, 1997; Hägerhäll and Hederstedt, 1996; Hederstedt, 1998; Kita *et al.*, 1997). Each cytochrome *b* component in the di-heme cytochromes, designated b_H (high potential) and b_L (low potential), exhibits unique thermodynamic and spectroscopic properties. b_H has a high midpoint potential, is reducible by succinate and, in most cases, shows a symmetrical α-peak in the visible spectrum (Hederstedt, 1998). On the other hand, b_L has a low redox potential, it is not reducible by succinate but can be reduced by a strong reductant like dithionite, and it shows an asymmetrical α-peak in the reduced state. In the mono-heme cytochromes of the *E. coli*, the *A. suum*, and the bovine SDHs, the apparent midpoint redox potentials are +36 mV, −34 mV, and −185 mV, respectively. Whereas the *E. coli* cytochrome b_{556} is reducible by succinate (Kita *et al.*, 1989; Vibat *et al.*, 1998), the low potential cytochrome b_{560} of bovine SDH is not readily reducible by succinate, though it is easily oxidized by fumarate and ubiquinone-2

Table 1.1

Properties of Quinones and Hemes in Selected SDHs and FRDs

Enzyme	Quinone (mV)	Heme (mV)	TM	Conserved His
T. acidophilum SDH	MMQ (− 74)	b_H: (+ 75) b_L: (− 150)	6	4
B. subtilis SDH	MQ (− 74)	b_H: (+ 65) b_L: (− 95)	5	4
W. succinogenes FRD	MQ (− 74)	b_H: (+ 20) b_L: (− 200)	5	4
E. coli SDH	UQ (− 113)	(+ 36)	6	2
Bovine heart SDH	UQ (− 113)	(− 185)	6	2
P. denitrificans SDH	UQ (− 113)	(− 175)	6	2
A. suum FRD	RQ (− 63)	(− 34)	6	2

The data are adapted from (Hägerhäll, 1997; Hederstedt, 1998; Schirawski and Unden, 1998). The abbreviations used are: MQ, menaquinone; MMQ (thermoplasmaquinone), methylated menaquinone; UQ, ubiquinone; RQ, rhodoquinone; TM, transmembrane segments. The E_m values for quinones and hemes are in parenthesis.

if pre-reduced with dithionite (Hatefi and Galante, 1980; Yu *et al.*, 1987). Similarly, the low potential cytochrome *b* of *A. suum* is only partially reducible by succinate (Takamiya *et al.*, 1986; Takamiya *et al.*, 1990). In contrast to the heme-containing enzymes, the *Sulfolobus acidocaldarius* SDH (Moll and Schäfer, 1991) and the *E. coli* (Cole *et al.*, 1985) and *Desulfovibrio multispirans* (He *et al.*, 1986) FRDs lack heme. It is also generally believed that the *S. cerevisiae* SDH does not contain heme (Hägerhäll, 1997; Hägerhäll and Hederstedt, 1996; Schilling *et al.*, 1982; Vibat *et al.*, 1998).

The possible role of heme in these enzymes is enigmatic. The variations in the number and the thermodynamic properties of heme, coupled with its absence in some species, has elicited questions about the functional role of heme in intramolecular electron transport. The EPR and optical spectra of heme are sensitive to inhibitors that block electron transfer from center 3 to ubiquinone in the bovine SDH (Yu *et al.*, 1987). Similarly, magnetic interactions between Center 3 and the mono-heme group of the *P. denitrificans* SDH have been demonstrated by EPR (Waldeck *et al.*, 1997). These observations are consistent with a possible role of heme in electron transfer between center 3 and quinone. However, the observation that some SDHs/FRDs do not contain heme, yet, efficiently reduce quinone, obviates an obligatory role for the heme moiety in electron transport. In addition, the high stability of the radical form and positive redox potential of the $Q/Q^{\cdot}$ couple ($E^{\circ\prime} = +100$ mV) (Ackrell *et al.*, 1992; Hederstedt and Ohnishi, 1992) make the need for a low potential reduction less obvious and the funneling of both electrons for quinone reduction through center 3 an increasing possibility. A structural role has been demonstrated for cytochrome b_{558} in the *B. subtilis* SDH (Hederstedt and Rutberg, 1980). A similar role has been suggested for the heme *b* of *E. coli* SDH when heme synthesis is blocked (Nakamura *et al.*, 1996). In contrast, heme *b* does not seem to have any role, structural or catalytic, in *E. coli* SDH when the heme ligands are mutated (Vibat *et al.*, 1998). Recently, it has been postulated that the cytochrome in complex II may interact with the ubisemiquinone radical to reduce the production of superoxide free radicals (Ishii *et al.*, 1998). Further studies will be required to test this possibility.

1.4.7. Interaction with Quinones

Although the catalytic dimer can reduce artificial electron acceptors like ferricyanide, PMS and DCPIP, the reduction of natural quinones and quinone analogs requires the presence of functional anchor polypeptides, indicating that they contain binding sites for this substrate (Yang *et al.*, 1997; Yu and Yu, 1980; Yu *et al.*, 1987). The involvement of the anchor polypeptides in quinone binding is further supported by the detection of ubisemiquinone radicals in intact or reconstituted SDHs. EPR studies of the bovine SDH have shown a thermodynamically stable ubisemiquinone pair ($Q^{\cdot -}Q^{\cdot -}$) in the vicinity of iron-sulfur center 3 (Ackrell *et al.*, 1992; Hägerhäll, 1997; Hederstedt and Ohnishi, 1992). Stable semiquinone pairs have also been observed in mitochondria from *N. crassa* (Rich and Bonner, 1978) and some green algae (Rich *et al.*, 1977). The stability of the semiquinone radicals in a hydrophobic milieu is indicative of interactions with protein. Moreover, photoaffinity labeling experiments have shown that the anchor polypeptides interact with quinones (Lee *et al.*, 1995; Shenoy *et al.*, 1997; Yang *et al.*, 1998; Yu and Yu, 1980; Yu and Yu, 1981a).

SDHs and FRDs interact with a variety of quinone substrates *in vitro*, though at different rates (Hägerhäll, 1997; Van Hellemond and Tielens, 1994). However, the enzymes are highly specific in their interaction with quinone *in vivo*, which may reflect the physiological direction of electron flow. Generally, SDH interacts with quinones having a higher standard redox potential like the benzoquinone, ubiquinone ($E^{\circ\prime} = +100$ mV). On the other hand, FRD generally interacts with quinones with a lower redox potential like the naphthoquinone, menaquinone ($E^{\circ\prime} = -70$ mV). The preferred quinone substrate *in vivo* often reflects the redox potential of iron-sulfur center 3, which most likely interacts with the quinone. The *B. subtilis* SDH interacts with menaquinone *in vivo* rather than ubiquinone (Lemma *et al.*, 1991). This enzyme is more FRD-like kinetically (Ackrell *et al.*, 1993) and in having a center 3 with a low standard redox potential (Maguire *et al.*, 1986). Similarly, anaerobically functioning adult parasitic helminths (Tielens and Van Hellemond, 1998) possess an SDH that functions in the direction of fumarate reduction and interacts with rhodoquinone, a benzoquinone with a standard redox potential similar to that of menaquinone ($E^{\circ\prime} = -63$ mV).

1.4.8. Intramolecular Electron Transfer

The electron transfer pathway within the succinate:quinone oxidoreductases remains controversial despite years of extensive research efforts. Nevertheless, the available data (Ackrell *et al.*, 1992; Hägerhäll, 1997; Hederstedt, 1998; Hederstedt and Ohnishi, 1992) indicate that the electron transfer sequence within these enzymes is most likely to be:

succinate/fumarate ↔ FAD ↔ [center 1 ↔ center 2 ↔ center 3] ↔ Q/QH_2

The iron-sulfur centers are 1-electron carriers while FAD and quinone are primarily 2-electron carriers. However, their stable semiquinone forms allow them to function as n=2 to n=1 electron-gating systems (Hederstedt and Ohnishi, 1992). During succinate oxidation, FAD is most likely the first electron acceptor from succinate. Experimental evidence confirming this comes from the analysis of two FAD deficient *B. subtilis* mutants (Maguire *et al.*, 1986). The iron-sulfur clusters of the mutant enzymes are not reducible by succinate, but are reducible by reverse electron-transfer from NADH via menaquinone. This places FAD prior to the iron-sulfur clusters in the electron transfer pathway between succinate and quinone. The $E_{m,7}$ values of the $FAD/FADH_2$ redox couple are −90 mV in the bovine SDH and −55 mV in the *E. coli* FRD. Two electrons are transferred from succinate to the flavin ring to form dihydroquinone during succinate oxidation. Reoxidation of the flavin then occurs in two sequential 1-electron steps via its univalent intermediate radical, flavosemiquinone. The flavosemiquinone is stable enough to permit the reduction of iron-sulfur clusters of the enzyme in sequential 1-electron steps. As discussed in section 1.1.4, the iron-sulfur centers 1 and 3 have E_m values that are high enough to be reducible by succinate. The high potential iron-sulfur center 3 is in close proximity to quinone and as such it is the most likely immediate electron donor to quinone. On the other hand, the E_m of center 2 is extremely low and this center is not reducible by succinate. It is possible that center 2 performs a structural role (Kowal *et al.*, 1995) or facilitates electron transfer between centers 1 and 3 (Salerno and Yan, 1987).

Like FAD, the reduction of quinone is thought to proceed in two sequential 1-electron transfer steps via semiquinone intermediates (Ackrell *et al.*, 1992; Hägerhäll, 1997; Hederstedt and Ohnishi, 1992). The existence of thermodynamically stable interacting semiquinone radicals has been detected in many members of the succinate:quinone oxidoreductase superfamily (section 1.4.7). A prototype for this formulation is present with the Q_A and Q_B sites of bacterial reaction centers that are involved in the initial photochemical reactions (see section 1.6.3). This is also similar to the Q_o and Q_i sites of the *bc*$_1$ complex (see section 1.3.3.2). In this model, two asymmetrically arranged quinone-binding sites are thought to exist in SDHs/FRDs. The primary quinone, Q_A, is assumed to be distal to the high potential iron-sulfur center 3 while the secondary quinone, Q_B, is thought to be proximal (Westenberg *et al.*, 1993; Yankovskaya *et al.*, 1996). This asymmetric arrangement is reminiscent of the quinone-binding site of *bc*$_1$ complex. In the bacterial RCs, Q_A and Q_B are on the same side of the membrane. Quinones interacting at the Q_A site are tightly bound and non-exchangeable. They cycle between the fully oxidized (Q) and the semiquinone ($Q^{\cdot-}$) states, thereby mediating single electron transfer between the high potential iron-sulfur center 3 and the Q_B site. Quinone species interacting at the Q_B site are in equilibrium with the Q/QH pool. As such, they are exchangeable with the quinone pool after protonation/deprotonation. Consequently, 2 quinone-binding sites have been proposed for the bovine (Lee *et al.*, 1995; Shenoy *et al.*, 1997; Yankovskaya *et al.*, 1996), the *B. subtilis* (Smirnova *et al.*, 1995) and the *P. denitrificans* (Waldeck *et al.*, 1997) SDHs and for the *E. coli* FRD (Westenberg *et al.*, 1993; Yankovskaya *et al.*, 1996).

Since fumarate reduction is the reverse reaction of succinate oxidation, it is believed to proceed essentially by the reversal of the above steps (Cole *et al.*, 1985; Van Hellemond and Tielens, 1994). Two electrons are transferred from quinol by 2 successive 1-electron steps at separate sites (Q_A and Q_B) to iron-sulfur center 3. The electrons are then transferred to FAD, with center 1 probably acting as an intermediary or electron storage site. Like succinate oxidation, FAD is thought to be directly involved in fumarate reduction.

Although the linear sequence of electron transfer in succinate oxidation and fumarate reduction may be similar, it is possible that the two reactions differ mechanistically as suggested by direct voltammetry measurements (see section 1.4.1). This seems to introduce another complexity to the mechanism of intramolecular electron transfer in SDHs/FRDs. How are the same redox components and structure adapted to carry out mechanistically different reversible reactions? Hence succinate:quinone oxidoreductases may provide good model systems for understanding the directionality of long-range electron transfer reactions.

As already discussed in section 1.4.6, the role of protoheme IX in electron transfer between succinate/fumarate and Q/QH_2 is uncertain. However, EPR studies indicate the protoheme IX is located closer to the high potential iron-sulfur center 3. This places heme between center 3 and quinone in the electron transfer pathway between succinate/fumarate and the Q/QH_2 couples.

1.4.9. Topological Organization of SDH and FRD

Structural information on succinate:quinone oxidoreductases is essential for a detailed understanding of the mechanism of catalysis and of intramolecular electron transfer. However, to date no direct x-ray crystallographic information on any succinate:quinone oxidoreductase is available. A combination of approaches including molecular genetics, photolabeling, chemical modification, and biophysical techniques have provided information on the overall topological outline of succinate:quinone oxidoreductases (Ackrell *et al.*, 1992; Cole *et al.*, 1985; Hägerhäll, 1997; Hederstedt and Ohnishi, 1992; Ohnishi, 1987; Scheffler, 1998).

A widely accepted topological model of SDH has the Sdh2p subunit serving as a link between the anchor domain and the matrix-oriented Sdh1p (Fig. 1.11). The model is consistent with many lines of experimentation. Ferricyanide, a membrane-impermeant artificial electron acceptor, is reducible by succinate in submitochondrial particles but not in intact mitochondria (Klingenberg, 1970). In another experiment, the succinate oxidase activity of submitochondrial particles is inhibited by antibodies directed against the holoenzyme and by the hydrophilic protein-modifying reagent, diazobenzene sulfonate (DABS) (Merli *et al.*, 1979). These results show that the catalytic domain is oriented to the matrix side of inner mitochondrial membrane. In addition, evidence that Sdh2p links Sdh1p and the anchor domain is provided by radiolabeling experiments (Merli *et al.*, 1979). [^{35}S]DABS selectively labels the Sdh1p subunit in submitochondrial particles prepared from bovine heart. In contrast, when intact mitochondria are used in the labeling experiment, the Sdh1p is not labeled. In either case, no significant labeling of the Sdh2p subunit is observed, indicating that this subunit is masked. Similarly, photolabeling of bovine SDH in phosphatidylcholine proteoliposomes by aryloazidophospholipid demonstrates that the two anchor polypeptides and the Sdh2p are intercalated into the interior of the lipid bilayer (Girdlestone *et al.*,

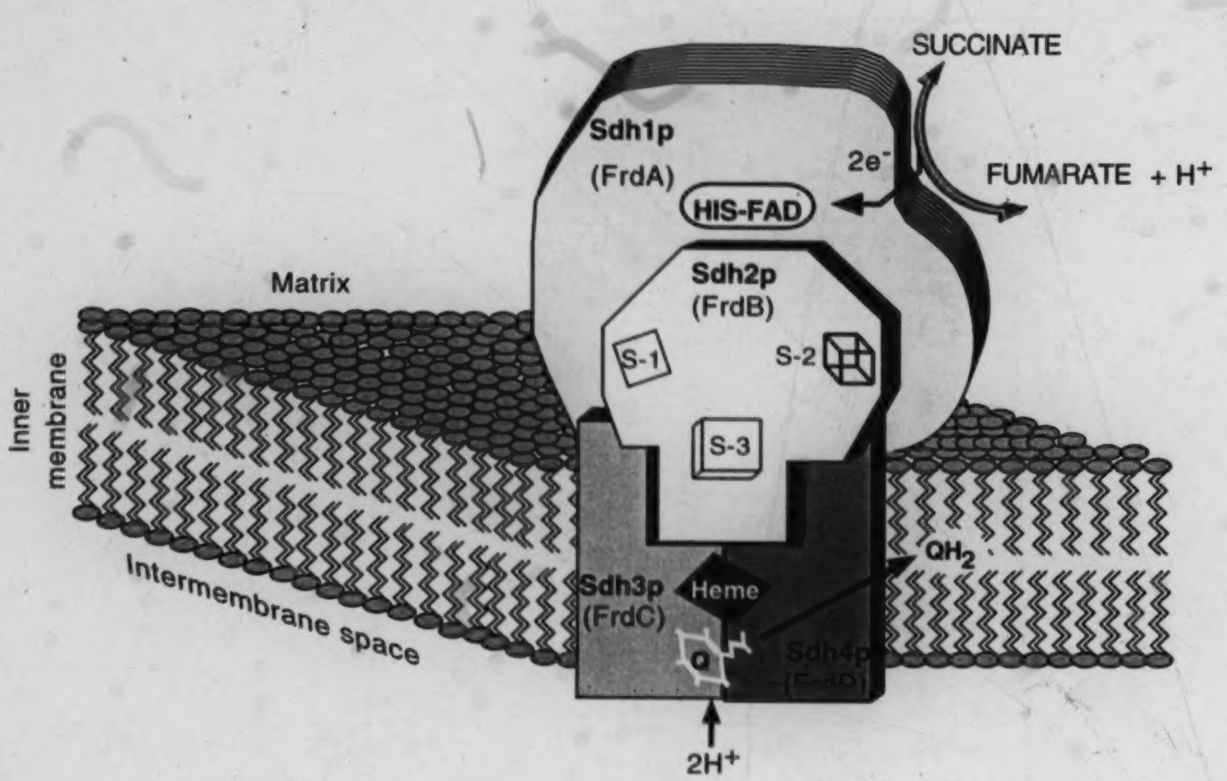
SUCCINATE
Sdh1p
(FrdA)
2e⁻
FUMARATE + H⁺
HIS-FAD
Matrix
Sdh2p
(FrdB)
S-1
S-2
S-3
Inner membrane
QH₂
Sdh3p
(FrdC)
Heme
Intermembrane space
Q
Sdh4p
(FrdD)
2H⁺

Figure 1.11 Topological Model of Succinate Dehydrogenase and Fumarate Reductase.

1981). Analogous transmembrane orientations for bacterial SDH/FRD have been demonstrated by antibody probing, limited proteolysis, radiolabeling, and electron microscopy (Hederstedt and Rutberg, 1981; Hederstedt and Rutberg, 1983; Lemire *et al.*, 1983; Unden and Kröger, 1980). Furthermore, hydropathy analysis of the primary sequences of all the anchor polypeptides suggests several hydrophobic segments that are potential transmembrane α-helices, 3 in each polypeptide in the tetrameric enzyme and 5 in the single anchor of the trimeric enzyme (Ackrell *et al.*, 1992; Hägerhäll, 1997; Hederstedt, 1998; Hederstedt and Ohnishi, 1992). The transmembrane topology has been confirmed for *B. subtilis* SDH by analyzing alkaline phosphatase fusion of various C-terminally truncated SdhC polypeptides (Hägerhäll *et al.*, 1995).

Several lines of experimentation have shown that the anchor polypeptides are essential for membrane docking of the catalytic domain (Ackrell *et al.*, 1992; Hägerhäll, 1997; Hederstedt and Ohnishi, 1992; Scheffler, 1998; Van Hellemond and Tielens, 1994). In enzymes with two anchor polypeptides, both are necessary for interaction with the subunits of the catalytic domain. This has been rigorously demonstrated in experiments with the *E. coli* FRD. *E. coli* cells were transformed with a variety of plasmids encoding the individual or combinations of FRD subunits. The experiments show that each of the anchor polypeptides plays an essential role in binding the catalytic domain to the membrane and in interacting with quinones (Cecchini *et al.*, 1986a; Cole *et al.*, 1985; Condon and Weiner, 1988; Latour and Weiner, 1989). Similar conclusions have been reached in reconstitution experiments with the bovine SDH (Hatefi, 1985). However, the structural interactions between the anchor polypeptides and the catalytic domain is poorly understood. Chemical modification studies show that histidines, amino groups, and carboxyl groups are essential for membrane docking (Choudhry *et al.*, 1985; Paudel *et al.*, 1991; Xu *et al.*, 1987; Yu and Yu, 1981b). Genetic studies in the *B. subtilis* SDH have identified the loop connecting transmembrane helices IV and V as essential in membrane docking (Fridén *et al.*, 1987). Replacement of G-168 in this loop with Asp results in an anchor polypeptide with normal spectroscopic properties for heme but unable to bind the catalytic domain. Studies of C-terminally truncated *E. coli* FRD mutants have provided a clearer picture on the role of various segments of the anchor polypeptides in membrane docking (Cecchini *et al.*, 1986b; Westenberg *et al.*, 1990). FrdC lacking 60 amino acid residues and FrdD lacking 80 amino acid residues at the C-termini still retain significant abilities to bind the catalytic domain. However, these mutants are defective in quinone-mediated electron transfer activities. This suggests that the amino acid residues in the truncated regions are not involved in membrane docking.

1.5. Assembly of Succinate-quinone Oxidoreductases

The biogenesis of succinate:quinone oxidoreductases is a rather complex process. This is due to the oligomeric nature of the enzyme, the presence of multiple prosthetic groups, and the fact that the enzymes are integral membrane proteins. There is a further complication in eukaryotes due to the fact that all the polypeptides, with few exceptions, are nuclear encoded and thus synthesized extra-mitochondrially (Ackrell *et al.*, 1992; Hägerhäll, 1997; Hederstedt and Ohnishi, 1992; Scheffler, 1998). These have to be translocated across the mitochondrial membranes. Therefore, subunits and cofactors must be synthesized, transported, and assembled at compatible rates. In addition, a plethora of accessory gene products are required for the assembly of these proteins, some of which remain to be identified (Attardi and Schatz, 1988; Grivell, 1995; Neupert, 1997; Pfanner and Meijer, 1997; Schatz, 1996). Generally, eukaryotic SDHs are synthesized as precursors, which contain cleavable N-terminal mitochondrial targeting presequences. In contrast, the bacterial subunits are synthesized without leader sequences (Ackrell *et al.*, 1992; Cole *et al.*, 1985; Hägerhäll, 1997;

Hederstedt and Ohnishi, 1992; Van Hellemond and Tielens, 1994). Understanding the biogenesis of SDH/FRD requires knowledge of the pathway and the temporal aspects of assembly, as well as intersubunit interactions in the quaternary structure of the enzyme. The available data indicate that complex assembly begins with the incorporation of the prosthetic groups to the appropriate subunits (Ackrell *et al.*, 1992; Cole *et al.*, 1985; Hägerhäll, 1997; Hederstedt and Ohnishi, 1992; Scheffler, 1998; Van Hellemond and Tielens, 1994). This is followed by subunit association to form the functional holoenzyme, with the anchor subunits being the first to be inserted into the membrane.

1.5.1. The Temporal Order of Assembly

The assembly of succinate:quinone oxidoreductases has been studied extensively using reconstituted and *in vivo* systems (Ackrell *et al.*, 1992; Cole *et al.*, 1985; Hägerhäll, 1997; Hederstedt and Ohnishi, 1992; Scheffler, 1998; Van Hellemond and Tielens, 1994). Many observations are consistent with the view that the synchronous insertion of the anchor subunits into the membrane constitutes an early event in assembly. Pulse-chase experiments with the *E. coli* FRD (Latour and Weiner, 1989) and with the *B. subtilis* SDH (Hederstedt and Rutberg, 1980) show that the anchor subunits are rapidly inserted into the plasma membrane. Mutants of the *B. subtilis* SDH lacking either the SdhA or B subunits were shown to contain correctly inserted anchor subunit (Hederstedt *et al.*, 1982; Hederstedt and Rutberg, 1980). Several lines of experimentation in bacteria also show that in the absence of functional anchor polypeptides, the catalytic domains accumulate in the cytoplasm (Ackrell *et al.*, 1992; Fridén and Hederstedt, 1990; Hederstedt and Ohnishi, 1992). These results demonstrate that membrane insertion of the anchor polypeptides is the initial step of complex assembly. This temporal order of assembly is consistent with the established docking role of the anchor polypeptides (Ackrell *et al.*, 1992; Hederstedt and Ohnishi, 1992; Scheffler, 1998).

Whether the subunits comprising the catalytic domain dimerize prior to membrane docking or dock in a stepwise fashion is an open question. Evidence has been advanced for both the concerted docking of pre-assembled catalytic dimer and the sequential docking of individual subunits. For example, in *E. coli*, FrdA and FrdB subunits form a soluble, active heterodimer when they are expressed in the absence of the membrane anchor subunits (Lemire *et al.*, 1982). Similarly, pre-assembled catalytic dimers of the *E. coli* FRD and the mammalian SDH can be added to their respective anchor domains to reconstitute functional succinate:quinone oxidoreductases (Ackrell *et al.*, 1992; Cecchini *et al.*, 1986a). The existence of a pre-assembled catalytic dimer is also indicated in *S. cerevisiae* by the observation that the absence of either Sdh1p or Sdh2p leads to rapid degradation of the other subunit (Schmidt *et al.*, 1992). There are several observations that are inconsistent with the notion that the catalytic domain is pre-assembled prior to membrane docking. Pulse-chase experiments in *E. coli* suggest that FrdA attaches to the membrane before the docking of FrdB (Latour and Weiner, 1989). In some mutants of the *B. subtilis* SDH lacking the anchor polypeptide, the SdhA and SdhB subunits are found in the cytoplasm as monomers (Hederstedt *et al.*, 1982; Hederstedt and Rutberg, 1980). Despite this seeming discrepancy, the docking of a pre-assembled catalytic domain is a very attractive possibility.

1.5.2. Incorporation of the Prosthetic Groups

Incorporation of the prosthetic groups (FAD, iron-sulfur clusters, and heme) into succinate:quinone oxidoreductases has also been studied (Ackrell *et al.*, 1992; Hederstedt and Ohnishi, 1992). In the case of FAD and iron-sulfur clusters, the available data indicates that incorporation of the cofactors into the appropriate subunits occurs prior to assembly of the catalytic dimer or membrane docking.

The mechanism by which the iron-sulfur clusters are assembled is unknown. Some data suggest that the iron-sulfur clusters may form independently of each other and play a role in membrane docking (Ackrell *et al.*, 1992; Johnson *et al.*, 1988; Manodori *et al.*, 1992). Soluble enzymes that are formed in the absence of anchor polypeptides contain iron-sulfur clusters, suggesting that cluster formation precedes membrane docking (Cecchini *et al.*, 1986a; Johnson *et al.*, 1988; Lemire *et al.*, 1982). Similarly, there is evidence that incorporation of some of the iron-sulfur clusters may precede the formation of the catalytic domain (AEvarsson and Hederstedt, 1988; Hederstedt and Ohnishi, 1992). In contrast to iron-sulfur cluster formation, incorporation of FAD into Sdh1p/FrdA is not obligatory for either dimerization with Sdh2p/FrdB or for membrane docking. However there is evidence that FAD attachment most likely occurs before the Sdh1p/FrdA subunit is assembled with other subunits. For example, when SDH assembly has been prevented in *B. subtilis* by heme depletion or the lack of a functional anchor polypeptide, SdhA containing covalently attached FAD accumulates in the cytoplasm (Hederstedt *et al.*, 1982; Hederstedt and Rutberg, 1980). Similar experiments in *E. coli* (Cecchini *et al.*, 1986a; Cole *et al.*, 1985) and *W. succinogenes* (Unden and Kröger, 1981) show that FrdA containing covalent FAD can be independently expressed.

There are conflicting reports concerning the role of heme in the assembly of SDH and FRD. This is not surprising since some members of the succinate:quinone oxidoreductase superfamily are devoid of this prosthetic group. Experiments with *B. subtilis* heme-deficient mutants suggest that incorporation of heme is an obligatory step in SDH assembly (Hederstedt and Rutberg, 1981). SdhA and SdhB are synthesized, but are unable to dock on the membrane. Similarly, mutations in the *B. subtilis* SDH that abolish heme binding lead to the accumulation of inactive SdhA and SdhB polypeptides in the cytoplasm (Fridén and Hederstedt, 1990). In contrast, bovine SDH lacking heme can be reconstituted *in vitro*, suggesting that incorporation of heme is not obligatory for enzyme assembly (Ackrell *et al.*, 1992; Hatefi and Galante, 1980; Yu and Yu, 1980). However, higher heme contents have been shown to result in better reconstitutive capacities. Similarly, experiments with the *E. coli* SDH have demonstrated that heme is not necessary for the assembly of a functional complex (Vibat *et al.*, 1998).

1.5.3. Assembly of Eukaryotic SDHs

It is becoming increasingly clear that the assembly of eukaryotic SDHs, like that of other respiratory complexes, is not a spontaneous event, but one that is mediated by a large number of specific and general accessory proteins (Attardi and Schatz, 1988; Grivell, 1995; Neupert, 1997; Tzagoloff and Dieckmann, 1990). Understanding the pathway and the temporal aspects of assembly of the respiratory complexes constitutes a major challenge in mitochondrial biogenesis. The *S. cerevisiae* SDH, consisting of only 4 nuclear-encoded subunits, is a potentially good model for studying the assembly of a respiratory complex. Two accessory proteins involved in the assembly of *S. cerevisiae* SDH have been identified. The Abc1p, a chaperone-like protein with a high degree of evolutionary conservation across species, has been shown to be essential for proper conformation and efficient functioning of the bc_1 complex (Bousquet *et al.*, 1991; Brasseur *et al.*, 1997). The observation that its absence affects efficient functioning of the neighboring complexes, SDH and cytochrome oxidase, indicates that it may be equally involved in the correct assembly of these enzymes. Abc1p may be necessary for the formation or insertion of the active site iron-sulfur cluster of the Rieske protein of complex III. However, the role of Abc1p in SDH assembly and/or function is unclear. Recently, the *TCM62* gene, encoding a member of the hsp60 family of molecular chaperones, was shown to be specifically required for SDH biogenesis (Dibrov *et al.*, 1998). Tcm62p is found exclusively associated with SDH when solubilized mitochondrial proteins are resolved by blue native gel electrophoresis. The presence of Tcm62p in substoichiometric amounts indicates that it may play a catalytic role in the assembly of SDH. Overexpression of Tcm62p results in the production of inclusion bodies containing Sdh1p and Sdh2p subunits. Several excellent reviews have treated other specific accessory proteins involved in the assembly of mitochondrial respiratory chain proteins (Grivell, 1995; McEwen *et al.*, 1986; Poyton and McEwen, 1996; Tzagoloff and Dieckmann, 1990).

1.6. The Mechanism of Q-mediated Electron Transfer: The Two Quinone-binding Site Hypothesis

Ubiquinone is a lipophilic and ubiquitous molecule that is capable of mediating redox reactions. These properties and its presence in mitochondria, led to the proposal that ubiquinone is a member of the electron-transport chain (Crane, 1977; Crane *et al.*, 1957). The participation of ubiquinone as an obligatory redox component of the electron-transport chain is now well-established (Crane, 1977; Hatefi, 1985; Ragan and Reed, 1986; Trumpower, 1980; Trumpower and Katki, 1979; Wikström and Saraste, 1984). In addition, ubiquinone may mediate the vectorial transport of protons across the mitochondrial inner membrane as predicted by the chemiosmotic theory (Mitchell, 1969).

The redox chemistry of quinones imposes restrictions for interacting with one-electron carriers like the iron-sulfur centers, with which quinones often interact. In order to facilitate the coupling of one-electron and two-electron carriers, quinone-binding proteins often have at least two quinone-binding sites (Ackrell *et al.*, 1992; Allen *et al.*, 1987b; Degli Esposti and Ghelli, 1994; Hägerhäll, 1997; Paddock *et al.*, 1989; Trumpower, 1990b). Typically, one of these sites is primarily responsible for stabilizing the semiquinone radical whereas the other acts as the electron input/output site. One of the binding sites (Q_B) is in dynamic equilibrium with the quinone pool. The second site (Q_A) has a high affinity for ubiquinone, stabilizes a semiquinone species, and is located physically close to the immediate electron donor, e.g. center 3 of SDHs.

1.6.1. Structure and Properties of Quinones

How does the chemistry of ubiquinone relate to its biological functions? The structural and physicochemical properties of quinones are well-suited to their biological role. Ubiquinone is a 1,4-benzoquinone with one or more isoprenoid side chains (Fig. 1.12). In mammals, the most commonly occurring form of ubiquinone is ubiquinone-10 (Q-10), which contains 10 isoprene units (Trumpower, 1980; Trumpower and Katki, 1979). An exception is the occurrence of Q-9 in the rat. Ubiquinone-6, which occurs in certain yeasts including *S. cerevisiae*, is the shortest side-chain homologue found in nature. The hydrophobic nature of ubiquinone makes it difficult to use experimentally. Hence, ubiquinone analogs with shorter side chains, and consequently greater water solubility, are usually employed. A commonly used quinone analog is decylubiquinone, DB (Fig. 1.12).

It is the 1,4-ubiquinone nucleus that is mainly responsible for the redox properties of ubiquinone, while the various ring substituents confer additional physicochemical properties. Since the isoprenoid structure imposes strict limits on internal rotation about single bonds, it contributes to molecular rigidity rather than fluidity, contrary to popular belief. The extended dimensions of the Q-10 and the Q-6 molecules have been estimated to be 56 and 36 Å, respectively (Trumpower, 1980; Trumpower and Katki, 1979). Hence, natural ubiquinone molecules are comparable in length to the transverse dimensions of a simple phospholipid bilayer (40–50 Å).

Quinones are 2-electron acceptors/donors (Fig. 1.13). However, quinones can form semiquinone radicals, $Q^{\cdot}$, which allows them to transfer electrons in

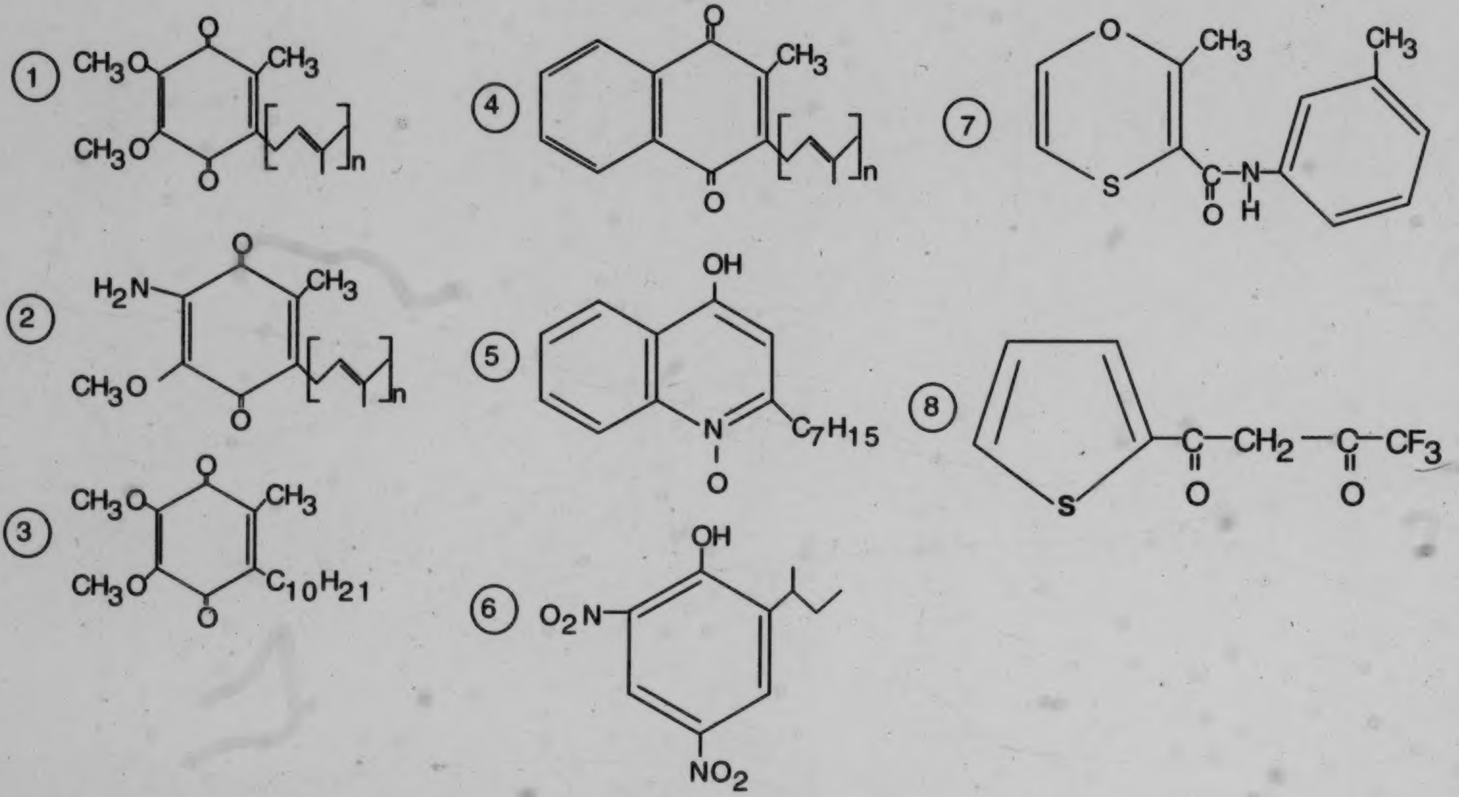

Figure 1.12 Structures of Quinones, Quinone Analogs, and Inhibitors.

1, Ubiquinone; 2, Rhodoquinone; 3, Decylubiquinone; 4, Menaquinone; 5, HQNO; 6, 2-*sec*-butyl-4,6-dinitrophenol; 7, 3′-methyl carboxin; 8, TTFA; n = 1–10.

Ubiquinone

Ubisemiquinone

Ubiquinol

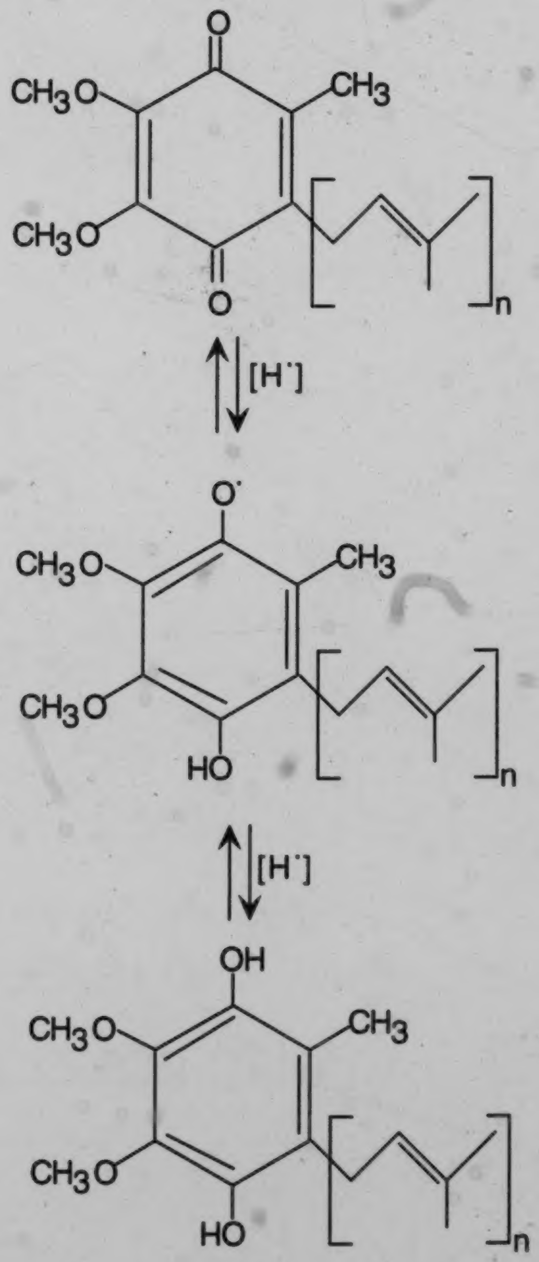
O
CH_3O
CH_3
CH_3O
O
n
$[H^{\cdot}]$
$O^{\cdot}$
CH_3O
CH_3
CH_3O
HO
n
$[H^{\cdot}]$
OH
CH_3O
CH_3
CH_3O
HO
n

Figure 1.13 The Oxidation States of Ubiquinone

discrete univalent steps (Mitchell, 1976). Experimental evidence indicates that long-lived ubisemiquinone radicals exist as intermediates in the electron transport chain (Ackrell *et al.*, 1992; de Vries *et al.*, 1981; de Vries *et al.*, 1980; Hägerhäll, 1997; Hederstedt and Ohnishi, 1992; Meinhardt *et al.*, 1987; Ohnishi and Trumpower, 1980; Trumpower and Gennis, 1994). Another molecular species of ubiquinone is the non-protonated, fully reduced form, UQ^{2-}, which has a transient existence in both the photosynthetic reaction center (Allen *et al.*, 1987b; Paddock *et al.*, 1989) and the cytochrome bc_1 complex (Trumpower and Gennis, 1994). The benzoquinone ring substituent may contribute to the stability of ubisemiquinone. The 2 methoxy groups increase semiquinone stability by resonance delocalization of the unpaired electrons of the carbonyl oxygens. The isoprenoid side chains may contribute to semiquinone stability by forming a 6-membered ring involving the carbonyl oxygen proximal to the side chain and the first isoprenoid double bond (Trumpower and Katki, 1979). This is supported by molecular orbital calculations (Breen, 1975). Therefore, it is very likely that protein ligands stabilize a ubisemiquinone radical by enhancing delocalization of the unpaired electron. Aromatic amino acid residues frequently found at the Q_A sites of bacterial RCs may perform such a role via π-π interactions with the benzoquinone ring. In the bacterial RCs, where the structures of quinone-binding sites have been solved to high-resolution, it is the two carbonyl oxygens of the benzoquinone ring that are involved in H-bonding with the polypeptide side chains (Allen *et al.*, 1987b; Paddock *et al.*, 1989).

1.6.2. Quinone-binding Sites in SDHs and FRDs

Although SDHs/FRDs are known to interact with quinones via the membrane anchor domains, little is known about the quinone-binding sites. To date, only a few membrane anchor polypeptides have been analyzed for quinone-binding pockets (Lee *et al.*, 1995; Shenoy *et al.*, 1997; Shenoy *et al.*, 1999;

Westenberg *et al.*, 1990; Westenberg *et al.*, 1993; Yang *et al.*, 1998). Even then, no common structural motif has emerged (Ackrell *et al.*, 1992; Hägerhäll, 1997; Hederstedt and Ohnishi, 1992; Van Hellemond and Tielens, 1994). The progress made on understanding the quinone interactions in the bc_1 complex has emphasized the utility of specific inhibitors and mutants (Colson, 1993; Link *et al.*, 1993). Similar approaches have been applied to the study of protein-quinone interactions in SDHs/FRDs. The quinone-binding sites are localized to the membrane domain and may resemble the Q_A and Q_B sites of bacterial photoreaction centers (Ackrell *et al.*, 1992; Hägerhäll, 1997; Hederstedt, 1998; Yankovskaya *et al.*, 1996). A dual-pathway model of electron transfer for SDH/FRD was proposed from thermodynamic considerations (Cammack *et al.*, 1986). Unlike the bacterial RCs where the 2 sites are located on the same side of the membrane (Allen *et al.*, 1987b; Paddock *et al.*, 1989), Q_A is thought to be proximal to the iron-sulfur center 3 in SDHs/FRDs and the Q_B site is thought to be distal. This asymmetric arrangement is reminiscent of the location of the Q_o and Q_i sites in complex III (Brandt, 1998; Colson, 1993; Trumpower, 1990a; Trumpower and Gennis, 1994).

Several inhibitors are known to interfere with quinone binding in succinate:quinone oxidoreductases (Fig. 1.12). The commonest are 2-thenoyltrifluoroacetone (TTFA), 3-methylcarboxin (a carboxanilide), 2-*n*-heptyl-4-hydroxyquinoline-*N*-oxide (HQNO) (Ackrell *et al.*, 1992; Hägerhäll, 1997), and, recently, 2-alkyl-4,6-dinitrophenols (Saitoh *et al.*, 1992; Yankovskaya *et al.*, 1996). There are variations in the sensitivities of the enzymes to these inhibitors, possibly reflecting differences in the quinone-binding pockets.

TTFA and carboxins are structurally related compounds that are potent inhibitors of the bovine SDH. These inhibitors have shown the existence of a quinone-binding site that is proximal to iron-sulfur center 3 (Ackrell *et al.*, 1992; Hägerhäll, 1997). EPR studies show that the inhibitors block reoxidation of reduced iron-sulfur center 3 with quinone but do not interfere with the reduction of the cluster by succinate (Ackrell *et al.*, 1977). This suggests that the inhibitors bind at a site that is distinct from, but very close to the quinone-binding site. A similar conclusion is indicated by the their mixed inhibition kinetics (Mowery *et al.*, 1977). In submitochondrial particles prepared from bovine heart mitochondria, TTFA was shown to quench the hyperfine splitting that originates from the semiquinone pair in SDH (Ingledew and Ohnishi, 1977; Salerno and Ohnishi, 1980). In addition, the inhibitor increased the signal amplitude of iron-sulfur center 3 and shifted its E_m. Taken together, these data show a close interaction between one or both of the quinone-binding sites and center 3. These observations have been confirmed and extended in the analyses of carboxin-resistant mutants of *Ustilago maydis* and *P. denitrificans*. A mutation in the *U. maydis* Sdh2 conferring resistance to carboxin was found to be a Leu to His substitution in the iron-sulfur cluster 3 ligation motif (Broomfield and Hargreaves, 1992; Keon *et al.*, 1994). The *P. denitrificans* mutant resistant to carboxin contains an Asp89—Gly substitution in the loop connecting predicted helices II and III of the SdhD subunit (Hägerhäll, 1997). This shows that both the anchor polypeptides and the Sdh2p subunits contribute to carboxin binding site and that the iron-sulfur cluster 3 is in close proximity to a quinone-binding site.

The 2-alkyl-4,6-dinitrophenol derivatives (Fig. 1.12) are well-established protonophore-type uncouplers (Miyoshi *et al.*, 1990). They have also been shown to inhibit all the mitochondrial electron-transport complexes except complex IV (Saitoh *et al.*, 1992), suggesting that they are universal inhibitors of quinone-mediated electron transport. The inhibition patterns and potencies differ depending on the respiratory complex and the nature of the 2-alkyl substituent. Based on the kinetics of inhibition by the 2-alkyl-4,6-dinitrophenol derivatives, two quinone-binding sites have been proposed for the bovine SDH and the *E. coli* FRD (Yankovskaya *et al.*, 1996). *s*-BDNP inhibits both enzymes in a noncompetitive, biphasic manner, which suggests the existence of two nonequivalent inhibitor binding sites. The noncompetitive inhibition kinetics indicate that *s*-BDNP may interact at a site separate from the quinone binding site and may sterically block electron exchange between the Q_A and Q_B sites. Molecular orbital calculation studies have shown that the α-branching conformation of the alkyl substituent at the 2-position, which is nearly perpendicular to the benzene ring, is similar to the isoprenoid side chain of ubiquinone (Saitoh *et al.*, 1992). It is possible that this stereochemical similarity contributes to the inhibitory potency of 2-alkyl-4,6-dinitrophenols.

The two-quinone binding site formulation is consistent with a number of observations. Photoaffinity labeling of the hydrophobic domain of the bovine SDH has shown that there are 2 quinone-binding pockets residing on opposite sides of the inner mitochondrial membrane (Lee *et al.*, 1995; Yu *et al.*, 1985). Similarly, a comprehensive search for quinone-binding sites was carried out in *E. coli* FRD (Westenberg *et al.*, 1990; Westenberg *et al.*, 1993). Residues involved in quinone interaction map to opposite sides of the membrane. Spectroscopic studies of *B. subtilis* SDH mutants and the inhibitory effect of HQNO support the existence of 2 quinone-binding sites (Smirnova *et al.*, 1995). One site is proximal to the iron-sulfur center 3, oriented toward the positive side of the membrane near heme b_H, while the other site is distal, close to heme b_L at the negative side of the membrane. Recently, the existence of two quinone-binding sites was demonstrated in the *P. denitrificans* SDH by EPR studies (Waldeck *et al.*, 1997). Exactly how the 2 quinone binding sites function in electron transfer has yet to be determined.

1.6.3 The Q_A and Q_B Sites of Bacterial Photosystems

The photosynthetic reaction center (RC) is an integral membrane pigment-protein complex that mediates the initial photochemical reactions in the conversion of light energy to chemical energy (Coleman and Youvan, 1990;

Deisenhofer and Michel, 1992; Okamura and Feher, 1992; Parson, 1996). Photosynthesis is remarkably similar to respiration. Both processes transduce energy via the generation of a transmembrane protonmotive force (Mitchell, 1969; Mitchell, 1977). In addition, the two processes share common redox cofactors like cytochromes, quinones, and iron-sulfur centers. The major difference between the two systems is the nature of the primary generator of protonmotive force (Δp). The RCs of purple bacteria, where light-induced electron transfer steps are coupled to proton transfer reactions, have been well characterized. High-resolution crystal structures have been obtained for RCs of *Rhodopseudomonas viridis* (Deisenhofer and Michel, 1989; Deisenhofer and Michel, 1995; El-Kabbani *et al.*, 1991) and *Rhodobacter sphaeroides* (Allen *et al.*, 1987a; Allen *et al.*, 1987b; Chirino *et al.*, 1994; Ermler *et al.*, 1994). The major structural elements of these RCs are a pair of polypeptides designated L (light) and M (medium), each of which has five transmembrane α-helices. A third polypeptide, H (heavy), adopts a more globular conformation and sits at the cytoplasmic surface of the membrane, but also has one transmembrane α-helix. In addition to the major polypeptides, the *Rb. sphaeroides* RC contains the following redox cofactors: four bacteriochlorophylls, two bacteriopheophytins, two ubiquinone molecules (Q_A and Q_B), one non-heme iron atom and the carotenoid, spheroidene. These associate with the L and M subunits in the membrane via non-covalent interactions.

The initial photochemical reactions involve the light-induced electron transfer from a primary electron donor, D (a bacteriochlorophyll dimer) through a series of univalent redox cofactors to the primary quinone, Q_A (Fig. 1.14). The electron is then transferred to a secondary quinone, Q_B. Subsequently, the doubly reduced quinone (Q_B^{2-}) accepts two protons, taken from the aqueous phase on the cytoplasmic side of the membrane, to form dihydroquinone (QH_2). The QH_2 is released into the membrane where it is reoxidized by the cytochrome bc_1 complex. The net reaction involves proton translocation from the cytoplasmic side to the

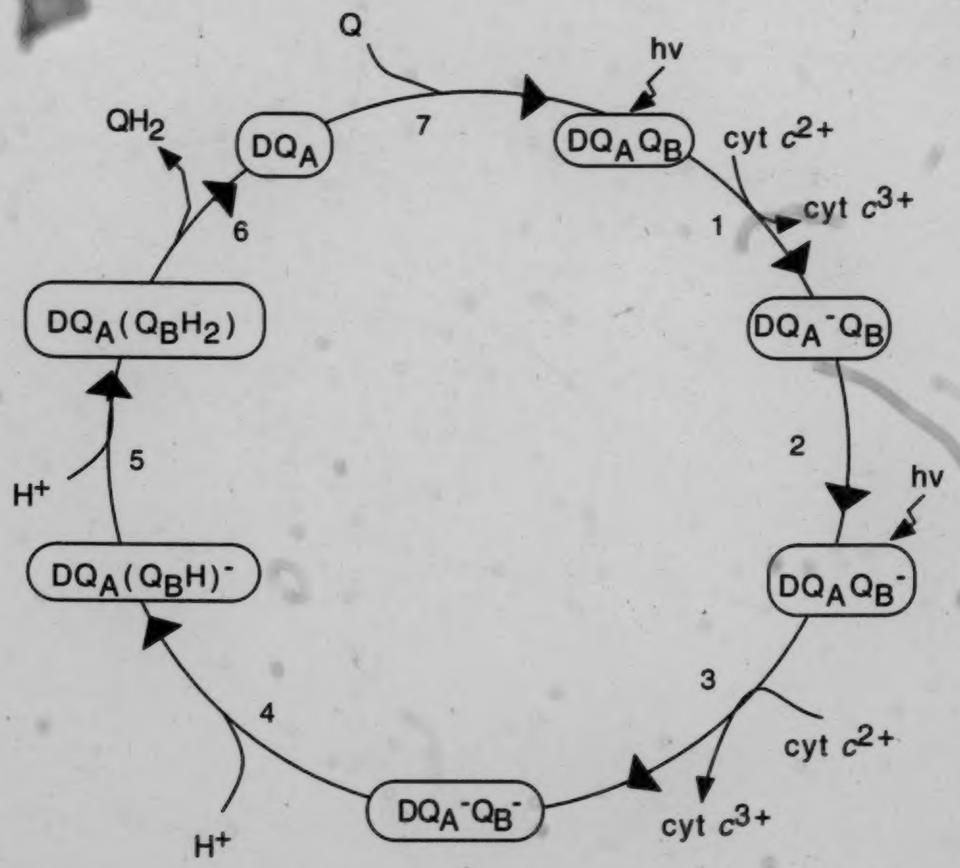
Q
hv
QH2
DQA
7
DQAQB
cyt c2+
cyt c3+
1
6
DQA(QBH2)
DQA-QB
2
hv
5
H+
DQA(QBH)-
DQAQB-
3
4
cyt c2+
DQA-QB-
cyt c3+
H+

Figure 1.14 Quinone-mediated Electron Transport in the Bacterial Reaction Center.

The sequence of reactions is indicated by numbers. Excitation of the special pair of bacteriochlorophyll dimer, D leads to the oxidation of cytochrome *c* (cyt *c*). The electron is first transferred to quinone bound at the Q_A site (1) and then to the Q_B site (2). A second photochemical oxidation of cytochrome *c* (3) leads to the reduction of Q_A. While the Q_A site can only accept one electron, the Q_B site functions as a 'two-electron gate', which after protonation (Q_BH_2) leaves its binding site and is re-oxidized by the cytochrome bc_1 complex.

periplasmic side of the plasma membrane. This generates a transmembrane electrochemical potential gradient that can drive the synthesis of ATP in accord with the chemiosmotic theory. Proton transfer to Q_B^{2-} is considered to be the primary step in the formation of the chemiosmotic potential. A model for Q-mediated electron transfer is depicted in Fig. 1.14 (Lancaster, 1998; Okamura and Feher, 1992). Electron transfer proceeds vectorially from Q_A to Q_B. Two successive electron transfer events and protonation convert a quinone to dihydroquinone. Q_A shuttles between the oxidized, Q, and the anionic semiquinone, $Q^{\cdot-}$ forms and never becomes fully reduced. In contrast, Q_B is doubly reduced and, after protonation, diffuses to the bulk quinone pool. Q_A and Q_B thus serve as a two-electron gate, converting the one-electron photochemical event into a two-electron transfer.

X-ray crystallographic structures of RCs have revealed amino acid residues forming the two quinone-binding pockets (Allen *et al.*, 1987a; Allen *et al.*, 1987b; Allen and Williams, 1998; El-Kabbani *et al.*, 1991; Ermler *et al.*, 1994; Paddock *et al.*, 1989). Generally, the Q_A environment is more hydrophobic than that of the Q_B and this contributes to the different functional properties of the two sites. Q_A is located near the cytoplasmic side of the RC. The two carbonyl oxygens of Q_A are within hydrogen-bonding distance of the peptide nitrogen of Ala M260 and the side chain of Thr M222 in *Rb. sphaeroides* (Allen *et al.*, 1987b; Paddock *et al.*, 1989). In the *Rp. viridis* RC, the carbonyl oxygens of Q_A (a menaquinone) form hydrogen bonds with the peptide nitrogen of Ala M258 (equivalent to M260 of *Rb. sphaeroides*) and the imidazole ring of His M217. In addition, several aromatic residues are located near Q_A. These include Phe M251 and Trp M252, which are conserved in all sequenced bacterial and plant photosystems (Deisenhofer and Michel, 1992). Trp M252 makes van der Waals contact with both Q_A and Phe M251. Similarly, Q_B is also located near the cytoplasmic side of the RC. In contrast to Q_A, Q_B interacts with several ionizable residues, making the environment more polar (Allen *et al.*, 1987b; Lancaster, 1998; Paddock *et al.*, 1989). Two carbonyl oxygens of Q_B are within hydrogen-bonding distance of $N_{\delta 1}$ of His L190 and the side chain of Ser L223. The latter residue is conserved in all bacterial and plant photosystems and has been altered in several herbicide-resistant RC mutants. Mutation of Ser L223 can confer resistance to triazine herbicides, which are believed to interact with the quinone-binding site (Deisenhofer and Michel, 1992). In addition, the acidic residues, Glu L212 (which is conserved across species), and Asp L213 are in van der Waals contact with the quinone ring. Mutation studies have shown that Glu L212 is involved in the protonation of Q_B (Paddock *et al.*, 1989). The acidic residues are thought to form a "bucket brigade" that aids the protonation of Q_B. Studies of the quinone-binding site of the *E. coli* FRD shows that Glu29, which is located in putative helix I of FrdC, may perform a similar role (Westenberg *et al.*, 1993).

1.7. Thesis Problem

Most of the information on the components involved in mitochondrial respiration has been accumulated using mammalian sources. However, the experimental advantages of using microbial systems have long been recognized (Lloyd, 1974). Such systems are amenable to facile genetic manipulations, allowing the study of structure-function relationships. *S. cerevisiae* is a good model system for studying the structural and functional properties of respiratory chain complexes. Being a facultative anaerobe, *S. cerevisiae* is able to grow on fermentable carbon sources, where SDH is not required or on nonfermentable carbon sources, where functional SDH is required. This feature allows the study of SDH and other respiratory complexes by mutational approaches. Moreover, *S. cerevisiae* grows rapidly and has a small, fully sequenced genome (Goffeau *et al.*, 1996). In addition, the ability to construct gene disruptions in *S. cerevisiae* with relative ease makes the organism an invaluable tool in determining the effects of mutations on protein function (Rothstein, 1991).

The *S. cerevisiae* SDH is composed of four subunits encoded by the nuclear *SDH1* (Chapman *et al.*, 1992; Robinson and Lemire, 1992; Robinson *et al.*, 1991; Schülke *et al.*, 1992), *SDH2* (Lombardo *et al.*, 1990), *SDH3* (Abraham *et al.*, 1994; Daignan-Fornier *et al.*, 1994), and *SDH4* (Bullis and Lemire, 1994) genes. Recently a gene encoding an isoform of the Sdh1p subunit, *SDH1b*, has been identified (Colby *et al.*, 1998). *SDH1b* gene can suppress the respiratory growth defect caused by a mutation in the *SDH1* gene. However, the expression level of *SDH1b* gene, as judged by β-galactosidase activities of *SDH1*- and *SDH1b-lacZ* fusions, is 100–500 times lower compared to that of *SDH1* gene. This indicates that the isoenzyme encoded by the *SDH1b* gene is unlikely to play a major role in mitochondrial respiration.

We are interested in several aspects of SDH structure and function. Does the *S. cerevisiae* SDH contain heme? What are the structural requirements of the membrane domain for anchoring, quinone interaction and electron transport? Undoubtedly, purified proteins will be invaluable tools in addressing such questions. Hence, my initial goal was to overexpress and purify recombinant SDH for detailed biochemical and biophysical studies. However, several attempts with heterologous and homologous expression systems were unsuccessful. The progress made with the bc_1 complex shows the importance of genetic approaches in structure-function studies (Colson, 1993). Therefore, we exploited similar approaches in studying the *S. cerevisiae* SDH.

It is generally believed that the *S. cerevisiae* SDH does not contain *b*-type heme (Hägerhäll, 1997; Hägerhäll and Hederstedt, 1996; Schilling *et al.*, 1982; Vibat *et al.*, 1998). However, recent reports show that *S. cerevisiae* SDH may interact with heme (Bruel *et al.*, 1996; Bruel *et al.*, 1995). Therefore, in Chapter 2 we address the question of whether or not the yeast enzyme contains a stoichiometric amount of heme. To do this, a property of the bovine cytochrome b_{560} was exploited. In the bovine SDH, excess fumarate rapidly oxidizes dithionite-reduced cytochrome b_{560} (Hatefi and Galante, 1980; Yu *et al.*, 1987). By exploiting this property, we determined the cytochrome *b* content of the yeast SDH in whole mitochondria and compared it with the covalent FAD content. In addition, a disruption mutant of the *SDH3* gene was constructed and characterized biochemically in order to gain insight into its role in anchoring, electron transfer, and heme binding.

Although the anchor polypeptides are known to be necessary for quinone interactions (Bullis and Lemire, 1994; Daignan-Fornier *et al.*, 1994), the structural requirements for such interactions have yet to be determined. Chapters 3, 4, and 5 address this question by random, directed, and deletion mutagenesis of the *SDH3* and *SDH4* genes. The mutants were characterized *in vivo* for respiratory growth, and *in vitro* for quinone reduction, enzyme assembly and stability, and sensitivity to a quinone analog inhibitor. These experiments lead to the identification of amino acid residues involved in quinone binding and/or reduction and the postulation of a two-quinone binding site for the yeast SDH.

1.8. Bibliography

Abraham, P. R., Mulder, A., van't Riet, J., and Raué, H. A. (1994). Characterization of the *Saccharomyces cerevisiae* nuclear gene *CYB3* encoding a cytochrome *b* polypeptide of respiratory complex II. *Mol. Gen. Genet.* **242,** 708-716.

Ackrell, B. A., Armstrong, F. A., Cochran, B., Sucheta, A., and Yu, T. (1993). Classification of fumarate reductases and succinate dehydrogenases based upon their contrasting behaviour in the reduced benzylviologen/fumarate assay. *FEBS Lett.* **326,** 92-94.

Ackrell, B. A., Ball, M. B., and Kearney, E. B. (1980). Peptides from complex II active in reconstitution of succinate-ubiquinone reductase. *J. Biol. Chem.* **255,** 2761-2769.

Ackrell, B. A., Kearney, E. B., and Edmondson, D. (1975). Studies on succinate dehydrogenase. XXVIII. Mechanism of reductive activation of succinate dehydrogenase. *J. Biol. Chem.* **250,** 7114-7119.

Ackrell, B. A. C., Cochran, B., and Cecchini, G. (1989). Interactions of oxaloacetate with Escherichia coli fumarate reductase. *Arch. Biochem. Biophys.* **268,** 26-34.

Ackrell, B. A. C., Johnson, M. K., Gunsalus, R. P., and Cecchini, G. (1992). Structure and function of succinate dehydrogenase and fumarate reductase. In Chemistry and biochemistry of flavoenzymes, F. Müller, ed. (Boca Raton, Florida: CRC Press, Inc.,), pp. 229-297.

Ackrell, B. A. C., Kearney, E. B., Coles, C. J., Singer, T. P., Beinert, H., Wan, Y. P., and Folkers, K. (1977). Kinetics of the reoxidation of succinate dehydrogenase. *Arch. Biochem. Biophys.* **182,** 107-117.

Addink, A. D., Boer, P., Wakabayashi, T., and Green, D. E. (1972). Enzyme localization in beef-heart mitochondria. A biochemical and electron-microscopic study. *Eur. J. Biochem.* **29,** 47-59.

AEvarsson, A., and Hederstedt, L. (1988). Ligands to the 2Fe iron-sulfur center in succinate dehydrogenase. *FEBS Lett.* **232,** 298-302.

Allen, J. P., Feher, G., Yeates, T. O., Komiya, H., and Rees, D. C. (1987a). Structure of the reaction center from *Rhodobacter sphaeroides* R-26: the cofactors. *Proc. Natl. Acad. Sci. USA* **84,** 5730-5734.

Allen, J. P., Feher, G., Yeates, T. O., Komiya, H., and Rees, D. C. (1987b). Structure of the reaction centre from *Rhodobacter sphaeroides* R-26, *the protein subunits. Proc. Natl. Acad. Sci. USA* **84,** 6162-6166.

Allen, J. P., and Williams, J. C. (1998). Photosynthetic reaction centers. *FEBS Lett.* **438,** 5-9.

Aquila, H., Link, T. A., and Klingenberg, M. (1987). Solute carriers involved in energy transfer of mitochondria from homologous protein family. *FEBS Lett.* **212,** 1-9.

Arikawa, Y., Enomoto, K., Muratsubaki, H., and Okazaki, M. (1998). Soluble fumarate reductase isoenzymes from *Saccharomyces cerevisiae* are required for anaerobic growth. *FEMS Microbiology Letters* **165,** 111-116.

Attardi, G., and Schatz, G. (1988). Biogenesis of Mitochondria. *Annu. Rev. Cell Biol.* **4,** 289-333.

Bechmann, G., Schulte, U., and Weiss, H. (1992). Mitochondrial ubiquinol-cytochrome *c* oxidoreductase. In Molecular mechanisms in bioenergetics, L. Ernster, ed. (New York: Elsevier Sciece Publishers), pp. 199-216.

Bixon, M., Jortner, J., and Michel-Beyerle, M. E. (1991). On the mechanism of the primary charge separation in bacterial photosynthesis. *Biochim. Biophys. Acta* **1056,** 301-315.

Blaut, M., Whittaker, K., Valdovinos, A., Ackrell, B. A. C., Gunsalus, R. P., and Cecchini, G. (1989). Fumarate reductase mutants of *Escherichia coli* that lack covalently bound flavin. *J. Biol. Chem.* **264,** 13599-13604.

Bonen, L. (1991). The mitochondrial genome: so simple yet so complex. *Curr. Opin. Genet. Dev.* **1,** 515-522.

Bousquet, I., Dujardin, G., and Slonimski, P. P. (1991). *ABC1*, a novel yeast nuclear gene has a dual function in mitochondria: it suppresses a cytochrome *b* mRNA translation defect and is essential for the electron transfer in the bc_1 complex. *EMBO J.* **10,** 2023-2031.

Brand, M. D., Reynafarje, B., and Lehninger, A. L. (1976). Re-evaluation of the H+/site ratio of mitochondrial electron transport with the oxygen pulse technique. *J. Biol. Chem.* **251,** 5670-5679.

Brandt, U. (1996). Bifurcated ubihydroquinone oxidation in the cytochrome bc_1 complex by proton-gated charge transfer. *FEBS Lett.* **387,** 1-6.

Brandt, U. (1997). Proton-translocation by membrane-bound NADH:ubiquinone-oxidoreductase (complex I) through redox-gated ligand conduction. *Biochim. Biophys. Acta* **1318,** 79-91.

Brandt, U. (1998). The chemistry and mechanics of ubihydroquinone oxidation at center P (Qo) of the cytochrome bc1 complex. *Biochim. Biophys. Acta* **1365,** 261-268.

Brandt, U., and Djafarzadeh-Andabili, R. (1997). Binding of MOA-stilbene to the mitochondrial cytochrome bc_1 complex is affected by the protonation state of a redox-Bohr group of the 'Rieske' iron-sulfur protein. *Biochim. Biophys. Acta* **1321,** 238-242.

Brandt, U., Haase, U., Schägger, H., and von Jagow, G. (1991). Significance of the "Rieske" iron-sulfur protein for formation and function of the ubiquinol-oxidation pocket of mitochondrial cytochrome *c* reductase (bc_1 complex). *J. Biol. Chem.* **266,** 19958-19964.

Brandt, U., Schägger, H., and von Jagow, G. (1988). Characterisation of binding of the methoxyacrylate inhibitors to mitochondrial cytochrome *c* reductase. *Eur. J. Biochem.* **173,** 499-503.

Brasseur, G., Tron, G., Dujardin, G., Slonimski, P. P., and Brivet-Chevillotte, P. (1997). The nuclear ABC1 gene is essential for the correct conformation and functioning of the cytochrome *bc*$_1$ complex and the neighbouring complexes II and IV in the mitochondrial respiratory chain. *Eur. J. Biochem.* **246,** 103-111.

Breen, D. L. (1975). Coenzyme Q: a molecular orbital study. *J. Theor. Biol.* **53,** 101-113.

Broomfield, P. L., and Hargreaves, J. A. (1992). A single amino-acid change in the iron-sulphur protein subunit of succinate dehydrogenase confers resistance to carboxin in *Ustilago maydis*. *Curr. Genet.* **22,** 117-121.

Brown, S., Colson, A. M., Meunier, B., and Rich, P. R. (1993). Rapid screening of cytochromes of respiratory mutants of *Saccharomyces cerevisiae*. Application to the selection of strains containing novel forms of cytochrome-c oxidase. *Eur. J. Biochem.* **213,** 137-145.

Bruel, C., Brasseur, R., and Trumpower, B. L. (1996). Subunit 8 of the *Saccharomyces cerevisiae* Cytochrome *bc*1 Complex Interacts with Succinate-Ubiquinone Reductase Complex. *J. Bioenerg. Biomembr.* **28,** 59-68.

Bruel, C., di Rago, J.-P., Slonimski, P. P., and Lemesle-Meunier, D. (1995). Role of the Evolutionarily Conserved Cytochrome *b* Tryptophan 142 in the Ubiquinol Oxidation Catalyzed by the *bc*1 Complex in the Yeast *Saccharomyces cerevisiae*. *J. Biol. Chem.* **270,** 22321-22328.

Bullis, B. L., and Lemire, B. D. (1994). Isolation and characterization of the *Saccharomyces cerevisiae SDH4* gene encoding a membrane anchor subunit of succinate dehydrogenase. *J. Biol. Chem.* **269,** 6543-6549.

Burger, G., Lang, B. F., Reith, M., and Gray, M. W. (1996). Genes encoding the same three subunits of respiratory complex II are present in the mitochondrial DNA of two phylogenetically distant eukaryotes. *Proc. Natl. Acad. Sci. USA* **93,** 2328-2332.

Calhoun, M. W., Thomas, J. W., and Gennis, R. B. (1994). The cytochrome oxidase superfamily of redox-driven proton pumps. *Trends Biochem. Sci.* **19,** 325-330.

Cammack, R., Crowe, B. A., and Cook, N. B. (1986). Dual-pathway models of electron transfer in succinate dehydrogenase and fumarate reductase. *Biochem. Soc. Trans.* **14,** 1207-1208.

Capaldi, R. A. (1990). Structure and function of cytochrome *c* oxidase. *Annu. Rev. Biochem.* **59,** 569-596.

Cecchini, G., Ackrell, B. A. C., Deshler, J. D., and Gunsalus, R. (1986a). Reconstitution of quinone reduction and characterization of *Escherichia coli* fumarate reductase activity. *J. Biol. Chem.* **261,** 1808-1814.

Cecchini, G., Thompson, C. R., Ackrell, B. A., Westenberg, D. J., Dean, N., and Gunsalus, R. P. (1986b). Oxidation of reduced menaquinone by the fumarate reductase complex in *Escherichia coli* requires the hydrophobic FrdD peptide. *Proc. Natl. Acad. Sci. USA* **83,** 8898-8902.

Chance, B. (1977). Electron transfer: pathways, mechanisms, and controls. *Annu. Rev. Biochem.* **46,** 967-980.

Chapman, K. B., Solomon, S. D., and Boeke, J. D. (1992). *SDH1*, the gene encoding the succinate dehydrogenase flavoprotein subunit from *Saccharomyces cerevisiae*. *Gene* **118,** 131-136.

Chazotte, B., and Hackenbrock, C. R. (1989). Lateral diffusion as a rate-limiting step in ubiquinone-mediated mitochondrial electron transport. *J. Biol. Chem.* **264,** 4978-4985.

Chirino, A. J., Lous, E. J., Huber, M., Allen, J. P., Schenck, C. C., Paddock, M. L., Feher, G., and Rees, D. C. (1994). Crystallographic analyses of site-directed mutants of the photosynthetic reaction center from *Rhodobacter sphaeroides*. *Biochemistry* **33,** 4584-4593.

Choudhry, Z. M., Gavrikova, E. V., Kotlyar, A. B., Tushurashvili, P. R., and Vinogradov, A. D. (1985). Pyridoxal phosphate-induced dissociation of the succinate: ubiquinone reductase. *FEBS Lett.* **182,** 171-175.

Colby, G., Ishii, Y., and Tzagoloff, A. (1998). Suppression of *SDH1* mutations by the *SDH1b* gene of *Saccharomyces cerevisiae*. *Yeast* **14,** 1001-1006.

Cole, S. T., Condon, C., Lemire, B. D., and Weiner, J. H. (1985). Molecular biology, biochemistry, and bioenergetics of fumarate reductase, a complex membrane-bound iron-sulfur flavoenzyme of *Escherichia coli*. *Biochim. Biophys. Acta* **811,** 381-403.

Cole, S. T., and Guest, J. R. (1980). Genetic and physical characterization of lambda transducing phages (lambda *frdA*) containing the fumarate reductase gene of *Escherichia coli* K12. *Mol. Gen. Genet.* **178,** 409-418.

Coleman, W. J., and Youvan, D. C. (1990). Spectroscopic analysis of genetically modified photosynthetic reaction centers. *Annu. Rev. Biophys. Biophys. Chem.* **19,** 333-367.

Colson, A.-M. (1993). Random mutant generation and its utility in uncovering structural and functional features of cytochrome *b* in *Saccharomyces cerevisiae*. *J. Bioenerg. Biomembr.* **25,** 211-220.

Condon, C., and Weiner, J. H. (1988). Fumarate reductase of *Escherichia coli*: an investigation of function and assembly using *in vivo* complementation. *Mol. Microbiol.* **2,** 43-52.

Crane, F. L. (1977). Hydroquinone dehydrogenases. *Annu. Rev. Biochem.* **46,** 439-469.

Crane, F. L., Hatefi, Y., Lester, R. L., and Widmer, C. (1957). Isolation of a quinone from beef-heart mitochondria. *Biochim. Biophys. Acta* **25,** 220.

Crofts, A. R., and Berry, E. A. (1998). Structure and function of the cytochrome bc_1 complex of mitochondria and photosynthetic bacteria. *Curr. Opin. Struct. Biol.* **8,** 501-509.

Crouse, B. R., Yu, C.-A., Yu, L., and Johnson, M. K. (1995). Spectroscopic identification of the axial ligands of cytochrome b_{560} in bovine heart succinate-ubiquinone reductase. *FEBS Lett.* **367,** 1-4.

Crowe, B. A., Owen, P., Patil, D. S., and Cammack, R. (1983). Characterization of succinate dehydrogenase from *Micrococcus luteus* (*lysodeikticus*) by electron-spin-resonance spectroscopy. *Eur. J. Biochem.* **137,** 191-196.

Daignan-Fornier, B., Valens, M., Lemire, B. D., and Bolotin-Fukuhara, M. (1994). Structure and regulation of *SDH3*, the yeast gene encoding the cytochrome b_{560} subunit of respiratory complex II. *J. Biol. Chem.* **269,** 15469-15472.

Darlison, M. G., and Guest, J. R. (1980). Nucleotide sequence encoding the iron-sulfur protein subunit of the succinate dehydrogenase of *Escherichia coli*. *Biochem. J.* **223,** 507-517.

Davis, K. A., Hatefi, Y., Poff, K. L., and Butler, W. L. (1973). The *b*-type cytochromes of bovine heart mitochondria: absorption spectra, enzymatic properties, and distribution in the electron transfer complexes. *Biochim. Biophys. Acta* **325,** 341-356.

de Vries, S., Albracht, S. P. J., Berden, J. A., and Slater, É. C. (1981). A new species of bound ubisemiquinone anion in QH_2: cytochrome *c* oxidoreductase. *J. Biol. Chem.* **256,** 11996-11998.

de Vries, S., Berden, J. A., and Slater, E. C. (1980). Properties of a semiquinone anion located in the QH_2:cytochrome *c* oxidoreductase segment of the mitochondrial respiratory chain. *FEBS Lett.* **122,** 143-148.

de Vries, S., and Marres, C. A. M. (1987). The mitochondrial respiratory chain of yeast. Structure and biosynthesis and the role in cellular metabolism. *Biochim. Biophys. Acta* **895,** 205-239.

de Vries, S., Van Witzernburg, R., Grivell, L. A., and Marres, C. A. M. (1992). Primary structure and import pathway of the rotenone-insensitive NADH-ubiquinone oxidoreductase of mitochondria from *Saccharomyces cerevisiae*. *Eur. J. Biochem.* **203,** 587-592.

Decker, K. F. (1993). Biosynthesis and function of enzymes with covalently bound flavin. *Annu. Rev. Nutr.* **13,** 17-41.

Degli Esposti, M. (1998). Inhibitors of NADH-ubiquinone reductase: an overview. *Biochim. Biophys. Acta* **1364,** 222-235.

Degli Esposti, M., De Vries, S., Crimi, M., Ghelli, A., Patarnello, T., and Meyer, A. (1993). Mitochondrial cytochrome *b*: evolution and structure of the protein. *Biochim. Biophys. Acta* **1143,** 243-271.

Degli Esposti, M., and Ghelli, A. (1994). The mechanism of proton and electron transport in mitochondrial complex I. *Biochim. Biophys. Acta* **1187,** 116-120.

Deisenhofer, J., and Michel, H. (1989). The photosynthetic reaction center from the purple bacterium *Rhodopseudomonas viridis*. *Science* **254,** 1463-1473.

Deisenhofer, J., and Michel, H. (1992). High-resolution crystal structures of bacterial photosynthetic reaction centers. In Molecular mechanisms in bioenergetics, L. Ernster, ed. (Armsterdam: Elsevier Science Publishers B. V.), pp. 103-120.

Deisenhofer, J., and Michel, H. (1995). Crystallographic refinement at 2.3 Å resolution and refined model of the photosynthetic reaction center from *Rhodopseudomonas viridis*. *J. Mol. Biol.* **246,** 429-457.

Dibrov, E., Fu, S., and Lemire, B. D. (1998). The *Saccharomyces cerevisiae TCM62* gene encodes a chaperone necessary for the assembly of the mitochondrial succinate dehydrogenase (complex II). *J. Biol Chem.* **273,** 32042-32048.

Ding, H., Moser, C. C., Robertson, D. E., Tokito, M. K., Daldal, F., and Dutton, P. L. (1995). Ubiquinone pair in the Qo site central to the primary energy conversion reactions of cytochrome bc_1 complex. *Biochemistry* **34,** 15979-15996.

Ding, H., Robertson, D. E., Daldal, F., and Dutton, P. L. (1992). Cytochrome bc_1 complex [2Fe-2S] cluster and its interaction with ubiquinone and ubihydroquinone at the Qo site: a double-occupancy Qo site model. *Biochemistry* **31,** 3144-3158.

Dutton, P. L., Moser, C. C., Sled, V. D., Daldal, F., and Ohnishi, T. (1998). A reductant-induced oxidation mechanism for complex I. *Biochim. Biophys. Acta* **1364,** 245-257.

Edmondson, D. E., and Singer, T. P. (1973). Oxidation-reduction properties of 8α-substituted flavins. *J. Bio. Chem.* **248,** 8144-8149.

El-Kabbani, O., Chang, C. H., Tiede, D., Norris, J., and Schiffer, M. (1991). Comparison of reaction centers from *Rhodobacter sphaeroides* and

Rhodopseudomonas viridis: overall architecture and protein-pigment interactions. *Biochemistry* **30,** 5361-5369.

Enomoto, K., Ohki, R., and Muratsubaki, H. (1996). Cloning and sequencing of the gene encoding the soluble fumarate reductase from *Saccharomyces cerevisiae*. *DNA Research* **3,** 263-267.

Erecinska, M., Chance, B., Wilson, D. F., and Dutton, P. L. (1972). Aerobic reduction of cytochrome b_{566} in pigeon-heart mitochondria (succinate-cytochrome c_1 reductase-stopped-flow kinetics). *Proc. Natl. Acad. Sci. U.S.A.* **69,** 50-54.

Ermler, U., Fritzsh, G., Buchanan, S. K., and Michel, H. (1994). Structure of the photosynthetic reaction center from *Rhodobacter sphaeroides* at 2.65 Å resolution: cofactors and protein-cofactor interactions. *Structure* **2,** 925-936.

Escobar Galvis, M. L., Allen, J. F., and Hakansson, G. (1998). Protein synthesis by isolated pea mitochondria is dependent on the activity of respiratory complex II. *Curr. Genet.* **33,** 320-329.

Fearnley, I. M., and Walker, J. E. (1993). Conservation of sequences of subunits of mitochondrial complex I and their relationships with other proteins. *Biochim. Biophys. Acta* **1140,** 105-134.

Finel, M. (1993). The proton-translocating NADH: ubiquinone oxidoreductase : a discussion of selected topics. *J. Bioenerg. Biomembr.* **25,** 357-366.

Finel, M. (1998). Organization and evolution of structural elements within complex I. *Biochim. Biophys. Acta* **1364,** 112-121.

Fridén, H., and Hederstedt, L. (1990). Role of His residues in *Bacillus subtilis* cytochrome *b*558 for haem binding and assembly of succinate:quinone oxidoreductase (complex 11). *Mol. Microbiol.* **4,** 1045-1056.

Fridén, H., Rutberg, L., Magnusson, K., and Hederstedt, L. (1987). Genetic and biochemical characterization of *Bacillus subtilis* mutants defective in expression and function of cytochrome b_{558}. *Eur. J. Biochem.* **168,** 695-701.

Friedrich, T., Abelmann, A., Brors, B., Guenebaut, V., Kintscher, L., Leonard, K., Rasmussen, T., Scheide, D., Schlitt, A., Schulte, U., and Weiss, H. (1998). Redox components and structure of the respiratory NADH:ubiquinone oxidoreductase (complex I). *Biochim. Biophys. Acta* **1365,** 215-219.

Friedrich, T., Stenmüller, K., and Weiss, H. (1995). The proton-pumping respiratory complex I of bacteria and mitochondria and its homologue in chloroplasts. *FEBS Lett.* **367,** 107-111.

Friedrich, T., Weidner, U., Nehls, U., Fecke, W., Schneider, R., and Weiss, H. (1993). Attempts to define distinct parts of NADH:ubiquinone oxidoreductase (complex I). *J. Bioenerg. Biomembr.* **25,** 331-337.

Friedrich, T., Weiss, H., Hirst, J., Ackrell, B. A. C., and Armstrong, F. A. (1997). Modular evolution of the respiratory NADH-ubiquinone oxidoreductase and the origin of its modules. Global observation of hydrogen/deuterium isotope effects on bidirectional catalytic electron transport in an Enzyme: Direct measurement by protein film voltammetry. *J. Theor. Biol.* **187,** 529-540.

Girdlestone, J., Bisson, R., and Capaldi, R. A. (1981). Interaction of succinate-ubiquinone reductase (complex II) with aryloazido-phospholipids. *Biochemistry* **20,** 152-156.

Goffeau, A., Barrell, B. G., Bussey, H., Davis, R. W., Dujon, B., Feldmann, H., Galibert, F., Hoheisel, J. D., Jacq, C., Johnston, M., Louis, E. J., Mewes, H. W., Murakami, Y., Philippsen, P., Tettelin, H., and Oliver, S. G. (1996). Life with 6000 genes. *Science* **274,** 546, 563-567.

Gray, H. B., and Winkler, J. R. (1996). Electron transfer in proteins. *Annu. Rev. Biochem.* **65,** 537-561.

Gray, M. W. (1993). Origin and evolution of organelle genomes. *Curr. Opin. Genet. Dev.* **3,** 884-890.

Grivell, L. A. (1995). Nucleo-Mitochondrial Interactions in Mitochondrial Gene Expression. *Crit. Rev. Biochem. Mol. Biol.* **30,** 121-164.

Guénebaut, V., Schlitt, A., Weiss, H., Leonard, K., and Friedrich, T. (1998). Consistent structure between bacterial and mitochondrial NADH:ubiquinone oxidoreductase (complex I). *J. Mol. Biol.* **276,** 105-112.

Guest, J. R. (1981). Partial replacement of succinate dehydrogenase function in phage and plasmid-specified fumarate reductase in *Escherichia coli*. *J. Gen. Microbiol.* **32,** 5455-5465.

Gupte, S. S., and Hackenbrock, C. R. (1988a). Multidimensional diffusion modes and collision frequencies of cytochrome *c* with its redox partners. *J. Biol. Chem.* **263,** 5241-5247.

Gupte, S. S., and Hackenbrock, C. R. (1988b). The role of cytochrome *c* diffusion in mitochondrial electron transport. *J. Biol, Chem.* **263,** 5248-5253.

Hägerhäll, C. (1997). Succinate:quinone Oxidoreductases: Variations on a conserved theme. *Biochim. Biophys. Acta* **1320,** 107-141.

Hägerhäll, C., Fridén, H., Aasa, R., and Hederstedt, L. (1995). Transmembrane topology and axial ligands to hemes in the cytochrome *b* subunit of *Bacillus subtilis* succinate:menaquinone reductase. *Biochemistry* **34,** 11080-11089.

Hägerhäll, C., and Hederstedt, L. (1996). A structural model for the membrane-integral domain of succinate:quinone oxidoreductases. *FEBS Lett.* **389,** 25-31.

Hatefi, Y. (1985). The mitochondrial electron transport and oxidative phosphorylation system. *Annu. Rev. Biochem.* **54,** 1015-1069.

Hatefi, Y., and Galante, Y. M. (1980). Isolation of Cytochrome b_{560} from Complex 11 (Succinate:Ubiquinone Oxidoreductase) and Its Reconstitution with Succinate Dehydrogenase. *J. Biol. Chem.* **255,** 5530-5537.

He, S. H., DerVartanian, D. V., and LeGall, J. (1986). Isolation of fumarate reductase from *Desulfovibrio multispirans*, a sulfate reducing bacterium. *Biochem. Biophys. Research. Commun.* **135,** 1000-10007.

Hederstedt, L. (1998). The membrane-integral domain of succinate:quinone oxidoreductases-a secretive haem-containing domain. *Biochem. Soc. Transactions* **26,** 408-413.

Hederstedt, L., Bergman, T., and Jörnvall, H. (1987). Processing of *Bacillus subtilis* succinate dehydrogenase and cytochrome b_{558} polypeptides. Lack of covalently bound flavin in the *Bacillus* enzyme expressed in *Escherichia coli*. *FEBS Lett.* **213,** 385-390.

Hederstedt, L., Magnusson, K., and Rutberg, L. (1982). Reconstitution of succinate dehydrogenase in *Bacillus subtilis* by protoplast fusion. *J. Bacteriol.* **152,** 157-165.

Hederstedt, L., and Ohnishi, T. (1992). Progress in Succinate:quinone Oxidoreductase Research. In Molecular mechanisms in bioenergetics, L. Ernster, ed. (New York: Elsevier Science Publishers), pp. 163-197.

Hederstedt, L., and Rutberg, L. (1980). Biosynthesis and membrane binding of succinate dehydrogenase in *Bacillus subtilis*. *J. Bacteriol.* **144,** 941-951.

Hederstedt, L., and Rutberg, L. (1981). Succinate dehydrogenase-a comparative review. *Microbiol. Rev.* **45,** 542-555.

Hederstedt, L., and Rutberg, L. (1983). Orientation of succinate dehydrogenase and cytochrome b_{558} in the *Bacillus subtilis* cytoplasmic membrane. *J. Bacteriol.* **153,** 57-65.

Heering, H. A., Weiner, J. H., and Armstrong, F. A. (1997). Direct detection and measurement of electron relays in a multicentered enzyme: Voltammetry of electrode-surface films of *E. coli* fumarate reductase, an iron-sulfur flavoprotein. *J. Am. Chem. Soc.* **119,** 11628-11638.

Hofhaus, G., Weiss, H., and Leonard, K. (1991). Electron microscopic analysis of the peripheral and membrane parts of mitochondrial NADH dehydrogenase (complex I). *J. Mol. Biol.* **221,** 1027-1043.

Ingledew, W. J., and Ohnishi, T. (1977). The probable site of action of thenoyltrifluoroacetone on the respiratory chain. *Biochem. J.* **164,** 617-620.

Ishii, N., Fujii, M., Hartman, P. S., Tsuda, M., Yasuda, K., Senoo-Matsuda, N., Yanase, S., Ayusawa, D., and Suzuki, K. (1998). A mutation in succinate dehydrogenase cytochrome *b* causes oxidative stress and ageing in nematodes. *Nature* **394,** 694-697.

Iwata, S., Lee, J. W., Okada, K., Lee, J. K., Iwata, M., Rasmussen, B., Link, T. A., Ramaswamy, S., and Jap, B. K. (1998). Complete structure of the 11-subunit bovine mitochondrial cytochrome bc_1 complex. *Science* **281,** 64-71.

Iwata, S., Ostermeier, C., Ludwig, B., and Michel, H. (1995). Structure at 2.8 Å resolution of cytochrome *c* oxidase from *Paracoccus denitrificans. Nature* **376,** 660-669.

Jap, B. K., and Walian, P. J. (1990). Biophysics of the structure and function of porins. *Quart. Rev. Biophys.* **23,** 367-403.

Johnson, M. K., Kowal, A. T., Morningstar, J. E., Oliver, M. E., Whittaker, K., Gunsalus, R. P., Ackrell, B. A., and Cecchini, G. (1988). Subunit location of the iron-sulfur clusters in fumarate reductase from *Escherichia coli. J. Biol. Chem.* **263,** 14732-14738.

Karpefors, M., Adelroth, P., Aagaard, A., Sigurdson, H., Svensson Ek, M., and Brzezinski, P. (1998). Electron-proton interactions in terminal oxidases. *Biochim. Biophys. Acta* **1365,** 159-169.

Keon, J. P., Broomfield, P. L., White, G. A., and Hargreaves, J. A. (1994). A mutant form of the succinate dehydrogenase iron-sulphur protein subunit confers resistance to carboxin in the maize smut pathogen *Ustilago maydis. Biochem. Soc. Trans.* **22,** 234-237.

Kim, H., Xia, D., Yu, C. A., Xia, J. Z., Kachurin, A. M., Zhang, L., Yu, L., and Deisenhofer, J. (1998). Inhibitor binding changes domain mobility in the iron-sulfur protein of the mitochondrial bc_1 complex from bovine heart. *Proc. Natl. Acad. Sci. USA* **95,** 8026-8033.

Kita, K., Hirawake, H., and Takamiya, S. (1997). Cytochromes In the Respiratory Chain of Helminth Mitochondria. *Int. J. Parasitol.* **27,** 617-630.

Kita, K., Takamiya, S., Furushima, R., Ma, Y. C., Suzuki, H., Ozawa, T., and Oya, H. (1988). Electron-transfer complexes of *Ascaris suum* muscle mitochondria. III. Composition and fumarate reductase activity of complex II. *Biochim. Biophys. Acta* **935,** 130-140.

Kita, K., Vibat, C. R., Meinhardt, S., Guest, J. R., and Gennis, R. B. (1989). One-step purification from *Escherichia coli* of complex II (succinate: ubiquinone oxidoreductase) associated with succinate-reducible cytochrome b_{556}. *J. Biol. Chem.* **264,** 2672-2677.

Klingenberg, M. (1970). Localization of the glycerol-phosphate dehydrogenase in the outer phase of the mitochondrial inner membrane. *Eur. J. Biochem.* **13,** 247-252.

Knaff, D. B. (1993). The cytochrome bc_1 complexes of photosynthetic purple bacteria. *Photosynth. Rs.* **35,** 117-133.

Korman, E. F., Addink, A. D., Wakabayashi, T., and Green, D. E. (1970). A unified model of mitochondrial morphology. *J. Bioenerg.* **1,** 9-32.

Kotlyar, A. B., and Vinogradov, A. D. (1984a). Evidence for an essential arginine residue in the substrate binding site of the mammalian succinate dehydrogenase. *Biochem. Int.* **8,** 545-552.

Kotlyar, A. B., and Vinogradov, A. D. (1984b). Interaction of the membrane-bound succinate dehydrogenase with substrate and competitive inhibitors. *Biochim. Biophys. Acta* **784,** 24-34.

Kowal, A. T., Werth, M. T., Manodori, A., Cecchini, G., Schröder, I., Gunsalus, R. P., and Johnson, M. K. (1995). Effect of cysteine to serine mutations on the properties of the [4Fe-4S] center in *Escherichia coli* fumarate reductase. *Biochemistry* **34,** 12284-12293.

Krämer, R., and Palmieri, F. (1992). Metabolite carriers in mitochondria. In Molecular mechanisms in bioenergetics, L. Ernster, ed. (New York: Elsevier Science Publishers), pp. 359-384.

Krishnamoorthy, G., and Hinkle, P. C. (1988). Studies on the electron transfer pathway, topography of iron-sulfur centers, and site of coupling in NADH-Q oxidoreductase. *J. Biol. Chem.* **263,** 17566-17575.

Lancaster, C. R. D. (1998). Ubiquinone reduction and protonation in the photosynthetic reaction centers from *Rhodopseudomonas viridis*: x-ray structures and their functional implications. *Biochim. Biophys. Acta* **1365,** 143-150.

Larsson, S. (1998). Electron transfer in proteins. *Biochim. Biophys. Acta* **1365,** 294-300.

Latour, D. J., and Weiner, J. H. (1989). Assembly of *Escherichia coli* fumarate reductase holoenzyme. *Biochem. Cell Biol.* **67,** 251-259.

Lederer, F. (1991). Flavocytochrome b_2. In chemistry and biochemistry of the flavoenzymes, f. Muller, ed. (Boca Raton, Florida: CRC Press), pp. 153-242.

Lee, G. Y., He, D.-Y., Yu, L., and Yu, C.-A. (1995). Identification of the ubiquinone-binding domain in QPs1 of succinate-ubiquinone reductase. *J. Biol. Chem.* **270,** 6193-6198.

Lee, G. Y., Zhu, J., Yu, L., and Yu, C.-A. (1998). Reconstitution of cytochrome b_{560} (QPs1) of bovine heart mitochondrial succinate-ubiquinone reductase. *Biochim. Biophys. Acta* **1363,** 35-46.

Lemire, B. D., Robinson, J. J., Bradley, R. D., Scraba, D. G., and Weiner, J. H. (1983). Structure of fumarate reductase on the cytoplasmic membrane of *Escherichia coli*. *J. Bacteriol.* **155,** 391-397.

Lemire, B. D., Robinson, J. J., and Weiner, J. H. (1982). Identification of Membrane Anchor Polypeptides of *Escherichia coli* Fumarate Reductase. *J. Bacteriol.* **152,** 1126-1131.

Lemma, E., Hagerhall, C., Geisler, V., Brandt, U., von Jagow, G., and Kroger, A. (1991). Reactivity of the *Bacillus subtilis* succinate dehydrogenase complex with quinones. *Biochim. Biophys. Acta* **1059,** 281-285.

Lenaz, G. (1998). Quinone specificity of Complex I. *Biochim. Biophys. Acta* **1364,** 207-221.

Link, T. A., Hasse, U., Brandt, U., and von Jagow, G. (1993). What information do inhibitors provide about the structure of the hydroquinone oxidation site of ubihydroquinone:cytochrome *c* oxidoreductase? *J. Bioenerg. Biomembr.* **25,** 221-232.

Lloyd, D. (1974). Respiration and the respiratory components in mitochondria of microorganisms. In The mitochondria of microorganisms (New York: Academic Press), pp. 82-158.

Lohmeier, E., Hagen, D. S., and Weiner, J. H. (1981). Cloning and expression of fumarate reductase gene of *Escherichia coli*. *Can. J. Biochem.* **59,** 158-164.

Lombardo, A., Carine, K., and Scheffler, I. E. (1990). Cloning and characterization of the iron-sulfur subunit gene of succinate dehydrogenase from *Saccharomyces cerevisiae*. *J. Biol. Chem.* **265,** 10419-10423.

Maguire, J. J., Magnusson, K., and Hederstedt, L. (1986). *Bacillus subtilis* mutant succinate dehydrogenase lacking covalently bound flavin: identification of the primary defect and studies on the iron-sulfur clusters in mutated and wild-type enzyme. *Biochemistry* **25,** 5202-5208.

Maklashina, E., Berthold, D. A., and Cecchini, G. (1998). Anaerobic expression of *Escherichia coli* succinate dehydrogenase: functional replacement of fumarate reductase in the respiratory chain during anaerobic growth. *J. Bacteriol.* **180,** 5989-5996.

Manodori, A., Cecchini, G., Schroder, I., Gunsalus, R. P., Werth, M. T., and Johnson, M. K. (1992). [3Fe-4S] to [4Fe-4S] cluster conversion in *Escherichia coli* fumarate reductase by site-directed mutagenesis. *Biochemistry* **31,** 2703-2712.

McEwen, J. E., Ko, C., Kloeckner-Gruissem, B., and Poyton, R. O. (1986). Nuclear functions required for cytochrome *c* oxidase biogenesis in *Saccharomyces cerevisiae*. Characterization of mutants in 34 complementation groups. *J. Biol. Chem.* **261,** 11872-11879.

Meinhardt, S. W., Yang, X., Trumpower, B. L., and Onishi, T. (1987). Identification of a stable ubisemiquinone and characterization of the effects of ubiquinone oxidation-reduction status on the Rieske iron-sulfur protein in the three-subunit ubiquinol-cytochrome *c* oxidoreductase complex of *Paracoccus denitrificans*. *J. Biol. Chem.* **262,** 8702-8706.

Merli, A., Capaldi, R. A., Ackrell, B. A. C., and Kearney, E. B. (1979). Arrangement of complex II (succinate-ubiquinone reductase) in the mitochondrial inner membrane. *Biochemistry* **18,** 1393-1400.

Mewies, M., McIntire, W. S., and Scrutton, N. S. (1998). Covalent attachment of flavin adenine dinucleotide (FAD) and flavin mononucleotide (FMN) to enzymes: The current state of affairs. *Protein Sci.* **7,** 7-20.

Michel, H., Behr, J., Harrenga, A., and Kannt, A. (1998). Cytochrome *c* oxidase: structure and spectroscopy. *Ann. Rev. Biophys. Biomol. Struct.* **27,** 329-356.

Mitchell, P. (1961). Coupling of phosphorylation to electron and proton transfer by a chemiosmotic type of mechanism. *Nature* **191,** 144-148.

Mitchell, P. (1969). Chemiosmotic coupling and energy transduction. *Theor. Exp. Biophys.* **2,** 159-216.

Mitchell, P. (1976). Possible molecular mechanisms of the protonmotive function of cytochrome systems. *J. Theor. Biol.* **62,** 327-367.

Mitchell, P. (1977). Vectorial chemiosmotic processes. *Annu. Rev. Biochem.* **46,** 996-1005.

Mitchell, P. (1987). Respiratory chain systems in theory and practice. In Advances in membrane biochemistry and bioenergetics, C. H. Kim, H. Tedeschi, J. J. Diwan and J. C. Salerno, eds. (New York: Plenum), pp. 25-52.

Mitchell, R., West, I. C., Moody, A. J., and Mitchell, P. (1986). Measurement of the proton-motive stoichiometry of the respiratory chain of rat liver mitochondria: the effect of N-ethylmaleimide. *Biochim. Biophys. Acta* **849,** 229-235.

Miyoshi, H. (1998). Structure-activity relationships of some complex I inhibitors. *Biochim. Biophys. Acta* **1364,** 236-244.

Miyoshi, H., Tsujishita, H., Tokutake, N., and Fujita, T. (1990). Quantitative analysis of uncoupling activity of substituted phenols with physicochemical substituent and molecular parameters. *Biochim. Biophys. Acta* **1016,** 99-106.

Moll, R., and Schäfer, G. (1991). Purification and characterisation of an archaebacterial succinate dehydrogenase complex from the plasma membrane of the thermoacidophile *Sulfolobus acidocaldarius*. *Eur. J. Biochem.* **201,** 593-600.

Møller, I. M., Rasmusson, A. G., and Fredlund, K. M. (1993). NAD(P)H-ubiquinone oxidoreductases in plant mitochondria. *J. Bioenerg. Biomembr.* **25,** 377-384.

Moore, A. L., Bonner, W. D. J., and Rich, P. R. (1978). The determination of the protonmotive force during cyanide insensitive respiration in plant mitochondria. *Arch. Biochem. Biophys.* **186,** 298-306.

Moser, C. C., and Dutton, P. L. (1996). Outline of theory of protein electron transfer. In Protein electron transfer, D. S. Bendall, ed. (Oxford, UK: BIOS Scientific Publishers), pp. 1-21.

Mowery, P. C., Steenkamp, D. J., Ackrell, A. C., Singer, T. P., and White, G. A. (1977). Inhibition of mammalian succinate dehydrogenase by carboxins. *Arch. Biochem. Biophys.* **178,** 495-506.

Muratsubaki, H., and Enomoto, K. (1998). One of the fumarate reductase isoenzymes from *Saccharomyces cerevisiae* is encoded by the OSM1 gene. *Arch. Biochem. Biophys.* **352,** 175-181.

Nakamura, K., Yamaki, M., Sarada, M., Nakayama, S., Vibat, C. R., Gennis, R. B., Nakayashiki, T., Inokuchi, H., Kojima, S., and Kita, K. (1996). Two hydrophobic subunits are essential for the heme *b* ligation and functional assembly of complex II (succinate-ubiquinone oxidoreductase) from *Escherichia coli*. *J. Biol. Chem.* **271,** 521-527.

Neupert, W. (1997). Protein import into mitochondria. *Annu. Rev. Biochem.* **66,** 863-917.

Nicholls, D. G., and Ferguson, S. J. (1992). Respiratory chains. In Bioenergetics 2 (New New York: Academic Press), pp. 107-154.

Ohnishi, T. (1987). Structure of the succinate-ubiquinone oxidoreductase (Complex II). *Curr. Top. Bioenerg.* **15,** 37-65.

Ohnishi, T., King, T. E., Salerno, J. C., Blum, H., Bowyer, J. R., and Maida, T. (1981). Thermodynamic and electron paramagnetic resonance characterization of flavin in succinate dehydrogenase. *J. Biol. Chem.* **256,** 5577-5582.

Ohnishi, T., and Trumpower, B. L. (1980). Differential effects of antimycin on ubisemiquinone bound in different environments in isolated succinate-cytochrome c reductase complex. *J. Biol. Chem.* **255,** 3278-3284.

Okamura, M. Y., and Feher, G. (1992). Proton transfer in reaction centers from photosynthetic bacteria. *Annu. Rev. Biochem.* **61,** 861-896.

Ostermeier, C., Harrenga, A., Ermler, U., and Michel, H. (1997). Structure at 2.7 Å resolution of the *Paracoccus denitrificans* two-subunit cytochrome *c* oxidase complexed with an antibody FV fragment. *Proc. Natl. Acad. Sci. USA* **94,** 10547-10553.

Packer, L. (1974). Membrane structure in relation to function of energy-transducing organelles. *Ann. N. Y. Acad. Sci.* **227,** 166-174.

Paddock, M. L., Rongey, S. H., Feher, G., and Okamura, M. Y. (1989). Pathway of proton transfer in bacterial reaction centers: replacement of glutamic acid 212 in the L subunit by glutamine inhibits quinone (secondary acceptor) turnover. *Proc. Natl. Acad. Sci. USA* **86,** 6602-6606.

Palmer, J. M., and Hall, D. O. (1972). The mitochondrial membrane system. *Prog. Biophys. Mol. Biol.* **24,** 125-176.

Papa, S., Lorusso, M., and Capitanio, N. (1995). On the mechanism of proton pumps in respiratory chains. In Biochemistry of cell membranes: a compendium of selected topics, S. Papa and J. M. Tager, eds. (Boston: Birkhäuser Verlag), pp. 151-166.

Parson, W. W. (1996). Photosynthetic bacterial reaction centres. In Protein electron transfer, D. S. Bendall, ed. (Oxford, UK: BIOS Scientific Publishers Ltd), pp. 125-160.

Paudel, H. K., Yu, L., and Yu, C. A. (1991). Involvement of a histidine residue in the interaction between membrane-anchoring protein (QPs) and succinate dehydrogenase in mitochondrial succinate-ubiquinone reductase. *Biochim. Biophys. Acta* **1056,** 159-165.

Peterson, J., Vibat, C., and Gennis, R. B. (1994). Identification of the axial heme ligands of cytochrome b_{556} in succinate:ubiquinone oxidoreductase from *Escherichia coli*. *FEBS Lett.* **355,** 155-156.

Pfanner, N., and Meijer, M. (1997). Mitochondrial biogenesis: the Tom and Tim machine. *Curr. Biol.* **7,** R100-R103.

Poyton, R. O., and McEwen, J. E. (1996). Crosstalk between nuclear and mitochondrial genomes. *Annu. Rev. Biochem.* **65,** 563-607.

Ragan, C. I. (1987). Structure of NADH-ubiquinone reductase (complex I). *Curr. Top. Bioenerg.* **15,** 1-36.

Ragan, C. I. (1990). Structure and function of an archetypal respiratory chain complex: NADH-ubiquinone reductase. *Biochem. Soc. Trans.* **18,** 515-516.

Ragan, C. I., and Reed, J. S. (1986). Regulation of electron transfer by the quinone pool. *J. Bioenerg. Biomembr.* **18,** 403-418.

Rich, P. R. (1996). Electron transfer complexes coupled to ion translocation. In Protein electron transfer, D. S. Bendall, ed. (Oxford, UK: BIOS Scientific Publishers Ltd), pp. 217-248.

Rich, P. R., and Bonner, W. D., Jr. (1978). An EPR analysis of cyanide-resistant mitochondria isolated from the mutant strain of *Neurospora crassa*. *Biochim. Biophys. Acta* **504,** 345-363.

Rich, P. R., Moore, A. L., Ingledew, W. J., and Bonner, W. D., Jr. (1977). EPR studies of higher plant mitochondria. I Ubisemiquinone and its relation to alternative respiratory oxidations. *Biochim. Biophys. Acta* **462,** 501-514.

Robertson, D. E., Ding, H., Chelminski, P. R., Slaughter, C., Hsu, J., Moomaw, C., Tokito, M., Daldal, F., and Dutton, P. L. (1993). Hydroquinone-cytochrome c_2 oxidoreductase from *Rhodobacter capsulatus*: definition of a minimal, functional isolated preparation. *Biochemistry* **32,** 1310-1317.

Robinson, K. M., and Lemire, B. D. (1992). Isolation and nucleotide sequence of the *Saccharomyces cerevisiae* gene for the succinate dehydrogenase flavoprotein subunit. *J. Biol. Chem.* **267,** 10101-10107.

Robinson, K. M., and Lemire, B. D. (1995). Flavinylation of succinate: ubiquinone oxidoreductase from *Saccharomyces cerevisiae*. *Methods Enzymol.* **260,** 34-51.

Robinson, K. M., and Lemire, B. D. (1996a). Covalent attachment of FAD to the yeast succinate dehydrogenase flavoprotein requires import into mitochondria, presequence removal, and folding. *J. Biol. Chem.* **271,** 4055-4060.

Robinson, K. M., and Lemire, B. D. (1996b). A requirement for matrix processing peptidase but not for mitochondrial chaperonin in the covalent attachment of FAD to the yeast succinate dehydrogenase flavoprotein. *J. Biol. Chem.* **271,** 4061-4067.

Robinson, K. M., Rothery, R. A., Weiner, J. H., and Lemire, B. D. (1994). The covalent attachment of FAD to the flavoprotein of *Saccharomyces cerevisiae* succinate dehydrogenase is not necessary for import and assembly into mitochondria. *Eur. J. Biochem.* **222,** 983-990.

Robinson, K. M., von Kieckebusch-Gück, A., and Lemire, B. D. (1991). Isolation and Characterization of a *Saccharomyces cerevisiae* Mutant Disrupted for the Succinate Dehydrogenase Flavoprotein subunit. *J. Biol. Chem.* **266,** 21347-21350.

Roos, M. H., and Tielens, A. G. (1994). Differential expression of two succinate dehydrogenase subunit-B genes and a transition in energy metabolism during the development of the parasitic nematode *Haemonchus contortus. Mol. Biochem. Parasitol.* **66,** 273-281.

Rothstein, R. (1991). Targeting, disruption, replacement, and allele rescue: integrative DNA transformation in yeast. *Methods Enzymol.* **194,** 281-301.

Rottenberg, H. (1998). The generation of proton electrochemical potential gradient by cytochrome *c* oxidase. *Biochim. Biophys. Acta* **1364,** 1-16.

Saitoh, I., Miyoshi, H., Shimizu, R., and Iwamura, H. (1992). Comparison of structure of quinone redox site in the mitochondrial cytochrome bc_1 complex and photosystem II (Q_B site). *Eur. J. Biochem.* **209,** 73-79.

Salerno, J. C., Lim, J., King, T. E., Blum, H., and Ohnishi, T. (1979). The spatial relationships and structure of the binuclear iron-sulfur clusters in succinate dehydrogenase. *J. Biol. Chem.* **254,** 4828-4835.

Salerno, J. C., and Ohnishi, T. (1980). Studies on the stabilized ubisemiquinone species in the succinate-cytochrome *c* reductase segment of the intact mitochondrial membrane. *Biochem. J.* **192,** 769-781.

Salerno, J. C., and Yan, X. (1987). Aspects of spin coupling between even and odd electron systems: applications to succinate: Q reductase. In Cytochrome systems: molecular biology and bioenergetics, S. Papa, B. Chance and L. Ernster, eds. (New York: Plenum Press), pp. 467-471.

Samain, E., Patil, D. S., DerVartanian, D. V., Albagnac, G., and LeGall, J. (1987). Isolation of succinate dehydrogenase from *Desulfobulbus elongatus*, a propionate oxidizing, sulfate reducing bacterium. *FEBS Lett.* **216,** 140-144.

Saraste, M. (1990). Structural features of cytochrome oxidase. *Quart. Rev. Biophys.* **23,** 331-366.

Saruta, F., Kuramochi, T., Nakamura, K., Takamiya, S., Yu, Y., Aoki, T., Sekimizu, K., Kojima, S., and Kita, K. (1995). Stage-specific isoforms of complex II (succinate-ubiquinone oxidoreductase) in mitochondria from the parasitic nematode, *Ascaris suum. J. Biol. Chem.* **270,** 928-932.

Schägger, H., Link, T. A., Engel, W. D., and von Jagow, G. (1986). Isolation of the eleven protein subunits of the bc_1 complex from beef heart. *Methods Enzymol.* **126,** 224-237.

Schatz, G. (1996). The protein import system of mitochondria. *J. Biol. Chem.* **271,** 31763-31766.

Scheffler, I. E. (1998). Molecular genetics of succinate:quinone oxidoreductase in eukaryotes. *Prog. Nucleic Acid Res. Mol. Biol.* **60,** 267-315.

Schilling, R. J., Baldwin, T., and Palmer, G. (1982). The characterization of highly purified complex II from baker's yeast. *Fed. Proc.* **41,** 896.

Schirawski, J., and Unden, G. (1998). Menaquinone-dependent succinate dehydrogenase of bacteria catalyzes reversed electron transport driven by the proton potential. *Eur. J. Biochem.* **257,** 210-215.

Schmidt, D. M., Saghbini, M., and Scheffler, I. M. (1992). The C-terminus of the succinate dehydrogenase IP peptide of *Saccharomyces cerevisiae* is significant for assembly of complex II. *Biochemistry* **31,** 8442-8448.

Schröder, I., Gunsalus, R. P., Ackrell, B. A. C., Cochran, B., and Cecchini, G. (1991). Identification of active site residues of *Escherichia coli* fumarate reductase by site-directed mutagenesis. *J. Biol. Chem.* **266,** 13572-13579.

Schülke, N., Blobel, G., and Pain, D. (1992). Primary structure, import, and assembly of the yeast homolog of succinate dehydrogenase flavoprotein. *Proc. Natl. Acad. Sci. USA* **89,** 8011-8015.

Shenoy, S. K., Yu, L., and Yu, C. A. (1997). The smallest membrane anchoring subunit (QPs3) of bovine heart mitochondrial succinate-ubiquinone reductase. Cloning, sequencing, topology, and Q-binding domain. *J. Biol. Chem.* **272,** 17867-17872.

Shenoy, S. K., Yu, L., and Yu, C. A. (1999). Identification of quinone-binding and heme-ligating residues of the smallest membrane-anchoring subunit (QPs3) of bovine heart mitochondrial succinate:ubiquinone reductase. *J. Biol. Chem.* **274,** 8717-8722.

Shulz, G. E. (1995). Structure and function of membrane channel porin. In Biochemistry of cell membranes: a compendium of selected topics, S. P. a. J. M. Tager, ed. (Boston: Birkhaüser Verlag), pp. 327-338.

Simon, J., Gross, R., Ringel, M., Schmidt, E., and Kroger, A. (1998). Deletion and site-directed mutagenesis of the *Wolinella succinogenes* fumarate reductase operon. *Eur. J. Biochem.* **251,** 418-426.

Singer, T. P., and Edmondson, D. E. (1974). 8α-substituted flavins of biological importance. *FEBS Lett.* **42,** 1-14.

Singer, T. P., and Johnson, M. K. (1985). The prosthetic groups of succinate dehydrogenase: 30 years from discovery to identification. *FEBS Lett.* **190,** 189-198.

Singer, T. P., Kearney, E. B., and Kennedy, W. C. (1973). Succinate dehydrogenase. *Adv. Enzymol.* **37,** 189.

Singer, T. P., and McIntire, W. S. (1984). Covalent attachment of flavin to flavoproteins: occurence, assay, and synthesis. *Methods Enzymol.* **106,** 369-378.

Singer, T. P., and Ramsay, R. R. (1992). NADH-ubiquinone oxidoreductase. In Molecular mechanisms in bioenergetics, L. Ernster, ed. (New York: Elsevier Science Publishers), pp. 145-162.

Skulachev, V. P. (1992). Chemiosmotic systems and the basic principles of cell energetics. In Molecular mechanisms in bioenergetics, L. Ernster, ed. (Amsterdam: Elsevier Science Publishers B. V.), pp. 37-73.

Smirnova, I. A., Hägerhäll, C., Konstantinov, A. A., and Hederstedt, L. (1995). HOQNO interaction with cytochrome *b* in succinate:menaquinone oxidoreductase from *Bacillus subtilis*. *FEBS Lett.* **359,** 23-26.

Sucheta, A., Ackrell, B. A. C., Cochran, B., and Armstrong, F. A. (1992). Diode-like behaviour of a mitochondrial electron-transport enzyme. *Nature (London)* **356,** 361-362.

Sucheta, A., Cammack, R., Weiner, J., and Armstrong, F. A. (1993). Reversible electrochemistry of fumarate reductase immobilized on an electrode surface. direct voltammetric observations of redox centers and their participation in rapid catalytic electron transport. *Biochemistry* **32,** 5455-5465.

Taanman, J.-W. (1999). The mitochondrial genome: structure, transcription, translation and replication. *Biochim. Biophys. Acta* **1410,** 103-123.

Takamiya, S., Furushima, R., and Oya, H. (1986). Electron-transfer complexes of *Ascaris suum* muscle mitochondria. II. Succinate-coenzyme Q reductase (complex II) associated with substrate-reducible cytochrome b_{558}. *Biochim. Biophys. Acta* **848,** 99-107.

Takamiya, S., Kita, K., Matsuura, K., Furushima, R., and Oya, H. (1990). Oxidation-reduction potentials of cytochromes in *Ascaris* muscle mitochondria: high-redox-potential cytochrome b_{558} in complex II (succinate-ubiquinone reductase). *Biochemistry* **21,** 1073-1083.

Tielens, A. G., and Van Hellemond, J. J. (1998). The electron transport chain in anaerobically functioning eukaryotes. *Biochim. Biophys. Acta* **1365,** 71-78.

Trumpower, B. L. (1980). New concepts on the role of ubiquinone in the mitochondrial respiratory chain. *J. Bioener. Biomembr.* **13,** 1-24.

Trumpower, B. L. (1990a). Cytochrome *bc_1* complexes of microorganisms. *Microbiol. Rev.* **54,** 101-129.

Trumpower, B. L. (1990b). The protonmotive Q cycle-energy transduction by coupling of proton translocation to electron transfer by the cytochrome *bc_1* complex. *J. Biol. Chem.* **265,** 11409-11412.

Trumpower, B. L., and Gennis, R. B. (1994). Energy transduction by cytochrome complexes in mitochondrial and bacterial respiration: the enzymology of coupling electron transfer reactions to transmembrane proton translocation. *Annu. Rev. Biochem.* **63,** 675-716.

Trumpower, B. L., and Katki, A. G. (1979). Succinate-cytochrome *c* reductase complex of the mitochondrial electron transport chain. In Membrane proteins in energy transduction, R. A. Capaldi, ed. (New York, New York: Marcel Dekker, Inc.), pp. 89-200.

Tsukihara, T., Aoyama, H., Yamashita, E., Tomizaki, T., Yamaguchi, H., Shinzawa-Itoh, K., Nakashima, R., Yaono, R., and Yoshikawa, S. (1995). Structures of metal sites of oxidized bovine heart cytochrome *c* oxidase at 2.8 Å. *Science* **269,** 1069-1074.

Tsukihara, T., Aoyama, H., Yamashita, E., Tomizaki, T., Yamaguchi, H., Shinzawa-Itoh, K., Nakashima, R., Yaono, R., and Yoshikawa, S. (1996). The whole structure of the 13-subunit oxidized cytochrome *c* oxidase at 2.8 Å resolution. *Science* **272,** 1136-1144.

Tushurashvili, P. R., Gavrikova, E. V., Ledenev, A. N., and Vinogradov, A. D. (1985). Studies on the succinate dehydrogenating system. Isolation and properties of the mitochondrial succinate-ubiquinone reductase. *Biochim. Biophys. Acta* **809,** 145-159.

Tzagoloff, A., and Dieckmann, C. L. (1990). *PET* Genes of *Saccharomyces cerevisiae*. *Microbiol. Rev.* **54,** 211-225.

Unden, G., and Kröger, A. (1980). An essential sulphydryl group at the substrate site of the fumarate reductase of *Vibrio succinogenes*. *FEBS Lett.* **177,** 323-326.

Unden, G., and Kröger, A. (1981). The function of the subunits of fumarate reductase complex of *Vibrio succinogenes*. *Eur. J. Biochem.* **120,** 577-584.

Van Hellemond, J. J., and Tielens, A. G. M. (1994). Expression and functional properties of fumarate reductase. *Biochem. J.* **304,** 321-331.

Vibat, C. R. T., Cecchini, G., Nakamura, K., Kita, K., and Gennis, R. B. (1998). Localization of histidine residues responsible for heme axial ligation in cytochrome b_{556} of complex II (succinate:ubiquinone oxidoreductase) in *Escherichia coli*. *Biochemistry* **37,** 4148-4159.

Viehmann, S., Richard, O., Boyen, C., and Zetsche, K. (1996). Genes for two subunits of succinate dehydrogenase form a cluster on the mitochondrial genome of *Rhodophyta*. *Curr. Genet.* **29,** 199-201.

Vik, S. B., and Hatefi, Y. (1981). Possible occurrence and role of an essential histidyl residue in succinate dehydrogenase. *Proc. Natl. Acad. Sci. U.S.A.* **78,** 6749-6753.

Vinogradov, A. D. (1993). Kinetics, control and mechanism of ubiquinone reduction by the mammalian respiratory chain-linked NADH-ubiquinone reductase. *J. Bioenerg. Biomembr.* **25,** 367-376.

Waldeck, A. R., Stowell, M. H. B., Lee, H. K., Hung, S. C., Matsson, M., Hederstedt, L., Ackrell, B. A. C., and Chan, S. I. (1997). Electron paramagnetic resonance studies of succinate:ubiquinone oxidoreductase from *Paracoccus denitrificans*. Evidence for a magnetic interaction between the 3Fe-4S cluster and cytochrome *b*. *J. Biol. Chem.* **272,** 19373-19382.

Walker, J. E. (1992). The NADH:ubiquinone oxidoreductase (complex I) of respiratory chains. *Q. Rev. Biophys.* **25,** 253-324.

Weiss, H., and Friedrich, T. (1991). Redox-linked proton translocation by NADH-ubiquinone reductase (complex I). *J. Bioenerg. Biomembr.* **23,** 743-754.

Weiss, H., Friedrich, T., Hofhaus, G., and Preis, D. (1991). The respiratory chain NADH dehydrogenase (complex I) of mitochondria. *Eur. J. Biochem.* **197,** 563-576.

Weiss, H., and Kolb, H. J. (1979). Isolation of mitochondrial succinate: ubiquinone reductase, cytochrome *c* reductase and cytochrome *c* oxidase from *Neurospora crassa* using nonionic detergent. *Eur. J. Biochem.* **99,** 139-149.

West, I. C. (1986). A theoretical analysis of the effect of phosphate on apparent H+/O stoichiometries in oxygen-pulse experiments with rat liver mitochondria. *Biochim. Biophys. Acta* **849**.

Westenberg, D. J., Gunsalus, R. P., Ackrell, B. A. C., and Cecchini, G. (1990). Electron transfer from menaquinol to fumarate. Fumarate reductase anchor polypeptide mutants of *Escherichia coli*. *J. Biol. Chem.* **265,** 19560-19567.

Westenberg, D. J., Gunsalus, R. P., Ackrell, B. A. C., Sices, H., and Cecchini, G. (1993). *Escherichia coli* fumarate reductase *frdC* and *frdD* mutants. Identification of amino acid residues involved in catalytic activity with quinones. *J. Biol. Chem.* **268,** 815-822.

Wikström, M., Morgan, J. E., and Verkhovsky, M. I. (1998). On the mechanism of proton translocation by respiratory enzymes. *J. Bioenerg. Biomembr.* **30,** 139-145.

Wikström, M. K., and Berden, J. A. (1972). Oxidoreduction of cytochrome *b* in the presence of antimycin. *Biochim. Biophys. Acta* **283,** 403-420.

Wikström, M. K. F., and Saraste, M. (1984). The mitochondrial respiratory chain. In Bioenergetics, L. Ernster, ed. (New York: Elsevier), pp. 49-94.

Wood, D., Darlison, M. G., Wilde, R. J., and Guest, J. R. (1984). Nucleotide sequence encoding the flavoprotein and hydrophobic subunits of the succinate dehydrogenase of *Escherichia coli*. *Biochem. J.* **222,** 519-534.

Xia, D., Yu, C. A., Kim, H., Xian, J. Z., Kachurin, A. M., Zhang, L., Yu, L., and Deisenhofer, J. (1997). Crystal structure of the cytochrome bc_1 complex from bovine heart mitochondria. *Science* **277,** 60-66.

Xu, J. X., Yu, L., and Yu, C. A. (1987). Involvement of a carboxyl group in the interaction between succinate dehydrogenase and its membrane-anchoring protein (QPs) fraction. *Biochemistry* **26,** 7674-7679.

Yang, X. D., Yu, L., He, D., and Yu, C. A. (1998). The quinone-binding site in succinate-ubiquinone reductase from *Escherichia coli*. *J. Biol. Chem.* **273,** 31916-31923.

Yang, X. D., Yu, L., and Yu, C. A. (1997). Resolution and reconstitution of succinate-ubiquinone reductase from *Escherichia coli*. *J. Biol. Chem.* **272,** 9683-9689.

Yankovskaya, V., Sablin, S. O., Ramsay, R. R., Singer, T. P., Ackrell, B. A. C., Cecchini, G., and Miyoshi, H. (1996). Inhibitor probes of the quinone binding sites of mammalian complex II and *Escherichia coli* fumarate reductase. *J. Biol. Chem.* **271,** 21020-21024.

Yoshikawa, S., Shinzawa-Itoh, K., and Tsukihara, T. (1998). Crystal structure of bovine heart cytochrome *c* oxidase at 2.8 Å resolution. *J. Bioenerg. Biomembr.* **30,** 7-14.

Yu, C.-A., Nagaoka, S., Yu, L., and King, T. E. (1978). Evidence for the existence of a ubiquinone protein and its radical in the cytochromes *b* and c_1 region in the mitochondrial electron transport chain. *Biochem. Biophys. Res. Commun.* **82,** 1070-1078.

Yu, C. A., Xia, D., Kim, H., Deisenhofer, J., Zhang, L., Kachurin, A. M., and Yu, L. (1998). Structural basis of functions of the mitochondrial cytochrome bc_1 complex. *Biochim. Biophys. Acta* **1365,** 151-158.

Yu, C. A., and Yu, L. (1980). Isolation and properties of a mitochondrial protein that converts succinate dehydrogenase into succinate-ubiquinone oxidoreductase. *Biochemistry* **19,** 3579-3585.

Yu, C. A., and Yu, L. (1981a). Ubiquinone-binding proteins. *Biochim. Biophys. Acta* **639,** 99-128.

Yu, L., Xu, J. X., Haley, P. E., and Yu, C. A. (1987). Properties of bovine heart mitochondrial cytochrome b_{560}. *J. Biol. Chem.* **262,** 1137-1143.

Yu, L., Yang, F. D., and Yu, C. A. (1985). Interaction and identification of ubiquinone-binding proteins in ubiquinol-cytochrome *c* reductase by azido-ubiquinone derivatives. *J. Biol. Chem.* **260,** 963-973.

Yu, L., and Yu, C.-A. (1982). Quantitative resolution of succinate-cytochrome *c* reductase into succinate-ubiquinone and ubiquinol-cytochrome *c* reductases. *J. Biol. Chem.* **257,** 2016-2021.

Yu, L., and Yu, C. A. (1981b). The participation of primary amino groups of succinate dehydrogenase in the formation of succinate-Q reductase. *Biochim. Biophys. Acta* **637,** 383-386.

Zhang, Z., Huang, L., Shulmeister, V. M., Chi, Y. I., Kim, K. K., Hung, L. W., Crofts, A. R., Berry, E. A., and Kim, S. H. (1998). Electron transfer by domain movement in cytochrome bc_1. *Nature* **392,** 677-684.

Zhu, Q. S., Berden, J. A., De Vries, S., and Slater, E. C. (1982). On the role of ubiquinone in the respiratory chain. *Biochim. Biophys. Acta* **680,** 69-79.

Chapter 2

The *S. cerevisiae* SDH Contains a Stoichiometric Amount of Heme *b*[*]

---

[*] A version of this chapter has been published. Oyedotun, K. S. and Lemire, B. D. (1999) *FEBS Lett.* **422**, 203–207.

2.1. Introduction

Succinate-ubiquinone reductase, also called succinate dehydrogenase (SDH), is a membrane bound enzyme of the Krebs cycle and the mitochondrial respiratory chain. It catalyzes the oxidation of succinate to fumarate coupled to the reduction of quinone. A related enzyme, fumarate reductase (FRD), which catalyzes the reduction of fumarate to succinate coupled to quinone oxidation, is present in anaerobic cells respiring with fumarate as the terminal electron acceptor. This enzyme is functionally and structurally similar to SDH (Ackrell *et al.*, 1992; Hägerhäll, 1997; Hederstedt and Ohnishi, 1992; Lemire *et al.*, 1982).

Generally, SDH is a tetramer of non-equivalent subunits: a flavoprotein subunit (about 70 kDa), an iron-sulfur protein subunit (about 27 kDa) and two smaller hydrophobic polypeptides of about 17 and 13 kDa (Ackrell *et al.*, 1992; Cole *et al.*, 1985; Hägerhäll, 1997; Hederstedt and Ohnishi, 1992). The flavoprotein and the iron-sulfur protein subunits comprise the catalytic domain. The dicarboxylate active site resides in the flavoprotein subunit near a covalently attached FAD cofactor. The iron-sulfur protein subunit contains 3 iron-sulfur clusters that are involved in electron transfer from FAD to quinone (Ackrell *et al.*, 1992). This catalytic domain can transfer electrons from succinate to artificial electron acceptors such as phenazine methosulphate (PMS) or potassium ferricyanide. However, the reduction of natural quinones or quinone analogs requires the presence of the membrane-anchoring domain, which is typically comprised of the two smaller polypeptides (Ackrell *et al.*, 1992; Bullis and Lemire, 1994; Daignan-Fornier *et al.*, 1994; Hägerhäll and Hederstedt, 1996). The membrane domain attaches the catalytic subunits to the inner membrane of mitochondria or to the cytoplasmic membrane of bacteria. In addition, it contains the binding site(s) for quinone and may also ligand one or two *b*-type hemes.

The flavoprotein and the iron-sulfur subunits are well conserved across species at the primary amino acid level. In contrast, there is considerable variability in subunit composition and primary amino acid sequence of the membrane domain (Hägerhall *et al.*, 1992; Hederstedt, 1980; Kita *et al.*, 1989; Takamiya *et al.*, 1986; Takamiya *et al.*, 1990; Yu *et al.*, 1987). Some SDHs have a single anchor subunit while others have 2; some have two hemes in their anchor subunits, while others have one or none. This variability has made it difficult to identify residues that may be involved in cofactor binding or in subunit-subunit interactions through sequence comparisons. In the absence of high-resolution structural information, the yeast SDH promises to be a good model system for studying structural requirements for cofactor interactions through genetic approaches. *Saccharomyces cerevisiae* is able to grow either by fermentation, where functional SDH is not required, or by respiration, where its presence is essential (Bullis and Lemire, 1994; Daignan-Fornier *et al.*, 1994; Lombardo and Sheffler, 1989; Robinson *et al.*, 1991).

The membrane-intrinsic domain of the *S. cerevisiae* SDH is composed of the two hydrophobic polypeptides, Sdh3p (Abraham *et al.*, 1994; Daignan-Fornier *et al.*, 1994) and Sdh4p (Bullis and Lemire, 1994). Each subunit is predicted to contain three membrane-spanning domains on the basis of hydrophobicity analysis. Based on heme content and the number of anchor polypeptides, SDH and FRD membrane anchor domains have been classified into 4 types, A-D (Hägerhäll, 1997; Hägerhäll and Hederstedt, 1996; Hederstedt, 1998). The yeast SDH and the *Escherichia coli* FRD fall into the D structural subtypes, containing 2 anchor polypeptides without heme. The supposed absence of heme is based on a published abstract (Schilling *et al.*, 1982). In this earlier report, the authors isolated SDH by a procedure involving cholate solubilization, ammonium sulfate fractionation, and density gradient centrifugation. This yielded a preparation containing a substoichiometric molar ratio of heme to flavin (less than 0.2). The final purification step involved immuno-affinity chromatography, which further reduced the heme to flavin molar ratio to 0.06. The influence of this abstract has persisted in the literature (Hägerhäll, 1997; Hägerhäll and Hederstedt, 1996; Vibat *et al.*, 1998). Recently, investigators working with the yeast complex III demonstrated the presence of a fumarate-oxidizable heme in dithionite-reduced mitochondria corresponding to cytochrome *b* in SDH (Bruel *et al.*, 1996; Bruel *et al.*, 1995). Selective oxidation of cytochrome *b* by fumarate, after pre-reduction with dithionite, is also a property of the bovine SDH (Hatefi and Galante, 1980; Yu *et al.*, 1987).

In this report, we demonstrate the presence of a stoichiometric amount of heme in the yeast SDH by monitoring the fumarate-oxidizable spectrum in dithionite-reduced mitochondria. This produces a peak centered at 562 nm, hence, we designate the heme as cytochrome b_{562} (previous reports have referred to the putative heme of yeast SDH as cytochrome b_{560}, by analogy to cytochrome b_{560} of the bovine SDH (Abraham *et al.*, 1994; Daignan-Fornier *et al.*, 1994). In addition, we also construct and characterize an *SDH3* disruption mutant as a preliminary step to understanding its structural and functional role.

2.2. Materials and Methods

Media and Culture Conditions. The yeast media used are: SD (0.67% yeast nitrogen base, 2% glucose); SG (0.67% yeast nitrogen base, 3% glycerol); YPD (1% yeast extract, 2% peptone, 2% glucose); YPD-0.6 (1% yeast extract, 1% peptone, 0.6% glucose, 0.1% KH_2PO_4, 0.12% ammonium sulfate, pH 6.2); and semisynthetic media (0.3% yeast extract, 0.1% KH_2PO_4, 0.1% NH_4Cl, 0.05% NaCl, 0.06% $MgSO_4.7H_2O$, 0.05% $CaCl_2$, 0.003% $FeCl_3$, 2% galactose or 2% lactate). Generally, yeast strains were initially cultivated on minimal SD plates for 2-3 days to select for plasmid retention. Single colonies were picked to inoculate 100 ml of semisynthetic galactose or lactate medium and grown aerobically at 30

°C for 24 hours. The precultures were diluted 100-fold into semisynthetic galactose or lactate medium and grown aerobically at 30 °C to an OD_{600} of about 3, yielding approximately 3 g (wet weight) of cell paste/liter of culture. For the isolation of submitochondrial membranes, yeast strains were grown aerobically to stationary phase on YPD-0.6%. *E. coli* strains were grown aerobically on Luria-Bertani medium (1% tryptone, 0.5% yeast extract, and 1% NaCl) or Terrific Broth (1.2% bacto-tryptone, 2.4% yeast extract, 0.4% glycerol, 17 mM KH_2PO4, and 72 mM K_2HPO4) supplemented with 100 μg/ml ampicillin to select for plasmid retention.

Strains and Plasmids. The parental strain, MH125 (*Mata ura3-52 leu2-3, -112 his3 his4 rme rho*$^+$) was used for constructing disruption mutants and as a source of wild type mitochondria and submitochondrial particles. The sdh4W2 (*Mata ura3-52 leu2-3, -112 his3 his4 rme sdh4::TRP1 ρ*+) is an *SDH4* disruption mutant that was constructed from MH125 by targeted gene disruption. sdh3W3 (*Mata ura3-52 leu2-3, -112 his3 his4 rme sdh3::TRP1 rho*$^+$) is an *SDH3* disruption mutant that was constructed by targeted gene disruption (Rothstein, 1991) as described below. MS10 (*Matα kar1-1 leu2-3 canR rho*^{0}) was used for mating when checking for mitochondrial petite strains. The plasmid pYCSDH3 was constructed by sub-cloning a 0.988-kb *Eco*RI-*Bgl*II fragment containing the entire *SDH3* gene into the *Eco*RI-*Bam*HI sites of the *E. coli*-yeast shuttle vector, YCplac111 (Gietz and Sugino, 1988). pSDH4-17 (Bullis and Lemire, 1994) bears the wild type *SDH4* gene on the *E. coli*-yeast shuttle vector, pRS416. The *E. coli* strain DH5α (F^-φ80d/*lacZ*ΔM15 *endA1 recA1 hsdR17* (r_k^- m_k^-) *supE44 thi-1 gyrA relA1* Δ(*lacZYA-argF*) U169 $\lambda^-\lambda^-$) was used for all DNA manipulations.

Mutant construction. Briefly, an internal 0.13-kb *Kpn*1 fragment was removed from *SDH3* gene, borne on the plasmid pYC22SDH3, and replaced with a 0.83-kb *Kpn*1 fragment containing the *TRP1* gene to yield the plasmid pSDH3-TRP1. A 1.7-kb fragment (containing the disrupted *SDH3* gene) was isolated and transformed into the yeast strain, MH125. Tryptophan prototrophs were selected on SD medium supplemented with 20 μg/ml each of histidine, uracil, adenine sulfate, leucine, and lysine. At least five stably transformed tryptophan prototrophs had lost the ability to grow on minimal SG and were further examined.

Isolation of Mitochondria and Submitochondrial Particles. For the preparation of submitochondrial particles, yeast strains were grown in YPD-0.6%, harvested, and re-suspended in 20 mM HEPES-KOH buffer, pH 7.4, containing 1 mM phenylmethylsulfonyl fluoride, to form a cell suspension of 0.3 g of cells ml^{-1}. Cells were disrupted by two passages through a French pressure cell (American Instrument Co., Silver Spring, MD) at 20,000 p.s.i. and 4 °C. Cell suspensions were cooled briefly on ice after each passage. This process ruptures the yeast cells and produces fragments of yeast mitochondria. Typically, 75–85% of the yeast cells were broken as judged by microscopic examination. Unlysed cells, nuclei, and envelopes were removed by centrifugation at 11,000 × *g* for 10 min, and the supernatant was spun at 160,000 × *g* for 60 min. The pellet of submitochondrial particles was re-suspended in 20 mM HEPES-KOH, pH 7.4 at concentrations >30 mg ml^{-1} and stored at –70 °C.

Mitochondria were prepared from *S. cerevisiae* strains by differential centrifugations. Lactate or galactose-grown cells (6-7 g, wet weight) were washed once in water (0.1 volume of the original culture), resuspended in 50 ml of Tris-SO_4 buffer (0.1 M Tris-SO_4, pH9.4, 10 mM DTT) and incubated for 15 min at 30°C with shaking. After a wash in 50 ml of sorbitol buffer (1.2 M sorbitol; 20 mM KPi, pH 7.4), cells were resuspended in sorbitol buffer (3 ml/g of original pellet) and converted to spheroplasts by adding 5 mg of Zymolyase-20T per g of cells and incubating the mixture at 30 °C for 30-45 min. All subsequent steps were performed at 4 °C. Spheroplasts were sedimented at 3,500 × *g* for 5 min, washed twice in sorbitol buffer and resuspended (3 mg/g) in hypotonic sorbitol buffer (0.6 M sorbitol, 20 mM HEPES-KOH, pH 7.4, 1 mM PMSF). After homogenization using 15 strokes of a Dounce homogenizer, samples were diluted with an equal volume of 0.65 M sorbitol buffer and centrifuged at 3000 × *g* for 5 min. The supernatant was decanted and the pellet was similarly rehomogenized and centrifuged. The supernatants were pooled and centrifuged at 18000 × *g* for 10 min. The mitochondrial pellet was washed thrice and resuspended in 0.65 M sorbitol buffer at a concentration of 15-20 mg/ml.

Measurement of Covalent FAD. Covalently attached FAD was determined on a Perkin Elmer Luminescence Spectrometer model LS50 using riboflavin as a standard (de Kok *et al.*, 1975; Singer and McIntire, 1984). Values are averages of at least three independent measurements, after subtracting background levels.

Cytochrome content determination. Total absorption spectra of yeast mitochondria were measured as the dithionite-reduced minus ferricyanide-oxidized spectra. The heme content of SDH was determined spectrally as the dithionite-reduced minus the dithionite-reduced/fumarate-oxidized difference spectrum (Brasseur *et al.*, 1997; Bruel *et al.*, 1995). Mitochondria isolated from strains grown on semisynthetic lactate or galactose medium (Oyedotun and Lemire, 1997) were suspended to 185 pmol of acid-precipitable FAD/ml (2.5-3.2 mg protein/ml) in 0.65 M sorbitol, 10 mM KH_2PO_4, 2 mM $MgCl_2$, 0.3% fatty acid-free bovine serum albumin, pH 6.5. Lauryl maltoside (Boehringer Mannheim) was added to a final concentration of 0.1% to reduce spectral noise. Spectra were recorded at 22°C on a Hewlett Packard 8453 diode array spectrophotometer with a 1 cm path length. The molar absorption coefficients used were: 21.4 mM^{-1} cm^{-1} for cytochrome aa_3, 18 mM^{-1} cm^{-1} for cytochrome cc_1, and 24 mM^{-1} cm^{-1} for cytochrome $b_{562} + b_{565}$ (Meunier-Lemesle *et al.*, 1980). This latter value was also used for the fumarate-oxidizable cytochrome b_{562} (Bruel *et al.*, 1995).

Electrophoresis and Western blot analyses. Mitochondrial proteins (10 µg) were separated using a 13 % Tricine gel system (Schägger and Von Jagow, 1987) and transferred electrophoretically to a polyvinylidene difluoride membrane using the semi-dry blotting method as described (Schägger *et al.*, 1994). The blot was treated with a rabbit polyclonal antiserum raised against a peptide consisting of the amino-terminal dodecapeptide of the mature Sdh3p. Detection of antigens was with a peroxidase-labeled goat anti-rabbit secondary antibody and the enhanced chemiluminescence detection system (Amersham).

Polymerase chain reaction. Genomic DNA was isolated from the *SDH3* knockout strain, sdh3W3 and the parental strain, MH125 and used as templates in the polymerase chain reactions. The following primers were used:

Upstream primer: 5′-GTTAAAGGATGTTCTAGTGG-3′, corresponding to nucleotides –307 to –326 of the *SDH3* gene; and

Downstream primer: 5′-ATAGGTTTGTGTTAATCGGC-3′, corresponding to nucleotides +719 to +738 of the *SDH3* gene.

The oligonucleotides were synthesized on an Applied Biosystems 392 DNA Synthesizer in the Department of Biochemistry DNA Core Facility, University of Alberta. PCR conditions were as previously described (Robinson *et al.*, 1991).

Enzyme Assays. The succinate-dependent, phenazine methosulfate (PMS)-mediated reduction of dichlorophenol indophenol (DCPIP) was determined as a measure of the membrane-associated Sdh1p/Sdh2p dimer. This assay is a measure of the membrane-associated Sdh1p/Sdh2p dimer; the assay does not require catalytically competent Sdh3p and Sdh4p subunits, though membrane association of the Sdh1p/Sdh2p dimer requires intact anchor subunits (Bullis and Lemire, 1994; Robinson *et al.*, 1991). The succinate-PMS reductase activity was measured as the malonate-sensitive, PMS-mediated reduction of DCPIP at 22 °C in 50 mM

Tris-SO_4, 0.1 mM EDTA, 0.1% Triton X-100, 1 mM NaCl, pH 7.4, in a Pye Unicam split beam spectrophotometer. DCPIP is added a final concentration of 70 μM, PMS to 120 μg ml^{-1}, succinate and malonate to 20 mM each. The extinction coefficient for DCPIP at 600 nm is 21 cm^{-1} mM^{-1}. The succinate-DB reductase activity was monitored at 22 °C as the succinate-dependent, malonate-sensitive reduction of 2,3-dimethoxy-5-methyl-6-decyl-1,4-benzoquinone (DB)-mediated reduction of DCPIP. The assay medium contains 0.05 mM EDTA, 2.5 mM potassium phosphate buffer, pH 7.4. DB was added to a final concentration of 50 μM, DCPIP to 75 μM, succinate and malonate to 20 mM each. Succinate-cytochrome *c* reductase activity was measured as the malonate-sensitive reduction of cytochrome *c* in 100 mM Tris-SO_4 buffer, pH 7.4, 1.6 mg ml^{-1} horse heart cytochrome *c* (Sigma Chemical Co.), 1 mM NaCN. Succinate and malonate were added to a final concentration of 20 mM each. For antimycin A-sensitive NADH- or glycerol-1-phosphate-cytochrome *c* reductase activities, freshly prepared NADH is added to 0.1 mM or glycerol-1-phosphate to 10 mM. The extinction coefficient of cytochrome *c* at 550 nm is 19.23 mM^{-1} cm^{-1}. Succinate and NADH oxidase activities were measured at room temperature in a Clark-type oxygen electrode (Rank Brothers, Cambridge, England). Rates were determined from the slope of a plot of oxygen concentration versus time. Mitochondria (0.5 mg) were incubated in a standard Clark electrode buffer (CEB) containing 0.5 mM EDTA, 2 mM $MgCl_2$, 20 mM phosphate buffer, pH 7.4, 0.6 mM sorbitol and 1 mg ml^{-1} fatty acid-free bovin serum albumin. The substrates, succinate and NADH, were added to 5 mM and 0.5 mM final concentrations, respectively.

Miscellaneous Methods. Standard procedures were used for transforming *E. coli*, for DNA manipulations, and for plasmid isolation from *E. coli*. Protein determination was carried out by a modified Lowry method, using bovine serum albumin as standard (Markwell *et al.*, 1978). Yeast transformations were done by the lithium acetate transformation method (Ito *et al.*, 1983). Genomic DNA was isolated from yeast as described (Philippsen *et al.*, 1991).

2.3. Results

Characterization of the *SDH3* knockout mutant. The *SDH3* gene was disrupted with the *TRP1* marker gene and integrated into the chromosomal *SDH3* locus of the strain MH125 by homologous recombination to yield sdh3W3. The disruption was confirmed by PCR (Fig. 2.1) and Western blotting (Fig. 2.2). Interestingly, Sdh3p is not detectable in mitochondria isolated from sdh4W2 (Fig. 2.2, lane 3). This suggests that in the absence of Sdh4p, Sdh3p is not stable. The mutant was characterized *in vivo* for respiratory growth on synthetic and complex glycerol media and *in vitro* for enzymatic activities. sdh3W3 has lost the ability to grow on minimal medium with glycerol as the sole carbon source unless a plasmid-borne wild type *SDH3* gene is introduced. However, the mutant can grow slowly on complex medium containing glycerol. That the impaired respiration did not result from a spontaneous mutation in the mitochondrial genome was verified by mating with a rho^0 strain, MS10. The resulting diploid is fully competent to grow on glycerol containing media. These data indicate that the Sdh3p subunit is essential for respiration. We further measured the enzymatic activities in submitochondrial particles prepared from the mutant strain, sdh3W3 and the wild type strains, MH125 and sdh3W3 pYCSDH3 (Table 2.1). sdh3W3 membranes show severely reduced levels of malonate-sensitive succinate-DB reductase, succinate-PMS reductase, succinate-cytochrome *c* reductase, and succinate oxidase activities as compared to the wild type strains, MH125 and sdh3W3 pYCSDH3. Similarly, the level of acid precipitable flavin is severely reduced in the mutant. In contrast, the levels of antimycin A-sensitive NADH oxidase and glycerol-1-phosphate dehydrogenase activities are unaffected in the mutant. These

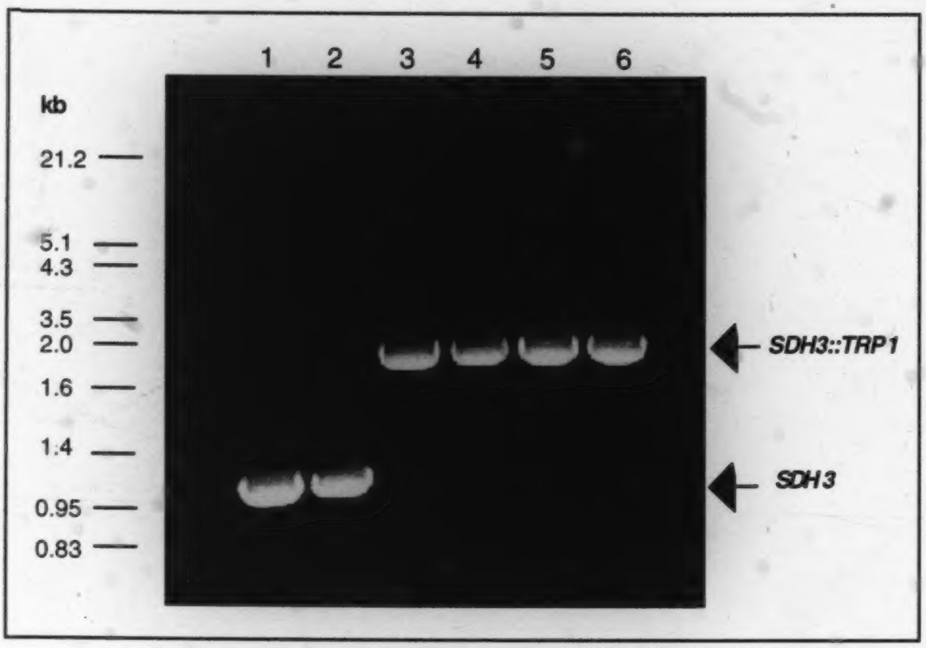

Figure 2.1 Agarose Gel Analysis of PCR Products.

The PCR products were obtained using the upstream and downstream primers (see "Materials and Methods") with MH125 genomic DNA (lanes 1 and 2) or genomic DNA from tryptophan prototrophic, respiration deficient transformants carrying the *SDH3* disruption mutations (lanes 3-6). The deletion of 0.13-kb of SDH3 coding sequence and the insertion of the 0.83-kb TRP1 DNA is expected to result in the production of a 1.76-kb band in the mutant as opposed to a 1.06-kb in the wild type.

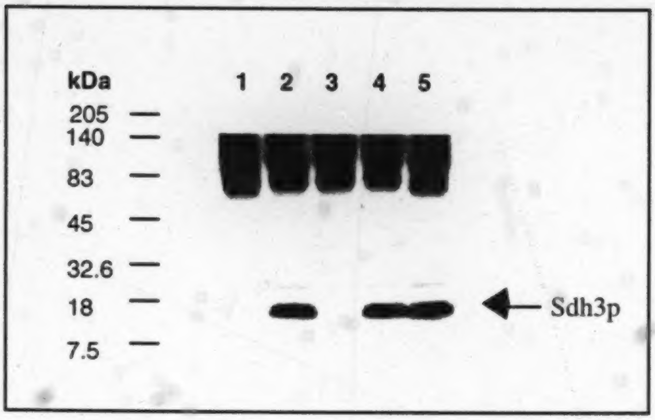

Figure 2.2 Western Blot Analysis of Mutant and Wild Type Mitochondria.

Mitochondria were isolated from galactose-grown MH125, sdh3W3 and sdh4W2 knock-out strains and 10 µg electrophoresed on 13 % Tricine SDS-PAGE, and immunoblotted using anti-Sdh3p antibody. Lanes 1 to 5 are: sdh3w3, sdh3W3/pYC111SDH3, sdh4W2, sdh4W2/pSDH4-17, and MH125, respectively.

Table 2.1

Enzymatic Activities of Submitochondrial Particles

	MH125	Sdh3W3-pYCSDH3	sdh3W3
Succinate-DB/DCPIP reductase[a]	130	99	ND (> 5%)
Succinate-cytochrome *c* reductase[b]	65	55	ND (> 3%)
Succinate oxidase[c]	50	45	ND (> 6%)
Succinate-PMS/DCPIP reductase[a]	170	145	ND (> 4%)
NADH oxidase[c]	130	148	120
Glycerol-1-P-cytochrome *c* reductase[b]	85	75	60
Covalent FAD[e]	40	35	ND (> 6%)

Enzymatic activities are assayed in submitochondrial particles as described under "Material and Methods". Each value represents the mean of three independent determinations. [a] Activities are expressed as nanomoles of DCPIP reduced min^{-1} mg^{-1} of protein; [b] Activities are expressed as nanomoles of cytochrome *c* reduced min^{-1} mg^{-1} of protein; [c] Activities are expressed as nanoatoms of oxygen min^{-1} mg^{-1} of protein; [d] Acid precipitable flavin contents are expressed as picomoles of flavin mg^{-1} of protein; ND, not detectable.

observations indicate that the disruption specifically affected SDH and confirm the role of the Sdh3p subunit as necessary for SDH function.

Fumarate-oxidizable Spectrum of Yeast Mitochondrial Membranes. Since cytochrome b_{562} of complex III is considerably more abundant than that of SDH in *S. cerevisiae*, the spectrum of the latter is not readily observable in the classical difference absorption spectrum of yeast mitochondria. In the bovine SDH, excess fumarate rapidly oxidizes dithionite-reduced cytochrome b_{560}. The other chromophores reduced by dithionite can be subsequently reoxidized by ferricyanide (Hatefi and Galante, 1980), suggesting it is a unique property of cytochrome b_{560} to be selectively oxidized by fumarate after dithionite reduction. By exploiting this property, investigators working on yeast complex III have demonstrated the presence of a *b*-type cytochrome in SDH (Brasseur *et al.*, 1997; Bruel *et al.*, 1995). We used a similar approach to determine the cytochrome *b* content of the yeast SDH. Shown in Fig. 2.3 is the fumarate-oxidizable spectrum of mitochondria isolated from lactate-grown MH125 cells. The major peak, which appears within 1 minute after the addition of fumarate, is symmetrical and is centered at 562 nm. There is only a small peak at 605 nm, indicating that cytochrome aa_3 remains reduced. Addition of ferricyanide leads to the reoxidation of cytochromes cc_1, complex III associated cytochrome *b*, and cytochrome aa_3 (Data not shown). The amount of cytochrome b_{562} calculated from the spectrum is 0.92 ± 0.11 moles/moles of covalent FAD (Table 2.2), suggesting the presence of a single heme per SDH holoenzyme. Also shown in Table 2.2 are the mitochondrial contents of cytochromes aa_3, $c + c_1$, and $b_{562} + b_{565}$ calculated from the dithionite-reduced minus ferricyanide-oxidized difference spectrum (Fig. 2.4).

Difference Absorption Spectra of Mutant and Wild Type Mitochondrial Membranes. Residues likely to be involved in heme coordination are usually contributed by the SDH anchor polypeptides (Hägerhäll, 1997; Hägerhäll and Hederstedt, 1996). We investigated the effects of *SDH3* and *SDH4*

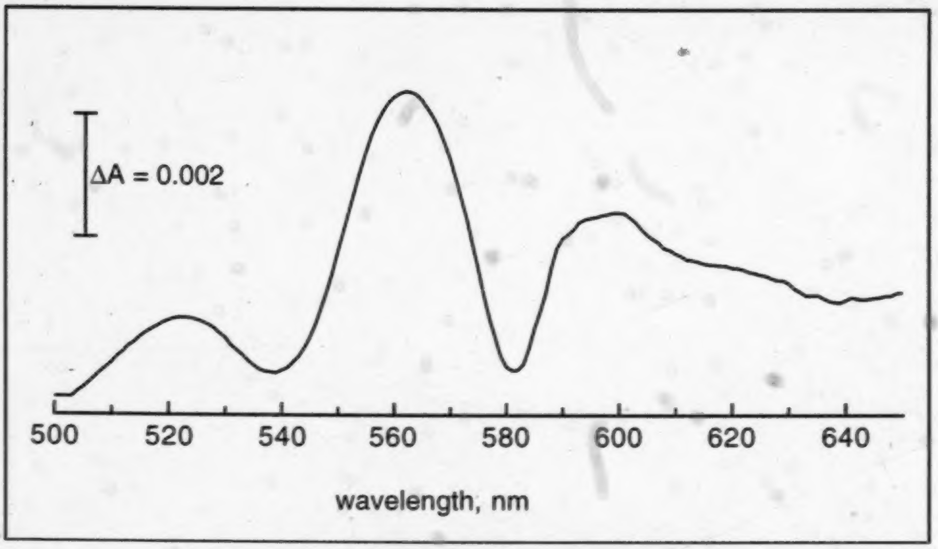

Figure 2.3 Fumarate-oxidizable Absorption Spectrum of Mitochondria Isolated from Lactate-grown MH125 Cells.

Mitochondria, prepared from lactate-grown MH125 cells, were suspended to a covalent flavin level of 185 pmol/ml and the dithionite-reduced minus dithionite-reduced/fumarate-oxidized spectrum determined. Mitochondria were reduced by adding a few grains of dithionite and oxidized with 40 mM fumarate (final concentration).

Table 2.2

Concentrations of Cytochromes in Yeast Mitochondrial Membranes

Cytochrome	Wavelength Pair (nm)	Concentration[a]
aa_3	605-630	6.5 ± 0.1
$c + c_1$	550-540	12.9 ± 1.1
$b_{562}+b_{565}$ (Complex III)	562-590	8.1 ± 1.1
b_{562} (complex II)	562-578	0.92 ± 0.11

Concentrations of the cytochromes aa_3, $c+c_1$, and $b_{562}+b_{565}$ were calculated, using the indicated wavelength pairs, from the dithionite-reduced minus ferricyanide-oxidized difference spectrum of MH125 mitochondria (Fig. 2.4) while that of cytochrome b_{562} of complex II was calculated from the spectrum in Fig. 2.3. [a] Concentrations are expressed as moles of cytochromes moles^{-1} of covalent FAD. Values represent the means of triplicate determinations ± S.E.M.

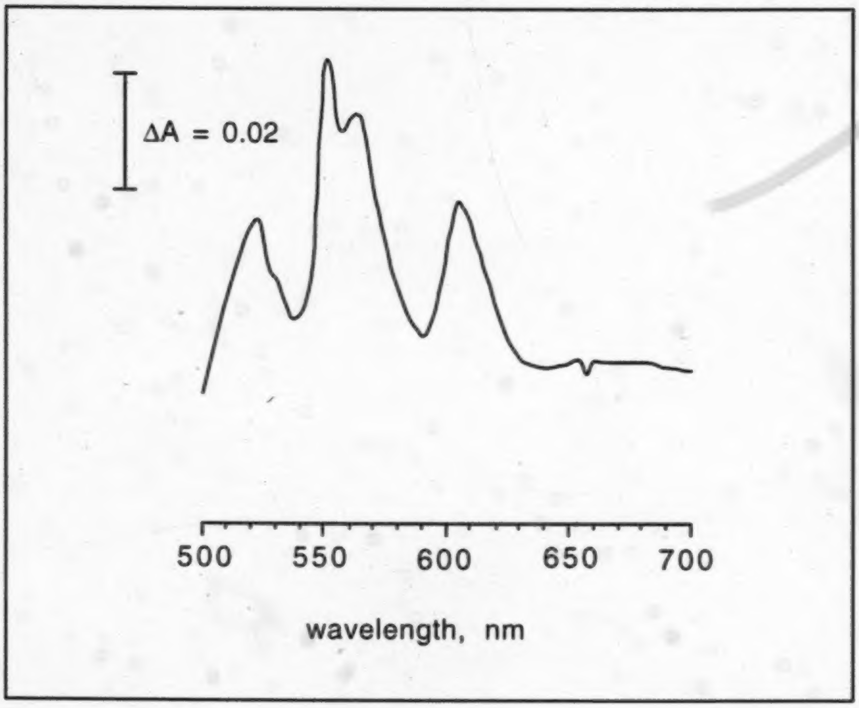

Figure 2.4 Difference Absorption Spectrum of Mitochondria Isolated from Lactate-grown MH125 Cells.

Mitochondria, prepared from lactate-grown MH125 cells, were suspended to a covalent flavin level of 185 pmol/ml and the dithionite-reduced minus ferricyanide-oxidized spectrum determined. Mitochondria were reduced by adding a few grains of dithionite and oxidized with 10 μM potassium ferricyanide (final concentration). The α absorption bands corresponding to cytochromes aa_3, b_{562} + b_{565}, and $c + c_1$ are 605, 562 and 550 nm, respectively.

knockout mutations on the mitochondrial contents of cytochrome b_{562}. Depicted in Fig. 2.5 are the absorption spectra of mitochondrial membranes isolated from galactose-grown mutant and wild type yeast strains. The total cytochrome spectra of mitochondria isolated from both wild type and mutant strains are comparable. Similarly, the fumarate-oxidizable cytochrome *b* peak, centered at 562 nm, is present in mitochondria from the wild type strain, MH125 or the plasmid complemented strains, sdh3W3/pYCSDH3 and sdh4W2/pSDH4-17 (Fig 2.6). In contrast, the fumarate-oxidizable cytochrome b_{562} spectrum is not detectable in sdh3W3 or sdh4W2 mitochondria (Fig. 2.6), strongly suggesting that it is a component of the yeast SDH.

To further demonstrate the reliability of the fumarate-oxidizable spectra in detecting a heme associated with SDH, we used the SDH-specific inhibitor, malonate. Malonate competes with succinate and fumarate for the SDH dicarboxylate-binding site. Thus, as expected, malonate prevents the oxidation of cytochrome b_{652} by preventing the binding of fumarate to the SDH holoenzyme present in MH125 mitochondria (Fig. 2.6).

2.4. Discussion

In summary, we demonstrate here that: (1) the *SDH3* gene is necessary for SDH function; (2) the *S. cerevisiae* SDH contains a stoichiometric amount of cytochrome b_{562}; (3) the fumarate-oxidizable heme is not detectable in the absence of either of the SDH anchor polypeptides, Sdh3p or Sdh4p or in the presence of malonate. A disruption of the *S. cerevisiae SDH3* gene, constructed by replacing the chromosomal copy of the *SDH3* gene with the mini-Mu transposon sequences, has earlier been reported (Daignan-Fornier *et al.*, 1994). *In vivo* characterization of this mutant shows that its growth on nonfermentable carbon sources is severely impaired. These observations are consistent with the results of the current study. We extend this study by further characterizing the mutant *in vitro* (Table 2.2). The

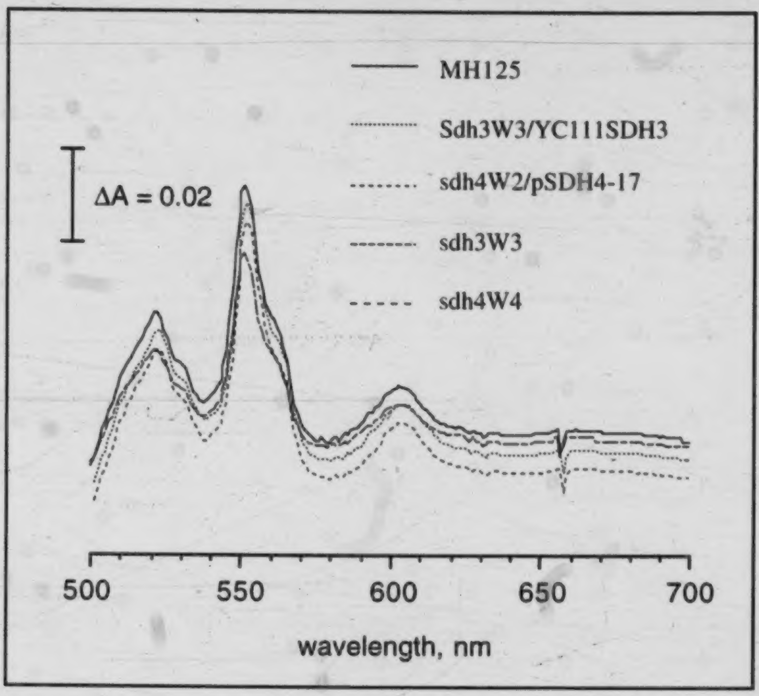

Figure 2.5 Difference Absorption Spectra of Mutant and Wild Type *S. cerevisiae* Strains.

Membranes were prepared from mitochondria isolated from galactose-grown cells by extraction with lauryl maltoside and centrifugation at 100,000 × *g* for 15 min. Mitochondrial proteins were normalized to a covalent flavin level of 185 pmol/ml and the dithionite-reduced minus ferricyanide-oxidized spectrum determined. Mitochondria were reduced by adding a few grains of dithionite and oxidized with 10 μM potassium ferricyanide (final concentration).

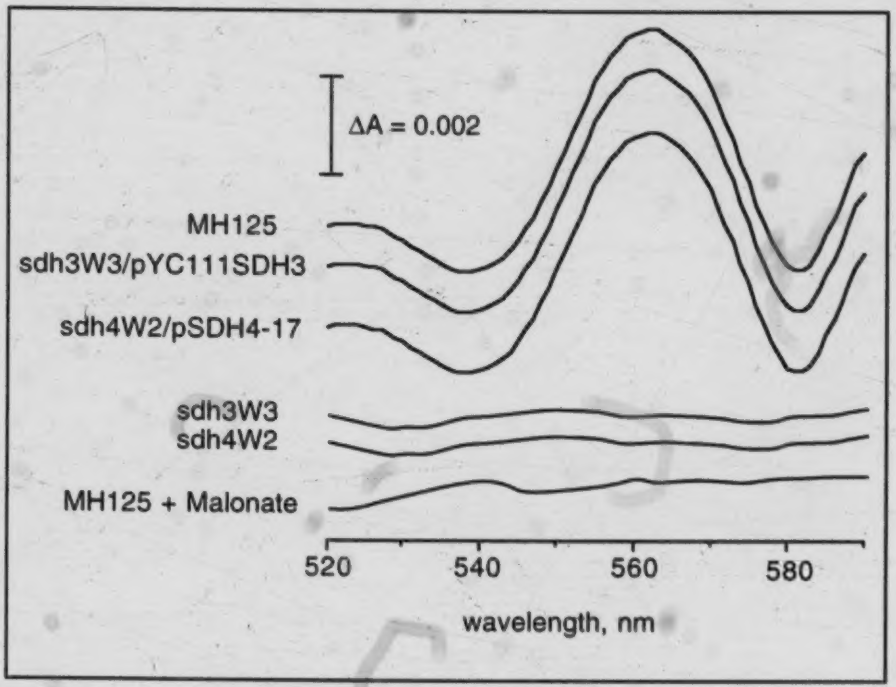

Figure 2.6 **Fumarate-oxidizable Spectra of Mutant and Wild Type *S. cerevisiae* Strains.**

Mitochondria were isolated from galactose-grown cells, suspended to a covalent flavin level of 185 pmol/ml and the dithionite-reduced minus dithionite-reduced/fumarate-oxidized spectrum determined. Mitochondria were reduced by adding a few grains of dithionite and oxidized with 40 mM fumarate (final concentration). Malonate was added to a final concentration of 40 mM prior to the addition of fumarate.

enzymatic activities of sdh3W3 membranes are consistent with the inability of this strain to grow on minimal glycerol.

The recently completed yeast genome project (Goffeau *et al.*, 1996) has unearthed a homologue of the *SDH3* gene, *YMR118C* (Accession number Z49702.1). This homologue is located on chromosome XIII and encodes a putative mitochondrial membrane protein (Swiss Protein Accession number Q04487) of 196 amino acid residues. The primary sequence is 57% identical and 72% similar to that of the Sdh3p subunit (Fig. 2.7). However, the function of this gene has yet to be determined. The data obtained in this study indicate that the *SDH3* gene is the major gene that is expressed under our assay conditions. Similarly, the yeast genome database contains two genes (*YLR164W* and *YOR297C*) encoding Sdh4p homologues (Fig. 2.8). YLR164W and YOR297C are respectively 52% and 36% identical and 74% and 57% similar to Sdh4p. An isoform of the yeast *SDH1* gene, *SDH1b*, was recently shown to suppress an *SDH1* mutation when overexpressed (Colby *et al.*, 1998). However, the extremely low expression level of this gene suggests that it may not play a major role in mitochondrial respiration. The *SDH1*, *2*, *3*, and *4* knockouts are respiration deficient and it does not appear that these isoforms are functionally redundant. Why *S. cerevisiae* should have multiple genes for SDH subunits is unclear at present. Future studies should investigate the conditions under which these genes are expressed and their roles, if any, in respiration.

The present study is the first to demonstrate the presence of a stoichiometric amount of heme in the yeast SDH. Our data contradict an earlier study reporting a substoichiometric molar ratio of heme to covalent FAD in an immuno-affinity purified SDH (Schilling *et al.*, 1982). We believe that the purification procedure employed in the earlier study leads to the loss of heme. The use of whole mitochondria in this study may have prevented such a loss. Even mammalian SDH, which is uniformly acknowledged to contain heme, is usually

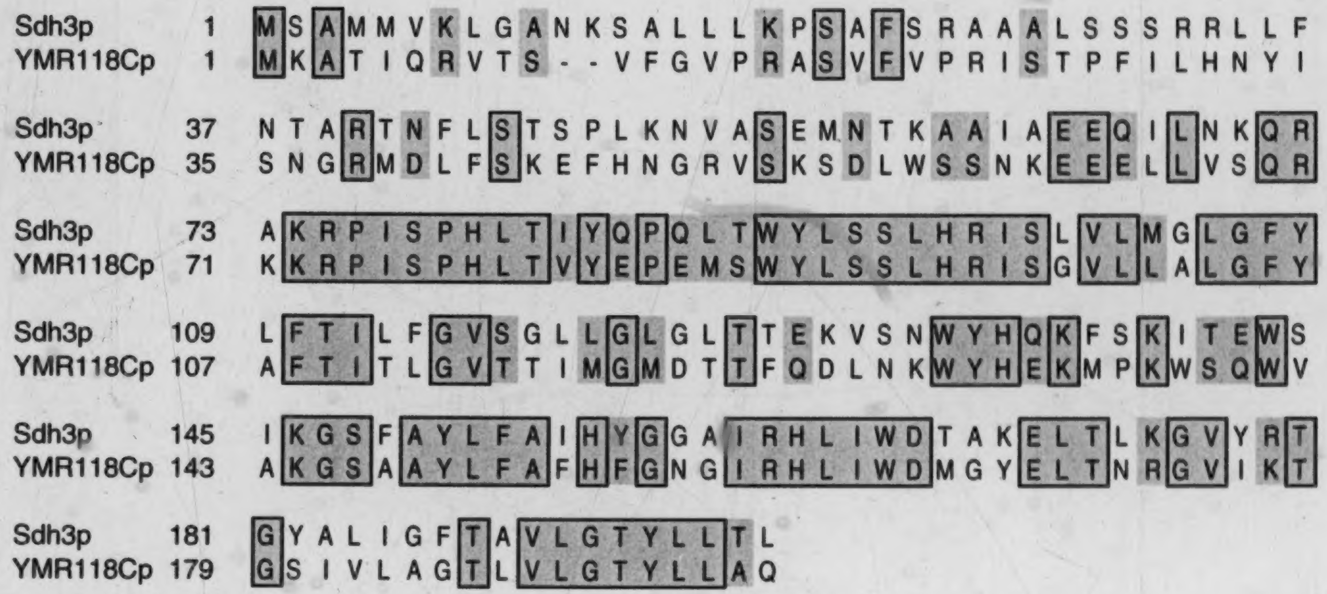
Sdh3p 1 M S A M M V K L G A N K S A L L L K P S A F S R A A A L S S S R R L L F
YMR118Cp 1 M K A T I Q R V T S - - V F G V P R A S V F V P R I S T P F I L H N Y I
Sdh3p 37 N T A R T N F L S T S P L K N V A S E M N T K A A I A E E Q I L N K Q R
YMR118Cp 35 S N G R M D L F S K E F H N G R V S K S D L W S S N K E E E L L V S Q R
Sdh3p 73 A K R P I S P H L T I Y Q P Q L T W Y L S S L H R I S L V L M G L G F Y
YMR118Cp 71 K K R P I S P H L T V Y E P E M S W Y L S S L H R I S G V L L A L G F Y
Sdh3p 109 L F T I L F G V S G L L G L G L T T E K V S N W Y H Q K F S K I T E W S
YMR118Cp 107 A F T I T L G V T T I M G M D T T F Q D L N K W Y H E K M P K W S Q W V
Sdh3p 145 I K G S F A Y L F A I H Y G G A I R H L I W D T A K E L T L K G V Y R T
YMR118Cp 143 A K G S A A Y L F A F H F G N G I R H L I W D M G Y E L T N R G V I K T
Sdh3p 181 G Y A L I G F T A V L G T Y L L T L
YMR118Cp 179 G S I V L A G T L V L G T Y L L A Q

Figure 2.7 Alignment of the *S. cerevisiae* Sdh3p Subunit and its Homologue, YMR118Cp.

Alignment of the protein sequences was generated using the PAM250 matrix with the program ClustalW 1.7 and edited with the program SeqVu. Gaps (*hyphens*) have been introduced to optimize the alignment. Identical residues are boxed while columns with 65% similar residues are shaded. The YMR118Cp sequence is from the Swiss protein database (Accession number Q04487).

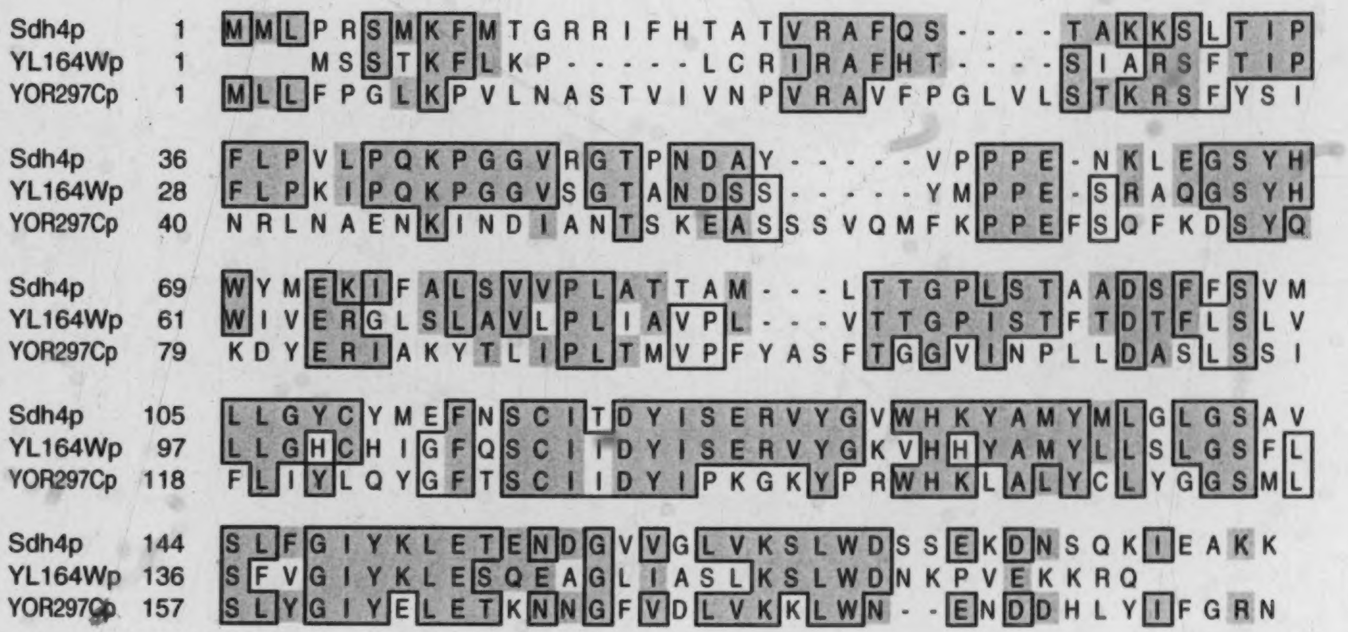
Sdh4p 1 M M L P R S M K F M T G R R I F H T A T V R A F Q S - - - - T A K K S L T I P
YL164Wp 1 M S S T K F L K P - - - - - L C R I R A F H T - - - - S I A R S F T I P
YOR297Cp 1 M L L F P G L K P V L N A S T V I V N P V R A V F P G L V L S T K R S F Y S I
Sdh4p 36 F L P V L P Q K P G G V R G T P N D A Y - - - - - V P P P E - N K L E G S Y H
YL164Wp 28 F L P K I P Q K P G G V S G T A N D S S - - - - - Y M P P E - S R A Q G S Y H
YOR297Cp 40 N R L N A E N K I N D I A N T S K E A S S S V Q M F K P P E F S Q F K D S Y Q
Sdh4p 69 W Y M E K I F A L S V V P L A T T A M - - - L T T G P L S T A A D S F F S V M
YL164Wp 61 W I V E R G L S L A V L P L I A V P L - - - V T T G P I S T F T D T F L S L V
YOR297Cp 79 K D Y E R I A K Y T L I P L T M V P F Y A S F T G G V I N P L L D A S L S S I
Sdh4p 105 L L G Y C Y M E F N S C I T D Y I S E R V Y G V W H K Y A M Y M L G L G S A V
YL164Wp 97 L L G H C H I G F Q S C I I D Y I S E R V Y G K V H H Y A M Y L L S L G S F L
YOR297Cp 118 F L I Y L Q Y G F T S C I I D Y I P K G K Y P R W H K L A L Y C L Y G G S M L
Sdh4p 144 S L F G I Y K L E T E N D G V V G L V K S L W D S S E K D N S Q K I E A K K
YL164Wp 136 S F V G I Y K L E S Q E A G L I A S L K S L W D N K P V E K K R Q
YOR297Cp 157 S L Y G I Y E L E T K N N G F V D L V K K L W N - - E N D D H L Y I F G R N

Figure 2.8 Alignment of the *S. cerevisiae* Sdh4p Subunit and its Homologues.

Alignment of the protein sequences was generated using the PAM250 matrix with the program ClustalW 1.7 and edited with the program SeqVu. Gaps (*hyphens*) have been introduced to optimize the alignment. Identical residues are boxed while columns with 65% similar residues are shaded.

purified with a substoichiometric amount of heme, suggesting the chromophore is easily lost (Ackrell *et al.*, 1992).

The results presented in Table 2.2 suggest a ratio of SDH to complex III of about 1:4 since complex III contains two *b*-type cytochromes. SDH to complex III ratios ranging from 1:2 to 1:10 have been reported for different respiratory chain sources (Trumpower and Katki, 1979). Our determination of a cytochrome b_{562} to covalent FAD ratio of 0.92 in SDH is not influenced by the stoichiometry of the individual respiratory chain complexes. The yeast respiratory chain may function in a kinetically different manner than mammalian respiratory chains (Boumans *et al.*, 1998).

Is it possible that the fumarate-oxidizable cytochrome b_{562} does not reside in SDH, but is linked to it by an electron transport pathway? We consider this possibility unlikely for two reasons. First, a fumarate-oxidizable cytochrome residing out of SDH has not been reported in any system. Second, we have constructed a mutant in Sdh4p, which will be discussed in Chapter 3, that renders the enzyme incapable of quinone reduction. Yet, this mutant still displays a fumarate-oxidizable cytochrome. Thus, electron transport beyond the quinone is not necessary to oxidize cytochrome b_{562}, placing it within SDH in an electron transport pathway between fumarate and ubiquinone.

Is there a role for cytochrome b_{562} in electron transfer from succinate to ubiquinone? Electron transfer in SDH from donor to acceptor occurs via multiple domains. The pathway of electron transfer in SDH is believed to be: succinate —> FAD —> iron-sulfur —> quinone (Ackrell *et al.*, 1992; Hederstedt and Ohnishi, 1992). For the reverse reaction, in which fumarate is reduced to succinate, the pathway of electron flow is in the opposite direction (Van Hellemond and Tielens, 1994). The role of heme in this scenario remains obscure. Many SDHs contain *b*-type hemes but the content and redox properties of these hemes vary considerably. The *B. subtilis* SDH contains two *b*-type hemes (Hägerhall *et al.*, 1992;

Hederstedt, 1980), while the *E. coli* and *Ascaris suum* SDHs have one (Kita *et al.*, 1989; Takamiya *et al.*, 1986; Takamiya *et al.*, 1990). In *B. subtilis*, the heme with the higher potential (E'_m = +65 mV) is reduced by succinate while the heme with the lower potential (E'_m = -95 mV) is not (Hägerhall *et al.*, 1992; Hederstedt, 1980). The heme in *E. coli* SDH is fully reducible (Kita *et al.*, 1989) while that of *A. suum* SDH is only partially reduced by succinate (Takamiya *et al.*, 1986; Takamiya *et al.*, 1990). Bovine SDH cytochrome b_{560} is not readily reducible by succinate (Yu *et al.*, 1987). In *B. subtilis* SDH, the cytochrome plays a structural role (Fridén and Hederstedt, 1990), while the loss of heme does not impair the assembly of the *E. coli* enzyme (Vibat *et al.*, 1998). The role of heme in the succinate-mediated reduction of ubiquinone will be addressed in further studies (Chapters 3-5).

All SDH cytochromes are known to be coordinated by 2 histidine residues (Hägerhäll, 1997; Hägerhäll and Hederstedt, 1996). In the yeast Sdh3p, His-106 is positioned in the putative transmembrane helix 2 and may be such a ligand. However, a second conserved His that serves as a heme ligand in other SDHs is replaced by Cys-78 in the yeast Sdh4p. Therefore, determining the heme ligands in the yeast SDH may reveal unusual coordination. Further studies will be required to define the redox properties of SDH cytochrome b_{562}. To do this, it will be necessary to overexpress or purify SDH, due to the paucity of this cytochrome in yeast mitochondria.

2.5. Bibliography

Abraham, P. R., Mulder, A., van 't Riet, J., and Raué, H. A. (1994). Characterization of the *Saccharomyces cerevisiae* nuclear gene *CYB3* encoding a cytochrome *b* polypeptide of respiratory complex II. *Mol. Gen. Genet.* **242,** 708-716.

Ackrell, B. A. C., Johnson, M. K., Gunsalus, R. P., and Cecchini, G. (1992). Structure and function of succinate dehydrogenase and fumarate reductase. In

Chemistry and biochemistry of flavoenzymes, F. Müller, ed. (Boca Raton, Florida: CRC Press, Inc.,), pp. 229-297.

Boumans, H., Grivell, L. A., and Berden, J. A. (1998). The respiratory chain in yeast behaves as a single functional unit. *J. Biol. Chem.* **273,** 4872-4877.

Brasseur, G., Tron, G., Dujardin, G., Slonimski, P. P., and Brivet-Chevillotte, P. (1997). The nuclear *ABC1* gene is essential for the correct conformation and functioning of the cytochrome bc_1 complex and the neighbouring complexes II and IV in the mitochondrial respiratory chain. *Eur. J. Biochem.* **246,** 103-111.

Bruel, C., Brasseur, R., and Trumpower, B. L. (1996). Subunit 8 of the *Saccharomyces cerevisiae* cytochrome *bc*1 complex interacts with succinate-ubiquinone reductase complex. *J. Bioenerg. Biomembr.* **28,** 59-68.

Bruel, C., di Rago, J.-P., Slonimski, P. P., and Lemesle-Meunier, D. (1995). Role of the evolutionarily conserved cytochrome *b* tryptophan 142 in the ubiquinol oxidation catalyzed by the *bc*1 complex in the yeast *Saccharomyces cerevisiae. J. Biol. Chem.* **270,** 22321-22328.

Bullis, B. L., and Lemire, B. D. (1994). Isolation and characterization of the *Saccharomyces cerevisiae SDH4* gene encoding a membrane anchor subunit of succinate dehydrogenase. *J. Biol. Chem.* **269,** 6543-9.

Colby, G., Ishii, Y., and Tzagoloff, A. (1998). Suppression of *SDH1* mutations by the *SDH1b* gene of *Saccharomyces cerevisiae. Yeast* **14,** 1001-6.

Cole, S. T., Condon, C., Lemire, B. D., and Weiner, J. H. (1985). Molecular biology, biochemistry, and bioenergetics of fumarate reductase, a complex membrane-bound iron-sulfur flavoenzyme of *Escherichia coli. Biochim. Biophys. Acta* **811,** 381-403.

Daignan-Fornier, B., Valens, M., Lemire, B. D., and Bolotin-Fukuhara, M. (1994). Structure and regulation of *SDH3*, the yeast gene encoding the cytochrome b_{560} subunit of respiratory complex II. *J. Biol. Chem.* **269,** 15469-72.

de Kok, J., Muller, J. L. M., and Slater, E. C. (1975). EPR studies on the respiratory chain of wild-type *Saccharomyces cerevisiae* and mutants with a deficiency in succinate dehydrogenase. *Biochim. Biophys. Acta* **387,** 441-450.

Fridén, H., and Hederstedt, L. (1990). Role of His residues in *Bacillus subtilis* cytochrome b_{558} for haem binding and assembly of succinate:quinone oxidoreductase (complex II). *Mol. Microbiol.* **4,** 1045-1056.

Gietz, R. D., and Sugino, A. (1988). New yeast-*Escherichia coli* shuttle vectors constructed with *in vitro* mutagenized yeast genes lacking six-base pair restriction sites. *Gene* **74,** 527-534.

Goffeau, A., Barrell, B. G., Bussey, H., Davis, R. W., Dujon, B., Feldmann, H., Galibert, F., Hoheisel, J. D., Jacq, C., Johnston, M., Louis, E. J., Mewes, H. W., Murakami, Y., Philippsen, P., Tettelin, H., and Oliver, S. G. (1996). Life with 6000 genes. *Science* **274,** 546, 563-567.

Hägerhäll, C. (1997). Succinate:quinone oxidoreductases: variations on a conserved theme. *Biochim. Biophys. Acta* **1320,** 107-141.

Hägerhall, C., Aasa, R., Von Wachenfeldt, C., and Hederstedt, L. (1992). Two hemes in *Bacillus subtilis* succinate:menaquinone oxidoreductase (complex II). *Biochemistry* **31,** 7411-7421.

Hägerhäll, C., and Hederstedt, L. (1996). A structural model for the membrane-integral domain of succinate:quinone oxidoreductases. *FEBS Lett.* **389,** 25-31.

Hatefi, Y., and Galante, Y. M. (1980). Isolation of cytochrome b_{560} from complex ii (succinate:ubiquinone oxidoreductase) and its reconstitution with succinate dehydrogenase. *J. Biol. Chem.* **255,** 5530-5537.

Hederstedt, L. (1980). Cytochrome *b* reducible by succinate in an isolated succinate dehydrogenase-cytochrome *b* complex from *Bacillus subtilis* membranes. *J. Bacteriol.* **144,** 933-940.

Hederstedt, L. (1998). The membrane-integral domain of succinate:quinone oxidoreductases-a secretive haem-containing domain. *Biochem. Soc. Trans.* **26,** 408-413.

Hederstedt, L., and Ohnishi, T. (1992). Progress in Succinate:quinone oxidoreductase research. In Molecular mechanisms in bioenergetics, L. Ernster, ed. (New York: Elsevier Science Publishers), pp. 163-197.

Ito, H., Fukuda, Y., Murata, K., and Kimura, A. (1983). Transformation of intact yeast cells treated with alkali cations. *J. Bacteriol.* **153,** 163-168.

Kita, K., Vibat, C. R. T., Meinhardt, S., Guest, J. R., and Gennis, R. B. (1989). One-step purification from *Escherichia coli* of complex II (succinate:ubiquinone oxidoreductase) associated with succinate-reducible cytochrome b_{556}. *J. Biol. Chem.* **264,** 2672-2677.

Lemire, B. D., Robinson, J. J., and Weiner, J. H. (1982). Identification of membrane anchor polypeptides of *Escherichia coli* fumarate reductase. *J. Bacteriol.* **152,** 1126-1131.

Lombardo, A., and Scheffler, I. E. (1989). Isolation and characterization of a *Saccharomyces cerevisiae* mutant with a disrupted gene for the IP subunit of succinate dehydrogenase. *J. Biol. Chem.* **264,** 18874-18877.

Markwell, M. A., Haas, S. M., Bieber, L. L., and Tolbert, N. E. (1978). A modification of the Lowry procedure to simplify protein determination in membrane and lipoprotein samples. *Anal. Biochem.* **87,** 206-10.

Meunier-Lemesle, D., Chevillotte-Brivet, P., and Pajot, P. (1980). Cytochrome b_{565} in *Saccharomyces cerevisiae*: use of mutants in the *Cox-Box* region of the mitochondrial DNA to study the functional role of this spectra species of cytochrome *b*. 1. Measurements of cytochrome *b*-562 and *b*-565 and selection of revertants devoid of cytochrome *b*-565. *Eur. J. Biochem.* **111,** 151-159.

Oyedotun, K. S., and Lemire, B. D. (1997). The carboxyl terminus of the *Saccharomyces cerevisiae* succinate dehydrogenase membrane subunit, sdh4p, is necessary for ubiquinone reduction and enzyme stability. *J. Biol. Chem.* **272,** 31382-31388.

Philippsen, P., Stotz, A., and Scherf, C. (1991). DNA of *Saccharomyces cerevisiae*. *Methods Enzymol.* **194,** 169-82.

Robinson, K. M., von Kieckebusch-Gück, A., and Lemire, B. D. (1991). Isolation and characterization of a *Saccharomyces cerevisiae* mutant disrupted for the succinate dehydrogenase flavoprotein subunit. *J. Biol. Chem.* **266,** 21347-21350.

Rothstein, R. (1991). Targeting, disruption, replacement, and allele rescue: integrative DNA transformation in yeast. *Methods Enzymol.* **194,** 281-301.

Schägger, H., Cramer, W. A., and Von Jagow, G. (1994). Analysis and oligomeric states of protein complexes by blue native electrophoresis and isolation of membrane protein complexes by two-dimensional native electrophoresis. *Anal. Biochem.* **217,** 220-230.

Schägger, H., and Von Jagow, G. (1987). Tricine-sodium dodecyl sulfate-polyacrylamide electrophoresis for the separation of proteins in the range from 1 to 100 kDa. *Anal. Biochem.* **166,** 368-379.

Schilling, R. J., Baldwin, T., and Palmer, G. (1982). The characterization of highly purified complex II from baker's yeast. *Fed. Proc.* **41,** 896.

Singer, T. P., and McIntire, W. S. (1984). Covalent Attachment of Flavin to Flavoproteins: Occurence, Assay, and Synthesis. *Methods Enzymol.* **106,** 369-378.

Takamiya, S., Furushima, R., and Oya, H. (1986). Electron-transfer complexes of *Ascaris suum* muscle mitochondria. II. Succinate-coenzyme Q reductase (complex II) associated with substrate-reducible cytochrome b_{558}. *Biochim. Biophys. Acta* **848,** 99-107.

Takamiya, S., Kita, K., Matsuura, K., Furushima, R., and Oya, H. (1990). Oxidation-reduction potentials of cytochromes in *Ascaris* muscle mitochondria:

high-redox-potential cytochrome b_{558} in complex II (succinate-ubiquinone reductase). *Biochemistry* **21,** 1073-1083.

Trumpower, B. L., and Katki, A. G. (1979). Succinate-cytochrome *c* reductase complex of the mitochondrial electron transport chain. In Membrane proteins in energy transduction, R. A. Capaldi, ed. (New York, New York: Marcel Dekker, Inc.), pp. 89-200.

Van Hellemond, J. J., and Tielens, A. G. M. (1994). Expression and functional properties of fumarate reductase. *Biochem. J.* **304,** 321-331.

Vibat, C. R. T., Cecchini, G., Nakamura, K., Kita, K., and Gennis, R. B. (1998). Localization of histidine residues responsible for heme axial ligation in cytochrome b_{556} of complex II (succinate:ubiquinone oxidoreductase) in Escherichia coli. *Biochemistry* **37,** 4148-4159.

Yu, L., Xu, J. X., Haley, P. E., and Yu, C. A. (1987). Properties of bovine heart mitochondrial cytochrome b_{560}. *J. Biol. Chem.* **262,** 1137-1143.

Chapter 3

Function of the Sdh4p Carboxyl-terminal Extension[*]

---

[*] A version of this chapter has been published. Oyedotun, K. S. and Lemire, B. D. (1997) *J. Biol. Chem.* **272**, 31382-31388.

3.1. Introduction

Succinate dehydrogenase (SDH) and fumarate reductase (FRD) form a family of structurally and functionally related respiratory chain proteins. They are typically composed of four nonidentical subunits: a large flavoprotein subunit of about 70 kDa to which is covalently attached an FAD cofactor, an iron-sulfur protein subunit of about 27 kDa that contains three iron-sulfur clusters, and two smaller hydrophobic membrane subunits of about 17 and 13 kDa. The flavoprotein and the iron-sulfur subunits together constitute the catalytic domain while the two hydrophobic subunits constitute the membrane-anchoring domain. The primary structures of the flavoprotein and the iron-sulfur subunits are conserved in SDHs and FRDs of different species, but this is not the case for the membrane anchor subunits (Ackrell *et al.*, 1992; Hägerhäll, 1997; Hägerhäll and Hederstedt, 1996; Hederstedt and Ohnishi, 1992). In addition to the differences in the primary structures, the composition of the membrane-anchoring domain is not conserved. In some SDHs and FRDs, the membrane-anchoring domains contain one larger polypeptide (Hägerhäll, 1997; Hägerhäll and Hederstedt, 1996; Hederstedt, 1998). Thus, the anchor subunits contribute to the unique properties of each enzyme. For example, the SDHs and FRDs from different sources interact with a variety of quinones and are differentially sensitive to quinone analog inhibitors (Ackrell *et al.*, 1992; Hägerhäll, 1997; Hägerhäll and Hederstedt, 1996; Hederstedt and Ohnishi, 1992). Furthermore, the hydrophobic subunits may determine the preferred direction of electron flow in SDH and FRD enzymes. To date, our understanding of the molecular details of electron flow through the membrane subunits is rather limited.

In the *Saccharomyces cerevisiae* SDH, the two hydrophobic subunits, Sdh3p (Abraham *et al.*, 1994; Daignan-Fornier *et al.*, 1994) and Sdh4p (Bullis and Lemire, 1994), are predicted to each contain three membrane-spanning domains.

Alignment of the Sdh4p subunits from different organisms reveals the presence of a 25-30 amino acid extension at the carboxyl-terminus of the *S. cerevisiae* Sdh4p (Fig. 3.1). A search for the presence of functional or structural motifs in the C-terminal extension failed to identify any. We were curious to determine whether the C-terminal extension was required for SDH function in yeast. In this study, we investigate the role of the Sdh4p C-terminal extension by deletion mutagenesis. Truncation of the C-terminus reveals that it is necessary for respiration on non-fermentable carbon sources, for quinone reduction, and for enzyme stability.

3.2. Materials and Methods

Strains, Media, and Culture conditions. The *S. cerevisiae* strains MH125, MS10, sdh4W2, and the *E. coli* strain, DH5α have been described in Chapter 2. Similarly, media and culture conditions were as described in Chapter 2.

Mutant Construction. Three *SDH4* deletion mutants were constructed by polymerase chain reactions with the plasmid, pSDH4-17 as template (Bullis and Lemire, 1994) and the following oligonucleotides as the downstream primers:

1) 5′-TACTTCTAGACGTCGACACCATCATTCTCGGTTTC-3′;

2) 5′-TACTTCTAGACCCATAGACTTTTTACTAAACC-3′; and

3) 5′-TACTTCTAGACTTTCTCGGAAGAATCCC-3′.

Stop codons, encoded within the *Xba*I restriction sites (underlined), were introduced into the *SDH4* gene following the Val-127, Trp-135, or Lys-140 codons (Fig. 3.1) to produce the SDH4ΔC23, SDH4ΔC15, and SDH4ΔC10 constructs, respectively. The oligonucleotides introduced the amino acids aspartate and valine, valine, and valine at the C-termini of the SDH4ΔC23, SDH4ΔC15, and SDH4ΔC10 constructs, respectively. The M13 forward primer, 5'-GTAAAACGACGGCCAGT-3', was used in conjunction with each of the above

Figure 3-1 Multiple Sequence Alignment of the Sdh4p Subunits.

A multiple alignment of the protein sequences was generated using a PAM250 matrix with the program CLUSTALW and edited with the program SeqVu. Gaps (*hyphens*) have been introduced to optimize the alignment. Residues identical to the yeast Sdh4p sequence are boxed. Columns with 65% identical residues are shaded, while putative transmembrane domains are underlined. The protein sources are: *Ec, Escherichia coli; Cb, Coxiella burnetii; Rp, Rickettsia prowazekii; Pp, Porphyra purpurea; Ra, Reclinomonas americana; Mp, Marcantia polymorpha; Cc, Chondrus cripus; Np, Natronobacterium pharanis; Sc, Saccharomyces cerevisiae.* The *S. cerevisiae* Sdh4p sequence is that of the mature polypeptide.

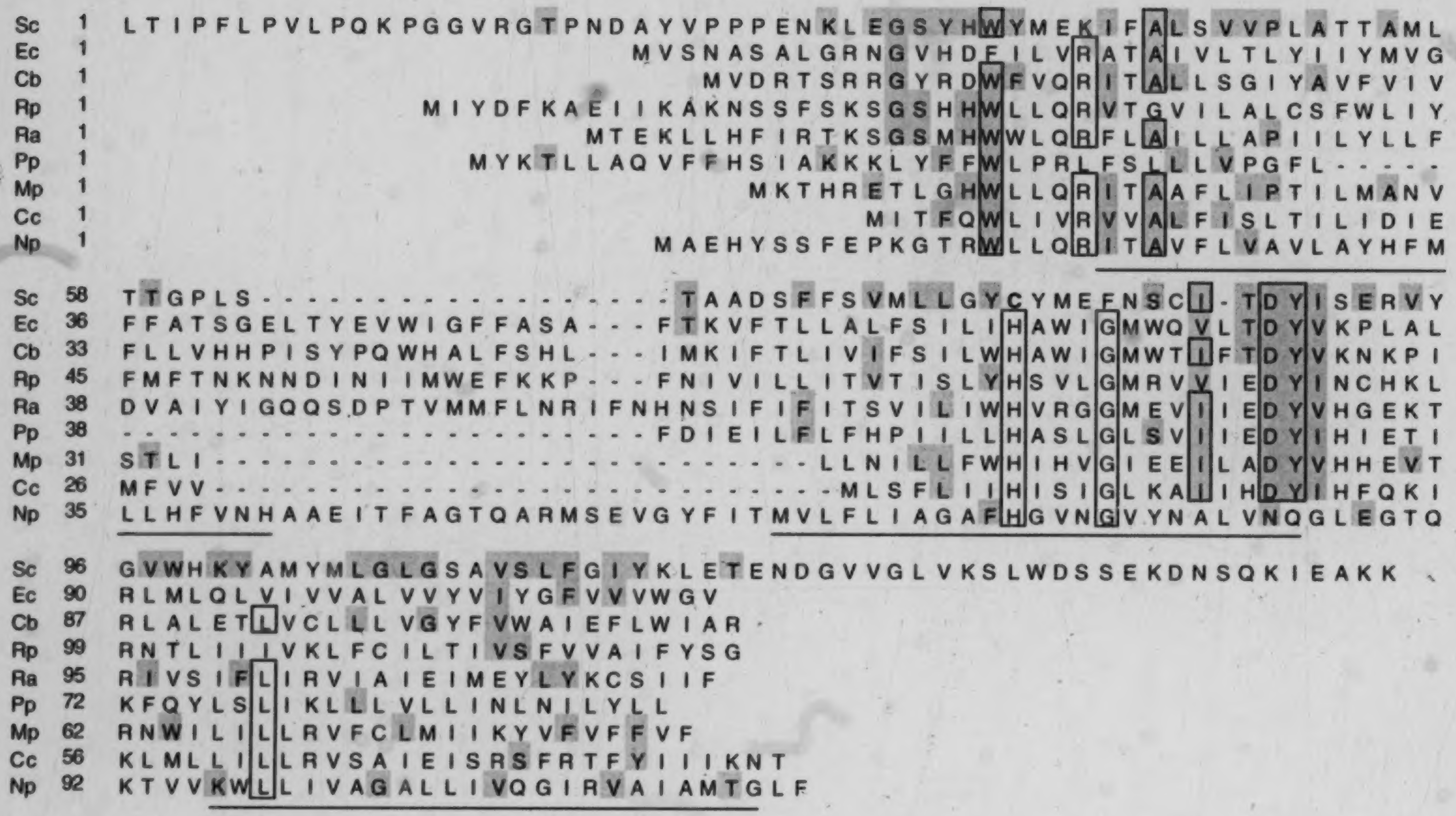

```
Sc   1 LTIPFLPVLPQKPGGVRGTPNDAYVPPPENKLEGSYHWYMEKIFALSVVPLATTAML
Ec   1                       MVSNASALGRNGVHDFILVRATAIVLTLYIIYMVG
Cb   1                          MVDRTSRRGYRDWFVQRITALLSGIYAVFVIV
Rp   1              MIYDFKAEIIKAKNSSFSKSGSHHWLLQRVTGVILALCSFWLIY
Ra   1                     MTEKLLHFIRTKSGSMHWWLQRFLAILLAPIILYLLF
Pp   1                MYKTLLAQVFFHSIAKKKLYFFWLPRLFSLLLVPGFL-----
Mp   1                            MKTHRETLGHWLLQRITAAFLIPTILMANV
Cc   1                                 MITFQWLIVRVVALFISLTILIDIE
Np   1                        MAEHYSSFEPKGTRWLLQRITAVFLVAVLAYHFM

Sc  58 TTGPLS------------------TAADSFFSVMLLGYCYMEFNSCI-TDYISERVY
Ec  36 FFATSGELTYEVWIGFFASA---FTKVFTLLALFSILIHAWIGMWQVLTDYVKPLAL
Cb  33 FLLVHHPISYPQWHALFSHL---IMKIFTLIVIFSILWHAWIGMWTIFTDYVKNKPI
Rp  45 FMFTNKNNDINIIMWEFKKP---FNIVILLITVTISLYHSVLGMRVVIEDYINCHKL
Ra  38 DVAIYIGQQSDPTVMMFLNRIFNHNSIFIFITSVILIWHVRGGMEVIIEDYVHGEKT
Pp  38 -----------------------FDIEILFLFHPIILLHASLGLSVIIEDYIHIETI
Mp  31 STLI--------------------------LLNILLFWHIHVGIEEILADYVHHEVT
Cc  26 MFVV---------------------------MLSFLIIHISIGLKAIIHDYIHFQKI
Np  35 LLHFVNHAAEITFAGTQARMSEVGYFITMVLFLIAGAFHGVNGVYNALVNQGLEGTQ

Sc  96 GVWHKYAMYMLGLGSAVSLFGIYKLETENDGVVGLVKSLWDSSEKDNSQKIEAKK
Ec  90 RLMLQLVIVVALVVYVIYGFVVVWGV
Cb  87 RLALETLVCLLLVGYFVWAIEFLWIAR
Rp  99 RNTLIIIVKLFCILTIVSFVVAIFYSG
Ra  95 RIVSIFLIRVIAIEIMEYLYKCSIIF
Pp  72 KFQYLSLIKLLLVLLINLNILYLL
Mp  62 RNWILILLRVFCLMIIKYVFVFFVF
Cc  56 KLMLLILLRVSAIEISRSFRTFYIIIKNT
Np  92 KTVVKWLLIVAGALLIVQGIRVAIAMTGLF
```

primers. Amplifications were performed using the Expand Long Template PCR System kit (Boehringer Mannheim) according to the manufacturer's instructions. The amplification products were purified, digested with *Xho*I and *Xba*I, and ligated into *Sal*I and *Xba*I-digested YEplac181 (Gietz and Sugino, 1988) to yield the plasmids, pSDH4ΔC23, pSDH4ΔC15, and pSDH4ΔC10. The deletions were confirmed by sequencing. Plasmids were introduced into sdh4W2 by lithium acetate mediated transformation (Ito *et al.*, 1983).

DNA Sequencing and Oligonucleotide synthesis. Oligonucleotides were synthesized as described in Chapter 2. DNA sequencing was carried out in the Department of Biochemistry DNA Core Facility using Sequenase and the Sequenase reaction kits, version 2, from the United States Biochemical Corporation.

Enzyme Assays and Thermal Stability Measurements. Enzymatic activities and covalent flavin contents of submitochondrial particles were measured as described in Chapter 2. For thermal stability measurements, submitochondrial particles (20 mg/ml) were incubated at 30°C in 50 mM potassium phosphate, pH 7.5, 1 mM EDTA and 20 mM succinate. Aliquots were assayed for succinate-DB reductase activity at 5-min intervals.

Analysis of Kinetic Data. Double reciprocal plots (Lineweaver-Burk) were fitted by a weighted least squares algorithm in the EnzymeKinetics software package (Trinity Software, Campton, U. S. A.) to evaluate the inhibition patterns and the apparent Michaelis parameters, K_m and V_{max}. Where non-competitive inhibition was indicated from the nature of the double reciprocal plots generated with different inhibitor concentrations, secondary plots of reciprocal intercepts on the abscissa (or slopes) against the inhibitor concentrations were produced. When the secondary plots were linear, as for the SDH4ΔC23 enzyme, suggesting simple, linear, non-competitive inhibition, the hypothesis was confirmed by performing a non-linear least squares fit to equation 1:

$$v = V\frac{A}{K\left(1+\frac{I}{K_{is}}\right)+A\left(1+\frac{I}{K_{ii}}\right)} \qquad (1)$$

where v is the initial velocity observed in the presence of a fixed inhibitor concentration I, K_{is} and K_{ii} are the slope and intercept inhibition constants, respectively, A is the varied substrate concentration, and K and V are the apparent K_m and V_{max} values, respectively (Cleland, 1979).

Where hyperbolic secondary plots were obtained, as for the wild type, the SDH4ΔC10, and the SDH4ΔC15 enzymes, the data were fitted to equation 2:

$$y = a\frac{\left(1+\frac{I}{K_{i1}}\right)}{\left(1+\frac{I}{K_{i2}}\right)} \qquad (2)$$

where y is the slope or intercept in the presence of a fixed concentration of the inhibitor I, a is the slope or intercept in the absence of inhibitor, and K_{i1} and K_{i2} are the high affinity and low affinity inhibition constants respectively (Cleland, 1979). The equation was compiled into proFit 5.0 (Quantum Soft, Zurich, Switzerland) and fitted by non-linear least squares using the Quasi-Newton algorithm. In all cases, the fit with the lowest sum of squares error (SSE) was chosen to describe the inhibition patterns.

Miscellaneous Methods. All other methods, including DNA manipulations, protein determinations, and preparations of mitochondria and submitochondrial particles have been described in Chapter 2.

3.3. Results

Construction of a Chromosomal *SDH4* Deletion Mutant. An *SDH4* disruption mutant, sdh4K7, previously made by insertion of the *LYS2* marker into the *SDH4* open reading frame still possessed low levels of succinate-quinone reductase activity (Bullis and Lemire, 1994). We surmised that the N-terminal peptide of 65-amino acid residues might retain partial Sdh4p function. A complete deletion of the *SDH4* gene in the parent strain, MH125, was constructed by Bonnie Bullis in which the entire *SDH4* open reading frame is replaced by the *TRP1* marker gene by targeted gene disruption to produce the strain, sdh4W2. The genotype was confirmed by Southern blot analysis (data not shown). As expected, sdh4W2 has lost the ability to use glycerol as the sole carbon source on synthetic medium unless a wild type *SDH4* gene is introduced.

***In vivo* Characterization of the Sdh4p C-Terminal Deletion Mutants.** The presence of the unusual C-terminal extension in the yeast Sdh4p sequence (Fig. 3.1) prompted us to determine whether this extension is required for proper enzyme function. Truncated, plasmid-borne *SDH4* genes were constructed and introduced into sdh4W2. Deletion of 23 amino acid residues in pSDH4ΔC23 severely impairs respiratory growth on the non-fermentable carbon sources, glycerol and lactate. That the impaired respiration did not result from a mutation in the mitochondrial genome was verified by mating with a rho° strain, MS10; the diploid is fully competent to grow on glycerol-containing media. These data indicate that the *SDH4* C-terminal extension is essential for SDH function *in vivo.*

To more precisely define the critical sequences in the C-terminal extension that are required for SDH function, two shorter truncations were constructed (Fig. 3.2). The plasmids pSDH4ΔC10 and pSDH4ΔC15 both conferred the ability to grow on glycerol-containing media to sdh4W2.

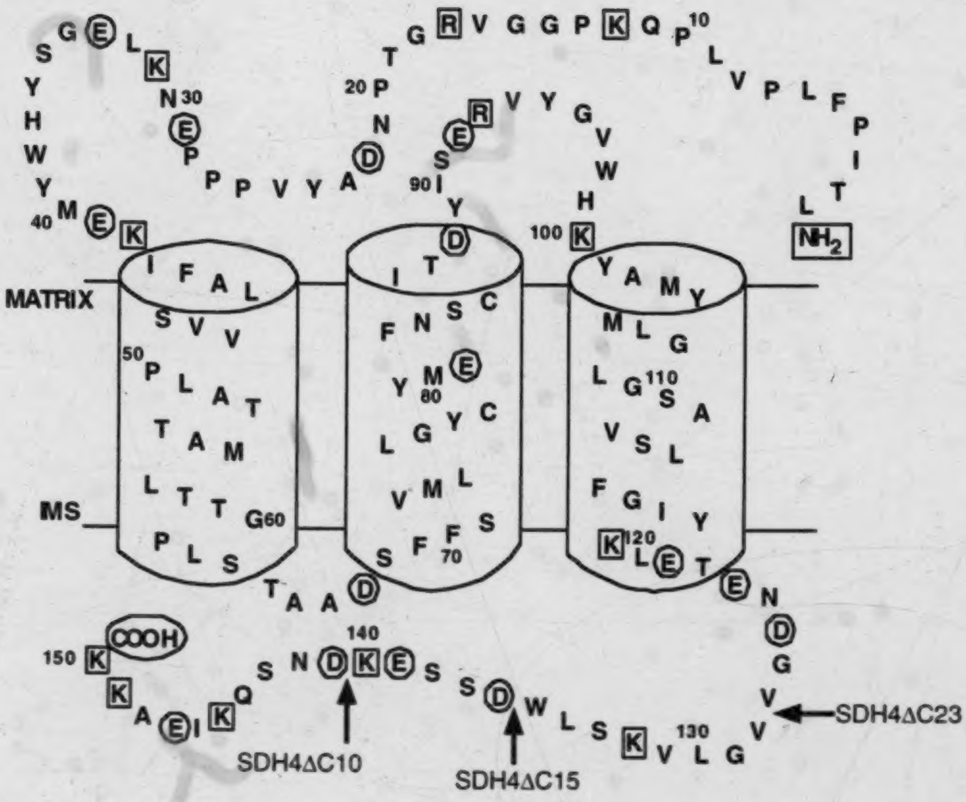
MATRIX
MS
NH_2
COOH
10
20
30
40
50
60
70
80
90
100
110
120
130
140
150
SDH4ΔC10
SDH4ΔC15
SDH4ΔC23

Figure 3.2 Topological Model for the Sdh4p Subunit.

The structure of the Sdh4p subunit was developed after hydropathy analysis. Positively charged amino acids are boxed while negatively charged residues are circled. Arrows indicate the positions of the Sdh4p C-terminal truncations.

In order to compare the respiratory growth abilities of the wild type and mutant strains, growth on semisynthetic medium containing 0.1, 0.2, 0.3, 0.4, or 0.5% galactose was monitored (Fig. 3.3). An initial growth phase is fermentative followed by a respiratory phase (Bruel *et al.*, 1995). Growth rates during the fermentative phases were similar for wild type and mutant strains (not shown) but were markedly different in the respiratory phases. The growth yields monitored as the optical densities at 600 nm of late stationary phase cultures reflect the respiratory capabilities of each strain and were plotted against the initial galactose concentrations (Fig. 3.3). The growth yields of the parent strain, MH125, and sdh4W2 carrying the plasmid, pSDH4-17 are similar. The deletion strain, sdh4W2, by fermentation alone achieves 11% of the growth yield of the respiration-proficient wild type on 0.5% galactose. The growth yield of 85% achieved with sdh4W2-pSDH4ΔC10 indicates that this deletion has only minor effects on respiratory growth. In contrast, the growth yield of sdh4W2-pSDH4ΔC23 is severely reduced (29%), while sdh4W2-pSDH4ΔC15 produces an intermediate value (59%). These data indicate that deletion of the C-terminal 23 amino acids of Sdh4p severely impairs respiratory growth *in vivo*, while deletion of 15 residues results in partial impairment.

Enzymatic Characterization of Deletion Mutants. To determine whether the impaired growth we observed is due to a loss of SDH activity or to decreased assembly of the enzyme into the membrane, we prepared mitochondrial membrane fractions for biochemical analysis (Table 3.1). sdh4W2-pSDH4ΔC23 mitochondrial membranes show greatly reduced turnover numbers for succinate-DB reductase, succinate-cytochrome *c* reductase, and malonate-sensitve succinate oxidase activities. As expected, these activities are not detectable in sdh4W2 mitochondrial membranes. Interestingly, the succinate-PMS reductase activity in sdh4W2-pSDH4ΔC23 membranes is the same as that of MH125 membranes. These data indicate that the SDH4ΔC23 enzyme is correctly assembled into

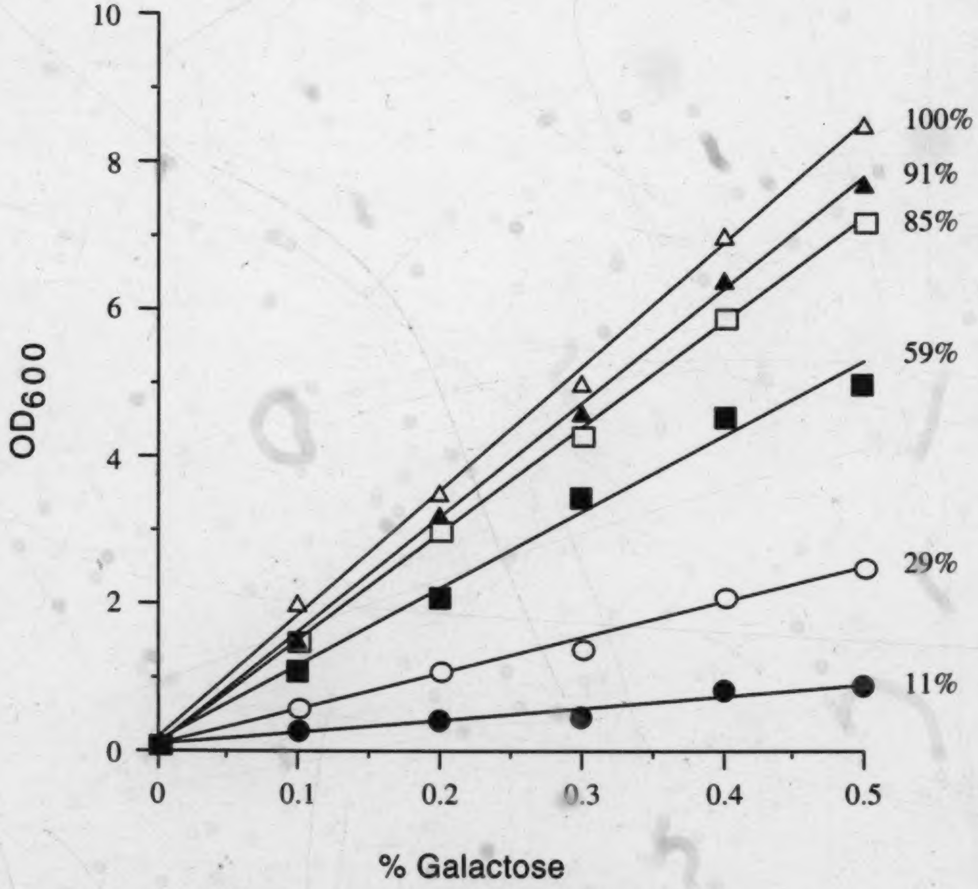

Figure 3-3 Growth of Yeast Strains on Galactose Media.

Yeast strains were grown at 30 °C on semisynthetic liquid medium containing 0.1, 0.2, 0.3, 0.4, and 0.5% galactose and the optical densities at 600 nm were measured (36, 37). Precultures were prepared on selective minimal medium containing 2% galactose and 0.01% glucose. This was used to inoculate the main culture at a starting OD_{600} of 0.1. The cultures were allowed to reach late stationary phase (approximately 100 hours). The relative growth yields were calculated using the final absorbance values reached on 0.5% galactose. The symbols used are: closed circles, sdh4W2; open circles, sdh4W2/SDH4ΔC23; closed squares, sdh4W2/SDH4ΔC15; open squares, sdh4W2/sdh4ΔC10; closed triangles, sdh4W2/pSDH4-17; open triangles, MH125.

Table 3.1

Respiratory Chain Activities of Mitochondrial Membranes

	MH125	sdh4W2-pSDH4-17	sdh4W2-pSDH4ΔC10	sdh4W2-pSDH4ΔC15	sdh4W2-pSDH4ΔC23	sdh4W2
Succinate-DB reductase[a]	3400	3500	3200	2600	600	ND
Succinate-cytochrome *c* reductase[b]	2300	3100	2500	1900	500	ND
Succinate oxidase[c]	2500	3100	2600	1700	700	ND
Succinate-PMS reductase[a]	4100	5100	4100	3700	4300	ND
NADH oxidase[c]	3800	4400	4700	3700	5200	95[e]
Glycerol-1-P-cytochrome *c* reductase[b]	2000	2000	2100	2600	2800	55[f]
Covalent flavin[d]	32	25	29	27	21	ND

[a] Activities are expressed as µmoles of DCPIP reduced min^{-1} µmol FAD^{-1}; [b] Activities are expressed as µmoles of cytochrome *c* reduced min^{-1} µmol FAD^{-1}; [c] Activities are expressed as µatoms of oxygen min^{-1} µmol FAD^{-1}; [d] Covalent flavin contents are expressed as picomoles of FAD mg protein^{-1}; [e] Activity is expressed as nanogram atoms of oxygen min^{-1} mg protein^{-1}; [f] Activity is expressed as nanomoles of cytochrome *c* reduced min^{-1} mg protein^{-1}; ND, activities are between 4 and 6% of wild type values.

mitochondria in near normal amounts and is able to reduce the artificial electron acceptor, PMS but is impaired in the reduction of ubiquinone or a ubiquinone analog (DB). To independently confirm enzyme assembly, we determined the trichloroacetic acid-precipitable flavin levels in mutant and wild type membranes. In *S. cerevisiae*, the amount of acid-precipitable flavin directly reflects the levels of Sdh1p (Robinson and Lemire, 1995; Robinson *et al.*, 1991). The covalent flavin levels of SDH4ΔC23 membranes are only slightly reduced compared to the wild type, supporting our conclusion that membrane assembly is only slightly impaired in this mutant. In contrast, the succinate-PMS reductase and covalent flavin levels in sdh4W2 membranes are not detectable. The levels of NADH oxidase and glycerol-1-phosphate-cytochrome *c* reductase activities are unaffected or even slightly elevated in sdh4W2-pSDH4ΔC23, indicating that the C-terminal deletion specifically affects SDH. Taken together, the results strongly suggest that the C-terminal extension of Sdh4p is not necessary for a membrane anchoring function, but is required for ubiquinone reduction.

As shown in Table 3.1, truncation of 15 amino acids from the C-terminus (SDH4ΔC15) had smaller effects on succinate-DB reductase, succinate-cytochrome *c* reductase, and succinate-oxidase activities, whereas the loss of 10 (SDH4ΔC10) amino acids had no appreciable effects; the results of the enzymatic assays are consistent with observed growth abilities in that the deletions of 10 or 15 amino acids do not greatly impair respiratory abilities. SDH4ΔC15 and SDH4ΔC10 membranes have normal levels of succinate-PMS reductase and covalent flavin. This suggests that the C-terminal decapeptide (DNSQKIEAKK) is dispensable for membrane anchoring and ubiquinone reduction while residues 136 to 140, missing in the SDH4ΔC15 enzyme, are required for optimal quinone reduction activity.

The SDH4ΔC23 Enzyme has a Lower Affinity for Quinones. Since the SDH4ΔC23 enzyme is partially active in quinone reduction, we tested whether its activity could be stimulated by higher quinone concentrations. We preincubated SDH4ΔC23 membranes at 22 °C with a 10-fold excess of DB (0.5 mM) before assaying succinate-DB reductase activity. A greater than 5-fold stimulation could be achieved (Fig. 3.4) with maximal stimulation occurring after a 5 minute incubation. In contrast, preincubation with DB had no effect on the activities of the wild type, the SDH4ΔC15, or the SDH4ΔC10 enzymes (data not shown).

We measured the apparent kinetic parameters K_m and V_{max} for DB reduction using the reporter DCPIP in a coupled enzyme assay. Succinate reduces exogeneous DB directly without interference from endogeneous Q_6 (Zhu and Beattie, 1988). In contrast to earlier observations (Grivennikova and Vinogradov, 1982), we did not observe a lag in enzyme activity. SDH4ΔC23 mitochondrial membranes were preincubated with varying concentrations of DB at room temperature and reactions were initiated by the addition of succinate and DCPIP. The apparent Michaelis constants K_m and V_{max} were calculated and are summarized in Table 3.2. The apparent K_m for DB of the SDH4ΔC23 enzyme (22 μM) is almost 7 times higher than that of the wild type enzyme (3.3 μM). The apparent K_ms for the SDH4ΔC15 and the SDH4ΔC10 enzymes are only slightly higher than that of the wild type. We suggest that the higher apparent K_m of the SDH4ΔC23 enzyme is an indication of a reduced quinone binding affinity due to an altered binding site.

Thermal Stabilities of Mutant Enzymes. Fig. 3.4 shows that preincubation of the SDH4ΔC23 enzyme with DB for longer than 5 minutes results in lower activities suggesting that the enzyme is unstable. We directly tested this possibility by incubating mitochondrial membranes at 30°C in 50 mM potassium phosphate, 20 mM succinate, 1 mM EDTA, pH 7.4. Aliquots were withdrawn at 5 minute intervals and assayed for succinate-DB reductase activity (Fig. 3.5). The wild type and SDH4ΔC10 enzymes are stable over the course of the experiment. The SDH4ΔC15 and SDH4ΔC23 enzyme activities drop rapidly

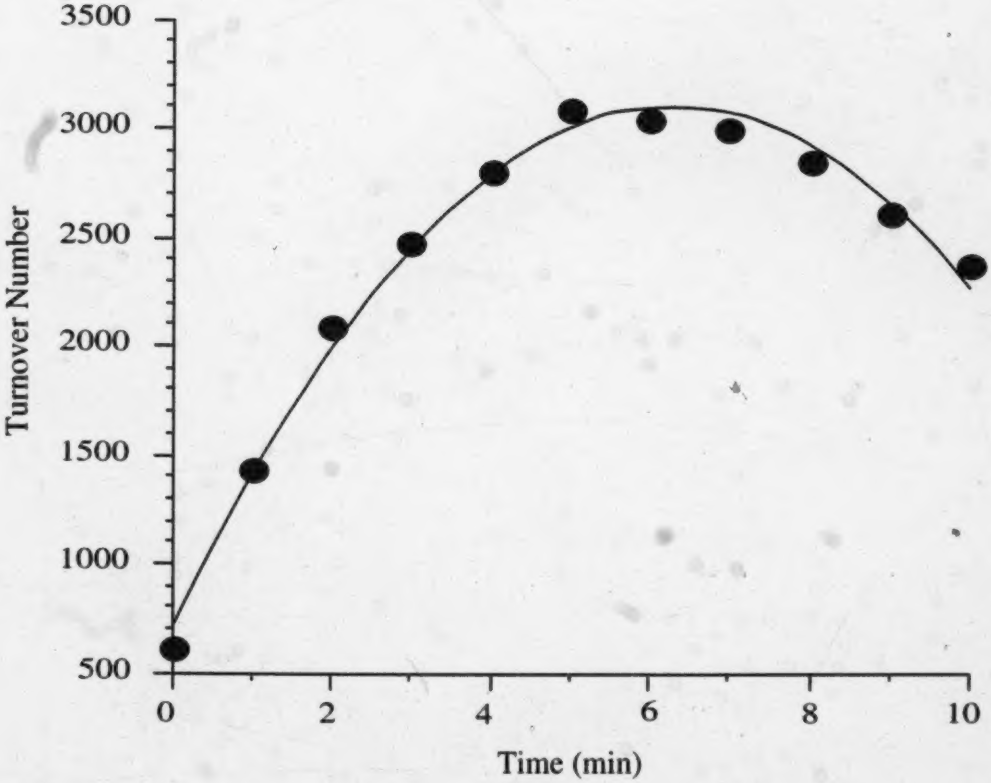

Figure 3-4 Stimulation of the SDH4ΔC23 Succinate-DB Reductase Activity.

Membrane fractions were incubated at room temperature for the indicated period in the presence of 0.5 mM DB and assayed for succinate-DB reductase activity as described under "Materials and Methods."

Table 3.2

Apparent Michaelis Constants for Quinone Reduction

Strain	K_m [a]	V_{max} [b]
MH125	3.3 ± 0.2[c]	3500 ± 200
sdh4W2-pSDH4ΔC10	4.5 ± 0.1	3400 ± 40
sdh4W2-pSDH4ΔC15	5.1 ± 0.2	2900 ± 100
sdh4W2-pSDH4ΔC23	22 ± 1	3400 ± 100

[a] Values are expressed as μMolar; [b] Values are expressed as μmoles DCPIP reduced min^{-1} μmoles FAD^{-1}; [c] Values represent means of triplicate determinations ± standard error of the mean

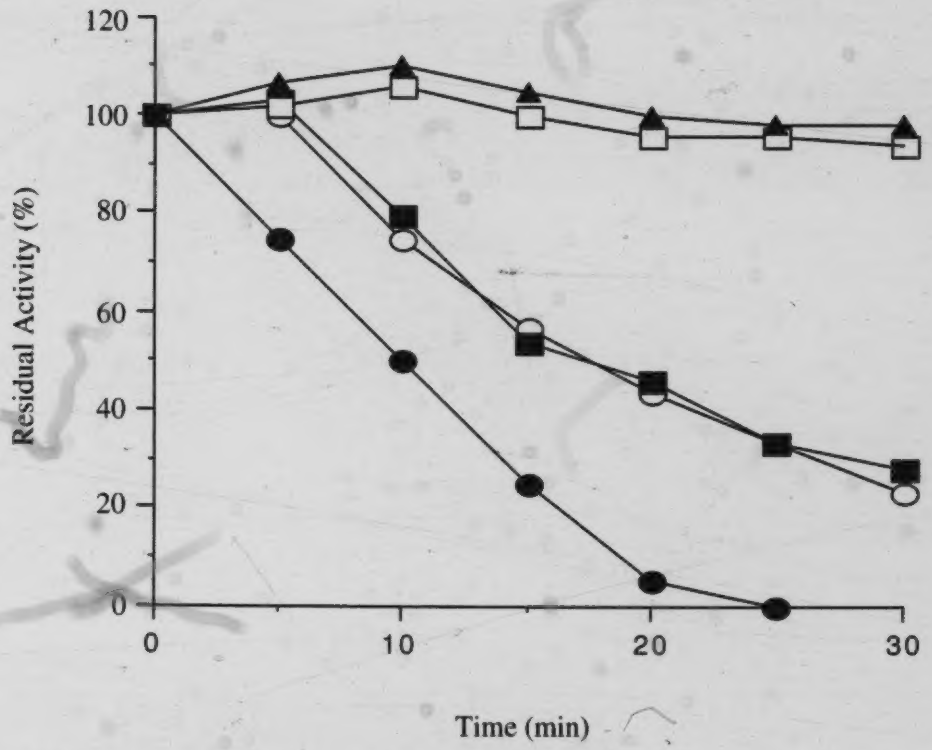

Figure 3-5 Stabilities of Mutant and Wild Type

Enzymes. Membrane fractions were incubated at 30 °C in 50 mM potassium phosphate, 20 mM succinate, 1 mM EDTA, pH 7.5 for up to 30 minutes. Succinate-DB reductase reactions were initiated with the addition of 50 μM DB and 75 μM DCPIP. The symbols used are: triangles, wild type; open squares, SDH4ΔC10; filled squares, SDH4ΔC15; open circles, SDH4ΔC23 incubated in the presence of 0.5 mM DB; closed circles, SDH4ΔC23.

with 50% losses at 20 and 11 minutes, respectively. Interestingly, the SDH4ΔC23 enzyme could be partially stabilized by incubating in the presence of DB. These data indicate that the Sdh4p C-terminal extension is also required for enzyme stability and that residues 136 to 140, missing in the SDH4ΔC15 enzyme are crucial to this function. Since the maximal velocities of the wild type and mutant enzymes are similar under our standard preincubation and assay conditions (Table 3.2), we do not believe that enzyme instability significantly affected the kinetic values reported in Tables 3.2 and 3.3.

Inhibition by 2-*sec*-butyl-4,6-dinitrophenol. Inhibitors have been very powerful tools in the elucidation of the mechanisms of quinone oxidation and reduction (Degli Esposti, 1998; Link *et al.*, 1993; Miyoshi, 1998). The 4,6-dinitrophenol derivatives effectively inhibit beef heart SDH and *E. coli* FRD (Yankovskaya *et al.*, 1996). We tested whether the *S. cerevisiae* SDH was similarly sensitive to 2-*sec*-butyl-4,6-dinitrophenol (s-BDNP). As with the bovine and the *E. coli* enzymes, we observed non-competitive inhibition of succinate-DB reductase activity with the yeast enzyme (Fig. 3.6).

The secondary plots of the abscissa intercepts against the inhibitor concentrations for the wild type, the SDH4ΔC10, and the SDH4ΔC15 enzymes showed hyperbolic curvature (Fig. 3.7). The data could best be described with equation 2 for non-competitive inhibition with two non-equivalent K_is. The sum of squares error (SSE) values for the wild type, the SDH4ΔC10, and the SDH4ΔC15 enzymes are 1.7×10^{-4}, 1.6×10^{-4}, and 2.0×10^{-4}, respectively. This suggests a two-site model for inhibitor binding, with two non-equivalent inhibition constants. Table 3.3 presents the estimates of the affinities of both inhibitor sites. The affinities of the inhibitor sites in the wild type and the SDH4ΔC10 enzymes are similar with an approximate 10-fold difference between the 2 sites. For the SDH4ΔC15 enzyme, the high affinity inhibitor site (0.06 mM) remains unchanged while the low affinity site has a 2-fold lower affinity (1.14 mM), consistent with a

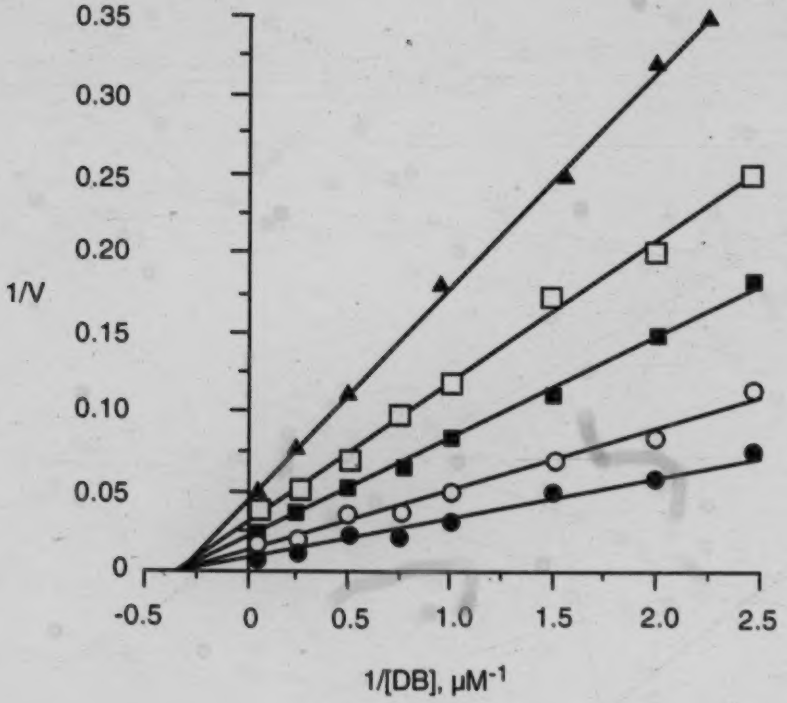

Figure 3.6 **Double-reciprocal Plots for the Inhibition of the Wild Type Enzyme by *s*-BDNP.**

Each value represents the mean of 3 independent determinations. The double-reciprocal plots were generated at the following inhibitor concentrations: 0 mM, closed circles; 0.04 mM, open circles; 0.1 mM, closed squares; 0.2 mM, open squares; 0.4 mM, triangles. 1/V values are expressed as nmoles^{-1} DCPIP reduced min mg of protein. The data were fitted by a least squares algorithm.

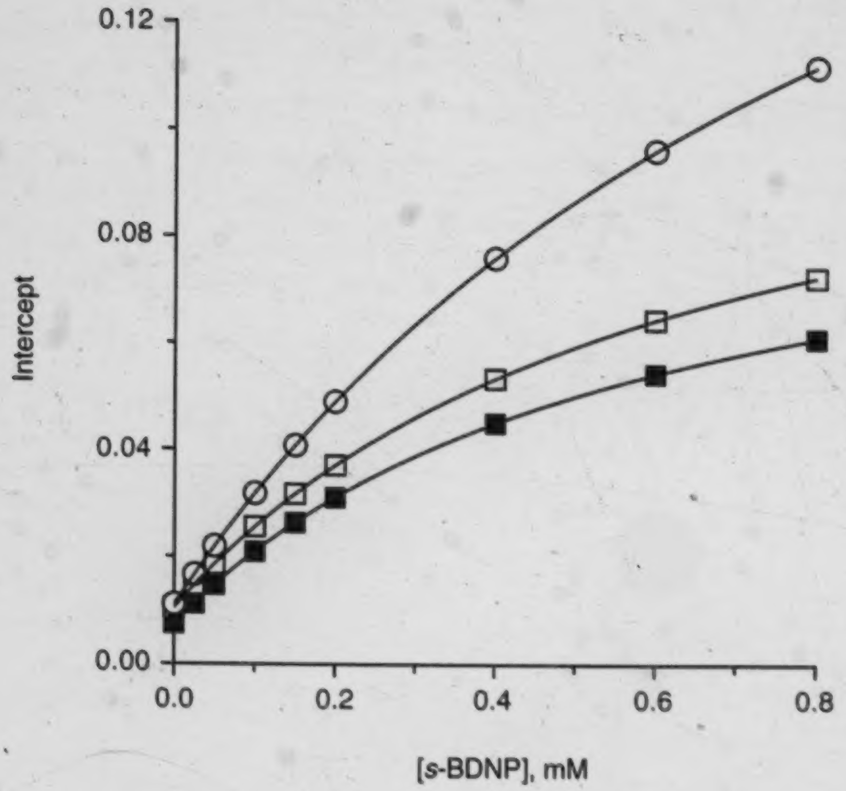

Figure 3.7 Nonlinear Kinetics of Inhibition of Quinone Reduction by s-BDNP.

Abscissa intercepts (reciprocal maximal velocities) were plotted against inhibitor concentrations. The data were fitted to equation 2 using the Quasi-Newton algorithm. The symbols used are: SDH4ΔC15, open circles; wild type, filled squares, SDH4ΔC10, open squares. Each value represents the mean of three independent determinations.

Table 3.3

Apparent Inhibition Constants for Quinone Reduction

Strain	K_{i1}[a]	K_{i2}
MH125	0.05 ± 0.01[b]	0.56 ± 0.06
sdh4W2-pSDH4ΔC10	0.06 ± 0.01	0.74 ± 0.1
sdh4W2-pSDH4ΔC15	0.06 ± 0.01	1.14 ± 0.12
sdh4W2-pSDH4ΔC23	0.08 ± 0.02	—

[a] Inhibition constants are expressed as mMolar; [b] Values represent means of triplicate determinations ± standard error of the mean.

small perturbation of the putative low affinity inhibitor binding site and a partial loss of quinone-reductase activity exhibited in growth and activity studies.

For the SDH4ΔC23 enzyme, non-competitive inhibition by *s*-BDNP is also observed, but the secondary plot of reciprocal maximal velocities against inhibitor concentrations is linear (Fig. 3.8). This suggests the presence of only one inhibitor binding site in the SDH4ΔC23 enzyme (Table 3.3). There is a good fit of the data to equation 1 (Fig. 3.9). The second inhibitor site may be non-functional or its affinity for *s*-BDNP may be too low to measure. Interestingly, the apparent K_i for the SDH4ΔC23 mutant enzyme (0.08 mM) is close to the value obtained for the high affinity inhibitor site in the wild type enzyme.

3.4. Discussion

The participation of ubiquinone in the mitochondrial electron transport chain is well established (Crane, 1977; Hatefi, 1985; Ragan and Reed, 1986; Trumpower, 1980; Trumpower and Katki, 1979; Wilkstrom and Saraste, 1984). However, the molecular details of its interactions with SDH are poorly understood. Studies on the bovine SDH (Lee *et al.*, 1995; Shenoy *et al.*, 1997; Shenoy *et al.*, 1999), the *E. coli* SDH (Yang *et al.*, 1998), and the *E. coli* FRD (Westenberg *et al.*, 1990; Westenberg *et al.*, 1993) have revealed that quinone substrates interact via the membrane anchor subunits.

Our data clearly demonstrate that the *S. cerevisiae* Sdh4p subunit is required for an anchoring role. The *SDH4* deletion mutant, sdh4W2, is unable to grow on glycerol, has undetectable levels of the ubiquinone-dependent enzyme activities, succinate oxidase and succinate-cytochrome *c* reductase, and undetectable levels of acid precipitable flavin (Table 3.1), consistent with absence of membrane-associated SDH. Similarly, as shown in Chapter 2, the Sdh3p subunit is essential for SDH assembly (Daignan-Fornier *et al.*, 1994).

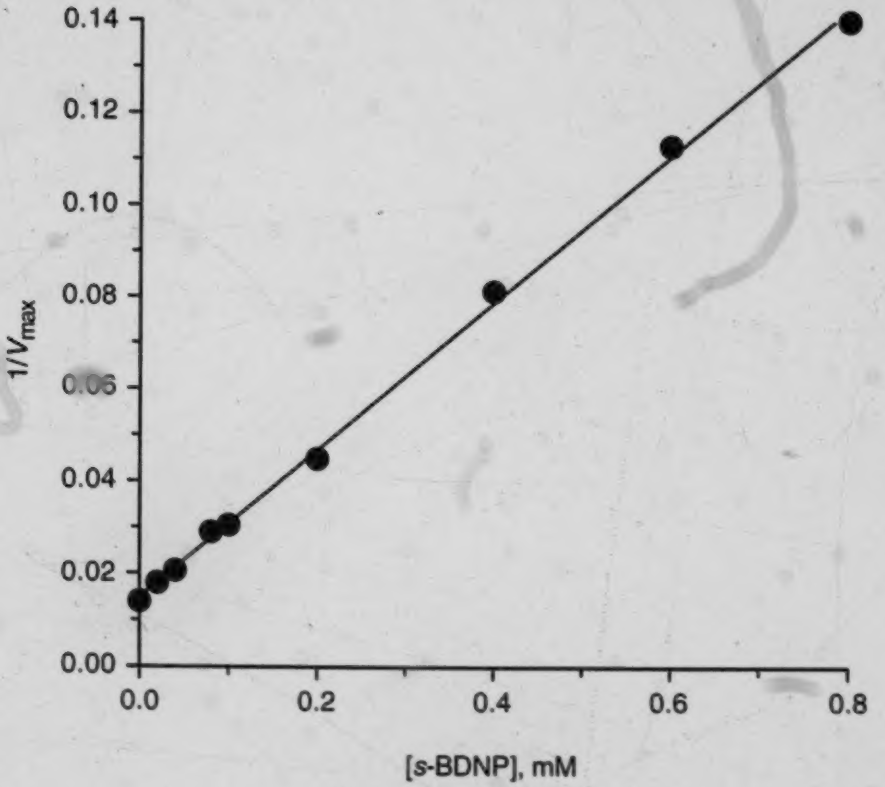

Figure 3.8 **Secondary Plot Showing Linear Inhibition Kinetics for the Reduction of Exogenous Quinone.**

Maximal velocities for the SDH4ΔC23 enzyme were obtained at the indicated inhibitor concentrations. Each value represents the mean of three independent determinations. Reciprocal V_{max} values are expressed as nmoles^{-1} DCPIP reduced min mg of protein.

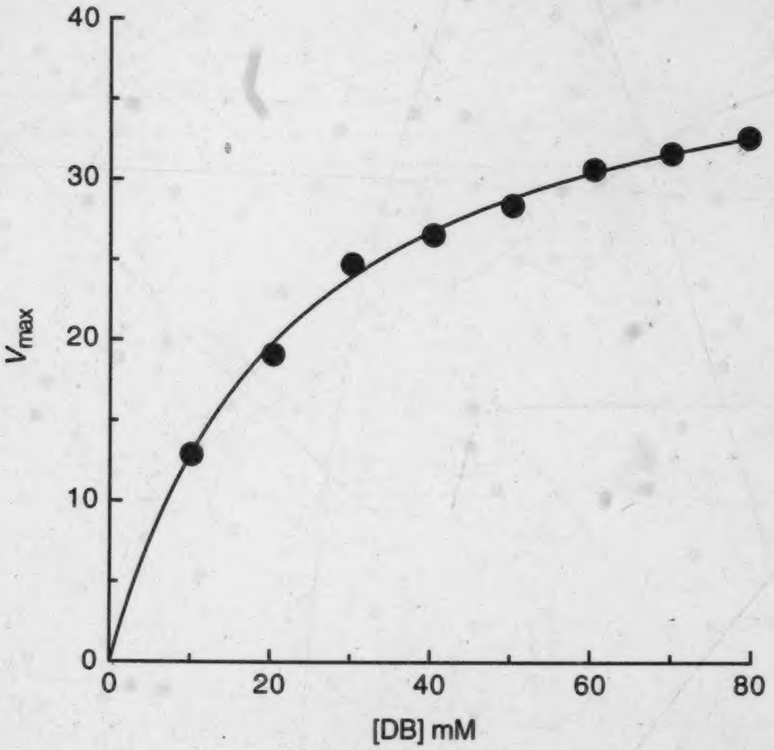

Figure 3.9 **Plot of Maximal Velocities versus Substrate Concentrations at Fixed Inhibitor Concentration for the SDH4ΔC23 Mutant Enzyme.**

The apparent maximal velocities obtained at a fixed inhibitor concentration (0.06 mM, Fig. 3.8) were plotted against substrate concentrations and fitted to equation 1 using the Quasi-Newton nonlinear least squares algorithm. Each value represents means of three independent determinations. V_{max} values are expressed as nmoles DCPIP reduced min^{-1} mg^{-1} of protein.

Our data also establish a role for the yeast Sdh4p subunit in ubiquinone reduction and more specifically for its terminal 23 amino acid residues. The loss of those 23 amino acids severely impairs SDH function *in vivo* (Fig. 3.3). The lack of respiratory growth is not due to a loss of Sdh4p anchoring function since mitochondrial membranes from sdh4W2-pSDH4ΔC23 have normal levels of succinate-PMS reductase activity (Table 3.1); this clearly indicates that the Sdh1p and Sdh2p subunits are membrane associated and active. This is further supported by the covalent flavin levels in SDH4ΔC23 membranes.

The SDH4ΔC23 enzyme is only poorly able to reduce the ubiquinone analog, DB (Table 3.1). Preincubation of the enzyme with 0.5 mM DB for 5 min at room temperature stimulates the succinate-DB reductase activity 5-fold (Fig. 3.4) and achieves a turnover number similar to the wild type enzyme (Table 3.2). Stimulation of activity by preincubation with DB is not observed for the wild type or for the other mutant enzymes. This indicates that the SDH4ΔC23 enzyme is fully catalytically competent when provided with saturating substrate (DB) levels. The apparent affinity of the SDH4ΔC23 enzyme for DB is about 7-fold lower than that of the wild type enzyme (Table 3.2). The data demonstrate that the Sdh4p C-terminal extension is involved in quinone reduction.

At the molecular level, at least two possibilities may account for these observations. The C-terminal extension may directly interact with DB and ubiquinone as part of a quinone-binding site. Alternatively, it may stabilize protein conformations necessary for the formation of a high affinity quinone-binding site. In either model, its loss impairs quinone binding and hence quinone reduction. Our data do not distinguish between these alternatives. Further insight should await a detailed structural analysis of the quinone binding sites in the *S. cerevisiae* SDH.

The Sdh4p residues 128-135, which are missing in the SDH4ΔC23 enzyme but not in the SDH4ΔC15 enzyme, are critical for the formation of a high affinity quinone binding site since it is only with the more extensive deletion that severely impaired quinone reduction is observed (Table 3.1). Residues 136 to 140, missing in the SDH4ΔC15 enzyme but not in the SDH4ΔC10 enzyme, are necessary for optimal quinone reducing activity. The enzymatic activities of the SDH4ΔC10 enzyme are comparable to those of the wild type enzyme, suggesting that the C-terminal decapeptide is dispensable.

In addition to the C-terminal extension's role in quinone reduction, it also serves to stabilize the enzyme. At 30 °C, the SDH4ΔC23 enzyme is extremely labile with a complete loss of succinate-DB reductase activity within 20 minutes (Fig. 3.5), whereas the wild type and the SDH4ΔC10 enzymes are stable. The SDH4ΔC15 enzyme is moderately unstable indicating that residues 136-140 are important for stability while the additional loss of residues 128-135 in the SDH4ΔC23 enzyme can be compensated for by higher DB concentrations.

The mechanism of how an iron-sulfur center, a one-electron carrier can fully reduce a two-electron acceptor like ubiquinone has been a focus of considerable attention. Studies on the photosynthetic reaction center (Coleman and Youvan, 1990; Deisenhofer and Michel, 1992; Parson, 1996) indicate that quinone reduction proceeds via two 'one-electron' steps carried out at separate quinone binding sites, Q_A and Q_B. In this model, a tightly bound quinone at the Q_A site cycles between the fully oxidized and the semiquinone states to mediate single electron transfer between the enzyme and a dissociable quinone at the Q_B site. A similar two-state model has earlier been postulated for SDH and FRD based on thermodynamic considerations (Cammack *et al.*, 1986). During quinone reduction by the beef heart SDH, two protein-stabilized ubisemiquinone radicals can be identified in the vicinity of the Center 3 iron-sulfur cluster (Ruzicka *et al.*, 1975). Consequently, photoaffinity labeling of the hydrophobic domain of the bovine SDH has shown that there are 2 quinone-binding pockets residing on opposite sides of the inner mitochondrial membrane (Lee *et al.*, 1995; Yu *et al.*, 1985). Similarly, a comprehensive search for quinone-binding sites was carried out in *E.*

coli FRD (Westenberg *et al.*, 1990; Westenberg *et al.*, 1993). Residues involved in quinone interaction were found to map to opposite sides of the membrane. Spectroscopic studies of *B. subtilis* SDH mutants and the inhibitory effect of HQNO have demonstrated the existence of 2 quinone-binding sites (Smirnova *et al.*, 1995). One site is proximal to the iron-sulfur Center 3, oriented toward the positive side of the membrane near heme b_H, while the other site is distal, close to heme b_L at the negative side of the membrane. Recently, the existence of two quinone-binding sites was demonstrated in the *P. denitrificans* SDH by EPR studies (Waldeck *et al.*, 1997).

Despite the absence of detailed structural information about the yeast anchor subunits, our observations can be rationalized in terms of a two-ubiquinone binding site model. The noncompetitive inhibition pattern of the enzyme by s-BDNP, an analog of ubiquinone, is best explained by 2 inhibitor-binding sites; these may correspond to the Q_A and Q_B sites. By analogy to the bacterial RCs and the model for the FRD Q_A and Q_B sites, the SDH Q_A site would be proximal to the high potential iron-sulfur cluster, Center 3, and the SDH Q_B would be distal. The Sdh4p C-terminal extension is predicted to be on the cytoplasmic face of the membrane (Fig. 3.2). Our data do not identify which of the two putative quinone binding sites is affected in the SDH4ΔC23 enzyme nor whether the inhibitor binding sites physically correspond to those sites, although the loss of quinone reductase activity is consistent with a perturbed Q_A site and with the topological model for Sdh4p (Bullis and Lemire, 1994).

This study clearly demonstrates that the SDH4 C-terminal extension is necessary for SDH activity and stability. It is interesting to note that of the 8 additional residues deleted in the SDH4ΔC23 enzyme as compared to the SDH4ΔC15 enzyme, only one, lysine-132, is charged, and only two, lysine-132 and serine-133 are potentially involved in hydrogen bonding. These residues are thus candidates for direct interactions with ubiquinone or for protein-protein interactions that produce a competent quinone binding conformation. The role of one of these residues, Lys-132, in SDH structure and function will be examined in the following chapter.

3.5. Bibliography

Abraham, P. R., Mulder, A., van 't Riet, J., and Raué, H. A. (1994). Characterization of the *Saccharomyces cerevisiae* nuclear gene *CYB3* encoding a cytochrome *b* polypeptide of respiratory complex II. *Mol. Gen. Genet.* **242,** 708-716.

Ackrell, B. A. C., Johnson, M. K., Gunsalus, R. P., and Cecchini, G. (1992). Structure and function of succinate dehydrogenase and fumarate reductase. In Chemistry and biochemistry of flavoenzymes, F. Müller, ed. (Boca Raton, Florida: CRC Press, Inc.,), pp. 229-297.

Bruel, C., Manon, S., Guerin, M., and Lemesle-Meunier, D. (1995). Decoupling of the bc_1 complex in *Saccharomyces cerevisiae*; point mutations affecting the cytochrome *b* gene bring new information about the structural aspect of the proton translocation. *J. Bioenerg. Biomembr.* **27,** 527-539.

Bullis, B. L., and Lemire, B. D. (1994). Isolation and characterization of the *Saccharomyces cerevisiae SDH4* gene encoding a membrane anchor subunit of succinate dehydrogenase. *J. Biol. Chem.* **269,** 6543-6549.

Cammack, R., Crowe, B. A., and Cook, N. B. (1986). Dual-pathway models of electron transfer in succinate dehydrogenase and fumarate reductase. *Biochem. Soc. Trans.* **14,** 1207-1208.

Cleland, W. W. (1979). Statistical analysis of enzyme kinetic data. *Methods Enzymol.* **63,** 103-138.

Coleman, W. J., and Youvan, D. C. (1990). Spectroscopic analysis of genetically modified photosynthetic reaction centers. *Annu. Rev. Biophys. Biophys. Chem.* **19,** 333-367.

Crane, F. L. (1977). Hydroquinone dehydrogenases. *Annu. Rev. Biochem.* **46,** 439-469.

Daignan-Fornier, B., Valens, M., Lemire, B. D., and Bolotin-Fukuhara, M. (1994). Structure and regulation of *SDH3*, the yeast gene encoding the cytochrome b_{560} subunit of respiratory complex II. *J. Biol. Chem.* **269,** 15469-15472.

Degli Esposti, M. (1998). Inhibitors of NADH-ubiquinone reductase: an overview. *Biochim. Biophys. Acta* **1364,** 222-235.

Deisenhofer, J., and Michel, H. (1992). High-resolution crystal structures of bacterial photosynthetic reaction centers. In Molecular Mechanisms in Bioenergetics, L. Ernster, ed. (Armsterdam: Elsevier Science Publishers B. V.), pp. 103-120.

Gietz, R. D., and Sugino, A. (1988). New yeast-*Escherichia coli* shuttle vectors constructed with *in vitro* mutagenized yeast genes lacking six-base pair restriction sites. *Gene* **74,** 527-534.

Grivennikova, V. G., and Vinogradov, A. D. (1982). Kinetics of ubiquinone reduction by the resolved succinate: ubiquinone reductase. *Biochim. Biophys. Acta* **682,** 491-495.

Hägerhäll, C. (1997). Succinate:quinone oxidoreductases: variations on a conserved theme. *Biochim. Biophys. Acta* **1320,** 107-141.

Hägerhäll, C., and Hederstedt, L. (1996). A structural model for the membrane-integral domain of succinate:quinone oxidoreductases. *FEBS Lett.* **389,** 25-31.

Hatefi, Y. (1985). The mitochondrial electron transport and oxidative phosphorylation system. *Annu. Rev. Biochem.* **54,** 1015-1069.

Hederstedt, L. (1998). The membrane-integral domain of succinate:quinone oxidoreductases-a secretive haem-containing domain. *Biochem. Soc. Transactions* **26,** 408-413.

Hederstedt, L., and Ohnishi, T. (1992). Progress in succinate:quinone oxidoreductase research. In Molecular mechanisms in bioenergetics, L. Ernster, ed. (New York: Elsevier Science Publishers), pp. 163-197.

Ito, H., Fukuda, Y., Murata, K., and Kimura, A. (1983). Transformation of intact yeast cells treated with alkali cations. *J. Bacteriol.* **153,** 163-168.

Lee, G. Y., He, D.-Y., Yu, L., and Yu, C.-A. (1995). Identification of the ubiquinone-binding domain in QPs1 of succinate-ubiquinone reductase. *J. Biol. Chem.* **270,** 6193-6198.

Link, T. A., Hasse, U., Brandt, U., and von Jagow, G. (1993). What information do inhibitors provide about the structure of the hydroquinone oxidation site of ubihydroquinone:cytochrome *c* oxidoreductase? *J. Bioenerg. Biomembr.* **25,** 221-232.

Miyoshi, H. (1998). Structure-activity relationships of some complex I inhibitors. *Biochim. Biophys. Acta* **1364,** 236-244.

Parson, W. W. (1996). Photosynthetic bacterial reaction centres. In Protein electron transfer, D. S. Bendall, ed. (Oxford, UK: BIOS Scientific Publishers Ltd), pp. 125-160.

Ragan, C. I., and Reed, J. S. (1986). Regulation of electron transfer by the quinone pool. *J. Bioenerg. Biomembr* **18,** 403-418.

Robinson, K. M., and Lemire, B. D. (1995). Flavinylation of succinate: ubiquinone oxidoreductase from Saccharomyces cerevisiae. *Methods Enzymol.* **260,** 34-51.

Robinson, K. M., von Kieckebusch-Gück, A., and Lemire, B. D. (1991). Isolation and characterization of a *Saccharomyces cerevisiae* mutant disrupted for the succinate dehydrogenase flavoprotein subunit. *J. Biol. Chem.* **266,** 21347-21350.

Ruzicka, F. J., Beinert, H., Schepler, K. L., Dunham, W. R., and Sands, R. H. (1975). Interaction of ubisemiquinone with a paramagnetic component in heart tissue. *Proc. Natl. Acad. Sci. USA* **72,** 2886-2890.

Shenoy, S. K., Yu, L., and Yu, C. A. (1997). The smallest membrane anchoring subunit (QPs3) of bovine heart mitochondrial succinate-ubiquinone reductase. Cloning, sequencing, topology, and Q-binding domain. *J. Biol. Chem.* **272,** 17867-17872.

Shenoy, S. K., Yu, L., and Yu, C. A. (1999). Identification of quinone-binding and heme-ligating residues of the smallest membrane-anchoring subunit (QPs3) of bovine heart mitochondrial succinate:ubiquinone reductase. *J. Biol. Chem.* **274,** 8717-8722.

Smirnova, I. A., Hägerhäll, C., Konstantinov, A. A., and Hederstedt, L. (1995). HOQNO interaction with cytochrome *b* in succinate:menaquinone oxidoreductase from *Bacillus subtilis*. *FEBS Lett.* **359,** 23-26.

Trumpower, B. L. (1980). New concepts on the role of ubiquinone in the mitochondrial respiratory chain. *J. Bioener. Biomembr.* **13,** 1-24.

Trumpower, B. L., and Katki, A. G. (1979). Succinate-cytochrome *c* reductase complex of the mitochondrial electron transport chain. In Membrane proteins in energy transduction, R. A. Capaldi, ed. (New York, New York: Marcel Dekker, Inc.), pp. 89-200.

Waldeck, A. R., Stowell, M. H. B., Lee, H. K., Hung, S. C., Matsson, M., Hederstedt, L., Ackrell, B. A. C., and Chan, S. I. (1997). Electron paramagnetic resonance studies of succinate:ubiquinone oxidoreductase from *Paracoccus denitrificans*. Evidence for a magnetic interaction between the 3Fe-4S cluster and cytochrome *b*. *J. Biol. Chem.* **272,** 19373-19382.

Westenberg, D. J., Gunsalus, R. P., Ackrell, B. A. C., and Cecchini, G. (1990). Electron transfer from menaquinol to fumarate. Fumarate reductase anchor polypeptide mutants of *Escherichia coli*. *J. Biol. Chem.* **265,** 19560-19567.

Westenberg, D. J., Gunsalus, R. P., Ackrell, B. A. C., Sices, H., and Cecchini, G. (1993). *Escherichia coli* fumarate reductase *frdC* and *frdD* mutants.

Identification of amino acid residues involved in catalytic activity with quinones. *J. Biol. Chem.* **268,** 815-822.

Wikström, M. K. F., and Saraste, M. (1984). The mitochondrial respiratory chain. In Bioenergetics, L. Ernster, ed. (New York: Elsevier), pp. 49-94.

Yang, X. D., Yu, L., He, D., and Yu, C. A. (1998). The quinone-binding site in succinate-ubiquinone reductase from *Escherichia coli*. *J. Biol. Chem.* **273,** 31916-31923.

Yankovskaya, V., Sablin, S. O., Ramsay, R. R., Singer, T. P., Ackrell, B. A. C., Cecchini, G., and Miyoshi, H. (1996). Inhibitor probes of the quinone binding sites of mammalian complex II and *Escherichia coli* fumarate reductase. *J. Biol. Chem.* **271,** 21020-21024.

Yu, L., Yang, F. D., and Yu, C. A. (1985). Interaction and identification of ubiquinone-binding proteins in ubiquinol-cytochrome *c* reductase by azido-ubiquinone derivatives. *J. Biol. Chem.* **260,** 963-973.

Zhu, Q. S., and Beattie, D. S. (1988). Direct interaction between yeast NADH-ubiquinone oxidoreductase, succinate-ubiquinone oxidoreductase, and ubiquinol-cytochrome *c* oxidoreductase in the reduction of exogenous quinones. *J. Biol. Chem.* **263,** 193-199.

Chapter 4

Mutagenesis of the *S. cerevisiae* Sdh4p Lys-132*

---

* A version of this chapter has been published. Oyedotun, K. S. and Lemire, B. D. (1999) *Biochim. Biophys. Acta* **1411**, 170-179.

4.1. Introduction

Generally the succinate:quinone oxidoreductases, succinate dehydrogenase (SDH) and fumarate reductase (FRD), are made up of two parts: a soluble catalytic domain and a membrane-anchoring domain (Ackrell *et al.*, 1992; Cole *et al.*, 1985; Hägerhäll, 1997; Hederstedt and Ohnishi, 1992). Unlike the subunits of the catalytic domain that are well conserved across species, there are considerable variations in subunit compositions and primary structures of the membrane-anchoring domains (Ackrell *et al.*, 1992; Hägerhäll, 1997; Hägerhäll and Hederstedt, 1996; Hederstedt and Ohnishi, 1992). In the *S. cerevisiae* SDH, the membrane-anchoring domain is composed of two small hydrophobic polypeptides, Sdh3p (Abraham *et al.*, 1994; Daignan-Fornier *et al.*, 1994) and Sdh4p (Bullis and Lemire, 1994). As shown in Chapters 2 and 3, the membrane-anchoring domain is necessary for interactions with heme and quinone, and for the assembly of a functional SDH. Moreover, the data presented in Chapter 3 suggests that this domain contains two quinone-binding sites by analogy to the bovine SDH (Lee *et al.*, 1995; Shenoy *et al.*, 1997; Yankovskaya *et al.*, 1996), the *Bacillus subtilis* SDH (Smirnova *et al.*, 1995), the *Escherichia coli* FRD (Westenberg *et al.*, 1993; Yankovskaya *et al.*, 1996), and the *P. denitrificans* SDH (Waldeck *et al.*, 1997). Although significant progress has been made in understanding the structural aspects of the anchor polypeptides from the bovine and the bacterial enzymes, little is known about those of the yeast enzyme.

The yeast Sdh4p subunit contains a matrix-localized amino terminus, 3 transmembrane helices, and a carboxyl terminus of about 30 amino acids that extends into the intermembrane space (Bullis and Lemire, 1994; Oyedotun and Lemire, 1997). The C-terminal extension of the yeast subunit is not shared by most other SDH or FRD anchor subunits (Fig. 3.1) (Burger *et al.*, 1996; Hägerhäll, 1997; Hägerhäll and Hederstedt, 1996). In Chapter 3, we showed that the carboxyl terminus of the yeast Sdh4p subunit is necessary for respiratory growth on nonfermentable carbon sources, for ubiquinone reduction, and for enzyme stability (Oyedotun and Lemire, 1997). Through a stepwise truncation, residues 128-135 were shown to be critical for the formation of a quinone-binding site. We noted that of the 8 additional residues deleted in the SDH4ΔC23 enzyme as compared to the SDH4ΔC15 enzyme, only one, lysine-132, is charged, and only two, lysine-132 and serine-133 are potentially involved in hydrogen bonding. These residues are thus candidates for direct interactions with ubiquinone or for protein-protein interactions that produce a competent quinone binding conformation. In this chapter, we further characterize the role of the Sdh4p C-terminus by identifying Lys-132 as a key residue in the establishment of a stable conformation compatible with heme assembly and quinone binding in the SDH hydrophobic domain.

4.2. Materials and Methods

Strains and media. The *E. coli* strains used for the mutagenesis reactions are JM109 (*endA1 recA1 gyrA96 thi hsdR17* (r_k^- m_k^+) *relA1 supE44 λ⁻ Δ(lac-proAB)* [F′ *traD36 proA⁺B⁺ lacI*^{q}ZΔM15]) and ES1301 *mut*S (l*acZ*53 *mut*S201::Tn5 *thy*A36 *rha*-5 *metB1 deoC* IN(*rrnD-rrnE*)). The yeast strains, MH125 and sdh4W2 and the *E. coli* strain, DH5α, have been described in Chapter 2. Similarly, media and culture conditions have been described therein.

Mutant construction. Five point mutations were constructed at the *SDH4* Lys-132 codon with the Altered Site® II *in vitro* Mutagenesis Kit (Promega, Madison, WI). Briefly, a *Xho*I-*Spe*I fragment of *SDH4* was ligated into the *Sal*I-*Xba*I sites of the pALTER®-1 vector to form pALSDH4 and used as a template for the mutagenesis reaction. The mutagenic oligonucleotides used were:

1. 5'-CCCATAGACTT(T/A/C)(C/G)TACTAAACCAAC-3': this is a degenerate oligonucleotide designed to generate the six codons, GAA, GTA,

GGA, CAA, CTA, CGA coding for Glu, Val, Gly, Gln, Leu, and Arg, respectively;

2. 5'-CCCATAGACTT(T/A/C)CTACTAAACCAAC-3': this is a degenerate oligonucleotide designed to generate the three codons, GAA, GTA, and GGA coding for Glu, Val and Gly, respectively; and

3. 5'-CCCATAGACTTCGTACTAAACCAAC-3': this is designed to generate the codon CGA coding for Arg.

Primers 1-3 are used in conjunction with the Ampicillin Repair oligonucleotide, 5′-pGTTGCCATTGCTGCAGGCATCGTGGTG-3′, and a Tetracycline Knockout oligonucleotide, 5′-pGCCGGGCCTCTTGCGGGCGTCCATTCC-3′ supplied by the manufacturer. The mutagenesis reactions were performed as described by the manufacturer using double-stranded DNA (Fig. 4.1). The mutations were confirmed by sequencing. The *SDH4* mutants were moved as *EcoR*I-*Hind*III fragments into the yeast shuttle vector, YCplac111 (Gietz and Sugino, 1988) to yield the plasmids, pSDH4K132E, pSDH4K132G, pSDH4K132Q, pSDH4K132R, and pSDH4K132V.

Thermal Stability Measurements and Enzyme Assays. Membrane fractions (20 mg/ml) were incubated at temperatures ranging from 25 °C to 65 °C in 50 mM potassium phosphate, 50 µM EDTA, pH 7.4, 2 mM KCN for 10 minutes and assayed immediately for succinate-DB reductase and succinate-PMS reductase activities. For the succinate-DB reductase assay, the reactions were initiated with the addition of 50 µM DB and 20 mM succinate while for the succinate-PMS reductase assay, the reactions were initiated with the addition of the dyes (PMS and DCPIP) and succinate. Unless otherwise stated, the succinate-DB reductase activity was determined by directly monitoring the reduction of DB using the wavelength pair, 280 and 325 nm (Bruel *et al.*, 1995a), with a Hewlett

Figure 4.1 Schematic Diagram of the *in vitro* Mutagenesis Procedure Using the pALTER®-1 Vector.

1. Clone the *SDH3* gene into the pALTER-1 vector; 2. Isolate double-stranded DNA; 3. Alkaline denature and anneal mutagenic oligonucleotide (oligo), Ampicillin Repair oligo, and Tetracycline Knockout oligo; 4. Synthesize mutant strand with T4 DNA Polymerase and T4 DNA Ligase; 5. Transform ES1301 *mut*S with mutagenesis reaction. Grow overnight with Ampicillin selection; 6. Purify plasmid DNA and transform JM109. Select mutants on Ampicillin plated; 7. Replica plate to identify Tetracycline sensitive isolates and screen for mutations in the *SDH3* gene by sequencing. 70-80% of the Amp^{r} and Tet^{s} isolates contain mutations in the *SDH3* gene. MCS, multiple cloning site; Amp^{r}, Ampicillin resistance marker gene; Amp^{s}, Ampicillin sensitive marker gene; Tet^{r}, Tetracycline resistance marker gene; Tet^{s}, Tetracycline sensitive marker gene; dashed lines indicate gene disruption.

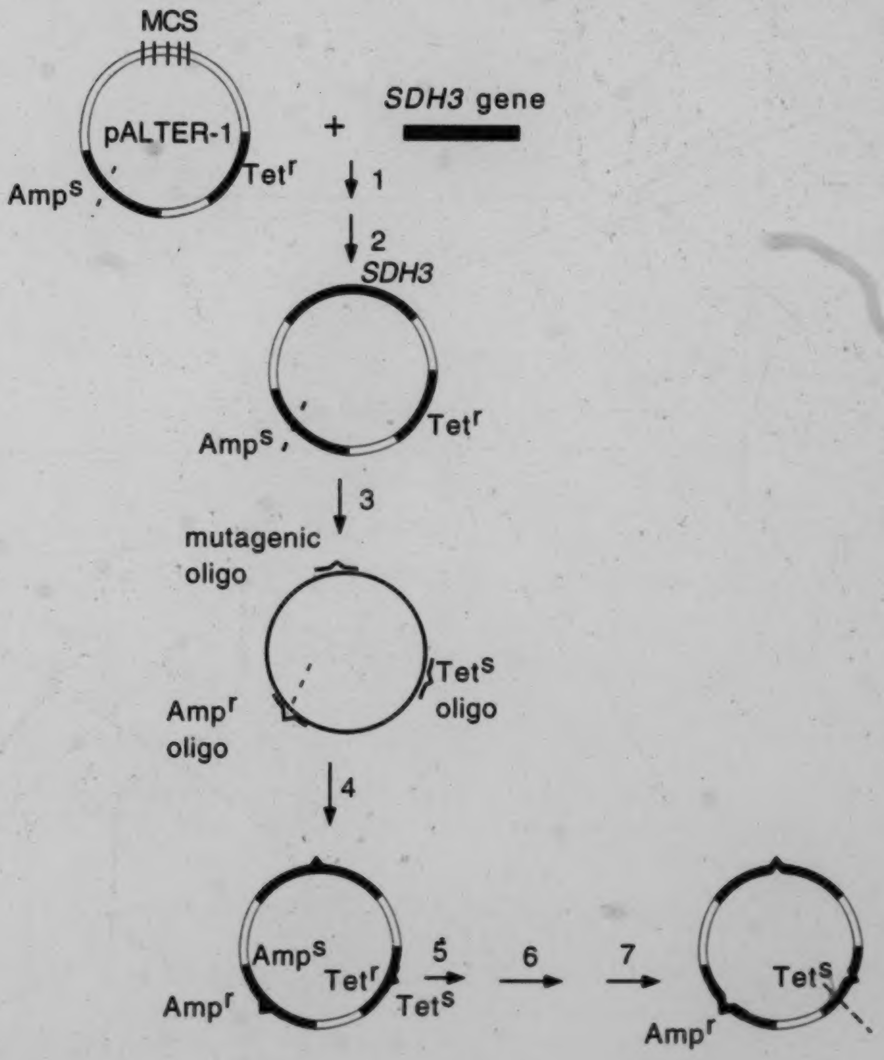
MCS
pALTER-1
+
SDH3 gene
Amp^s
Tet^r
1
2
SDH3
Amp^s
Tet^r
3
mutagenic oligo
Tet^s oligo
Amp^r oligo
4
Amp^s
Tet^r
Amp^r
Tet^s
5
6
7
Tet^s
Amp^r

Packard 8453 diode array spectrophotometer. The absorption coefficient is 16 mM^{-1} cm^{-1}. All other assays were carried out as described in Chapter 2.

Miscellaneous Methods. Measurements of SDH-associated cytochrome *b* content were carried out spectrally as described in Chapter 2. Determination of covalently bound flavin and protein contents, *E. coli* and yeast transformations, and recombinant DNA methods have been described in Chapter 2. The apparent Michaelis parameters, K_m and V_{max} were determined as described in Chapter 3. Synthesis of oligonucleotides and DNA sequencing were performed in the Department of Biochemistry DNA Core Facility as described in Chapters 2 and 3, respectively.

4.3. Results

***In vivo* Characterization of *SDH4* Point Mutants.** Lys-132 falls within the C-terminal sequence of Sdh4p (residues 128-135) that was recently shown to be necessary for quinone reduction and for enzyme stability through a stepwise truncation of the C-terminus (Oyedotun and Lemire, 1997). Since deletion mutagenesis has the potential for causing large structural perturbations, we further explored the role of the C-terminus by creating five point mutants in Lys-132. Lys-132 is the only charged amino acid residue within this sequence and was replaced by Arg, Glu, Gln, Gly, and Val (K132R, K132E, K132Q, K132G, and K132V). These substitutions have the potential for preserving the positive charge (K132R), removing the charge, but preserving the potential for hydrogen bonding (K132Q), introducing a negative charge (K132E), and removing both the charge and hydrogen-bonding capabilities (K132G and K132V). The mutant *SDH4* genes were introduced into the *SDH4* knockout strain, sdh4W2, and assayed for respiratory growth. Replacement of Lys-132 with Gln abolishes growth on minimal glycerol (SG) or lactate media, while the Glu, Gly, and Val substitutions lead to greatly impaired growth. In contrast, the K132R substitution grows almost as well as the wild type.

In order to compare quantitatively the respiratory growth abilities of the wild type and mutant strains, growth on a semisynthetic medium containing 0.1, 0.2, 0.3, 0.4, or 0.5% galactose was monitored. An initial growth phase is fermentative followed by a respiratory phase (Bruel *et al.*, 1995b). Growth rates during the fermentative phases were similar for wild type and mutant strains (data not shown) but were markedly different in the respiratory phases. The growth yields monitored as the optical densities at 600 nm of late stationary phase cultures reflect the respiratory capabilities of each strain and are plotted against the initial galactose concentrations (Fig. 4.2). A growth yield of less than about 30% is usually associated with a respiratory deficiency severe enough to prevent growth on minimal glycerol medium. The growth yields of the parent strain, MH125, sdh4W2 carrying the wild type *SDH4* plasmid, pSDH4-17, or sdh4W2 with the pSDH4K132R plasmid are similar. sdh4W2 achieves a 12% growth yield on 0.5% galactose by fermentation alone. The growth yields of sdh4W2 pSDH4K132E, sdh4W2 pSDH4K132G, sdh4W2 pSDH4K132V, and sdh4W2 pSDH4K132Q strains are severely reduced (51%, 41%, 38%, and 27%, respectively). We conclude that Lys-132 is critical for SDH function and respiratory competence.

Membrane-Association of the Catalytic Dimer. In order to examine the possibility that the mutation of Lys-132 compromises the anchoring role of Sdh4p, we determined the amounts of catalytic dimer on the mitochondrial membranes of the mutants. The Sdh1p subunit contains a covalently attached FAD and its presence is a measure of SDH assembly. The membrane-associated covalent flavin levels in sdh4W2 pSDH4-17 and sdh4W2 pSDH4K132R are similar to the wild type level, while those of sdh4W2 pSDH4K132E, sdh4W2 pSDH4K132G, sdh4W2 pSDH4K132Q, and sdh4W2 pSDH4K132V are slightly reduced (Table 4.1). We also measured the succinate-PMS reductase activities of mutant and wild

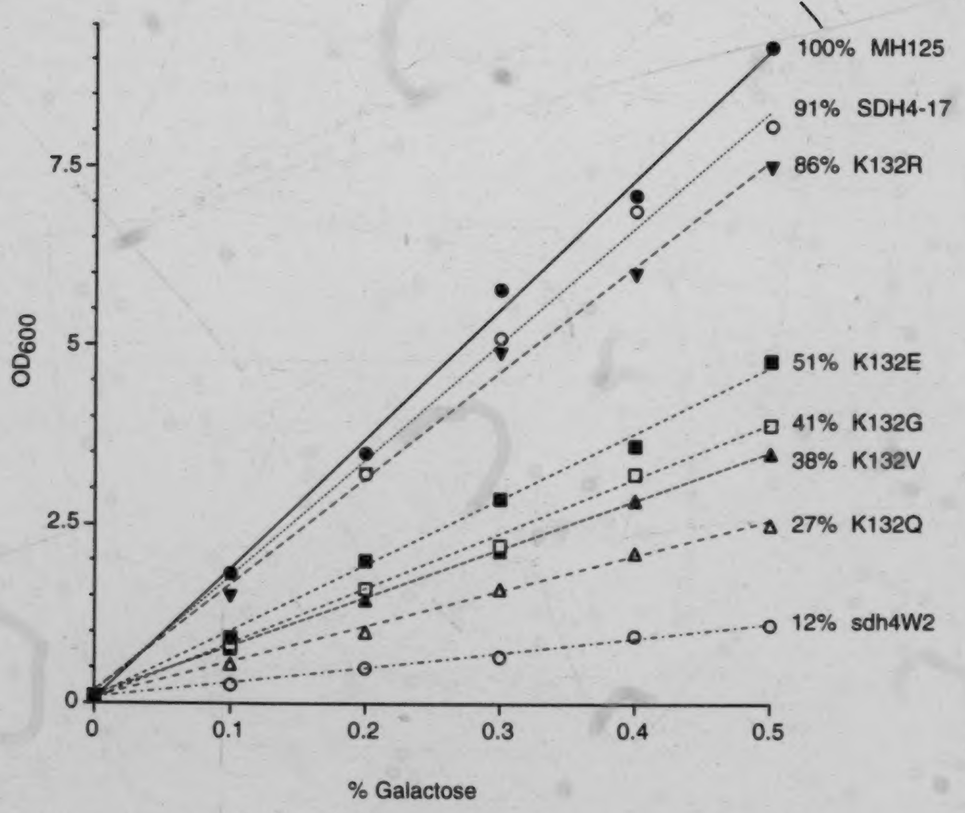

Figure 4.2 Growth of Yeast Strains on Galactose Media.

Precultures were prepared on selective minimal medium containing 2% galactose and 0.01% glucose and used to inoculate the main culture to a starting OD_{600} of 0.1. Growth was at 30 °C on semisynthetic liquid medium containing 0.1, 0.2, 0.3, 0.4, or 0.5% galactose and the optical densities at 600 nm were measured. The cultures were allowed to reach late stationary phase (approximately 100 hours). The relative growth yields were calculated using the final absorbance values reached on 0.5% galactose.

Table 4.1

Succinate Dehydrogenase Activities of Mitochondrial Membranes

Strain	Covalent flavin[a]	Specific activity[b]	Turnover numbers[c]
MH125	33 ± 5	135 ± 7	4100 ± 205
sdh4W2 pSDH4-17	31 ± 2	121 ± 5	3900 ± 156
sdh4W2 pSDH4K132E	25 ± 4	97 ± 5	3900 ± 195
sdh4W2 pSDH4K132G	22 ± 5	85 ± 3	3900 ± 117
sdh4W2 pSDH4K132Q	20 ± 4	78 ± 5	3900 ± 234
sdh4W2 pSDH4K132R	28 ± 3	112 ± 4	4000 ± 160
sdh4W2 pSDH4K132V	21 ± 3	82 ± 4	3900 ± 214
sdh4W2	ND	ND	ND

Each value represents the mean of triplicate determinations ± S. E. M. ND, not detectable or less than 4% of that of the wild type. [a] Covalent flavin contents are expressed as pmol of FAD mg^{-1} of protein. [b] Specific activities are expressed as μmol of PMS-mediated DCPIP reduced min^{-1} mg^{-1} of protein [c] Turnover numbers are expressed as μmol of PMS-mediated DCPIP reduced min^{-1} μmol^{-1} of FAD.

type enzym[illegible]his activity does not require that the anchor subunits be functional for quinone reduction. The turnover numbers in all the mutant strains are comparable to that of the wild type enzyme (Table 4.1). As expected, sdh4W2 membranes have undetectable levels of succinate-PMS reductase activity and covalent FAD. Taken together, the results indicate that membrane-association of Sdh1p/Sdh2p dimer proceeds normally with all the Lys-132 substituted Sdh4p subunits.

Respiratory activities of Sdh4p point mutants. Table 4.2 shows the quinone-dependent respiratory chain activities of mitochondrial membranes isolated from mutant and wild type strains. The SDH4K132E, SDH4K132G, SDH4K132Q, and SDH4K132V enzymes show 2-3 fold decreases in turnover numbers for succinate-DB reductase, succinate-cytochrome *c* reductase, and succinate oxidase activities. In contrast, the SDH4K132R enzyme activities are unaffected. sdh4W2 membranes lacking Sdh4p have undetectable levels of these enzymatic activities. NADH oxidase and glycerol-1-P-cytochrome *c* reductase activities are normal in all the mutants (Table 4.2). This clearly demonstrates that Lys-132 substitutions do not affect other respiratory complexes that may be associated with SDH.

Kinetics of exogenous quinone reduction. The succinate-DB reductase activities of all the mutant enzymes, except that of the K132R mutant, can be stimulated significantly when incubated with higher concentrations of DB at room temperature (data not shown). This suggests a possible structural perturbation in the vicinity of the quinone binding site(s). To further explore this, we measured the apparent Michaelis parameters, K_m and V_{max}, of the mutant and wild type enzymes by incubating membranes with different DB concentrations at room temperature for 5 minutes. Since the mutants have variable levels of covalent FAD, we also determine the k_{cat} (maximal turnover number). We observed approximately 3 fold increases in the apparent K_m for DB reduction of the

Table 4.2

Enzymatic Activities of Mitochondrial Membranes

	MH125	sdh4W2 pSDH4-17	sdh4W2 K132E	sdh4W2 K132G	sdh4W2 K132Q	sdh4W2 K132R	sdh4W2 K132V	sdh4W2
Succinate-DB reductase[b]	3500[a]	3400	1700	1500	1100	3300	1400	ND
Succinate-cytochrome *c* reductase[c]	2200	2200	1000	900	700	2100	800	ND
Succinate oxidase[d]	2000	2000	900	800	700	2000	700	ND
NADH oxidase[d]	4000	3800	3800	3700	3500	3900	3600	110[e]
Glycerol-1-P-cytochrome *c* reductase[c]	2700	2600	2200	2300	2400	2500	2300	65[f]

[a] Values represent the means of triplicate determinations . In all cases, the S. E. M. are within 5%. ND, not detectable or less than 4% of wild type activity. [b] Activities are expressed as µmoles of DB-mediated DCPIP reduced min^{-1} µmol^{-1} of FAD; [c] Activities are expressed as µmoles of cytochrome *c* reduced min^{-1} µmol FAD^{-1}; [d] Activities are expressed as µatoms of oxygen min^{-1} µmol FAD^{-1}; [e] Activity is expressed as ng atoms of oxygen min^{-1} mg protein^{-1}; [f] Activity is expressed as nmol of cytochrome *c* reduced min^{-1} mg protein^{-1}.

SDH4K132G, SDH4K132Q, and SDH4K132V enzymes, and a 2 fold increase in that of the SDH4K132E enzyme (Table 4.3). The apparent K_m for the SDH4K132R enzyme is similar to the plasmid-borne wild type *SDH4* gene, SDH4-17 and the parental strain, MH125. When normalized for covalent FAD contents, all mutant enzymes have maximal turnover numbers (k_{cat}) of at least 70% of the wild type when supplied with a saturating amount of DB (Table 4.3). We conclude that the Lys-132 mutations induce a structural defect in SDH that alters the local environment of a quinone-binding pocket.

Thermal stability profiles of mutant and wild type enzymes. The structural perturbations that lead to the differences in apparent K_m's for DB reduction in the mutant enzymes might also be expected to affect enzyme stability. We tested this possibility by incubating mitochondrial membranes at temperatures ranging from 25 to 65 °C (Figs. 4.3 and 4.4). Membranes were assayed for succinate-DB reductase activities by directly monitoring DB reduction at the wavelength pair 280 and 325 nm (Fig. 4.3; Bruel *et al.*, 1995a) or for succinate-PMS reductase activities (Fig. 4.4). The SDH4K132E, SDH4K132G, SDH4K132Q, and SDH4K132V mutant enzymes are significantly more thermolabile than the wild type enzyme or the SDH4K132R enzyme. Interestingly, there are no significant differences between the thermostability profiles for the succinate-PMS reductase activities of mutant and wild type enzymes (Fig. 4.4). This indicates a temperature-sensitive impairment of the quinone-binding site in the hydrophobic domains of the *SDH4* mutants.

SDH Cytochrome b_{562} Levels in Mutant and Wild Type Mitochondria. The cytochrome *b* from the mammalian SDH has the property of being selectively oxidized by fumarate after reduction with dithionite (Hatefi and Galante, 1980). Therefore, a dithionite-reduced minus dithionite-reduced plus fumarate-oxidized difference spectrum corresponds to the absorption spectrum of SDH cytochrome b_{562} (Brasseur *et al.*, 1997; Bruel *et al.*, 1995a; Hatefi and Galante,

Table 4.3

The Apparent Michaelis Constants for the Reduction of Decylubiquinone

Strain	K_m[a]	V_{max}[b]	k_{cat}[c]
MH125	3.5 ± 0.1	119 ± 4.9	3600 ± 150
sdh4W2 pSDH4-17	3.7 ± 0.2	109 ± 1.9	3500 ± 60
sdh4W2 pSDH4K132E	7.8 ± 0.1	75 ± 6.3	3000 ± 250
sdh4W2 pSDH4K132G	11.5 ± 0.6	64 ± 4.4	2900 ± 200
sdh4W2 pSDH4K132Q	13.2 ± 0.1	50 ± 5.2	2500 ± 260
sdh4W2 pSDH4K132R	3.9 ± 0.2	98 ± 2.8	3500 ± 100
sdh4W2 pSDH4K132V	12.2 ± 0.3	59 ± 4.2	2800 ± 200

The Michaelis constants were determined from double reciprocal plots as described in Section 2. Each value represents the mean of triplicate determinations ± S. E. M. [a] Values are expressed as μmol DB. [b] Values are expressed as nmol of DCPIP reduced min^{-1} mg^{-1} of protein. [c] Values are expressed as μmol of DCPIP reduced min^{-1} μmol of FAD^{-1}.

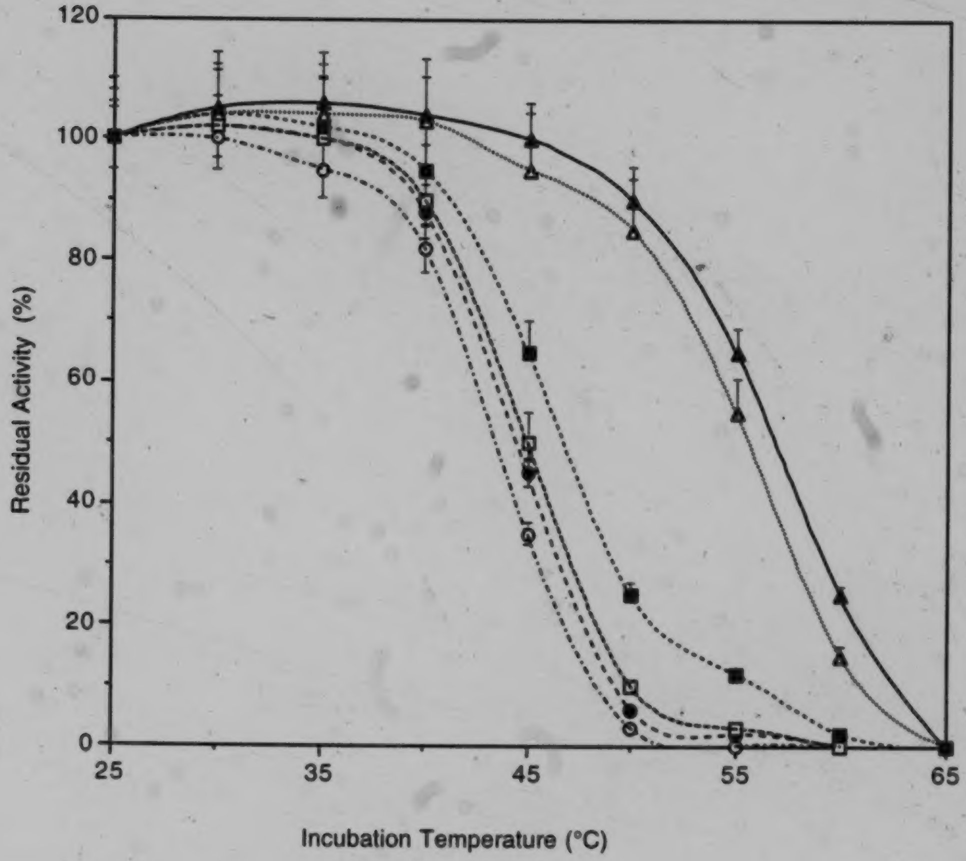

Figure 4.3 **Thermal stability profiles of succinate-DB reductase activities of mutant and wild type enzymes.**

DB reduction was monitored spectrophotometrically at the wavelength pair of 280 and 325 nm after incubating mitochondrial membranes at the indicated temperatures for 10 minutes. Activities are expressed as percentages of turnover numbers observed at 25 °C for each strain. The symbols used are: open circles, K132Q; closed circles, K132V; open squares, K132G; closed squares, K132E; open triangles, K132R; closed triangles, MH125. Error bars represent mean of triplicate determinations ± S.E.M.

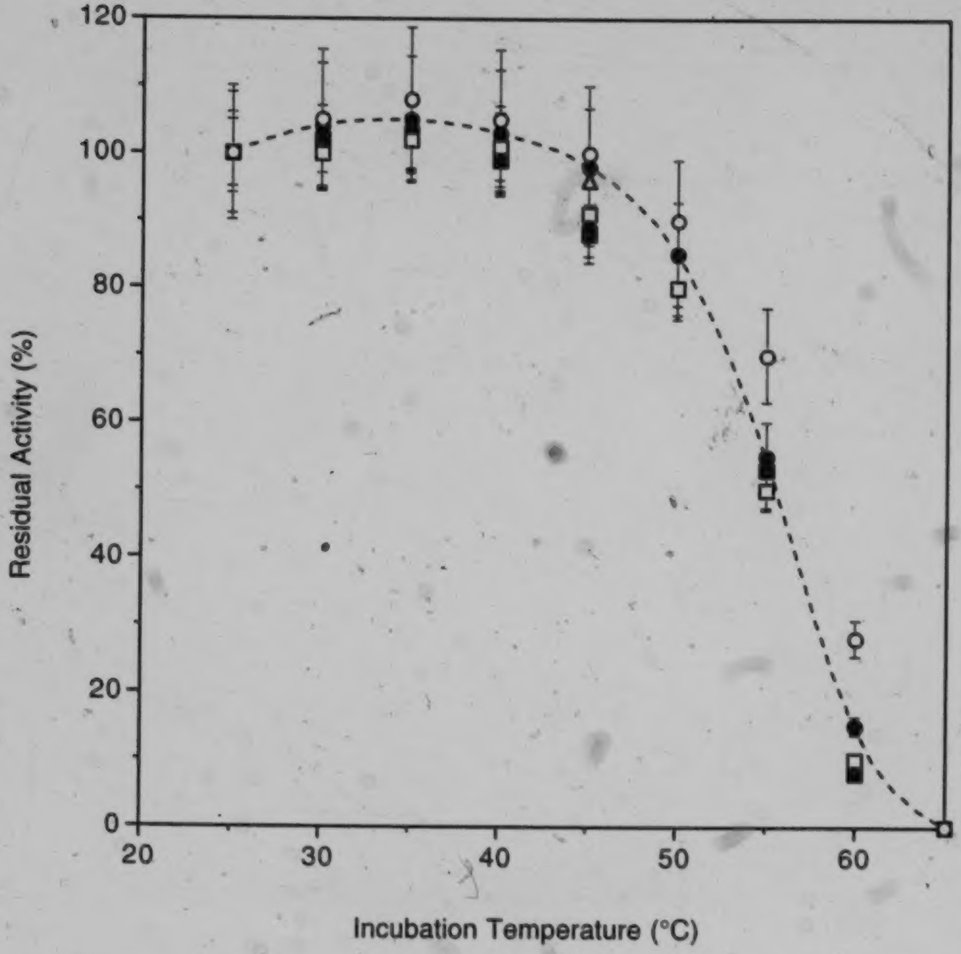

Figure 4.4 Thermal stability profiles of succinate-PMS reductase activities of mutant and wild type enzymes.

Mitochondrial membranes were incubated at the indicated temperatures for 10 minutes and assayed immediately for succinate-PMS reductase activity. Activities are expressed as percentage of turnover numbers observed at 25 °C for each strain. The symbols used are: open circles, wild type; closed circles, SDH4K132R; open squares, SDH4K132E; closed squares, SDH4K132G; open triangles, SDH4K132V closed triangles, SDH4K132Q. Error bars represent means of triplicate determinations ± S.E.M.

1980; Chapter 2). We used this approach to determine cytochrome b_{562} spectra of mutant and wild type mitochondria (Fig. 4.5). Spectra were normalized to covalent FAD levels. As expected, cytochrome b_{562} is not detected in the strain lacking the *SDH4* gene, sdh4W2. A 2-fold reduction in cytochrome b_{562} levels is observed in mitochondria from SDH4K132E, and a greater than 2-fold reduction in mitochondria from SDH4K132G, SDH4K132Q, and SDH4K132V compared to the wild type. In contrast, there is no significant difference between the cytochrome b_{562} contents of the SDH4K132R and the wild type mitochondria.

4.4. Discussion

Although relatively simple in subunit composition, the structure of SDH is still poorly understood due to a lack of information on the requirements for quinone binding and on intersubunit interactions. The variability in anchor subunit composition and primary amino acid sequence amongst SDH family members has made it difficult to compare results between the many SDH and FRD model systems. Yeast Sdh4p is unusual in its possession of a 30 amino acid extension at its C-terminus, suggesting that it may have an unusual function in this organism. The results presented in this report demonstrate the importance of Lys-132 of the Sdh4p C-terminus to the structure of the SDH hydrophobic domain.

We show that residue 132 of the yeast Sdh4p is important in the formation of a native conformation compatible with ubiquinone reduction, cytochrome b_{562} assembly, and enzyme stability. Of the five amino acid substitutions investigated, only the Arg substitution is benign, suggesting the need for a basic residue at this position. The K132E, K132G, K132Q, and K132V substitutions greatly impair SDH function *in vivo* (Fig. 4.2). The impaired respiratory growth is not due to a loss of Sdh4p anchoring function, since mitochondrial membranes from mutant strains have normal levels of succinate-PMS reductase activities and near normal levels of covalent FAD (Table 4.1). In *S. cerevisiae*, SDH is the major protein with

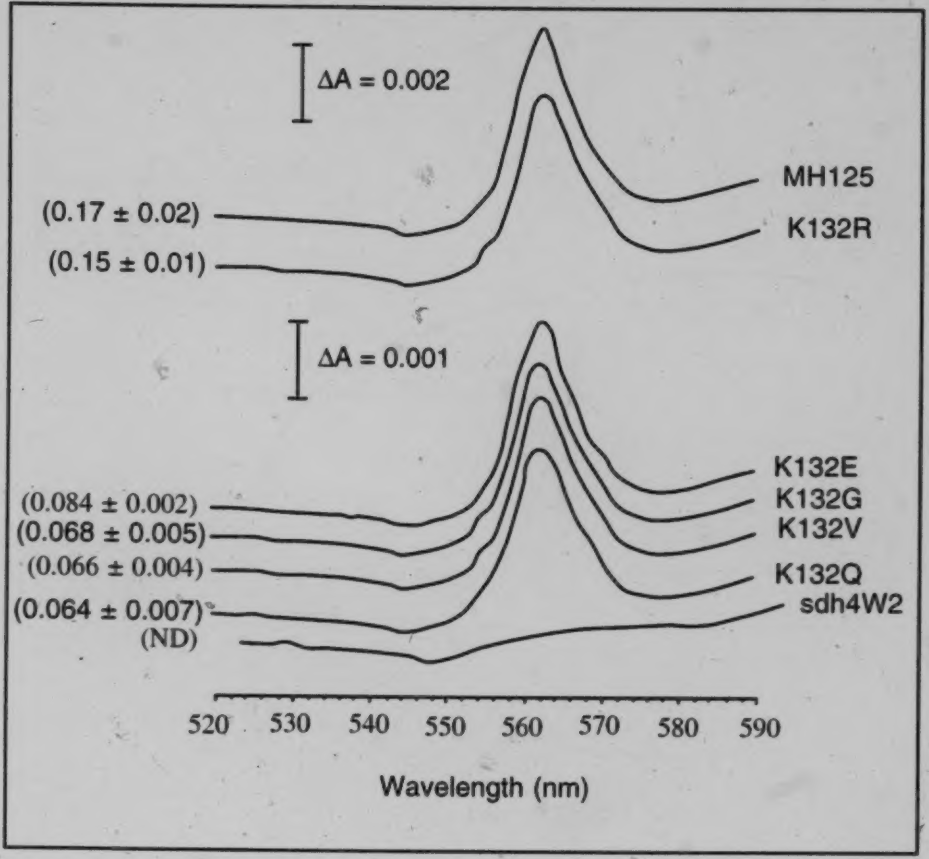

Figure 4.5 Spectra of SDH-associated Heme in Mitochondria from Wild Type and Mutant Strains.

Mitochondria were normalized to a covalent FAD level of 185 pmol/ml and the dithionite-reduced minus the dithionite-reduced/fumarate-oxidized difference spectra were determined. Spectra were recorded after adding a few grains of dithionite and 40 mM fumarate to the reference cuvette and a few grains of dithionite to the sample cuvette. Enclosed in parentheses are cytochrome concentrations (nmoles/185 pmol covalent FAD) calculated from the spectra, using the absorption coefficient of 24 mM^{-1} cm^{-1}. Values represent means of triplicate determinations ± S. E. M.

covalently bound flavin. The covalent flavin content of submitochondrial membranes provides an accurate measure of the membrane-associated Sdh1p (de Kok *et al.*, 1975; Robinson *et al.*, 1991; Singer and McIntire, 1984; Westenberg *et al.*, 1993). This directly reflects the assembly of the catalytic dimer, Sdh1p and Sdh2p, since the latter is not assembled in the absence of the former and vice versa (Schmidt *et al.*, 1992).

Replacing Sdh4p Lys-132 by Glu, Gln, Gly, or Val leads to significant decreases in the ability of SDH to reduce an exogenous quinone analog, DB (Table 4.2). However, when supplied with saturating DB concentrations, the mutant enzymes can achieve maximal turnover numbers approaching that of the wild type enzyme (Table 4.3). The Michaelis constant, K_m, is a very complex parameter. The differences in the apparent K_m's do not lead to concomitant changes in the k_{cat}'s (the maximal turnover numbers), suggesting that the rate of quinone reduction is not affected once the enzyme is supplied with a saturating amount of quinone. This raises the interesting question of how a residue located on the cytoplasmic side of the membrane can affect functions that are carried out in the membrane. Currently, the amino acid residues constituting the quinone binding site(s) of the yeast SDH are not known. By analogy to the bovine SDH and the *E. coli* FRD (Ackrell *et al.*, 1992; Hägerhäll, 1997; Hederstedt and Ohnishi, 1992; Lee *et al.*, 1995; Ohnishi, 1987; Scheffler, 1998; Shenoy *et al.*, 1997; Yankovskaya *et al.*, 1996), yeast SDH has been proposed to contain two quinone binding sites, Q_A and Q_B, located towards the matrix and the cytoplasmic sides of the inner mitochondrial membrane respectively (Oyedotun and Lemire, 1997). It seems unlikely that Lys-132 serves as a quinone ligand in a quinone-binding site. Our data favors the alternative possibility that the alteration of Lys-132 to a non-basic amino acid induces a structural perturbation that is propagated to the quinone binding sites in the membrane. The increased thermolability of the succinate-DB reductase activities and the unaffected thermostability of the succinate-PMS reductase activities of mutant enzymes (Fig. 4.4) support this conclusion. Thus, the structural changes induced by the mutations at Lys-132, although large enough to affect SDH enzyme stability, apparently only affect the hydrophobic domain. Furthermore, the differential thermal stability of the succinate-DB reductase and the succinate-PMS reductase activities indicates that an intact quinone-binding site is not necessary for the transfer of electrons from succinate to the artificial electron acceptor, PMS. The site of PMS reduction by the Sdh1p/Sdh2p dimer is unknown. From the data in Table 4.2, it is clear that the mutations have no effects on other respiratory chain complexes including the ubiquinol-cytochrome *c* reductase which may be intimately associated with SDH (Boumans *et al.*, 1998; Bruel *et al.*, 1996).

In addition to the effects on quinone reduction and enzyme stability, all the amino acid substitutions except the K132R substitution significantly impair cytochrome b_{562} assembly in SDH. Measurement of the fumarate-oxidizable spectrum provides a convenient means for detecting SDH-associated *b*-type heme in yeast (Oyedotun and Lemire, 1999). This spectrum is usually masked by that of the more abundant cytochrome *b* of complex III in the classical reduced minus oxidized difference absorption spectrum of mitochondria. The cytochrome contents in the mutant strains are about half that of the wild type, indicating that structural perturbations are propagated to the heme ligands since it is unlikely that Lys-132 participates in heme coordination. An alternative possibility is that the mutations significantly raise the midpoint potential of the heme such that it is less easily oxidizable by fumarate and not detected spectrophotometrically under our assay conditions. Deletion of the nuclear *ABC1* gene in yeast has been shown to lead to a drastic decrease in the amount of cytochrome b_{562} associated with SDH (Brasseur *et al.*, 1997). However, ours is the first report of point mutants in the yeast SDH that affect the cytochrome.

At present, the role of heme in electron transfer from succinate to ubiquinone is not clear. Our data indicate that heme does not play an essential role in quinone reduction. For example, in membranes of the K132Q mutant, which contain only 38% (0.064/0.17 nmol heme per 185 nmol of FAD^{-1}) the amount of heme per covalent FAD as wild type membranes (Fig. 4.5), we find 31% (1100/3500 μmol DCPIP min^{-1} μmol of FAD^{-1}) succinate-DB reductase activity (Table 4.2). However, activity can be stimulated to 69% (2500/3600 μmol DCPIP min^{-1} μmol of FAD^{-1}) under saturating DB concentrations (Table 3). The presence of approximately 2-fold more succinate-DB reductase activity under saturating DB conditions than heme content is also seen with the K132E, K132G, and K132V mutants. This observation is significant in that it suggests that heme is not involved in electron transfer from succinate to ubiquinone. This is in agreement with a recent observation that heme is not necessary for the catalytic function of the *E. coli* SDH (Vibat *et al.*, 1998). Recently, it has been postulated that the cytochrome in complex II interacts with the ubisemiquinone radical to reduce the production of superoxide free radicals (Ishii *et al.*, 1998). Further studies will be required to test these possibilities.

The impairments in quinone reduction, enzyme stability, and cytochrome *b* assembly strongly suggest that a structural change has occurred in SDH due to the substitutions at Lys-132 of Sdh4p. Our results are consistent with the possibility that Lys-132 of Sdh4p may be a determinant of structural integrity and conformation probably through salt-bridge formation. Of the five amino acid substitutions investigated, only the Arg substitution preserves both the charge and hydrogen bonding properties of Lys, and only the Arg substitution is benign at this position. We imagine that Lys-132 is part of either an intramolecular or an intermolecular salt-bridge with an acidic residue that stabilizes the native conformation of SDH hydrophobic domain. It should be possible to identify the interacting residue by the isolation of second-site revertants that restore wild type enzyme function. Such studies are currently in progress.

4.5. Bibliography

Abraham, P. R., Mulder, A., van 't Riet, J., and Raué, H. A. (1994). Characterization of the *Saccharomyces cerevisiae* nuclear gene *CYB3* encoding a cytochrome *b* polypeptide of respiratory complex II. *Mol. Gen. Genet.* **242,** 708-716.

Ackrell, B. A. C., Johnson, M. K., Gunsalus, R. P., and Cecchini, G. (1992). Structure and function of succinate dehydrogenase and fumarate reductase. In Chemistry and biochemistry of flavoenzymes, F. Müller, ed. (Boca Raton, Florida: CRC Press, Inc.,), pp. 229-297.

Boumans, H., Grivell, L. A., and Berden, J. A. (1998). The respiratory chain in yeast behaves as a single functional unit. *J. Biol. Chem.* **273,** 4872-4877.

Brasseur, G., Tron, G., Dujardin, G., Slonimski, P. P., and Brivet-Chevillotte, P. (1997). The nuclear ABC1 gene is essential for the correct conformation and functioning of the cytochrome bc_1 complex and the neighbouring complexes II and IV in the mitochondrial respiratory chain. *Eur. J. Biochem.* **246,** 103-111.

Bruel, C., Brasseur, R., and Trumpower, B. L. (1996). Subunit 8 of the *Saccharomyces cerevisiae* Cytochrome bc_1 complex interacts with succinate-ubiquinone reductase complex. *J. Bioenerg. Biomembr.* **28,** 59-68.

Bruel, C., di Rago, J.-P., Slonimski, P. P., and Lemesle-Meunier, D. (1995a). Role of the evolutionarily conserved cytochrome *b* tryptophan 142 in the ubiquinol oxidation catalyzed by the *bc*1 complex in the yeast *Saccharomyces cerevisiae. J. Biol. Chem.* **270,** 22321-22328.

Bruel, C., Manon, S., Guerin, M., and Lemesle-Meunier, D. (1995b). Decoupling of the bc_1 complex in *Saccharomyces cerevisiae*; point mutations affecting the cytochrome *b* gene bring new information about the structural aspect of the proton translocation. *J. Bioenerg. Biomembr.* **27,** 527-539.

Bullis, B. L., and Lemire, B. D. (1994). Isolation and characterization of the *Saccharomyces cerevisiae SDH4* gene encoding a membrane anchor subunit of succinate dehydrogenase. *J. Biol. Chem.* **269,** 6543-6549.

Burger, G., Lang, B. F., Reith, M., and Gray, M. W. (1996). Genes encoding the same three subunits of respiratory complex II are present in the mitochondrial DNA of two phylogenetically distant eukaryotes. *Proc. Natl. Acad. Sci. USA* **93,** 2328-2332.

Cole, S. T., Condon, C., Lemire, B. D., and Weiner, J. H. (1985). Molecular biology, biochemistry, and bioenergetics of fumarate reductase, a complex membrane-bound iron-sulfur flavoenzyme of *Escherichia coli*. *Biochim. Biophys. Acta* **811,** 381-403.

Daignan-Fornier, B., Valens, M., Lemire, B. D., and Bolotin-Fukuhara, M. (1994). Structure and regulation of *SDH3*, the yeast gene encoding the cytochrome b_{560} subunit of respiratory complex II. *J. Biol. Chem.* **269,** 15469-15472.

de Kok, J., Muller, J. L. M., and Slater, E. C. (1975). EPR studies on the respiratory chain of wild-type *Saccharomyces cerevisiae* and mutants with a deficiency in succinate dehydrogenase. *Biochim. Biophys. Acta* **387,** 441-450.

Gietz, R. D., and Sugino, A. (1988). New yeast-*Escherichia coli* shuttle vectors constructed with *in vitro* mutagenized yeast genes lacking six-base pair restriction sites. *Gene* **74,** 527-534.

Hägerhäll, C. (1997). Succinate:quinone oxidoreductases: variations on a conserved theme. *Biochim. Biophys. Acta* **1320,** 107-141.

Hägerhäll, C., and Hederstedt, L. (1996). A structural model for the membrane-integral domain of succinate:quinone oxidoreductases. *FEBS Lett.* **389,** 25-31.

Hatefi, Y., and Galante, Y. M. (1980). Isolation of cytochrome b_{560} from complex II (succinate:ubiquinone oxidoreductase) and its reconstitution with succinate dehydrogenase. *J. Biol. Chem.* **255,** 5530-5537.

Hederstedt, L., and Ohnishi, T. (1992). Progress in Succinate:quinone oxidoreductase research. In Molecular mechanisms in bioenergetics, L. Ernster, ed. (New York: Elsevier Science Publishers), pp. 163-197.

Ishii, N., Fujii, M., Hartman, P. S., Tsuda, M., Yasuda, K., Senoo-Matsuda, N., Yanase, S., Ayusawa, D., and Suzuki, K. (1998). A mutation in succinate dehydrogenase cytochrome *b* causes oxidative stress and ageing in nematodes. *Nature* **394,** 694-697.

Lee, G. Y., He, D.-Y., Yu, L., and Yu, C.-A. (1995). Identification of the ubiquinone-binding domain in QPs1 of succinate-ubiquinone reductase. *J. Biol. Chem.* **270,** 6193-6198.

Ohnishi, T. (1987). Structure of the succinate-ubiquinone oxidoreductase (complex II). *Curr. Top. Bioenerg.* **15,** 37-65.

Oyedotun, K. S., and Lemire, B. D. (1997). The carboxyl terminus of the *Saccharomyces cerevisiae* succinate dehydrogenase membrane subunit, Sdh4p, is necessary for ubiquinone reduction and enzyme stability. *J. Biol. Chem.* **272,** 31382-31388.

Oyedotun, K. S., and Lemire, B. D. (1999). The *Saccharomyces cerevisiae* succinate-ubiquinone reductase contains a stoichiometric amount of cytochrome b_{562}. *FEBS Lett.* **442,** 203-207.

Robinson, K. M., von Kieckebusch-Gück, A., and Lemire, B. D. (1991). Isolation and characterization of a *Saccharomyces cerevisiae* mutant disrupted for the succinate dehydrogenase flavoprotein subunit. *J. Biol. Chem.* **266,** 21347-21350.

Scheffler, I. E. (1998). Molecular genetics of succinate:quinone oxidoreductase in eukaryotes. *Prog. Nucleic Acid Res. Mol. Biol.* **60,** 267-315.

Schmidt, D. M., Saghbini, M., and Scheffler, I. M. (1992). The C-terminus of the succinate dehydrogenase IP peptide of *Saccharomyces cerevisiae* is significant for assembly of complex II. *Biochemistry* **31,** 8442-8448.

Shenoy, S. K., Yu, L., and Yu, C. A. (1997). The smallest membrane anchoring subunit (QPs3) of bovine heart mitochondrial succinate-ubiquinone reductase. Cloning, sequencing, topology, and Q-binding domain. *J. Biol. Chem.* **272,** 17867-17872.

Singer, T. P., and McIntire, W. S. (1984). Covalent attachment of flavin to flavoproteins: occurence, assay, and synthesis. *Methods Enzymol.* **106,** 369-378.

Smirnova, I. A., Hägerhäll, C., Konstantinov, A. A., and Hederstedt, L. (1995). HOQNO interaction with cytochrome *b* in succinate:menaquinone oxidoreductase from *Bacillus subtilis*. *FEBS Lett.* **359,** 23-26.

Vibat, C. R. T., Cecchini, G., Nakamura, K., Kita, K., and Gennis, R. B. (1998). Localization of histidine residues responsible for heme axial ligation in cytochrome b_{556} of complex II (succinate:ubiquinone oxidoreductase) in *Escherichia coli*. *Biochemistry* **37,** 4148-4159.

Waldeck, A. R., Stowell, M. H. B., Lee, H. K., Hung, S. C., Matsson, M., Hederstedt, L., Ackrell, B. A. C., and Chan, S. I. (1997). Electron paramagnetic resonance studies of succinate:ubiquinone oxidoreductase from *Paracoccus denitrificans*. Evidence for a magnetic interaction between the 3Fe-4S cluster and cytochrome *b*. *J. Biol. Chem.* **272,** 19373-19382.

Westenberg, D. J., Gunsalus, R. P., Ackrell, B. A. C., Sices, H., and Cecchini, G. (1993). *Escherichia coli* fumarate reductase *frdC* and *frdD* mutants. identification of amino acid residues involved in catalytic activity with quinones. *J. Biol. Chem.* **268,** 815-822.

Yankovskaya, V., Sablin, S. O., Ramsay, R. R., Singer, T. P., Ackrell, B A. C., Cecchini, G., and Miyoshi, H. (1996). Inhibitor probes of the quinone binding sites of mammalian complex II and *Escherichia coli* fumarate reductase. *J. Biol. Chem.* **271,** 21020-21024.

Chapter 5

Identification and Characterization of *S. cerevisiae* *SDH3* Mutants Involved in Quinone Interaction[*]

---

[*] A version of this chapter has been accepted for publication. Oyedotun, K. S. and Lemire, B. D. (1999) *J. Biol. Chem.*

5.1. Introduction

The mitochondrial respiratory chain carries out a series of reactions that generate an electrochemical potential across the inner membrane and drives the synthesis of ATP. It consists of several proteins and redox-active prosthetic groups arranged into four discrete molecular complexes (Hatefi, 1985; Mitchell, 1987; Trumpower and Gennis, 1994; Wikström and Saraste, 1984). These include: NADH:ubiquinone oxidoreductase (complex I; which is absent in *S. cerevisiae*); succinate:ubiquinone oxidoreductase, (complex II or succinate dehydrogenase, SDH); ubiquinol:cytochrome *c* oxidoreductase (complex III or bc_1 complex); and cytochrome *c* oxidase (complex IV). Ubiquinone, a small lipophilic molecule, plays a central role in linking the NADH and succinate oxidoreductases to complex III. A similar role is played by cytochrome *c* between complexes III and IV. Protein-quinone interactions and the mechanisms of quinone-mediated electron transfer are not yet fully understood. The relative abundance of quinone in comparison to other redox components in the inner mitochondrial membrane and its lipophilic nature led to the hypothesis that it functions as a homogeneous mobile carrier. Several dynamic and kinetic studies support the concept of pool function for quinone (Kroger and Klingenberg, 1973a; Kroger and Klingenberg, 1973b; Ragan and Cottingham, 1985; Ragan and Reed, 1986; Schneider *et al.*, 1982; Zhu *et al.*, 1982). Since free ubisemiquinone is highly unstable (Mitchell, 1975; Mitchell, 1976), the stability of these quinone species, which is usually observed in the membrane milieu, suggests that it must interact with protein (Ackrell *et al.*, 1992; Hägerhäll, 1997; Hederstedt and Ohnishi, 1992; Rich and Bonner, 1978; Rich *et al.*, 1977). It is now well established that the active species during quinone-mediated electron transfer are quinone-protein complexes (Lee *et al.*, 1995; Miki *et al.*, 1992; Shenoy *et al.*, 1997; Shenoy *et al.*, 1999; Trumpower and Gennis, 1994; Westenberg *et al.*, 1990; Westenberg *et al.*, 1993; Yang *et al.*, 1998).

Protein-quinone interactions have been studied extensively in bacterial photoreaction centers. High-resolution crystallographic structures are available for the Q_A-Q_B sites of the photosystems (Allen *et al.*, 1987a; Allen *et al.*, 1987b; Chirino *et al.*, 1994; Deisenhofer and Michel, 1989; Deisenhofer and Michel, 1995; El-Kabbani *et al.*, 1991; Ermler *et al.*, 1994). Quinone-binding sites have also been studied extensively in complex III (Iwata *et al.*, 1998; Kim *et al.*, 1998; Link *et al.*, 1993; Trumpower, 1990; Trumpower and Gennis, 1994; Xia *et al.*, 1997; Yu *et al.*, 1998; Zhang *et al.*, 1998). Despite these structures and the availability of sequences of many quinone-binding proteins, there is, as yet, no recognized general structural motif for these sites. Until additional structural data are available, insight into quinone-binding sites will continue to be gleaned from genetic and mutational analyses.

SDH and FRD constitute a family of structurally and functionally similar oxidoreductases (Ackrell *et al.*, 1992; Cole *et al.*, 1985; Hägerhäll, 1997; Hederstedt and Ohnishi, 1992). There has been a great deal of interest in identifying the amino acid residues involved in quinone binding in these enzymes. A comprehensive mutagenesis search for quinone-binding sites was carried out in the *E. coli* FRD. This led to the identification of a number of amino acid residues in FrdC and FrdD that are important for quinone-mediated enzyme activity (Westenberg *et al.*, 1990; Westenberg *et al.*, 1993). Since the quinone-binding sites in FRD are involved in oxidation, they are likely to differ from those of SDH, which are involved in reduction. Quite recently, a similar study has been undertaken on the *E. coli* SDH (Yang *et al.*, 1998). However, poor primary sequence similarity precludes a simple extrapolation of the findings from these studies to the yeast SDH. Quinone-binding sites have also been studied in the bovine SDH by photoaffinity labeling (Lee *et al.*, 1995; Shenoy *et al.*, 1997) and by directed mutagenesis (Shenoy *et al.*, 1999). The available evidence is consistent with the existence of two quinone-binding sites in SDHs and FRDs (Ackrell *et al.*, 1992; Hägerhäll, 1997; Waldeck *et al.*, 1997).

Although the *S. cerevisiae* SDH is known to interact with ubiquinone (Bullis and Lemire, 1994; Daignan-Fornier *et al.*, 1994), the amino acid residues involved in this interaction have yet to be determined. We have previously demonstrated the importance of residues 128-135 of the carboxyl terminus of the yeast Sdh4p (Oyedotun and Lemire, 1997). Sensitivity of the mutants to the quinone analog inhibitor, *s*-BDNP, suggests that the yeast SDH contains two quinone-binding sites and that one of these sites may be located toward the cytoplasmic face of the Sdh4p subunit. Furthermore, we showed that the positive charge provided by Sdh4p Lys-132 is crucial for establishing a stable conformation compatible with ubiquinone reduction (Oyedotun and Lemire, 1999a). We have also shown in Chapter 2 that the yeast SDH contains a stoichiometric amount of cytochrome b_{562} based on covalent flavin content (Oyedotun and Lemire, 1999b). However, the nature of the heme axial ligands and the function of heme in succinate-quinone reduction are not known. To further investigate the localization of the yeast SDH ubiquinone-binding sites and the role of the heme in succinate-quinone reductase activity, we isolated and characterized seven *SDH3* mutants. The mutant enzymes were characterized for their abilities to support respiratory growth as well as for enzyme stability, quinone reduction, heme assembly, and inhibitor sensitivity. From our analyses, we conclude that a ubiquinone-binding site is associated with the matrix-facing loop connecting Sdh3p transmembrane segments II and III. The yeast SDH is suggested to contain two ubiquinone-binding sites that are topologically localized to different faces of the membrane.

5.2. Materials and Methods

Strains, Media, and Culture Conditions. The *S. cerevisiae* strains, MH125 and sdh3W3, and the *E. coli* strain, DH5α, have been described earlier (Chapter 2). The yeast media used are YPDG (1% yeast extract, 2% peptone, 0.1% glucose, 2% glycerol) and YPG (1% yeast extract, 2% peptone, 2% glycerol). All other media and culture conditions have been described in Chapter 2.

Random Mutagenesis. An *Eco*RI-*Bgl*II fragment containing the promoter and the entire coding region of the *SDH3* gene was subcloned into a yeast-*E. coli* shuttle vector, YCplac111 (Gietz and Sugino, 1988) to yield the plasmid pYCSDH3 and transformed into the *E. coli* strain, DH5α. Cells were UV-irradiated at 254 nm (giving a dose rate of ~1.4 J m^{-1} s^{-1}) on LB plates in the dark for predetermined time points that resulted in 5-10 % survival. The plates were incubated at 37 °C overnight in the dark. Plasmids were isolated from colonies scraped from a total of 100 plates. For chemical mutagenesis, suspensions of the DH5α cells harboring pYCSDH3 were treated with 3 % ethyl methanesulfonate (EMS) (Lawrence, 1991). Plasmids were isolated from treatments that gave 5-10% survival on LB + Amp plates. Aliquots from the plasmids were transformed into the yeast strain sdh3W3, after which they were plated on SD medium for plasmid selection and incubated for three days at 30 °C. Leu^{+} transformants were replica-plated onto minimal SG and YPDG media. The plates were incubated at 30 °C. Colonies that are respiration-deficient as well as those that exhibited impaired growth were picked for further analysis. To ensure that any growth defects are plasmid-mediated, plasmids were recovered, re-transformed into sdh3W3 and the growth defect confirmed.

DNA Sequencing. Mutations were confirmed by sequencing the entire *SDH3* gene, using the M13 universal primers. Sequencing was performed in the Department of Biochemistry Core DNA facilities, University of Alberta as described in Chapter 3. To ensure that any phenotype observed is due to a mutation in the *SDH3* gene, a 0.988-kb *Eco*RI-*Hind*III fragment encoding the entire *SDH3* gene was subcloned into a non-mutagenized YCplac111 vector and retransformed into sdh3W3.

Enzyme Assays and Determination of the Kinetic Constants. All assays were carried out as described in Chapters 2 and 3. The determinations of the apparent Michaelis parameters, K_m and V_{max}, and the apparent inhibition constants, K_{i1} and K_{i2}, have been described elsewhere (Chapter 3).

Miscellaneous methods. Measurements of covalently bound flavin, yeast and *E. coli* transformations, and recombinant DNA methods have been described in Chapter 2. Similarly, determinations of protein and cytochrome contents of mitochondria, denaturing gel electrophoresis, and Western blot analysis were carried out as previously described in Chapter 2.

5.3. Results

Mutagenesis of the *SDH3* Gene. Unlike the succinate-quinone oxidoreductase catalytic domains, which are well conserved across species, the anchor polypeptides are much more variable in their primary amino acid sequences making it difficult to discern common structural features for quinone-binding sites. Random mutagenesis, followed by an appropriate selection scheme and biochemical characterization, is a powerful approach for identifying functional domains in proteins (Colson, 1993). We UV-mutagenized an *E. coli* strain carrying the plasmid-borne yeast *SDH3* gene and re-introduced the mutated plasmid into an *SDH3* knockout yeast strain. Mutagenesis in *E. coli*, rather than in yeast, greatly reduces the production of respiration-deficient mitochondrial petites. About 5000 Leu$^+$ sdh3w3 transformants were tested for respiratory growth on leucine-deficient minimal glycerol and YPDG media. Ten strains were impaired for growth, indicating a respiration deficiency. The strains were further analyzed by determining their growth yields on semisynthetic medium containing 0.5% galactose as carbon source. We isolated and sequenced 6 plasmids from colonies that resulted in growth yields of 10-50%. We have found that growth yields of less than 10 % are often associated with null alleles that abolish enzyme assembly. DNA sequencing revealed that five of the UV-induced mutants contain single base alterations (Table 5.1), resulting in the substitutions of Phe-103 with Val (F103V), His-106 with Tyr (H106Y), His-113 with Gln (H113Q), Trp-116 with Arg (W116R) and L-122 with a stop codon (L122stop). This latter lesion truncates Sdh3p by removing the third predicted transmembrane domain. A sixth mutant contained a single base deletion in the codon for Leu-52 that causes a frameshift mutation (L52FrShift). This truncates the *SDH3* gene product after the addition of 2 new amino acid residues, removing all three predicted transmembrane domains.

DH5α cells harboring pYCSDH3 were also treated with the chemical mutagen, EMS. Plasmids were re-isolated and tested for the presence of mutations by transformation into sdh3W3. Of the 1000 colonies screened, only one was incapable of respiratory growth. Sequencing revealed that the clone contained two A to T transversions in *SDH3* (Table 5.1), replacing His-106 and Asp-117 with Leu and Val, respectively (H106L/D117V).

Fig. 5.1 shows the growth of the mutants on semisynthetic medium containing 0.1-0.5% galactose. A growth yield of less than 30 % on this medium is usually associated with a respiratory deficiency severe enough to abolish growth on minimal glycerol medium. The growth yield of the *SDH3* knock out strain, sdh3W3, is 10% of its wild type parent, MH125; this represents fermentative growth. Similarly, the L52FrShift, the H106L/D117V, and the L122stop mutants achieved growth yields of 10% each. Since the L52FrShift is essentially an *SDH3* knockout, it was not characterized further. As expected, the growth yield of the sdh3W3 strain harboring the wild type *SDH3* plasmid, sdh3W3-pYCSDH3 was indistinguishable from the parental strain, MH125. The growth yield of the

Table 5.1

Summary of UV- and EMS-induced Mutations in the *SDH3* Gene

Mutant	Mutagen	Nucleotide change	Altered amino acid[a]
F103V	UV	T→G transversion	Phe-103→Val
H106Y	UV	C→T transition	His-106→Tyr
H113Q	UV	C→A transversion	His-113→Gln
W116R	UV	T→A transversion	Trp-116→Arg
H106L/D117V	EMS	A→T transversion A→T transversion	His-106→Leu Asp-117→Val
L122stop	UV	T→A transversion	Leu122→Stop
L52FrShift	UV	Deletion of 3' T of codon 155	Frameshift[b]

[a] The numbering of the amino acid residues is based on the mature sequence; [b] The frameshift caused the addition of 2 new amino acid residues at Leu 52 before premature truncation.

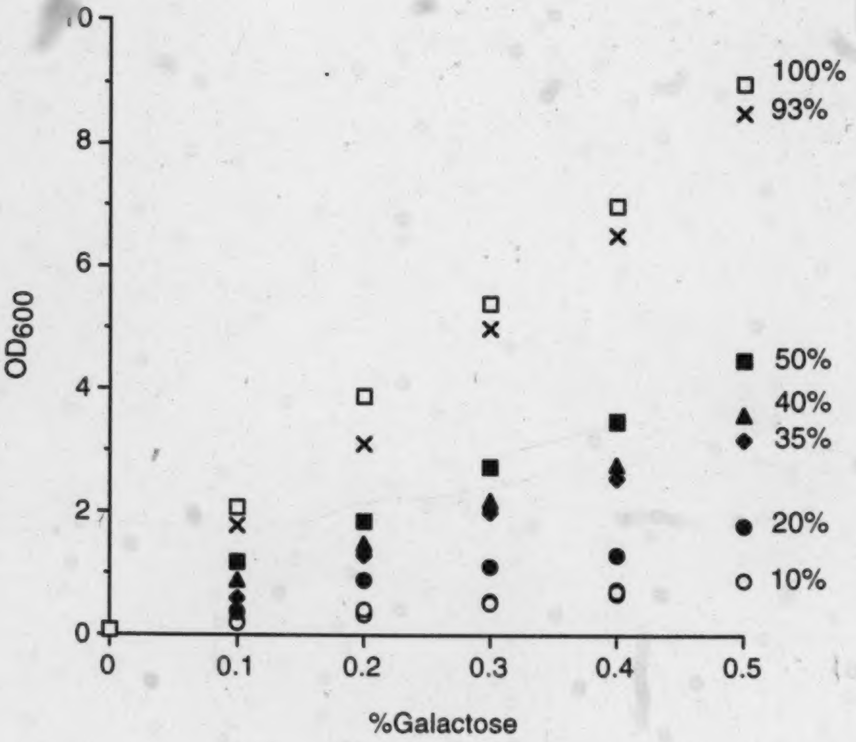

Figure 5.1 Growth of yeast strains on galactose media.

Yeast strains were grown at 30 °C on semisynthetic liquid medium containing 0.1, 0.2, 0.3, 0.4, and 0.5% galactose and the optical densities at 600 nm were measured. Precultures were prepared on selective minimal medium containing 2% galactose and 0.01% glucose. This was used to inoculate the main culture at a starting OD_{600} of 0.1. The cultures were allowed to reach late stationary phase (approximately 100 hours). The relative growth yields were calculated using the final absorbance values reached on 0.5% galactose. The symbols used are: open squares, MH125; crosses, sdh3W3/pYCSDH3; closed squares, H106Y; closed triangles, H113Q; closed diamond, F105V; closed circles, W116R; open circles, sdh3W3, L122stop, H106L/D117V, and L52FrShift. The growth characteristics of these latter 4 mutants are indistinguishable and for simplicity, only one symbol is used.

W116R mutant was severely reduced (20%), consistent with its inability to grow on minimal glycerol medium after 6 days of incubation at 30 °C. The F103V and H113Q mutants that achieve moderate growth yields of 35% and 40%, respectively, are also severely impaired for growth on minimal glycerol. The H106Y mutant retains a significant capacity for respiratory growth, with a 50% growth yield. These results indicate that Trp-116, Phe-103, His-113, and His-106 or Asp-117 are important residues in Sdh3p. In addition, loss of the third transmembrane segment in the L122stop mutant highlights the importance of this domain for SDH function.

Assembly of Mutant and Wild Type SDH Enzymes. To determine if the *SDH3* mutations interfere with enzyme assembly, we measured the levels of covalent FAD in mitochondrial membranes of mutant and wild type strains (Table 5.2). In *S. cerevisiae*, SDH is the major flavoprotein with covalently attached FAD and covalent flavin levels in mitochondrial membranes reflect the amount of Sdh1p associated with the membrane (Robinson and Lemire, 1995). The covalent FAD levels of the F103V, H113Q, and W116R strains are not significantly different from the wild type. We conclude that SDH assembly is not significantly impaired in these mutants. In contrast, the FAD levels of the H106Y, H106L/D117V, and the L122stop mutants are reduced, indicating some impairment of enzyme assembly with these lesions.

Also shown in Table 5.2 are the succinate-PMS reductase activities of mutant and wild type enzymes. Malonate-sensitive succinate-dependent PMS reductase activity in submitochondrial particles depends only on the membrane-anchoring function of the membrane domain and not on its catalytic competence. Since the mutants contain variable amounts of covalent FAD, we determined turnover numbers to compare catalytic efficiencies. The succinate-PMS reductase activities of the F103V, H106Y, H113Q, and W116R mutant enzymes are similar to that of the wild type enzyme in MH125 or sdh3W3 pYCSDH3. These data

Table 5.2

Covalent Flavin Levels and Succinate-PMS/DCPIP Reductase Activities in Mitochondrial Membranes of *S. cerevisiae* Strains

Yeast Strain	Covalent FAD[a]	Specific activity[b]	Turnover Number[c]
MH125	37 ± 4	148 ± 5	4000 ±135
sdh3W3/SDH3	34 ± 2	127 ± 6	3700 ± 185
F103V	33 ± 4	118 ± 3	3600 ± 100
W116R	32 ± 3	110 ± 4	3500 ± 126
H106Y	24 ± 3	77 ± 3	3160 ±50
H113Q	30 ± 3	103 ± 3	3400 ± 99
L122stop	19 ± 2	57 ± 2	3000 ± 111
H106L/D117V	17 ± 3	31 ± 1	1800 ± 65
Sdh3W3	ND[d]	ND	-[e]

Each value represents the mean of triplicate determinations ± S. E. M. [a] Covalent flavin contents are expressed as pmol FAD mg of protein^{-1}; [b] Specific activities are expressed as μmol of PMS-mediated DCPIP reduced min^{-1} mg^{-1} of protein; [c] Turnover numbers are expressed as μmol of PMS-mediated DCPIP reduced min^{-1} μmol of covalent FAD^{-1}; [d] Not detectable, less than 6% of wild type value; [e] Not determined.

confirm that the primary defects in these mutants are not due to impaired assembly on the membrane. Surprisingly, the L122stop mutant has a turnover number only slightly less than that of the wild type enzyme (75%). This indicates that the catalytic dimer assembled on the membrane retains wild type activity, although the lower level of covalent FAD in this mutant may indicate that the enzyme is only weakly attached to the membrane. In contrast, the turnover number of the H106L/D117V mutant enzyme is reduced (45%), suggesting that an altered Sdh3p structure can impair catalysis in the attached catalytic dimer.

Steady State Sdh3p Levels. The steady state levels of wild type and mutant Sdh3p subunits were compared by western blot analysis using a rabbit polyclonal antiserum raised against the N-terminal dodecapeptide of the mature Sdh3p (Fig. 5.2). The Sdh3p levels in mitochondrial membranes from the W116R, H106L/D117V, H113Q, H106Y, and F103V mutants (lanes 4 to 8 respectively) are similar to those of the wild type strains (lanes 2 and 9). Sdh3p is not detectable in the L122stop mutant (Lane 3). The truncated Sdh3p in this mutant is expected to migrate at about 13.8 kDa. Its absence may be due to protein degradation, enzyme instability, or to an altered behavior in the gel or blotting systems. The L122stop mutation does not eliminate enzyme assembly as judged by the covalent levels of isolated membranes. As expected, Sdh3p is absent in sdh3W3 (lane 1).

Quinone Reductase Activities of *SDH3* Mutants. Mitochondrial membranes of mutant and wild type strains were assayed for quinone-mediated electron transfer activities (Table 5.3). The succinate-DB reductase activities of the L122stop, F103V, H106L/D117V, and W116R mutants are severely reduced (25%, 24%, 20%, and 18% of the wild type turnover number, respectively). These data are consistent with the impaired growth phenotypes of these strains on minimal glycerol medium. The H113Q mutant enzyme retains a low but significant succinate-DB reductase activity (35% of wild type level), while the H106Y mutant is only slightly impaired (60% of wild type level). These values are

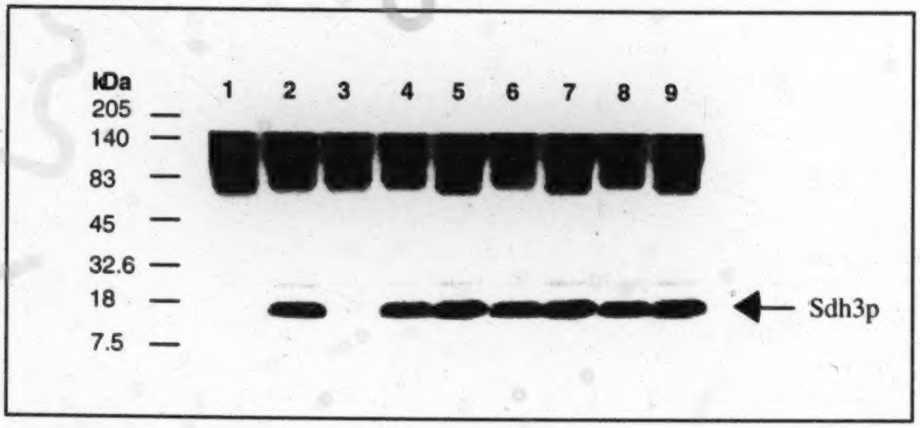
kDa
205
140
83
45
32.6
18
7.5
1
2
3
4
5
6
7
8
9
Sdh3p

Figure 5.2 Western Blot Analysis of Mutant and Wild Type Mitochondria.

Mitochondria were isolated from galactose-grown yeast strains and 10 μg electrophoresed on 13 % Tricine SDS-PAGE, and immunoblotted using anti-Sdh3p antibody. Lanes 1 to 9 are: sdh3w3, MH125, L122stop, W116R, H106V/D117L, H113Q, H106Y, F103V, and sdh3W3/pYCSDH3, respectively.

Table 5.3

Quinone-mediated Enzymatic Activities of *SDH3* Mutants and Wild Type Mitochondrial Membranes.

	MH125	sdh3W3 pYCSDH3	F103V	H106Y	H106L/ D117V	H113Q	W116R	L122stop	sdh3W3
Succinate-DB reductase[a]	3150[b]	3024	781	1890	630	1100	568	787	ND
Succinate-cytochrome *c* reductase[c]	2150	1978	538	1290	387	666	430	473	ND
Succinate oxidase[d]	1800	1689	450	1100	385	600	350	500	ND
NADH oxidase[d]	4150	4000	3711	3690	3500	3800	3300	3677	115[e]
Glycerol-1-P-cytochrome *c* reductase[c]	2500	2510	2000	2200	2183	2400	2342	2099	71[f]

Activities were measured in submitochondrial particles at saturating concentrations of all substrates.

[a] Activities are expressed as µmoles of DB-mediated DCPIP reduce min^{-1} µmol of covalent FAD^{-1}; [b] Each value represents the mean of triplicate determinations. In all cases, the S. E. M. are within 7% of mean values. ND, not detectable or less than 4% of wild type activity. [c] Activities are expressed as µmoles of cytochrome *c* reduced min^{-1} µmol of covalent FAD^{-1}; [d] Activities are expressed as µatoms of oxygen min^{-1} µmol FAD^{-1}; [e] Activity is expressed as ng atoms of oxygen min^{-1} mg^{-1} of protein; [f] Activity is expressed as nmol of cytochrome *c* reduced min^{-1} mg^{-1} of protein.

consistent with the levels of respiratory growth seen on galactose medium (Fig. 5.1). As expected, sdh3W3 has less than 4 % of the activity of wild type membranes.

We also measured the malonate-sensitive, succinate-dependent reduction of horse heart cytochrome *c* and succinate-oxidase activities (Table 5.3). The first assay depends on 2 segments of the mitochondrial respiratory chain (complexes II and III), while the second depends on 3 segments (complexes II-IV). Both assays rely on the reduction of endogenous ubiquinone. The succinate-cytochrome *c* reductase and succinate oxidase activities paralleled the succinate-DB reductase activities. In contrast, the membranes of *SDH3*-deficient strain, sdh3W3, have undetectable levels of these enzymatic activities. The NADH oxidase and glycerol-1-phosphate-cytochrome *c* reductase activities are largely unaffected in all the mutants. Since these activities do not depend on succinate as the source of electrons, they demonstrate the integrity of the remainder of the respiratory chain. From these data, we can conclude that the effects we have observed arise from defective SDH function and that the *SDH3* mutations do not have pleiotropic effects on other respiratory complexes present in the mitochondrial inner membrane.

Kinetics of exogenous quinone reduction. The kinetic parameters, K_m and V_{max}, were determined by varying the concentrations of DB at fixed concentrations of other substrates. The results are summarized in Table 5.4. The apparent K_m^{DB} of the W116R and the H113Q mutant enzymes are increased by 3-4 fold, while those of the F103V and the L122stop mutants are increased 2-fold. To compare the catalytic efficiencies of the enzymes, we also express the apparent V_{max} as maximal turnover numbers (k_{cat}) based on covalent FAD contents. We observed significant reductions in apparent k_{cat} values that are not paralleled by the turnover values determined with the succinate-PMS reductase assay, except for the H106L/D117V mutant (Table 5.2). This indicates that the W116R, H113Q,

Table 5.4

The Apparent Michaelis Constants for DB Reduction.

Strain	K_m[a]	V_{max}[b]	k_{cat}[c]
MH125	4.8 ± 0.1	126 ± 2.8	3400 ± 75
sdh3W3/SDH3	5.5 ± 0.2	123 ± 3.4	3250 ± 100
F103V	10 ± 0.3	33 ± 1.2	1000 ± 35
H106Y	7.0 ± 0.2	54 ± 1.7	2200 ± 70
H106L/D117V	7.3 ± 0.1	12 ± 0.3	690 ± 15
H113Q	15.0 ± 0.5	39 ± 1.5	1300 ± 50
W116R	18.0 ± 1.0	19 ± 0.9	612 ± 30
L122stop	11 ± 0.3	16 ± 0.4	820 ± 20

Kinetic parameters were determined by varying the concentrations of DB at fixed concentrations of succinate and DCPIP. K_m and V_{max} were calculated from a nonlinear regression fit to the Michaelis equation using initial estimates from the Lineweaver-Burk plots. Each value represents the mean of triplicate determinations ± S. E. M. [a]Values are expressed in µmol. [b] Values are expressed as µmol of DB-mediated DCPIP reduced min^{-1} mg^{-1} of protein. [c] Values are expressed as µmol of DB-mediated DCPIP reduced min^{-1} µmol of covalent FAD^{-1}.

F103V, and L122stop mutations affect the succinate-quinone reductase catalytic efficiencies, probably through defects in protein-quinone interaction as suggested by the apparent K_m^{DB} values. In contrast, we observed only a small increase in the apparent K_m^{DB} and a small decrease in the apparent k_{cat} of the H106Y mutant enzyme. The H106Y mutation likely does not affect this enzyme's catalytic efficiency.

Thermal Stability Profiles of the *SDH3* mutants. The Michaelis constant, K_m, is a complex parameter. Changes in apparent K_m may result from small structural perturbations that only alter the microenvironment of the quinone-binding pocket or from larger perturbations that are propagated to the remainder of the enzyme. To explore these two possibilities, we determined the thermostabilities of the mutant and wild type enzymes. We incubated mitochondrial membranes in the temperature range 25-65 °C and monitored the malonate-sensitive succinate-dependent reduction of DB directly at the wavelength pair of 280 and 325 nm (Fig. 5.3). All enzymes are stable at 25 °C. However, at higher temperatures, some of the mutant enzymes become thermolabile. The F103V, H106Y, and H106L/D117V mutant enzymes are considerably less stable than the wild type enzyme. This suggests that these mutations induce structural perturbations that destabilize the complex, possibly affecting the anchoring function of the membrane domain. In contrast, the thermal profiles of the H113Q and W116R mutant enzymes are comparable to the wild type enzyme. The structural perturbations produced by these lesions may be restricted in space.

Sensitivities of *SDH3* Mutants to a Quinone Analog Inhibitor. The pattern of inhibition by substrate analogs often gives an insight into the reaction mechanism. We have shown that the dinitrophenol derivative, 2-*sec*-butyl-4,6-dinitrophenol (*s*-BDNP) inhibits the yeast SDH with non-linear non-competitive kinetics (Oyedotun and Lemire, 1997). We hypothesize that a mutation that affects

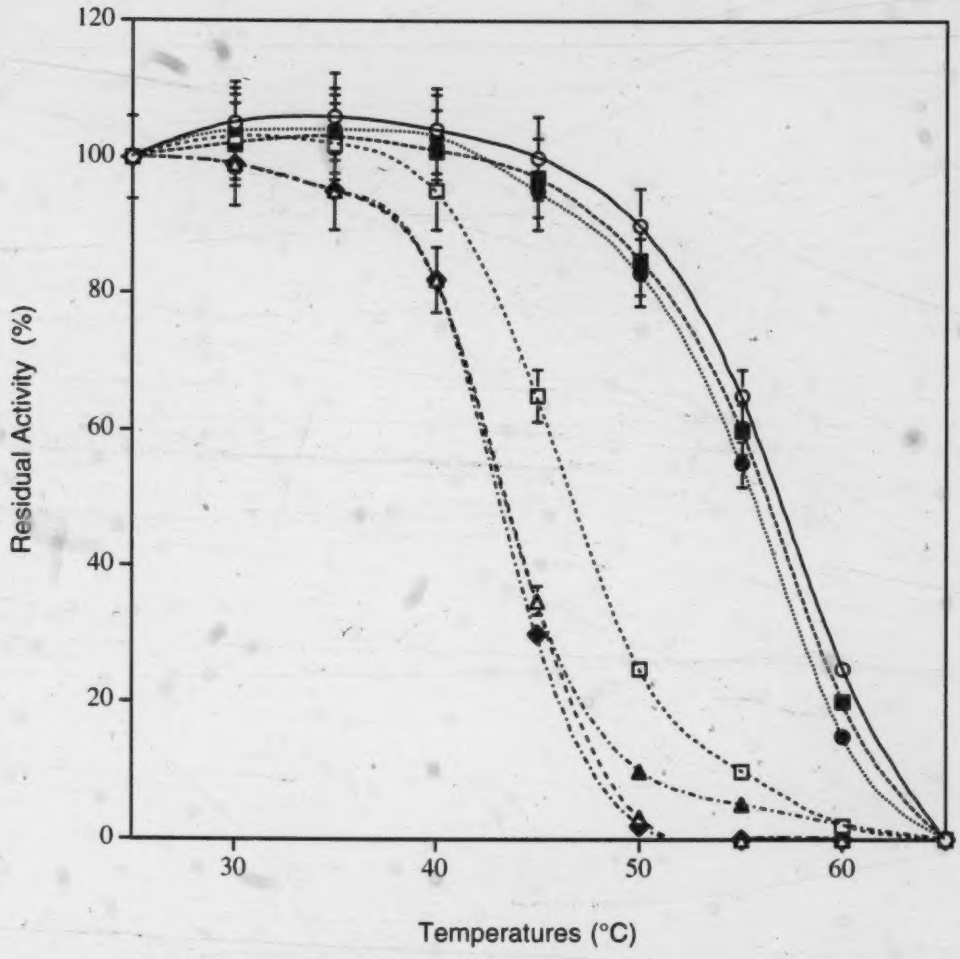

Figure 5.3 Thermal Stability Profiles of Succinate-DB Reductase Activities of Mutant and Wild Type Enzymes.

DB reduction was monitored spectrophotometrically at the wavelength pair of 280 and 325 nm after incubating mitochondrial membranes at the indicated temperatures for 10 minutes. Activities are expressed as percentages of turnover numbers observed at 25 °C for each strain. The symbols used are: open circles, MH125; closed circles, W116R; open squares, H106Y; closed squares, H113Q; open triangles, H106L/D117V; closed triangles, F103V; closed diamonds, L122stop. Error bars represent mean of triplicate determinations ± S.E.M.

the quinone reductase activity of an enzyme by altering a quinone-binding site will also alter that enzyme's sensitivity to a quinone analog inhibitor. We determined the inhibitor sensitivities of the H106Y, H113Q, and wild type enzymes. No reasonable estimates of the inhibition constants could be determined for the remaining mutants due to their low succinate-DB reductase activities. With all the mutants examined, complete inhibition of succinate-DB reductase activities could be attained at millimolar concentrations of *s*-BDNP. As previously reported (Oyedotun and Lemire, 1997), *s*-BDNP inhibits the *S. cerevisiae* succinate-ubiquinone reductase in a noncompetitive manner (Fig. 5.4, inset). The inhibition patterns of the mutants are also noncompetitive (data not shown). Re-plots of the abscissa intercepts against the inhibitor concentrations are hyperbolic for the wild type and the mutant enzymes (Fig. 5.4). Non-linearity of re-plots can result from a number of possibilities, including partial inhibition, allosteric effects, inhibition by an alternative product, or binding of the inhibitor to more than one site. In light of two-quinone binding site models for complex II and related enzymes (Hägerhäll, 1997; Waldeck *et al.*, 1997; Westenberg *et al.*, 1993; Yankovskaya *et al.*, 1996), we consider the latter possibility most likely. Accordingly, the hypothesis was tested by analyzing the data with the equation for a noncompetitive inhibition having two nonequivalent K_i values (Cleland, 1979):

$$y = a\frac{\left(1 + {}^{I}/_{K_{i1}}\right)}{\left(1 + {}^{I}/_{K_{i2}}\right)}$$

where y is the slope or intercept in the presence of a fixed concentration of the inhibitor I, a is the slope or intercept in the absence of inhibitor, and K_{i1} and K_{i2} are the high affinity and low affinity inhibition constants, respectively. There are good fits of the data to the equation (Fig. 5.4). The estimated K_i^{app} values for inhibitor binding at sites 1 and 2 (K_{i1} and K_{i2}) are presented in Table 5.5. Consistent with our earlier observations (Chapter 3), there is a difference of about 10-fold between the affinities of the two sites for *s*-BDNP. There is no significant

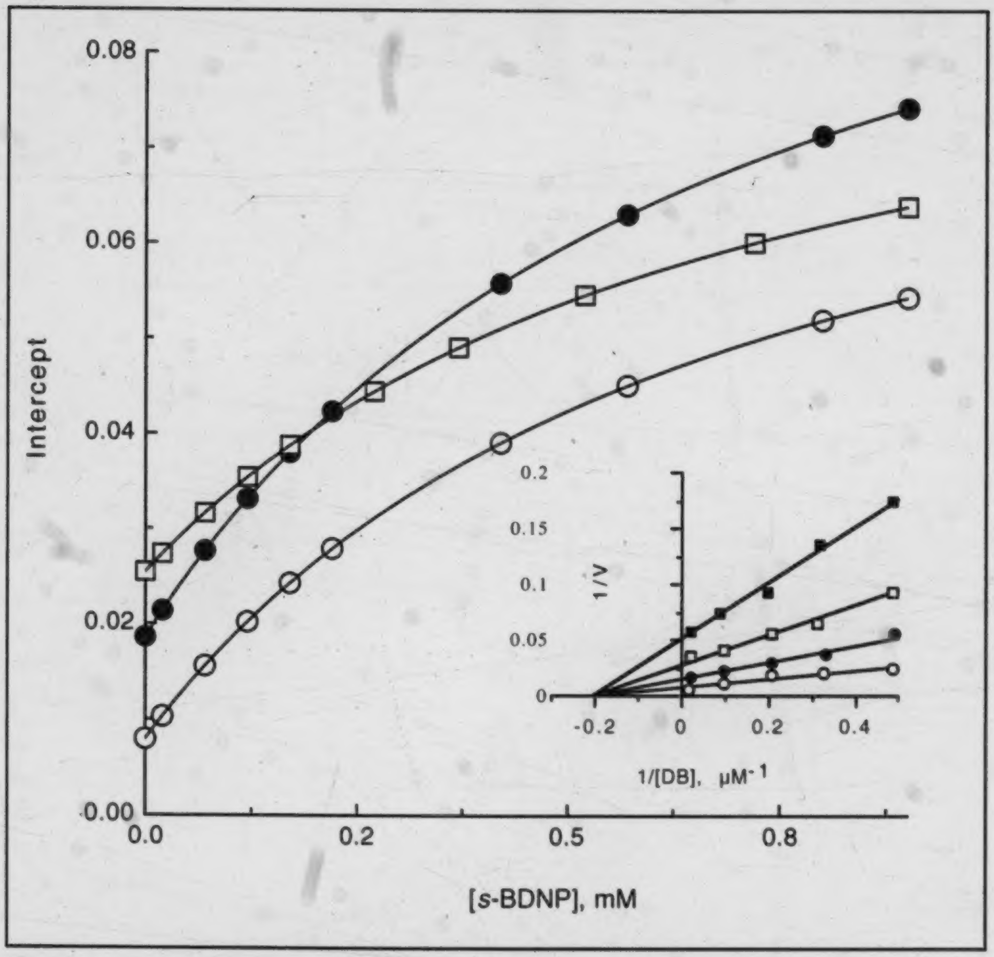

Figure 5.4 Inhibition of Quinone Reduction by 2-sec-butyl-4,6-dinitrophenol.

Secondary re-plots of intercepts (reciprocal maximal velocities) against inhibitor concentration (H113Q, filled circles; H106Y, open squares; wild type, open circles). The data were fitted to equation 1 by non-linear least squares using the quasi-Newton algorithm. Inset: Double-reciprocal plots showing non-competitive inhibition of succinate-DB reductase activity of the wild type enzyme by the inhibitor. The inhibitor concentrations are 0 mM, open circles; 0.07 mM, closed circles; 0.22 mM, open squares; 0.8 mM, closed squares.

Table 5.5

Apparent Inhibition Constants for Quinone Reduction

Strain	K_{i1}[a]	K_{i2}
MH125	0.060 ± 0.005[b]	0.67 ± 0.03
H113Q	0.19 ± 0.03	0.70 ± 0.01
H106Y	0.11 ± 0.01	0.69 ± 0.02

[a] Inhibition constants are expressed in mM; [b] Values represent the mean of triplicate determinations ± S. E. M.

difference at the low affinity inhibitor sites (K_{i2}^{app}) for the H106Y and the H113Q mutant enzymes compared to wild type value. In contrast, the K_i^{app} values for the high affinity sites in the H106Y and the H113 mutants are increased 2- and 3-fold, respectively. These results are consistent with a 2 quinone-binding site model where the H106Y and the H113 mutations only affect one of the sites.

SDH-Associated Cytochrome *b* Levels. The *S. cerevisiae* SDH possesses a fumarate-oxidizable cytochrome b_{562} (Brasseur *et al.*, 1997; Bruel *et al.*, 1995; Oyedotun and Lemire, 1999a; Oyedotun and Lemire, 1999b). In Chapter 2, we showed that this cytochrome is present in a stoichiometric amount based on covalent flavin level. To determine if SDH-associated cytochrome b_{562} assembly is affected by the mutations, we measured the dithionite-reduced, fumarate-oxidizable difference spectra of mitochondria isolated from wild type and mutant strains (Fig. 5.5). The cytochrome contents estimated from the spectra are significantly reduced in all mutant mitochondria. The cytochrome b_{562} levels decreased by about 2-fold in the F103V, H106Y, H113Q, W116R, and L122stop mitochondria, while there is a 3-fold reduction in those of H106Y and H106L/D117V mitochondria. There is no apparent correlation between the succinate-DB reductase activities (Table 5.2) and the cytochrome *b* contents of mitochondria. This may indicate that cytochrome *b* is not involved in the electron pathway between succinate and ubiquinone. Alternatively, it may suggest that the mutations have differential effects on the reverse reaction, the reduction of fumarate, which is required for cytochrome detection.

5.4. Discussion

Ubiquinone is an obligatory redox component of the respiratory and photosynthetic electron transport chains (Trumpower, 1980; Trumpower and Gennis, 1994). The chemiosmotic hypothesis predicts that ubiquinone might mediate the transport of H^+ outward across the inner mitochondrial membrane

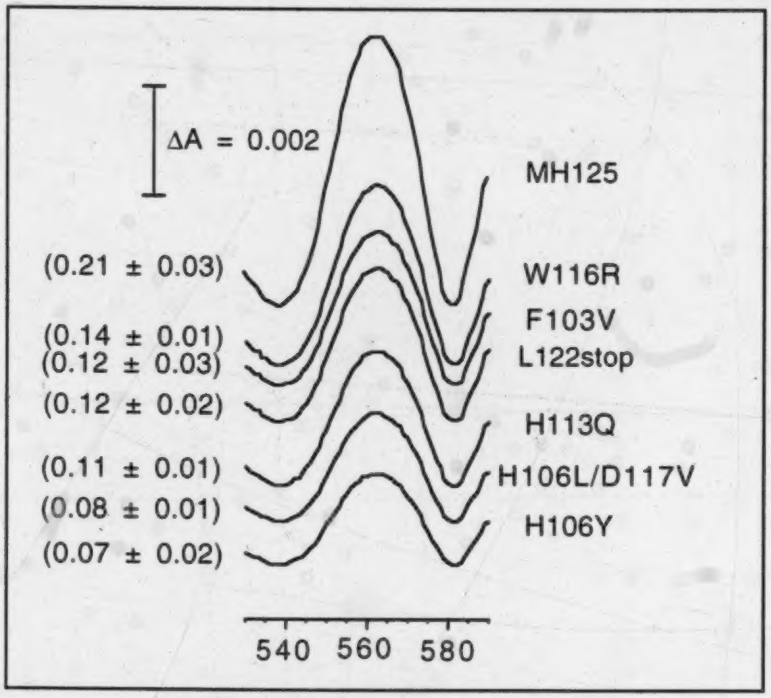

Figure 5.5 Spectra of SDH-associated Heme in Mitochondria from Wild Type and Mutant Strains.

Mitochondria were normalized to a covalent FAD level of 185 pmol/ml and the dithionite-reduced minus the dithionite-reduced/fumarate-oxidized difference spectra were determined. Spectra were recorded after adding a few grains of dithionite and 40 mM fumarate to the reference cuvette and a few grains of dithionite to the sample cuvette. Enclosed in parentheses are cytochrome concentrations (nmoles/185 pmol covalent FAD) calculated from the spectra, using the absorption coefficient of 24 mM^{-1} cm^{-1}. Values represent means of triplicate determinations ± S. E. M.

(Mitchell, 1961; Mitchell, 1977). Identifying the amino acid residues that interact with ubiquinone and their topographical locations in the membrane are central to understanding the mechanisms of quinone-mediated electron and or/proton transport.

In this study, we identify three amino acid residues (Phe-103, His-113, and Trp-116) in the *S. cerevisiae* Sdh3p subunit that are important in the formation of a quinone-binding site in SDH. Several lines of evidence indicate that mutations in these amino acid residues lead to a severe but specific impairment in the ability of SDH to reduce quinones. First, the three mutants demonstrate impaired but not abolished respiratory growth on galactose containing medium (Fig. 5.1). Second, the three mutants contain near normal levels of membrane-associated covalent FAD, wild type turnover numbers with the succinate-PMS reductase assay, which does not require catalytically functional membrane domain (Table 5.2), and wild type levels of Sdh3p polypeptide (Fig. 5.2). The mutant enzymes are thus assembled and inserted into the membrane in normal amounts. Third, these three mutants are significantly impaired in succinate-DB reductase, succinate-cytochrome *c* reductase, and succinate oxidase activities, assays that require the ability to reduce quinone. Fourth, the mutations lead to increases in the apparent K_m^{DB} values, with the highest increase observed for the W116R mutant enzyme. Fifth, two of the mutations, H113Q and W116R, do not affect the thermostabilities of the mutant enzymes suggesting that their structural perturbations are more localized. Sixth, for the H113Q mutation, the inhibitor sensitivity analysis suggests that only one of two inhibitor sites and by extension, one of two quinone-binding sites is affected. Finally, the Phe-103, His-113, and Trp-116 residues are topologically clustered (Fig. 5.6), strongly arguing for their involvement in the formation of a quinone-binding site in or near the loop connecting transmembrane segments II and III. The specific roles of these and neighboring residues in the formation of this site can now be further explored by site directed mutagenesis.

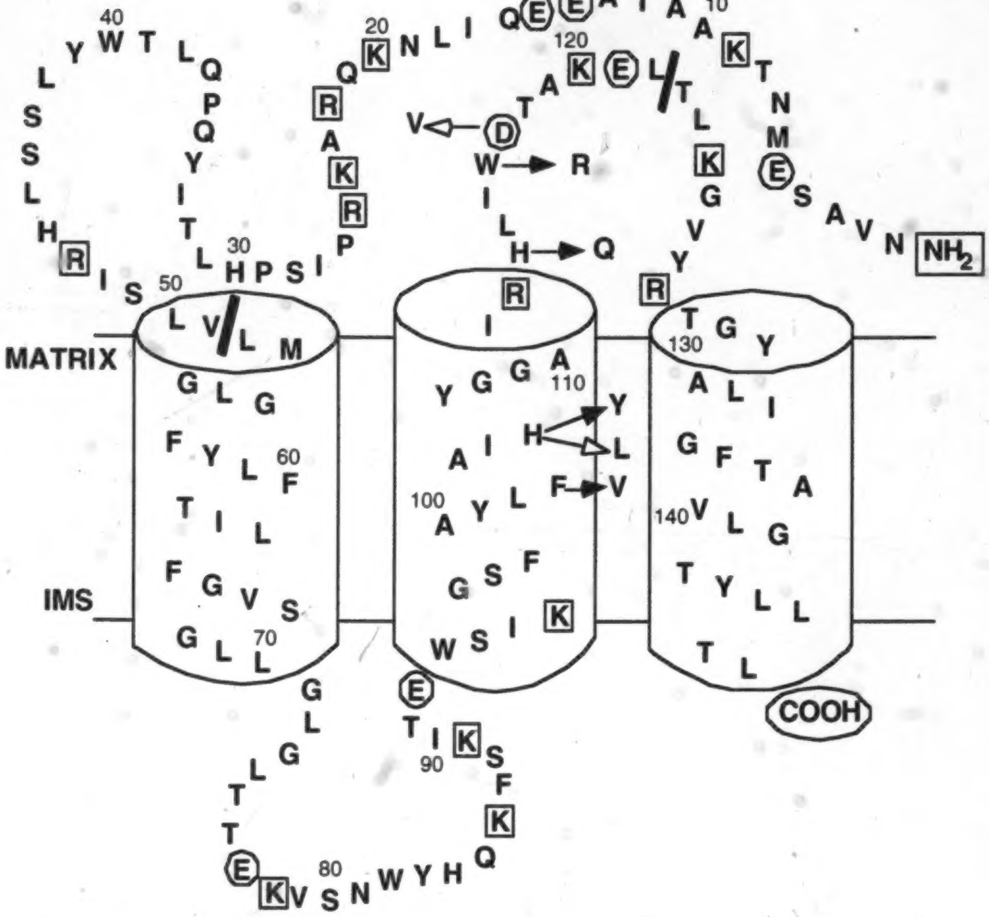
10
20
30
40
50
60
70
80
90
100
110
120
130
140
MATRIX
IMS
NH2
COOH
V
D
W
R
H
Q
Y
L
F

Figure 5.6 Topological Model of the Yeast Sdh3p Showing the Mutations Identified in this Study.

The model was developed from hydropathy analysis. Solid arrows indicate single amino acid substitutions, open arrows indicate double mutations, and solid lines indicate truncations.

The L122stop mutation results in many of the same effects as the F103V, the H113Q, and the W116R mutations, such as lowered succinate-DB reductase activity and an elevated K_m^{DB} value. However, it also results in lower covalent FAD (Table 5.2) and Sdh3p levels (Fig. 5.2), suggesting that the enzyme is not stably assembled. This conclusion is further supported by its thermostability profile (Fig. 5.3). It is perhaps not surprising that the L122stop mutation shares properties with the quinone-binding site mutants since it removes transmembrane segment III of Sdh3p and we postulate that a quinone-binding site is physically associated with the loop connecting transmembrane segments II and III. The loss of segment III likely impairs this loop's ability to adopt a conformation suited to quinone binding.

The H106L/D117V mutant has the very interesting property of having a reduced turnover number in the succinate-PMS reductase assay (Table 5.2), suggesting that these *SDH3* mutations propagate their effects into the catalytic dimer. We imagine that Asp-117 is located at the interface between the catalytic and the membrane-anchoring domains. As depicted in Fig. 5.6, the H106L lesion is expected to be within the bilayer and another mutation of this residue (H106Y; see below) does not significantly affect the succinate-PMS reductase activity. Thus, it is conceivable that the D117V mutation in the double mutant, H106L/D117V, accentuates the effect of the lesion at His-106. Similarly, the *Bacillus subtilis* SdhC Gly-168 is located in a hydrophilic stretch and its mutation to an Asp residue impairs binding of the catalytic dimer, placing it at the interface of the catalytic and the membrane-anchoring domains (Fríden *et al.*, 1987; Hederstedt, 1998). Alternatively, Asp-117 may be near to and perturb the catalytic dimer PMS binding site. Asp-117 is the first residue located in the membrane domain proposed to modulate electron transport of the catalytic domain in this family of enzymes. The specific role of Asp-117 can now be further explored by creating single point mutations at this residue and in its vicinity.

The turnover number of the H106Y mutant for succinate-DB reductase, succinate-cytochrome *c* reductase, and succinate-oxidase activities are all decreased by 40% while the apparent K_m^{DB} is only slightly elevated compared to the wild type enzyme. This suggests that His-106 does not play a direct role in quinone binding or reduction. Notably, the H106Y mutation causes the largest reduction of cytochrome b_{562} of all the mutants (Fig. 5.5).

Is His-106 then an axial ligand for heme *b*? In a multiple sequence alignment of SDH and FRD anchor polypeptides, the yeast Sdh3p His-106 aligns with an absolutely conserved histidine residue present in the second transmembrane segments of these enzymes (Hägerhäll, 1997). In some cases, such as His-70 of the *B. subtilis* SDH and His-84 of the *E. coli* SDH, this histidine residue has been experimentally shown to be a heme ligand (Fridén and Hederstedt, 1990; Hägerhäll *et al.*, 1995; Nakamura *et al.*, 1996; Vibat *et al.*, 1998). The conclusion that His-106 is a heme liganding residue can only be tentative because the two mutations involving this position (H106Y and H106L/D117V) do not completely abolish cytochrome b_{562} assembly. Cytochrome assembly may be impaired but not prevented by the loss of a single heme ligand (Fridén and Hederstedt, 1990; Hederstedt, 1998). In some cases, a natural ligand is apparently replaced by an alternative residue as suggested by the reconstitution of the bovine cytochrome b_{560} in either purified QPs1 (Q-binding protein in succinate-ubiquinone reductase) or QPs3 subunits (Lee *et al.*, 1998; Shenoy *et al.*, 1999). Further studies will be necessary to clarify the role of His-106.

The F103V, H113Q, and W116R mutations, which we suggest affect a quinone-binding site, also reduce the heme contents of the respective enzymes. Several possibilities may account for these reductions in heme *b* level, including structural changes that perturb cytochrome *b* assembly and alterations of the midpoint potential of the cytochrome that lead to underestimation of cytochrome content. Furthermore, it has yet to be determined if the electron transfer pathway between cytochrome b_{562} and fumarate involves quinone. Thus, lowered heme contents may reflect a disturbed quinone-binding site's ability to channel electrons between heme and fumarate.

The mutations analyzed in this study are localized to transmembrane segments II and the loop following it. This localization argues for the presence of a conserved quinone-binding site in SDH and FRD enzymes. Detailed mutagenesis studies in *E. coli* FRD have identified a number of amino acid residues that are critical for menaquinone binding and/or oxidation (Westenberg *et al.*, 1990; Westenberg *et al.*, 1993). In the FrdC subunit, which is analogous to the yeast Sdh3p, Glu-29, Phe-28, His-82, Trp-86 and Phe-87 interact with quinone. The latter three residues are in topologically similar positions to our mutants, being located in the loop following transmembrane segment II of the FrdC polypeptide. In the bovine SDH, photoaffinity-labeling experiments identified the loop connecting transmembrane segments II and III of Qps1 as a critical region for quinone binding (Lee *et al.*, 1995). In a recent study of the *E. coli* SDH, photoaffinity-labeling experiments identified the N-terminal end of the first transmembrane segment of the SdhC subunit as required for quinone binding (Yang *et al.*, 1998). This region corresponds to the location of the first two FrdC mutations mentioned above. It seems likely that residues close to the amino- and carboxyl-terminal ends of transmembrane segments I and II, respectively, contribute to the formation of a quinone-binding site. Our data do not exclude the presence of additional Sdh3p residues involved in quinone binding. Our screening procedure is biased against completely respiratory deficient cells and thus, might have prevented the isolation of mutations in another region of Sdh3p such as close to transmembrane segment I.

Inhibitors have been very powerful tools in the elucidation of the mechanisms of quinone-mediated electron transfer (Link *et al.*, 1993; Miyoshi, 1998; Ohnishi and Trumpower, 1980). In Chapter 3, we showed that the quinone analog, *s*-BDNP, inhibits the yeast SDH in a biphasic, noncompetitive manner (Oyedotun and Lemire, 1997). Earlier reports have shown similar inhibition patterns for the *E. coli* FRD and the bovine SDH (Yankovskaya *et al.*, 1996). We observed a biphasic inhibition of the wild type enzyme that can be explained by two inhibitor-binding sites with a 10-fold difference in affinities. The H113Q and H106Y mutants also showed biphasic inhibition patterns, but we observed significant increases in their apparent K_{i1} values compared to the wild type enzyme, suggesting a perturbation in the high affinity inhibitor-binding site. In our previous work (Oyedotun and Lemire, 1997), mutations involving the C-terminus of Sdh4p affected the apparent K_{i2} values for *s*-BDNP, indicating that the two inhibitor sites and by extension, the two quinone-binding sites, are spatially distinct in the yeast SDH. Similarly, two sites have been proposed for the *E coli FRD* and for the bovine SDH based on *s*-BDNP inhibition and the clustering of amino acid residues involved in quinone binding on opposite sides of the membrane (Lee *et al.*, 1995; Westenberg *et al.*, 1990; Westenberg *et al.*, 1993; Yankovskaya *et al.*, 1996; Yu *et al.*, 1985).

5.5. Bibliography

Ackrell, B. A. C., Johnson, M. K., Gunsalus, R. P., and Cecchini, G. (1992). Structure and function of succinate dehydrogenase and fumarate reductase. In Chemistry and biochemistry of flavoenzymes, F. Müller, ed. (Boca Raton, Florida: CRC Press, Inc.,), pp. 229-297.

Allen, J. P., Feher, G., Yeates, T. O., Komiya, H., and Rees, D. C. (1987a). Structure of the reaction center from *Rhodobacter sphaeroides* R-26: the cofactors. *Proc. Natl. Acad. Sci. USA* **84,** 5730-5734.

Allen, J. P., Feher, G., Yeates, T. O., Komiya, H., and Rees, D. C. (1987b). Structure of the reaction centre from *Rhodobacter sphaeroides* R-26, the protein subunits. *Proc. Natl. Acad. Sci. USA* **84,** 6162-6166.

Brasseur, G., Tron, G., Dujardin, G., Slonimski, P. P., and Brivet-Chevillotte, P. (1997). The nuclear *ABC1* gene is essential for the correct conformation and functioning of the cytochrome bc_1 complex and the neighbouring complexes II and IV in the mitochondrial respiratory chain. *Eur. J. Biochem.* **246,** 103-111.

Bruel, C., di Rago, J.-P., Slonimski, P. P., and Lemesle-Meunier, D. (1995). Role of the evolutionarily conserved cytochrome *b* tryptophan 142 in the ubiquinol oxidation catalyzed by the *bc*1 complex in the yeast *Saccharomyces cerevisiae*. *J. Biol. Chem.* **270,** 22321-22328.

Bullis, B. L., and Lemire, B. D. (1994). Isolation and characterization of the *Saccharomyces cerevisiae SDH4* gene encoding a membrane anchor subunit of succinate dehydrogenase. *J. Biol. Chem.* **269,** 6543-6549.

Chirino, A. J., Lous, E. J., Huber, M., Allen, J. P., Schenck, C. C., Paddock, M. L., Feher, G., and Rees, D. C. (1994). Crystallographic analyses of site-directed mutants of the photosynthetic reaction center from *Rhodobacter sphaeroides*. *Biochemistry* **33,** 4584-4593.

Cleland, W. W. (1979). Statistical analysis of enzyme kinetic data. *Methods Enzymol.* **63,** 103-138.

Cole, S. T., Condon, C., Lemire, B. D., and Weiner, J. H. (1985). Molecular biology, biochemistry, and bioenergetics of fumarate reductase, a complex membrane-bound iron-sulfur flavoenzyme of *Escherichia coli*. *Biochim. Biophys. Acta* **811,** 381-403.

Colson, A.-M. (1993). Random mutant generation and its utility in uncovering structural and functional features of cytochrome *b* in *Saccharomyces cerevisiae*. *J. Bioenerg. Biomembr.* **25,** 211-220.

Daignan-Fornier, B., Valens, M., Lemire, B. D., and Bolotin-Fukuhara, M. (1994). Structure and regulation of *SDH3*, the yeast gene encoding the cytochrome b_{560} subunit of respiratory complex II. *J. Biol. Chem.* **269,** 15469-15472.

Deisenhofer, J., and Michel, H. (1989). The photosynthetic reaction center from the purple bacterium *Rhodopseudomonas viridis*. *Science* **254,** 1463-1473.

Deisenhofer, J., and Michel, H. (1995). Crystallographic refinement at 2.3 Å resolution and refined model of the photosynthetic reaction center from *Rhodopseudomonas viridis*. *J. Mol. Biol.* **246,** 429-457.

El-Kabbani, O., Chang, C. H., Tiede, D., Norris, J., and Schiffer, M. (1991). Comparison of reaction centers from *Rhodobacter sphaeroides* and *Rhodopseudomonas viridis*: overall architecture and protein-pigment interactions. *Biochemistry* **30,** 5361-5369.

Ermler, U., Fritzsh, G., Buchanan, S. K., and Michel, H. (1994). Structure of the photosynthetic reaction center from *Rhodobacter sphaeroides* at 2.65 Å resolution: cofactors and protein-cofactor interactions. *Structure* **2,** 925-936.

Fridén, H., and Hederstedt, L. (1990). Role of His residues in *Bacillus subtilis* cytochrome *b*558 for haem binding and assembly of succinate:quinone oxidoreductase (complex 11). *Mol. Microbiol.* **4,** 1045-1056.

Fridén, H., Rutberg, L., Magnusson, K., and Hederstedt, L. (1987). Genetic and biochemical characterization of *Bacillus subtilis* mutants defective in expression and function of cytochrome b_{558}. *Eur. J. Biochem.* **168,** 695-701.

Gietz, R. D., and Sugino, A. (1988). New yeast-*Escherichia coli* shuttle vectors constructed with *in vitro* mutagenized yeast genes lacking six-base pair restriction sites. *Gene* **74,** 527-534.

Hägerhäll, C. (1997). Succinate:quinone oxidoreductases: variations on a conserved theme. *Biochim. Biophys. Acta* **1320,** 107-141.

Hägerhäll, C., Fridén, H., Aasa, R., and Hederstedt, L. (1995). Transmembrane topology and axial ligands to hemes in the cytochrome *b* subunit of *Bacillus subtilis* succinate:menaquinone reductase. *Biochemistry* **34,** 11080-11089.

Hatefi, Y. (1985). The mitochondrial electron transport and oxidative phosphorylation system. *Annu. Rev. Biochem.* **54,** 1015-1069.

Hederstedt, L. (1998). The membrane-integral domain of succinate:quinone oxidoreductases-a secretive haem-containing domain. *Biochem. Soc. Trans.* **26,** 408-413.

Hederstedt, L., and Ohnishi, T. (1992). Progress in Succinate:quinone oxidoreductase research. In Molecular mechanisms in bioenergetics, L. Ernster, ed. (New York: Elsevier Science Publishers), pp. 163-197.

Iwata, S., Lee, J. W., Okada, K., Lee, J. K., Iwata, M., Rasmussen, B., Link, T. A., Ramaswamy, S., and Jap, B. K. (1998). Complete structure of the 11-subunit bovine mitochondrial cytochrome bc_1 complex. *Science* **281,** 64-71.

Kim, H., Xia, D., Yu, C. A., Xia, J. Z., Kachurin, A. M., Zhang, L., Yu, L., and Deisenhofer, J. (1998). Inhibitor binding changes domain mobility in the iron-sulfur protein of the mitochondrial bc_1 complex from bovine heart. *Proc. Natl. Acad. Sci. USA* **95,** 8026-8033.

Kröger, A., and Klingenberg, M. (1973a). Further evidence for the pool function of ubiquinone as derived from the inhibition of the electron transport by antimycin. *Eur. J. Biochem.* **39,** 313-323.

Kröger, A., and Klingenberg, M. (1973b). The kinetics of the redox reactions of ubiquinone related to the electron-transport activity in the respiratory chain. *Eur. J. Biochem.* **34,** 358-368.

Lawrence, C. W. (1991). Classical mutagenesis techniques. *Methods Enzymol.* **194,** 273-281.

Lee, G. Y., He, D.-Y., Yu, L., and Yu, C.-A. (1995). Identification of the ubiquinone-binding domain in QPs1 of succinate-ubiquinone reductase. *J. Biol. Chem.* **270,** 6193-6198.

Lee, G. Y., Zhu, J., Yu, L., and Yu, C.-A. (1998). Reconstitution of cytochrome b_{560} (QPs1) of bovine heart mitochondrial succinate-ubiquinone reductase. *Biochim. Biophys. Acta* **1363,** 35-46.

Link, T. A., Hasse, U., Brandt, U., and von Jagow, G. (1993). What information do inhibitors provide about the structure of the hydroquinone oxidation site of ubihydroquinone:cytochrome *c* oxidoreductase? *J. Bioenerg. Biomembr.* **25,** 221-232.

Miki, T., Yu, L., and Yu, C. A. (1992). Characterization of ubisemiquinone radicals in succinate-ubiquinone reductase. *Arch. Biochem. Biophys.* **293,** 61-66.

Mitchell, P. (1961). Coupling of phosphorylation to electron and proton transfer by a chemiosmotic type of mechanism. *Nature* **191,** 144-148.

Mitchell, P. (1975). The protomotive Q-cycle: a general formulation. *FEBS Lett.* **59,** 137-139.

Mitchell, P. (1976). Possible molecular mechanisms of the protonmotive function of cytochrome systems. *J. Ther. Biol.* **62,** 327-367.

Mitchell, P. (1977). Vectorial chemiosmotic processes. *Annu. Rev. Biochem.* **46,** 996-1005.

Mitchell, P. (1987). Respiratory chain systems in theory and practice. In Advances in membrane biochemistry and bioenergetics, C. H. Kim, H. Tedeschi, J. J. Diwan and J. C. Salerno, eds. (New York: Plenum), pp. 25-52.

Miyoshi, H. (1998). Structure-activity relationships of some complex I inhibitors. *Biochim. Biophys. Acta* **1364,** 236-244.

Nakamura, K., Yamaki, M., Sarada, M., Nakayama, S., Vibat, C. R., Gennis, R. B., Nakayashiki, T., Inokuchi, H., Kojima, S., and Kita, K. (1996). Two hydrophobic subunits are essential for the heme *b* ligation and functional assembly of complex II (succinate-ubiquinone oxidoreductase) from *Escherichia coli*. *J. Biol. Chem.* **271,** 521-527.

Ohnishi, T., and Trumpower, B. L. (1980). Differential effects of antimycin on ubisemiquinone bound in different environments in isolated succinate-cytochrome *c* reductase complex. *J. Biol. Chem.* **255,** 3278-3284.

Oyedotun, K. S., and Lemire, B. D. (1997). The carboxyl terminus of the *Saccharomyces cerevisiae* succinate dehydrogenase membrane subunit, Sdh4p, is necessary for ubiquinone reduction and enzyme stability. *J. Biol. Chem.* **272,** 31382-31388.

Oyedotun, K. S., and Lemire, B. D. (1999a). The *Saccharomyces cerevisiae* succinate dehydrogenase anchor subunit, Sdh4p: mutations at the C-terminal Lys-132 perturb the hydrophobic domain. *Biochim. Biophys. Acta* **1411,** 170-179.

Oyedotun, K. S., and Lemire, B. D. (1999b). The *Saccharomyces cerevisiae* succinate-ubiquinone reductase contains a stoichiometric amount of cytochrome b_{562}. *FEBS Lett.* **442,** 203-207.

Ragan, C. I., and Cottingham, I. R. (1985). The kinetics of quinone pools in electron transport. *Biochim. Biophys. Acta* **811,** 13-31.

Ragan, C. I., and Reed, J. S. (1986). Regulation of electron transfer by the quinone pool. *J. Bioenerg. Biomembr.* **18,** 403-418.

Rich, P. R., and Bonner, W. D., Jr. (1978). An EPR analysis of cyanide-resistant mitochondria isolated from the mutant strain of *Neurospora crassa*. *Biochim. Biophys. Acta* **504,** 345-363.

Rich, P. R., Moore, A. L., Ingledew, W. J., and Bonner, W. D., Jr. (1977). EPR studies of higher plant mitochondria. I Ubisemiquinone and its relation to alternative respiratory oxidations. *Biochim. Biophys. Acta* **462,** 501-514.

Robinson, K. M., and Lemire, B. D. (1995). Flavinylation of succinate: ubiquinone oxidoreductase from *Saccharomyces cerevisiae*. *Methods Enzymol.* **260,** 34-51.

Schneider, H., Lemasters, J. J., and Hackenbrock, C. R. (1982). Lateral diffusion of ubiquinone during electron transfer in phospholipid- and ubiquinone-enriched mitochondrial membranes. *J. Biol. Chem.* **257,** 10789-10793.

Shenoy, S. K., Yu, L., and Yu, C. A. (1997). The smallest membrane anchoring subunit (QPs3) of bovine heart mitochondrial succinate-ubiquinone reductase. Cloning, sequencing, topology, and Q-binding domain. *J. Biol. Chem.* **272,** 17867-17872.

Shenoy, S. K., Yu, L., and Yu, C. A. (1999). Identification of quinone-binding and heme-ligating residues of the smallest membrane-anchoring subunit (QPs3) of bovine heart mitochondrial succinate:ubiquinone reductase. *J. Biol. Chem.* **274,** 8717-8722.

Trumpower, B. L. (1980). New concepts on the role of ubiquinone in the mitochondrial respiratory chain. *J. Bioener. Biomembr.* **13,** 1-24.

Trumpower, B. L. (1990). The protonmotive Q cycle-energy transduction by coupling of proton translocation to electron transfer by the cytochrome bc_1 complex. *J. Biol. Chem.* **265,** 11409-11412.

Trumpower, B. L., and Gennis, R. B. (1994). Energy transduction by cytochrome complexes in mitochondrial and bacterial respiration: the enzymology of coupling electron transfer reactions to transmembrane proton translocation. *Annu. Rev. Biochem.* **63,** 675-716.

Vibat, C. R. T., Cecchini, G., Nakamura, K., Kita, K., and Gennis, R. B. (1998). Localization of histidine residues responsible for heme axial ligation in cytochrome b_{556} of complex II (succinate:ubiquinone oxidoreductase) in *Escherichia coli*. *Biochemistry* **37,** 4148-4159.

Waldeck, A. R., Stowell, M. H. B., Lee, H. K., Hung, S. C., Matsson, M., Hederstedt, L., Ackrell, B. A. C., and Chan, S. I. (1997). Electron paramagnetic resonance studies of succinate:ubiquinone oxidoreductase from *Paracoccus denitrificans*. Evidence for a magnetic interaction between the 3Fe-4S cluster and cytochrome *b*. *J. Biol. Chem.* **272,** 19373-19382.

Westenberg, D. J., Gunsalus, R. P., Ackrell, B. A. C., and Cecchini, G. (1990). Electron transfer from menaquinol to fumarate. Fumarate reductase anchor polypeptide mutants of *Escherichia coli*. *J. Biol. Chem.* **265,** 19560-19567.

Westenberg, D. J., Gunsalus, R. P., Ackrell, B. A. C., Sices, H., and Cecchini, G. (1993). *Escherichia coli* fumarate reductase *frdC* and *frdD* mutants. Identification of amino acid residues involved in catalytic activity with quinones. *J. Biol. Chem.* **268,** 815-822.

Wikström, M. K. F., and Saraste, M. (1984). The mitochondrial respiratory chain. In Bioenergetics, L. Ernster, ed. (New York: Elsevier), pp. 49-94.

Xia, D., Yu, C. A., Kim, H., Xian, J. Z., Kachurin, A. M., Zhang, L., Yu, L., and Deisenhofer, J. (1997). Crystal structure of the cytochrome bc_1 complex from bovine heart mitochondria. *Science* **277,** 60-66.

Yang, X. D., Yu, L., He, D., and Yu, C. A. (1998). The quinone-binding site in succinate-ubiquinone reductase from *Escherichia coli*. *J. Biol. Chem.* **273,** 31916-31923.

Yankovskaya, V., Sablin, S. O., Ramsay, R. R., Singer, T. P., Ackrell, B. A. C., Cecchini, G., and Miyoshi, H. (1996). Inhibitor probes of the quinone binding sites of mammalian complex II and *Escherichia coli* fumarate reductase. *J. Biol. Chem.* **271,** 21020-21024.

Yu, C. A., Xia, D., Kim, H., Deisenhofer, J., Zhang, L., Kachurin, A. M., and Yu, L. (1998). Structural basis of functions of the mitochondrial cytochrome bc_1 complex. *Biochim. Biophys. Acta* **1365,** 151-158.

Yu, L., Yang, F. D., and Yu, C. A. (1985). Interaction and identification of ubiquinone-binding proteins in ubiquinol-cytochrome *c* reductase by azido-ubiquinone derivatives. *J. Biol. Chem.* **260,** 963-973.

Zhang, Z., Huang, L., Shulmeister, V. M., Chi, Y. I., Kim, K. K., Hung, L. W., Crofts, A. R., Berry, E. A., and Kim, S. H. (1998). Electron transfer by domain movement in cytochrome *bc*$_1$. *Nature* **392,** 677-684.

Zhu, Q. S., Berden, J. A., De Vries, S., and Slater, E. C. (1982). On the role of ubiquinone in the respiratory chain. *Biochim. Biophys. Acta* **680,** 69-79.

Chapter 6

General Discussion and Conclusions

The work presented in this thesis is aimed at understanding the structure and function of the *S. cerevisiae* SDH membrane-anchoring domain, which is composed of the Sdh3p and the Sdh4p subunits. Although significant progress has been made in understanding the structures and functions of SDHs and FRDs, the mechanism of quinone-mediated electron transport in these oxidoreductases is not known at the molecular level. The yeast SDH structural characteristics necessary for quinone binding have yet to be determined. Furthermore, the existence of a *b*-type cytochrome in the yeast SDH remains controversial. I have addressed these and other interesting questions about the yeast enzyme, which should contribute to a better understanding of SDHs and FRDs in general. The work presented in this thesis shows that the two anchor polypeptides are essential for aerobic respiration in *S. cerevisiae*. Specifically, I have demonstrated that: (1) the yeast SDH contains a stoichiometric amount of cytochrome b_{562}; (2) the carboxyl-terminal extension of the Sdh4p subunit is necessary for quinone reduction and enzyme stability; (3) the third predicted transmembrane helix in Sdh3p is necessary for SDH assembly and stability; (4) the Sdh3p amino acid residues Phe-103, His-113, and Trp-116 are involved in the formation of a quinone-binding pocket; and (5) the amino acid residue Asp-117 is in the interface between the catalytic domain and the membrane-anchoring domain.

In this chapter, I will discuss a model for quinone interaction that is compatible with these observations. In addition, I will try to answer some of the questions raised by the results of these studies and proffer some directions for future studies.

The SDH-associated Cytochrome b_{562} in Yeast.

The existence of a *b*-type heme in the yeast SDH is rather controversial. Based on a published abstract (Schilling *et al.*, 1982), it is generally believed that the *S. cerevisiae* SDH does not contain heme. In contrast, investigators working with the yeast complex III observed a fumarate-oxidizable heme in dithionite-reduced mitochondria corresponding to cytochrome *b* in SDH (Brasseur *et al.*, 1997; Bruel *et al.*, 1995). In Chapter 2, I confirm that the yeast SDH contains a fumarate-reducible *b*-type heme, which absorbs maximally at 562 nm. The molar ratio of this heme to the covalent FAD content is close to unity, suggesting the presence of a single heme per SDH holoenzyme. SDH is the major enzyme in yeast with covalently bound FAD, and the level of acid precipitable flavin reflects the level of SDH in mitochondrial membrane. We believe that the purification procedure employed in the earlier study (Schilling *et al.*, 1982) leads to the loss of heme. Although the bovine SDH is uniformly acknowledged to contain heme, it is usually purified with a substoichiometric amount of heme. This suggests that the chromophore is easily lost (Ackrell *et al.*, 1992). The use of whole mitochondria in our study may have avoided this problem.

The role of heme in SDH function is enigmatic. Our results indicate that heme is not required for electron transfer between succinate and ubiquinone. This is suggested by the lack of correlation between cytochrome contents and succinate-DB reductase activities. I show in Chapter 4 that decreases in the cytochrome contents of the Sdh4p Lys-132 mutants are not commensurate with the decreases of succinate-DB reductase activity. For example, while the cytochrome contents of the K132Q, K132E, K132G, and K132V mutants are reduced by about half, the succinate-DB reductase activities could be stimulated about 2-fold with increased DB concentrations and attain nearly wild type levels. Similarly, the results presented in Chapter 5 show that there is no correlation between the succinate-DB reductase activities of the *SDH3* mutant enzymes and their cytochrome contents. Further studies will be necessary to address the role of heme in this enzyme. An important step in addressing this question is the determination of the redox and thermodynamic properties of this cytochrome. The paucity of SDH in yeast mitochondria has so far hampered efforts in this direction.

Some level of overexpression of SDH may be necessary to achieve this goal. The facile genetics of *S. cerevisiae* can then be exploited by analyzing heme-deficient mutants for respiratory growth and for enzymatic activities and assembly. The hypothesis that the cytochrome in complex II interacts with the ubisemiquinone radical to reduce the production of superoxide free radicals (Ishii *et al.*, 1998) is very attractive and should be further explored. This hypothesis can be tested in a Mn-superoxide dismutase (SOD2)-deficient *S. cerevisiae* strain. The absence of this free radical scavenger will make cells sensitive to oxidative damage. If SDH-associated heme *b* plays a role in reducing superoxide production, its absence will make cells hypersensitive to oxidative stress.

Another fundamental question raised by this study is the validity of the assay, which relies on oxidation of the heme by fumarate. Two important observations argue against, but do not eliminate the possibility that this heme is a contaminant from the more abundant *b* cytochromes of complex III. First, the fumarate-oxidizable heme is not detectable in the absence of either of the SDH anchor polypeptides, Sdh3p and Sdh4p. Second, the spectrum is not detectable in the presence of the competitive inhibitor of the dicarboxylate-binding site, malonate. Independent methods for assaying the SDH-associated heme should be explored. These may include the use of *rho*$^-$ strains, which contain lesions in the mitochondrial genome (Lancashire and Mattoon, 1979). Since cytochrome *b* of complex III is encoded by the mitochondrial genome, *rho*$^-$ strains are devoid of this protein. *Rho*$^-$ strains can be induced efficiently by a wide variety of chemicals and treatments, including ethidium bromide, berenil, or ultraviolet irradiation (Lancashire and Mattoon, 1979). Alternatively, as done with the *Neurospora crassa* SDH, mitochondrial protein synthesis can be specifically inhibited by growing cells in the presence of chloramphenicol (Weiss and Kolb, 1979). Another approach is to label heme by growing yeast cells in the presence of a labeled heme precursor, such as δ-aminolevulinic acid. Labeled proteins could be resolved and identified by blue native gel electrophoresis (Schägger *et al.*, 1994; Schägger and von Jagow, 1991). Finally, the application of recombinant DNA technology in the production of partially or highly purified preparations of SDH cannot be overemphasized. The recent successful overexpression of the *E. coli* SDH offers a novel approach for the production of recombinant proteins (Maklashina *et al.*, 1998).

Axial Ligands for Heme.

The presence of heme in the yeast SDH also raises the important question of how this cofactor is coordinated. So far, all SDH cytochromes are known to be coordinated by 2 histidine residues (Hägerhäll, 1997; Hägerhäll and Hederstedt, 1996). The experiments reported in Chapter 2 suggest that the two anchor polypeptides, Sdh3p and Sdh4p, may be involved in heme coordination. The cytochrome b_{562} spectrum is abolished in the absence of either anchor polypeptide. In a multiple sequence alignment of SDH and FRD anchor polypeptides, the yeast Sdh3p His-106 aligns with an absolutely conserved histidine residue present in the second transmembrane segments of these enzymes (Hägerhäll, 1997). However, the two mutations involving this position (H106Y and H106L/D117V) do not completely abolish cytochrome b_{562} assembly. A second conserved His that serves as a heme ligand in other SDHs is replaced by Cys-78 in the yeast Sdh4p (Fig. 3.1). Should this residue be involved in heme ligation, it will reveal that heme coordination in the yeast SDH is novel. On the other hand, the possibility exists that a histidine residue at another location in the Sdh4p subunit serves as a heme ligand. A good candidate is His-99 at the matrix-facing end of the transmembrane segment III (Fig. 3.2). It is notable that this His residue is conserved in a yeast Sdh4p homologue, YL164Wp (Fig. 2.8). Site directed mutagenesis of all the histidine residues in the Sdh3p and Sdh4p subunits, as well as the Sdh4p Cys-78 at the canonical position, should clarify the nature of the axial heme ligands.

The Anchoring Role of the Membrane-Intrinsic Domain.

The two polypeptides of the membrane-anchoring domain, Sdh3p and Sdh4p, are clearly involved in the docking of the catalytic domain to the inner mitochondrial membrane. The absence of either of these polypeptides leads to undetectable levels of covalent FAD and succinate-PMS reductase activity in submitochondrial particles. However, the nature of the residues at the interface between the catalytic and the membrane domains is not known. Several observations indicate that Sdh3p Asp-117 may be close to or present at this interface. The H106L/D117V mutant has a greatly impaired covalent FAD level and a reduced turnover number in the succinate-PMS reductase assay (Table 5-2), suggesting that these *SDH3* mutations propagate their effects into the catalytic dimer. Alternatively, Asp-117 may modulate electron transport between the catalytic dimer and the artificial electron acceptor, PMS. This is conceivable if Asp-117 is in the vicinity of the PMS binding site on the catalytic dimer. Perturbation of this site by the H106L/D117V mutations would affect PMS-mediated electron transport. The specific role of Asp-117 should be further explored by creating single point mutations at this position and in its vicinity.

Furthermore, I observed that the third predicted transmembrane segment of the Sdh3p subunit is necessary for maintaining optimal conformation compatible with enzyme stability and quinone reduction. The Sdh3p L122stop mutation results in a lower content of membrane-associated covalent FAD (Table 5.2) and lower Sdh3p steady state levels (Fig. 5.2), suggesting that the enzyme is not stably assembled. This conclusion is further supported by its thermostability profile (Fig. 5.3). These observations highlight the crucial role of the loop connecting transmembrane segments II and III in the intersubunit interactions that maintain the native conformation of SDH. Site directed mutagenesis of the residues in this region, especially towards the transmembrane segment III end of the loop should give further insight into the interactions between the catalytic dimer and the membrane-anchoring domain.

The Role of the Sdh4p C-terminal extension.

This study demonstrates that the Sdh4p C-terminal extension is necessary for SDH activity and stability. The Sdh4p residues 128-135 are critical for the formation of a conformation that is compatible with high affinity quinone binding. This sequence is missing in the SDH4ΔC23 mutant enzyme, which shows a highly impaired ability to reduce exogenous quinone. In addition, kinetic analysis of the inhibition by *s*-DBNP indicates that a high affinity inhibitor-binding site, which may be equivalent to the Q_A site, is no longer present in the SDH4ΔC23 mutant enzyme. Moreover, residues 136 to 140, missing in the SDH4ΔC15 enzyme but not in the SDH4ΔC10 enzyme, are necessary for optimal quinone reducing activity. The C-terminal extension is hydrophilic and is predicted to be located on the cytoplasmic side of the inner mitochondrial membrane. Hence, it is very unlikely that the C-terminal extension participates directly in the formation of a quinone-binding pocket. However, it is conceivable that the effects of mutations in this region are propagated as structural perturbations to the quinone-binding site, arguing for the presence of a quinone-binding site associated with the cytoplasmic side of the Sdh4p subunit.

Furthermore, we showed in Chapter 4 that the positive charge provided by Sdh4p Lys-132 is crucial for establishing a stable conformation compatible with ubiquinone reduction (Oyedotun and Lemire, 1999). Since other SDHs and FRDs are missing the C-terminal extension, our observations raise the fundamental question of why the yeast SDH should have this peculiarity. The reason for this is not immediately obvious. However, the variability in the primary structures of the anchor polypeptides across species suggests that these subunits may determine the peculiar properties of the enzyme in each species. The observation that the positive charge provided by Lys-132 is critical suggests that the C-terminal extension may be involved in protein-protein interactions. It is interesting to note that the C-terminal extension, including the critical Lys-132, is conserved in a homologue of the yeast Sdh4p (Fig. 2.8), suggesting the functional importance of this region. Our results are consistent with the possibility that Lys-132 of Sdh4p may be a determinant of structural integrity and conformation probably through salt-bridge formation. Lys-132 may form a part of either an intramolecular or an intermolecular salt-bridge with an acidic residue that stabilizes the native conformation of the SDH hydrophobic domain. It should be possible to identify the interacting residue by the isolation of second-site revertants that restore wild type enzyme function on synthetic medium containing nonfermentable carbon sources.

Residues at the Quinone-Binding Site.

Three amino acid residues (Phe-103, His-113, and Trp-116) in the *S. cerevisiae* Sdh3p subunit are important for the formation of a quinone-binding site in SDH. Several lines of evidence, detailed in Chapter 5, indicate that mutations in these amino acid residues lead to severe but specific impairments in the ability of SDH to reduce exogenous quinones. This conclusion raises the fundamental question of the possible role of these residues in quinone binding and/or reduction. Site directed mutagenesis at these residues should give further insight into their roles in quinone interaction. Two sets of amino acid residues are usually present at quinone-binding sites (El-Kabbani *et al.*, 1991; Stowell *et al.*, 1997). One category is those having the ability to form hydrogen bonds with the carbonyl groups of the 1,4-benzoquinone ring. His-113 may fulfil such a role. The second category is amino acids having the ability to stabilize quinone binding through π-π interactions with the benzoquinone ring. The aromatic amino acids Phe-103 and Trp-116 are potential candidates for such functions. However, since the substitutions involving these residues are not isosteric, the specific role of these residues should be further explored by site directed mutagenesis.

As in the tetrameric SDHs and FRDs from other organisms (Ackrell *et al.*, 1992; Hägerhäll, 1997; Hederstedt and Ohnishi, 1992; Van Hellemond and Tielens, 1994), the data presented in this thesis indicate that amino acid residues provided by both anchor polypeptides are involved in quinone-binding of the yeast enzyme. A random mutagenesis study of the Sdh4p subunit should be undertaken in order to identify the amino acid residues that contribute to the formation of quinone-binding pockets.

A Model for SDH-Quinone Interactions.

The *SDH3* mutations that impaired quinone reduction are located in the Sdh3p transmembrane segment II and the loop following it. Similarly, truncations of the C-terminal extension of Sdh4p subunit suggest that a quinone-binding pocket may be located in the vicinity of transmembrane segment III, since the extension is at the end of transmembrane segment III. The asymmetric locations of these pockets suggest the existence of two quinone-binding sites in the yeast SDH. This hypothesis is further supported by kinetic analyses of *s*-BDNP inhibition. The quinone analog inhibits the yeast SDH with noncompetitive, biphasic kinetics, suggesting the existence of 2 nonequivalent inhibitor-binding sites. By extension, this corresponds to 2 nonequivalent quinone-binding sites, a high affinity and a low affinity quinone-binding sites that may be analogous to the Q_A and Q_B sites of the bacterial RCs, respectively (Deisenhofer and Michel, 1992; El-Kabbani *et al.*, 1991; Lancaster, 1998; Okamura and Feher, 1992; Parson, 1996).

Moreover, the two quinone-binding site hypothesis is further strengthened by the observation that mutations affecting succinate-quinone reduction have differential effects on the kinetics of inhibition by *s*-BDNP. The Sdh3p H113Q mutation, which has severely impaired quinone-mediated enzymatic activities, displays inhibition kinetics consistent with the perturbation of the high affinity inhibitor-binding site, corresponding to the high affinity quinone-binding site. On the other hand, the Sdh4ΔC23 truncation displays linear inhibition kinetics consistent with the loss of one inhibitor-binding site and by extension, one quinone-binding site. These data indicate that the two inhibitor-binding sites, and by extension the two quinone binding sites, are asymmetrically located in the membrane-anchoring domain, one proximal to the matrix side and the other, distal. This model is schematized in Fig. 6.1. It is not possible to assign specific locations for these sites from the data presented in this thesis. Hence, the model is based on that of the *E. coli* FRD for which more information is available.

There are a few predictions from this model that can be experimentally verified. First, the model predicts that residues involved in quinone binding would be clustered towards the matrix side of Sdh3p and the cytoplasmic side of the Sdh4p subunit. Second, it should be possible to find inhibitors, analogous to the complex III Q_o and Q_i inhibitors, which specifically affect either of the 2 quinone-binding sites. Third, perturbations of either of these sites (e.g. by mutations of important residues) should have differential effects on quinone-mediated electron transport. For instance, mutations affecting a high-affinity quinone-binding site would be expected to be more deleterious than those affecting a low-affinity quinone-binding site. These predictions are straightforward and should be easily verifiable experimentally.

It is not exactly known by what mechanism *s*-BDNP exerts its action. Molecular orbital calculation studies have shown that the α-branching conformation of the alkyl substituent at the 2-position, which is nearly perpendicular to the benzene ring, is similar to the isoprenoid side chain of ubiquinone (Saitoh *et al.*, 1992). It is possible that this stereochemical similarity is responsible for the inhibitory action of 2-alkyl-4,6-dinitrophenols. However, the noncompetitive inhibition kinetics indicate that *s*-BDNP may interact at a site

Figure 6.1 A Model of Quinone Interaction for the *S. cerevisiae* SDH

The model shows amino acid residues whose mutations affect SDH function. Ser-133, by virtue of its potential for H-bonding and proximity to Lys-132, may be involved in protein-protein interaction, which maintains SDH in optimal conformation for quinone reduction.

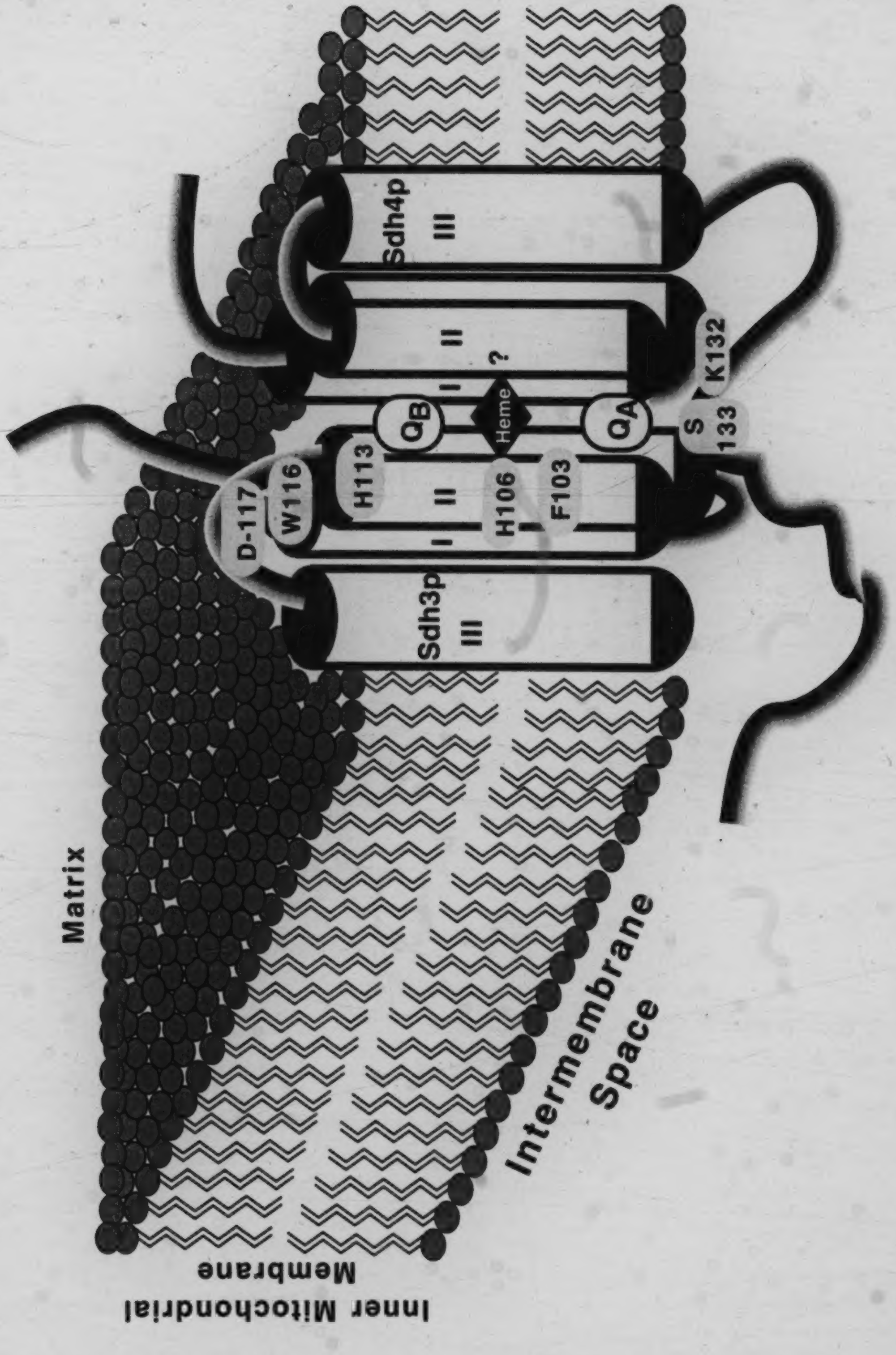
Matrix
Intermembrane Space
Inner Mitochondrial Membrane
Sdh4p
III
II
I
?
Heme
Q_B
Q_A
K132
S
133
H113
W116
D-117
H106
F103
Sdh3p
II
I
III

close to but distinct from the quinone-binding site. In that case, the inhibitor may sterically block electron exchange between the Q_A and Q_B sites. Alternatively, it may perturb the microenvironment of the Q_A and the Q_B sites and, thus, alters their quinone binding and/or reducing properties.

6.1. Bibliography

Ackrell, B. A. C., Johnson, M. K., Gunsalus, R. P., and Cecchini, G. (1992). Structure and function of succinate dehydrogenase and fumarate reductase. In Chemistry and biochemistry of flavoenzymes, F. Müller, ed. (Boca Raton, Florida: CRC Press, Inc.,), pp. 229-297.

Brasseur, G., Tron, G., Dujardin, G., Slonimski, P. P., and Brivet-Chevillotte, P. (1997). The nuclear *ABC1* gene is essential for the correct conformation and functioning of the cytochrome bc_1 complex and the neighbouring complexes II and IV in the mitochondrial respiratory chain. *Eur. J. Biochem.* **246,** 103-111.

Bruel, C., di Rago, J.-P., Slonimski, P. P., and Lemesle-Meunier, D. (1995). Role of the evolutionarily conserved cytochrome *b* tryptophan 142 in the ubiquinol oxidation catalyzed by the bc_1 complex in the yeast *Saccharomyces cerevisiae*. *J. Biol. Chem.* **270,** 22321-22328.

Deisenhofer, J., and Michel, H. (1992). High-resolution crystal structures of bacterial photosynthetic reaction centers. In Molecular mechanisms in bioenergetics, L. Ernster, ed. (Armsterdam: Elsevier Science Publishers B. V.), pp. 103-120.

El-Kabbani, O., Chang, C. H., Tiede, D., Norris, J., and Schiffer, M. (1991). Comparison of reaction centers from *Rhodobacter sphaeroides* and *Rhodopseudomonas viridis*: overall architecture and protein-pigment interactions. *Biochemistry* **30,** 5361-5369.

Hägerhäll, C. (1997). Succinate:quinone oxidoreductases: variations on a conserved theme. *Biochim. Biophys. Acta* **1320,** 107-141.

Hägerhäll, C., and Hederstedt, L. (1996). A structural model for the membrane-integral domain of succinate:quinone oxidoreductases. *FEBS Lett.* **389,** 25-31.

Hederstedt, L., and Ohnishi, T. (1992). Progress in succinate:quinone oxidoreductase research. In Molecular mechanisms in bioenergetics, L. Ernster, ed. (New York: Elsevier Science Publishers), pp. 163-197.

Ishii, N., Fujii, M., Hartman, P. S., Tsuda, M., Yasuda, K., Senoo-Matsuda, N., Yanase, S., Ayusawa, D., and Suzuki, K. (1998). A mutation in succinate dehydrogenase cytochrome *b* causes oxidative stress and ageing in nematodes. *Nature* **394,** 694-697.

Lancashire, W. E., and Mattoon, J. R. (1979). Genetics of oxidative phosphorylation: mitochondrial loci determining ossamycin-, venturicidin- and oligomycin-resistance in yeast. *Mol. Gen. Genet.* **176,** 255-264.

Lancaster, C. R. D. (1998). Ubiquinone reduction and protonation in the photosynthetic reaction centers from *Rhodopseudomonas viridis*: x-ray structures and their functional implications. *Biochim. Biophys. Acta* **1365,** 143-150.

Maklashina, E., Berthold, D. A., and Cecchini, G. (1998). Anaerobic expression of *Escherichia coli* succinate dehydrogenase: functional replacement of fumarate reductase in the respiratory chain during anaerobic growth. *J. Bacteriol.* **180,** 5989-5996.

Okamura, M. Y., and Feher, G. (1992). Proton transfer in reaction centers from photosynthetic bacteria. *Annu. Rev. Biochem.* **61,** 861-896.

Oyedotun, K. S., and Lemire, B. D. (1999). The *Saccharomyces cerevisiae* succinate dehydrogenase anchor subunit, Sdh4p: mutations at the C-terminal Lys-132 perturb the hydrophobic domain. *Biochim. Biophys. Acta* **1411,** 170-179.

Parson, W. W. (1996). Photosynthetic bacterial reaction centres. In Protein electron transfer, D. S. Bendall, ed. (Oxford, UK: BIOS Scientific Publishers Ltd), pp. 125-160.

Saitoh, I., Miyoshi, H., Shimizu, R., and Iwamura, H. (1992). Comparison of structure of quinone redox site in the mitochondrial cytochrome bc_1 complex and photosystem II (Q_B site). *Eur. J. Biochem.* **209,** 73-79.

Schägger, H., Cramer, W. A., and Von Jagow, G. (1994). Analysis and oligomeric states of protein complexes by blue native electrophoresis and isolation of membrane protein complexes by two-dimensional native electrophoresis. *Anal. Biochem.* **217,** 220-230.

Schägger, H., and von Jagow, G. (1991). Blue native electrophoresis for isolation of membrane protein complexes in enzymatically active form. *Anal. Biochem.* **199,** 223-231.

Schilling, R. J., Baldwin, T., and Palmer, G. (1982). The characterization of highly purified complex II from baker's yeast. *Fed. Proc.* **41,** 896.

Stowell, M. H., McPhillips, T. M., Rees, D. C., Soltis, S. M., Abresch, E., and Feher, G. (1997). Light-induced structural changes in photosynthetic reaction center: implications for mechanism of electron-proton transfer. *Science* **276,** 812-816.

Van Hellemond, J. J., and Tielens, A. G. M. (1994). Expression and functional properties of fumarate reductase. *Biochem. J.* **304,** 321-331.

Weiss, H., and Kolb, H. J. (1979). Isolation of mitochondrial succinate: ubiquinone reductase, cytochrome *c* reductase and cytochrome *c* oxidase from *Neurospora crassa* using nonionic detergent. *Eur. J. Biochem.* **99,** 139-149.